Transient Heme-Protein Interactions: Structural and Functional Studies on Interleukin-36α and Amyloid-β

Dissertation

zur Erlangung des Doktorgrades (*Dr. rer. nat.*)
der
Mathematisch-Naturwissenschaftlichen Fakultät
der
Rheinischen Friedrich-Wilhelms-Universität Bonn

vorgelegt von

Amelie Wißbrock

aus

Neustadt am Rübenberge

Bonn, im März 2019

Angefertigt mit Genehmigung der Mathematisch-Naturwissenschaftlichen Fakultät
der Rheinischen Friedrich-Wilhelms-Universität Bonn

1. Gutachter Prof. Dr. Diana Imhof
2. Gutachter Prof. Dr. Martin Hofmann-Apitius
Tag der Promotion: 9. Oktober 2019
Erscheinungsjahr: 2020

"Die Erkenntnis der Erkenntnis verpflichtet. Sie verpflichtet uns zu einer Haltung ständiger Wachsamkeit gegenüber der Versuchung der Gewißheit."

Humberto Maturana & Francisco Varela
Der Baum der Erkenntnis: Die biologischen Wurzeln menschlichen Erkennens

Abstract

The porphyrin heme is primarily known as a pivotal blood component. As functional part of hemoglobin, heme is responsible for the blood's vibrant red color and enables the transport of oxygen within the body. Moreover, biologically available heme acts as an effector and signaling molecule. As such, heme alters the activity and/or stability of proteins or evokes the formation of catalytically active complexes via transient heme-protein interactions. The latter was first observed for Amyloid beta (Aβ), whose aberrant accumulation is a hallmark of Alzheimer's disease (AD). Elevated heme levels are increasingly discussed in the context of assorted pathological conditions, such as inflammation and malaria as well as AD. Yet, intra- and extracellular heme concentrations are largely unknown due to the lack of suitable quantification methods. Within the scope of this work, a test system based on the catalytic activity of heme-peptide complexes was established to quantify biologically available heme in patient samples, such as *Liquor cerebrospinalis* (CSF). Beyond this, a potential interaction of heme with the proinflammatory cytokine interleukin-36α (IL-36α) was investigated.

Initially, a selection of heme-peptide complexes was examined with regard to their catalytic activity. A heme-binding 23mer peptide proved to be superior to Aβ and highly suitable for the application in a heme quantification assay. Subsequent studies with human CSF verified the correlation between substrate conversion and heme concentration. Heme binding to Aβ was characterized in more detail and the possible interplay between heme, the lipoprotein LDL, and Aβ, as it might occur in AD, was analyzed. Besides, a potential heme interaction with the proinflammatory cytokine IL-36α was subject of investigation. By means of different protein mutants and various spectroscopic methods, the binding of two heme molecules to distinct sequence motifs in IL-36α was confirmed. Structural analysis of the cytokine by 3D NMR spectroscopy provided detailed insights into the molecular basis of the heme-protein interaction. Furthermore, studies with fibroblast-like synoviocytes (FLS) isolated from knee joints of patients with rheumatoid arthritis revealed that heme binding to IL-36α as well as to IL-36β and IL-36γ attenuates IL-36 signaling.

The presented studies on the quantification of heme in patient samples and on the potentially heme-regulated protein IL-36α broaden the existing knowledge on the role of heme as an effector and signaling molecule in medical conditions. Hence, the findings contribute to the general disease understanding as well as to future development of therapy strategies.

Zusammenfassung

Das Porphyrin Häm ist vor allem als zentrale Komponente des Bluts bekannt. Als funktioneller Bestandteil des Hämoglobins verleiht es dem Blut seine leuchtend rote Farbe und ermöglicht den Transport von Sauerstoff innerhalb des Körpers. Darüber hinaus fungiert biologisch verfügbares Häm als Effektor- und Signalmolekül. Als solches beeinflusst Häm durch transiente Häm-Protein-Interaktionen die Aktivität und/oder Stabilität von Proteinen oder verursacht die Bildung katalytisch aktiver Komplexe. Letzteres wurde erstmals für Amyloid beta (Aβ) beobachtet, dessen aberrante Akkumulation ein Merkmal der Alzheimer-Krankheit ist. Erhöhte Hämspiegel werden zunehmend im Kontext mit verschiedenen pathologischen Zuständen, wie Entzündungen und Malaria sowie der Alzheimer-Krankheit, diskutiert. Dennoch sind intra- und extrazelluläre Häm-Konzentrationen mangels geeigneter Quantifizierungsmethoden weitgehend unbekannt. Im Rahmen dieser Arbeit wurde ein Testsystem basierend auf der katalytischen Aktivität von Häm-Peptid-Komplexen etabliert, um biologisch verfügbares Häm in Patientenproben, wie *Liquor cerebrospinalis* (CSF), zu quantifizieren. Darüber hinaus wurde eine mögliche Interaktion von Häm mit dem proinflammatorischen Zytokin Interleukin-36α (IL-36α) untersucht.
Zunächst wurde eine Auswahl von Häm-Peptid-Komplexen hinsichtlich ihrer katalytischen Aktivität analysiert. Ein Häm-bindendes 23mer-Peptid zeigte größeres Potential als Aβ und erwies sich für die Anwendung in einem Quantifizierungssystem als geeignet. Nachfolgende Studien mit humanem Liquor bestätigten die Korrelation zwischen Substratumsetzung und Hämkonzentration. Die Häm-Bindung an Aβ wurde weiter charakterisiert und eine mögliche Wechselwirkung zwischen Häm, dem Lipoprotein LDL und Aβ, wie sie bei der Alzheimer-Erkrankung auftreten kann, wurde untersucht. Darüber hinaus war eine potentielle Häm-Interaktion mit dem proinflammatorischen Zytokin IL-36α Gegenstand der Untersuchung. Mit Hilfe verschiedener Proteinmutanten und unterschiedlicher spektroskopischer Methoden wurde die Bindung von zwei Häm-Molekülen an unterschiedliche Sequenzmotive in IL-36α bestätigt. Die strukturelle Analyse des Zytokins mittels 3D-NMR-Spektroskopie lieferte detaillierte Einblicke in die molekularen Grundlagen der Häm-Protein-Interaktion. Des Weiteren zeigten Studien mit fibroblastenartigen Synoviozyten (FLS), die aus den Kniegelenken von Patienten mit rheumatoider Arthritis isoliert wurden, dass die Hämbindung an IL-36α sowie an IL-36β und IL-36γ die IL-36-vermittelte Signalübertragung verringert. Die dargelegten Studien zur Quantifizierung von Häm in Patientenproben und zum potenziell Häm-regulierten Protein IL-36α erweitern das vorhandene Wissen über die Rolle von Häm als Effektor- und Signalmolekül in Erkrankungen. Die Ergebnisse tragen so zum allgemeinen Krankheitsverständnis und zur zukünftigen Entwicklung von therapeutischen Strategien bei.

Contents

1 Introduction

"Blood is a very special juice", Mephistopheles states in Goethe's Faust.[1] Culturally speaking, blood has always been an entity that goes far beyond the physiological function.[2] The red fluid connects all body organs and tissues. 25 trillion (10^{12}) erythrocytes – also referred to as red blood cells (RBCs) – account for more than 60 % of human host cells.[3] Their main function, the transport of oxygen to and of carbon dioxide (CO_2) from tissues, is realized by hemoglobin, whose heme group is responsible for the blood's vibrant red color.[4] The central iron ion embedded in the tetrapyrrolic macrocycle of heme enables numerous vital physiological functions, and at the same time toxic redox activity.[5–10] What is the secret of the small molecule that is portrayed as the "one ring to rule them all", a "double-edged sword", the "friend turned foe" or "Dr. Jekyll or Mr. Hyde"?[11–14] While strict regulation under physiological conditions implements the pivotal effects of heme, the porphyrin's detrimental features emerge in a plethora of pathological situations as for example in porphyria, inflammation, and Alzheimer's disease.[10,13,15–20] Besides the cytotoxic properties of heme, heme-mediated regulation of proteins is part of the molecule's physiological and pathological role.[21,22] The regulatory function of heme is accomplished by transient heme-protein interactions.[22–32] An intricate network of heme-regulated proteins has been unravelled over the last 25 years, however, many questions remain unanswered and provide research opportunities at various levels.[21–25,27–32] Several studies indicate that the number of unidentified heme-regulated proteins is high.[28,33,34] Furthermore, methods that enable the quantification of biologically available heme *in vitro* and *in vivo* are rare and reliable numbers are largely missing.[35–39]

This thesis is dedicated to the field of biologically available heme. Based on the finding that the complex of heme and Amyloid beta (Aβ) exhibits a pseudoperoxidase activity, the catalytic activity of Aβ-derived and Aβ-independent heme-peptide complexes shall be analyzed initially.[40] Besides basic research, these studies aim at identifying a peptide that might be utilized for the diagnostic quantification of heme. Beyond that, a hitherto unknown, potentially heme-regulated protein, the human cytokine interleukin-36α, shall be investigated with regard to heme binding and a putative structural and functional impact of the interaction.

2 Theoretical Background

2.1 Chemistry and Biology of Heme

Dutch Antoni van Leeuwenhoek provided the first detailed description of RBCs in a letter addressed to the Royal Society, dated April 7, 1674: "I have divers times endeavoured to see and to know, what parts the *Blood* consists of; and at length I have observ'd, taking some Blood out of my own hand, that it consists of small round globuls driven thorough a Crystalline humidity or water".[41] A few years earlier Jan Swammerdam had observed RBCs in 1658 and Marcello Malpighi discovered the existence of the capillary system in 1661.[42,43] After identification of the predominant protein in RBCs, hemoglobin, by Fritz Ludwig Hünefeld in 1840, Felix Hoppe-Seyler, eponym of hemoglobin, described the reversible binding of oxygen to the protein in the 1860ies.[44,45] Two further findings of the 19$^{\text{th}}$ century are essential to our present understanding of hemoglobin and in particular the heme moiety. On the one hand, heme-driven generation of reactive oxygen species (ROS) along with cell and tissue damage may be caused by Fenton chemistry. The Fenton reaction, reported by Henry John Horstman Fenton, describes the oxidation of organic substrates catalyzed by iron salts with hydrogen peroxide (H_2O_2) in an acidic medium.[9,46,47] On the other hand, the specific absorbance band of porphyrins at $\sim$400 nm, also known as Soret band in honor of its discoverer Jacques-Louis Soret, provides the basis for a multitude of spectroscopic studies on heme and hemoproteins.[32,48] During the following decades, the interest in heme and related subjects has remained strong. In 1930, Hans Fischer was awarded with the Nobel Prize for the first total heme synthesis.[49,50] A few years later Max Perutz and John Cowdery Kendrew resolved the structures of hemoglobin and myoglobin, which was honored with the Nobel Prize in 1962.[50–52] The original belief that heme acts solely as a prosthetic group of proteins had to be dismissed in the 1990s when the porphyrin was found to modulate a protein's function by transient binding to distinct sequence motifs.[53] Several heme-regulated proteins, which act across diverse biological processes, are known by now (*cf.* Chapter 2.5).[21,22,31,40,54–57] To date, more than 50000 research articles on "heme" are deposited in the PubMed database, reflecting widespread interest in the porphyrin and related topics.[58]

Heme is a small molecule by definition, yet it is characterized by a high degree of chemical sophistication and intricacies. It is the chemical nature that makes heme one of the most versatile molecules in living organisms.[59] The porphyrin is a planar tetrapyrrole macrocycle, structurally related to chlorophyll and cobalamin (vitamin B_{12}).[60] By IUPAC definition heme molecules are "complexes consisting of an iron ion coordinated to a porphyrin acting as a tetradentate ligand, and to one or two axial ligands".[61] The complexing porphyrin ring is composed of four pyrroles, which are cyclically linked via methene bridges and are designated as A to D in a clockwise direction (Figure 1).[4,60,62] Four nitrogen atoms of the pyrroles coordinate the central heme iron ion, thereby allowing for two further coordinative bonds to complete the octahedral coordination.[4,28,60,62] The conjugated double bonds of the porphyrin scaffold facilitate the unique absorption and fluorescence properties distinctive for heme and other porphyrins.[63] As an amphiphilic, low-molecular iron chelate, heme can act in different milieus. The porphyrin ring, the methyl, and the vinyl groups add to the hydrophobic characteristics, whereas the propionate side chains and the iron ion account for hydrophilic features.[64,65] At physiological pH ferrous (Fe^{2+}) heme is electrically neutral, while ferric (Fe^{3+}) heme is positively charged.[9,64] The iron ion can appear in several oxidation and spin states.[9,66] Oxidative states ranging from Fe^{2+} to Fe^{5+} have been observed, however, the prevailing forms are Fe^{2+} and Fe^{3+}.[9] The iron ion enables heme to act as an electron donor/acceptor, to bind heteroatom-containing, proteinogenic amino acid side chains, to function as a pseudoperoxidase catalyzing Fenton-type reactions as well as to sense, transport, and store gaseous molecules (e.g. oxygen (O_2), carbon monoxide (CO), nitric oxygen (NO)).[9,21,28,67,68]

The porphyrin scaffold can be substituted by various functional groups, which determine the heme type (Figure 1).[9,28,68] Heme *b* (also referred to as protoporphyrin/protoheme IX), above all known for its presence in RBCs, is the most abundant form.[9,28] Heme *b* is characterized by a ferrous (Fe^{2+}) iron ion, methyl groups (C_1, C_3, C_5, C_8), vinyl groups (C_2, C_4), and propionic side chains (C_6, C_7, Figure 1).[9,28,68] In proteins (e.g. hemoglobin) it serves as a non-covalently bound cofactor.[9,28] In a two-step reaction heme *b* can be converted to heme *a*, which differs from heme *b* by a hydroxyethylfarnesyl group (C_2) and a formyl group (C_8).[9,28,68] Heme *a* is found in the mitochondrial cytochrome c oxidase (COX, complex IV) of the respiratory chain.[9,28,68] In heme *c* the two vinyl groups of heme *b* form thioesters (C_2, C_4) that are bound covalently to sulfhydryl groups of cysteine side chains (e.g. cytochrome c).[9,28,68] There are other types of heme (e.g. heme *i, m, d, o*), many of them being derivatives of heme *b*.[71,72] The oxidized, ferric forms of heme *b* are hemin or hematin, respectively. Both porphyrins are characterized by ferric (Fe^{3+}) iron ions and a fifth ligand, which is either a chloride ion (hemin) or an hydroxide ion (hematin, Figure 1).[73] Furthermore, ferriporphyrin crystals, referred to as malarial pigment

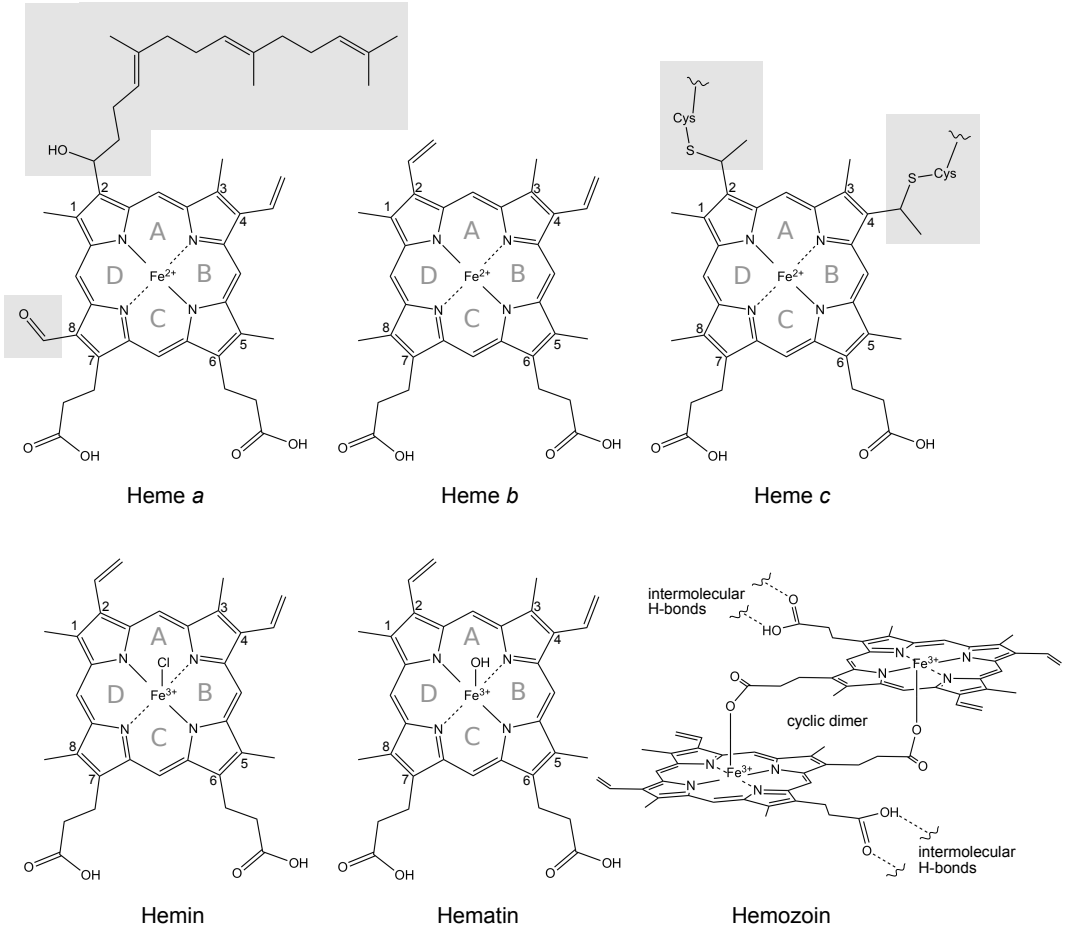

Figure 1. Chemical structures of heme *a* to *c*, hemin, hematin, and hemozoin (β-hematin). Carbon numbering and alphabetic designation of the pyrrol rings are given in the structures. The thioesters of heme *c* are covalently linked to cysteine residues in proteins. In hemozoin cyclic hematin dimers form larger structures via intermolecular H-bond formation.[9,28,68–70]

or hemozoin, occur in nature under certain circumstances, such as malaria infection (Figure 1).[69,70] During malaria infection, parasites of the genus *Plasmodium* crystallize reactive free heme from ingested hemoglobin into inert hemozoin. Hemozoin is composed of cyclic hematin dimers (β-hematin) consisting of two hematin molecules linked via reciprocal coordinative bonds from the iron ions to the oxygen atoms of the propionate side chains of the adjacent hematin molecule. The dimers assemble to form larger structures by intermolecular hydrogen bonds (H-bonds, Figure 1).[69,70]

Heme is not evenly distributed throughout the human body. About 80 % of the body's heme resides in the 25 trillion circulating RBCs.[3,59] 5×10^9 heme molecules are thought to be present in each RBC with an estimated heme concentration as high as 80 mM.[75] The remaining 20 % of the total heme quota are allocated to hepatic parenchyma cells (15 %) and other tissues (5 %).[59] Notably, all nucleated cells perform heme biosynthesis.[59] The sites with the highest levels of heme, RBCs and

hepatic cells, reflect two of the molecule's most important functions: oxygen transport and storage (hemoglobin) as well as mediation of redox reactions (cytochrome P_{450}, CYP_{450}).[6,10,21,28,76–78] These functions, like many others, are performed by hemoproteins.[9] Hemoproteins carry one or more heme molecule(s) as prosthetic group(s), which is/are bound covalently and/or non-covalently in a permanent fashion (Figure 2, 3). The heme moieties are often found in binding pockets enriched in aromatic residues.[9,26,28,79] Among the best-known hemoproteins are globins, cytochromes, peroxidases, and catalases.[6,78,80] In humans, not only in hemoglobin (blood) but also in myo- (muscle), neuro- (brain), and cytoglobin (intracellular) heme *b* is responsible for oxygen transport and storage.[78] Besides gas transport and storage, heme-based sensor proteins represent a prevailing system to recognize O_2, CO, and NO in humans. Gas binding to a heme-bound gas-sensing domain engenders a conformational change of the domain and thus a ligand-dependent switch of a second adjacent transmitter domain.[25,81] An often cited example is the NO-synthase (NOS) that forms an inactive ferrous-NO complex upon NO binding.[25,82] NOS catalyzes the conversion of arginine to citrulline while producing NO. The gas has a multitude of physiological functions, such as vasodilation, pathogen defense, and neurotransmitter activity (*cf.* Chapter 2.3).[83,84] Another example of a heme-bound gas-sensing domain is the Per-ARNT-Sim (PAS) motif (domain) that can be associated with various transmitter domains, as for example histidine kinase or phosphodiesterase domains.[29,81]

Peroxidases and catalases form a further group of essential hemoproteins that reduce H_2O_2 and other organoperoxides to less toxic compounds.[6,80,85] These enzymes share the common high-valent iron intermediate Compound I, presumably an oxoferryl porphyrin-π-cationic radical, that allows for oxidation and/or oxygenation to proceed.[86] In addition, heme can mediate electron transfer in respiratory cytochromes or in redox reactions catalyzed by cytochromes.[87,88] CYP_{450} enzymes

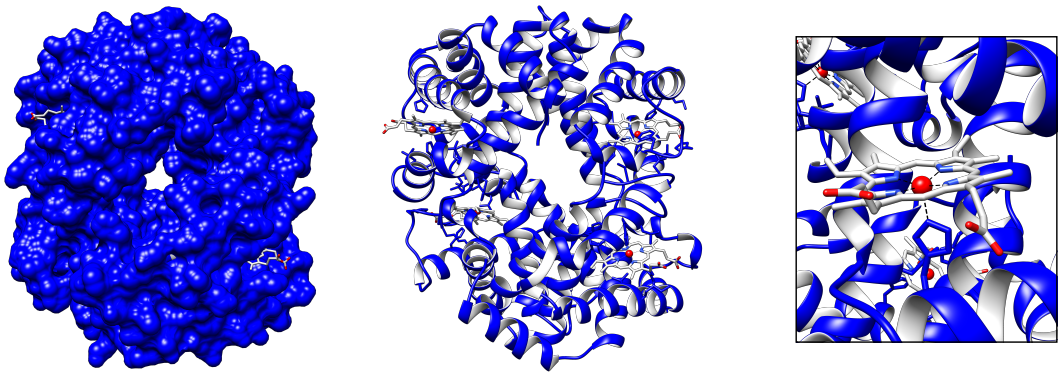

Figure 2. Structure of hemoglobin as surface (left) and ribbon (middle) diagram (PDB 1A3N[74]). A zoom-in (right) shows the coordination of one of the four heme molecules via a proximal histidine residue.

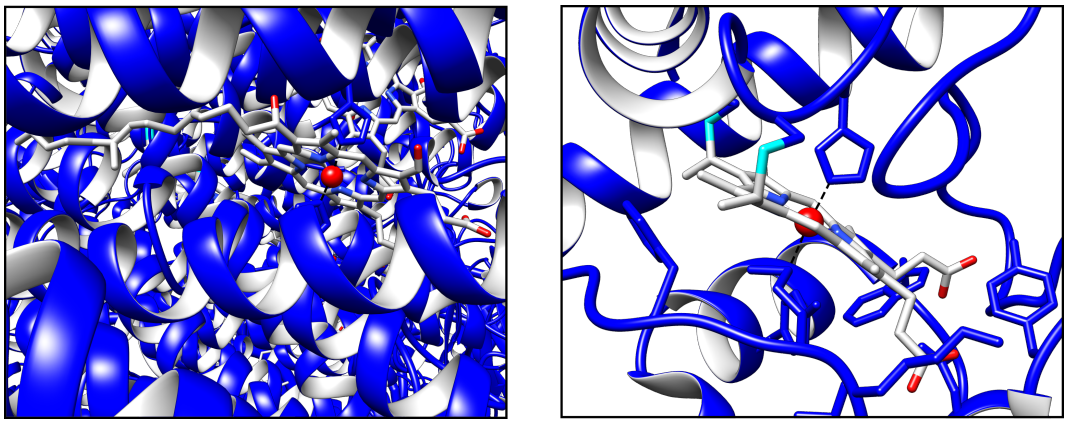

Figure 3. Heme *a* and heme *c* coordination in hemoproteins. Heme coordination sites of cytochrome c oxidase (heme *a*, PDB 1OCO,[90] left) and cytochrome c (heme *c*, PDB 1HRC,[91] right).

are of particular pharmaceutical interest, since they convert a plethora of drugs into readily removable forms as part of the phase I metabolic processes.[77] Moreover, the biosyntheses of vitamin D_3, retinoids, prostaglandins, and steroid hormones are CYP_{450}-dependent.[77] Two other vital hemoproteins are cytochrome c and COX (Figure 3). A covalently bound heme *c* molecule is found in cytochrome c, whereas two heme *a* (*a*, a_3) molecules are non-covalently bound in COX.[9] In the respiratory chain cytochrome c transports electrons along the inner mitochondrial matrix to the terminal electron acceptor COX by temporarily switching the redox state of the heme iron from Fe^{2+} to Fe^{3+}.[89]

Nowadays, it is generally accepted that besides permanently bound heme in hemoproteins, another pool of biologically available heme exerts alternative functions.[21–25,27–32] For many years the concept of heme as an effector molecule was questioned. The disbelief originated from the dogmatic assumption that heme *in toto* is readily incorporated into hemoproteins upon synthesis and is not trafficked from one cell or tissue to another.[92] This conviction was supported by the observed reactivity and toxicity of unbound heme and, moreover, by the chemical properties of heme which suggest that the porphyrin will eagerly interact with diverse molecules.[92]

To date there is strong evidence that one fraction of the cellular heme content is loosely associated to proteins within the cell serving for hemylation of hemoproteins and for heme-mediated signaling. Two observations support this concept. Firstly, heme has to be shielded in order to mitigate the molecule's toxicity. Secondly, heme is synthesized in the mitochondria, yet the molecule is found in virtually all organelles.[9,75,92] Accordingly, intracellular heme translocation is necessary. The characteristic attributes of the porphyrin suggest an escorted movement within the cell rather than free diffusion.[75,92]

Reversible heme binding to intracellular proteins for reasons of scavenging and transport is conceivable.[9,75,92] The exchangeable, dynamic pool of heme is often referred to as "labile heme", whereas the heme in hemoproteins is depicted as "inert heme" (Figure 4).[75,92] In addition, "free" heme can occur in pathological states. Demolition of hemoproteins elicits the liberation of large quantities of unbound heme.[9,18,93] The best-characterized example is hemolysis, during which high levels of extracellular, intra-, and extravascular, unbound heme are observed. A physiological back-up system scavenges unbound heme. Yet, persisting, recurring, and severe conditions can lead to exhaustion of the scavenging capacity and consequently heme-driven toxicity (Chapter 2.3).[9,10,62,94,95] There are various terms describing the heme fraction that is not permanently bound in hemoproteins in the literature, among them are "free", "uncommitted", "labile", or "not-determined" heme pool.[18,62,96,97] The present work is based on the assumption that heme occurs as "inert heme" in hemoproteins, as "labile heme" intracellular, and as "free heme" in pathological conditions (Figure 4). The latter ones, labile heme and free heme, can be grouped as "biologically available heme" and represent the heme pool responsible for alternative heme functions (regulatory heme).

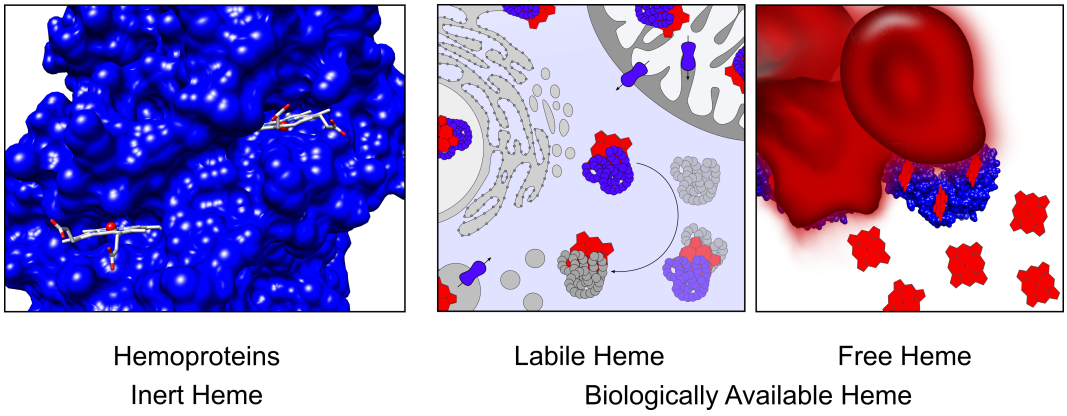

Figure 4. Designation of different heme pools. Heme can occur as "inert heme" in hemoproteins (e.g. hemoglobin, PDB 1A3N1[74]), as "labile heme" intracellular[75] as well as extracellular upon liberation from hemoproteins (e.g. during hemolysis). The latter is often referred to as "free heme". Labile and free heme represent the pool of biologically available heme, which may function as regulatory molecule.[21–25,27–32]

Unbound heme *b* is readily oxidized to hemin. For reasons of simplicity the generic term "heme" is used for hemin (Fe^{3+} heme) within this work unless in the context of hemoproteins (e.g. hemoglobin) and if not stated otherwise. To date, studies aiming at quantification of biologically available heme are still in their infancy.[36–39,98,99] Initial investigations utilized genetically encoded heme sensors and revealed cytosolic labile heme concentrations ranging from 25-300 nM depending on the cell type, which is equal to $\sim 10\,\%$ of the total cellular heme quota.[36,37,75,92,98]

As an effector molecule, heme can modulate the activity and stability of heme-regulated proteins by temporarily interacting with short heme-binding protein sequence stretches, termed heme-binding motifs (HBMs) or heme-regulatory motifs (HRMs), respectively.[32,100] Several peptide and protein examples have been established over the past decades, such as Aβ, known for its crucial role in Alzheimer's disease (AD) and tumor protein p53 (p53), a well-described tumor suppressor (*cf.* Chapter 2.4, 2.5).[40,57,101] So far, many studies have been based on *in vitro* assays and a detailed *in vivo* analysis is yet to be performed. Moreover, structural information on transient heme-protein interactions is rare and prospective studies are required to unravel the structural basis of different heme-binding modes.[21,22,28–32]

The chemistry and biology of heme is multifaceted at every level. Not for nothing tetrapyrroles have previously been depicted as the pigments of life.[60] The last decade has witnessed a renaissance in knowledge of the cell biology of heme, yet innumerable details remain uncovered.[92] The complex network of heme-associated biological reactions and pathways as well as its apparent importance in a plethora of pathological conditions, render it impossible to portray the heme's vital physiological role in its entirety. Accordingly, the following chapters are merely intended to provide a general insight and to address aspects relevant to the understanding of the research carried out in the context of this work.

2.2 Heme Homeostasis

Heme is essential for life, yet, due to the redox-active iron, high levels of unbound heme have deleterious effects on cells and tissues (*cf.* Chapter 2.3).[9] Therefore, heme homeostasis is a highly coordinated balancing act that is inevitably linked to erythropoiesis, erythrophagocytosis, and iron metabolism.[11,75,102] Since erythroblast maturation and thus hemoglobinization dramatically increase the demand for heme, erythroid cells are literally the "ultimate heme synthesizing factories in the body".[11,103] After travelling about 250 km throughout the cardiovascular system, the lifespan of an erythrocyte exceeds after 100 to 120 days, which explains the high physiological turnover of RBCs.[104] About 360 billion senescent RBCs are clarified by macrophages of the mononuclear phagocytic system (MPS, also referred to as reticuloendothelial system) during erythrophagocytosis every day. At the same time, erythropoiesis of an equivalent number of RBCs maintains a constant RBC count.[105–107] As a result of long-term membrane intercalation and subsequent destabilization, heme is substantially involved in RBC aging.[108] Once macrophages engulf senescent RBCs, hemoglobin is proteolytically degraded and the heme moiety is released. Liberated heme is thought to be almost exclusively transported from the erythrophagolysosome into the cytosol before degradation via the heme oxygenase (HO) system.[92,102,105,106]

A large part of the captured heme iron (25 mg) is recycled to ensure sufficient iron supply for erythropoiesis.[64,68,109] In fact, heme iron constitutes 95 % of the total iron quota (3-4 g in adults) and about 80 % of the 3-4 mg of iron that is circulating in the plasma is believed to be *en route* between the bone marrow and the MPS. Only a minor part (0.03 %, ca. 1 mg) of the iron pool is exchanged daily.[75,109] Depending on the amount of xenobiotics and consequently detoxification by CYP_{450}, heme synthesis is readily adapted to changing metabolic requirements in the liver.[110] The disparity in requirement for heme between erythroid versus non-erythroid cells is realized by different sets of enzymes, which are mostly derived from tissue-specific alternate splicing.[110,111] A short overview on the reactions and enzymes involved in heme synthesis and degradation will be given hereafter.

2.2.1 Heme Biosynthesis and Enzymatic Degradation

Heme is indispensable for almost all living organisms and the evolutionarily conserved heme biosynthetic pathway epitomizes one of the most vital metabolic routes. The pathway does not only provide heme as the final product, but, depending on the organism, also precursors for other eminent tetrapyrroles, such as chlorophyll and cobalamin.[112] In humans, heme synthesis proceeds following the Shemin pathway, yet, deviating pathways are known in other organisms (e.g. C_5 pathway).[4,113,114] Heme synthesis includes eight enzymatic reactions partitioned between the mitochondria (step 1, steps 6-8) and the cytoplasm (steps 2-5, Figure 5).[4,11,111,115,116] In mammals, the first and rate-limiting step is the condensation of glycine and succinyl-CoA to form δ-aminolevulinic acid (ALA) and CO_2 in the mitochondrial matrix. The reaction is catalyzed by ALA synthase (ALAS), a homodimeric, pyridoxal-5'-phosphate-dependent enzyme.[117] ATP-binding cassette subfamily B member 10 (ABCB10), which is located in the inner mitochondrial membrane, was believed to be involved in ALA transport to the cytosol. A recent study found ABCB10 to be crucial for hemoglobinization, however, the same study also suggests that ABCB10 is not involved in ALA transport. Therefore, the mechanism of mitochondrial ALA export remains to be resolved.[118,119] The following reactions take place in the cytosol and are catalyzed by porphobilinogen synthase (PBGS, also known as ALA dehydratase), porphobilinogen desaminase (PBGD), and uroporphyrinogen III synthase (UROS). Initially, the asymmetric condensation of two ALA molecules yields the monopyrrole porphobilinogen (PBG, step 2). The head-to-tail synthesis of four PBG molecules forms preuroporphyrinogen (hydroxymethylbilane, HMB), a reactive linear intermediate (step 3). By intramolecular rearrangement and spontaneous cyclization the first cyclic intermediate, uroporphyrinogen III, is formed in the presence of UROS (step 4). Subsequently, uroporphyrinogen III decarboxylase (UROD) catalyzes the decarboxylation of the four acetates of uroporphyrinogen III to form coproporphyrino-

gen III, which is presumably transported to the intermembrane space (IMS) via ATP-binding cassette subfamily B member 6 (ABCB6, step 5).[4,11,75,111,115,116,120] The following oxidative decarboxylation of the two A and B ring propionate side chains by coproporphyrinogen oxidase (CPOX), yields protoporphyrinogen IX and forms the vinyl groups of heme *b* (step 6). In the penultimate reaction six electrons are eliminated and protoporphyrinogen IX is oxidized to the aromatized protoporphyrin IX (PPIX) by porphyrinogen oxidase (PPO, step 7).[121] Ferrous iron (Fe^{2+}) is incorporated into the PPIX ring by ferrochelatase (FECH) on the matrix side of the inner mitochondrial membrane in the terminal reaction (step 8).[4,11,111,115,116]

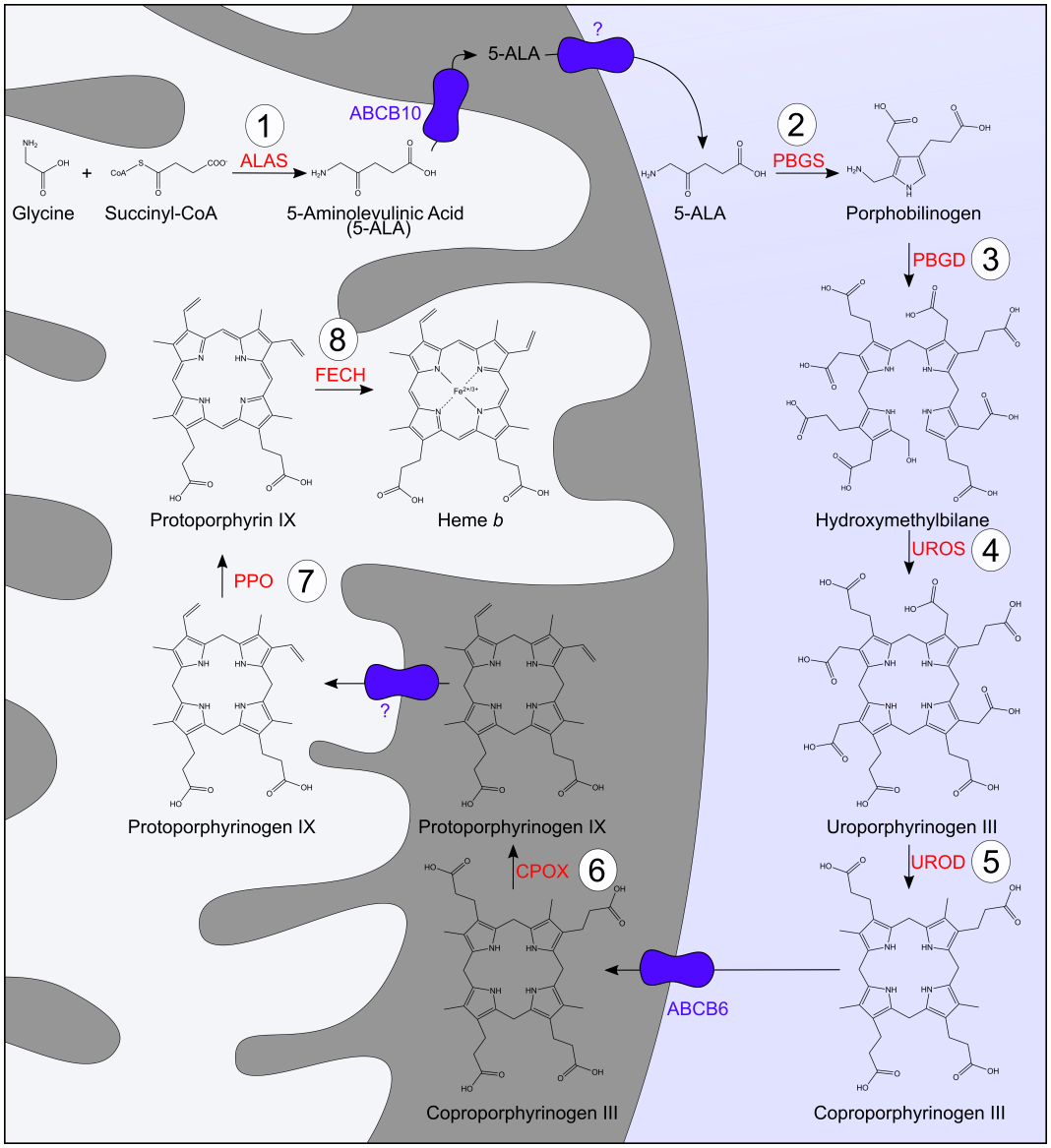

Figure 5. The mammalian pathway of heme biosynthesis. Partitioned between the mitochondria and the cytosol, eight enzymatic reactions yield the final product heme. Full enzyme names are given in the text.

Control mechanisms of heme synthesis in differentiating erythroid cells and hepatocytes vary significantly.[5,111,116,122,123] Two isoforms of ALAS, ALAS1 and ALAS2, ensure heme synthesis at the correct level depending on cell requirements. In non-erythroid cells and hepatocytes the non-specific housekeeping form ALAS1 is expressed, whereas ALAS2 is found in erythroid cells.[111,116] ALAS expression is encoded by hemA genes that are regulated by a broad range of transcriptional and posttranscriptional factors. The genes are located in chromosome 3 (ALAS1) and the X chromosome (ALAS2), respectively.[4,5,111,116,123,124] The gene of ALAS1 is also expressed in erythroid precursor cells but is turned off once differentiation and hemoglobin synthesis are initiated.[11] Heme acts as a positive feedback regulator for heme synthesis in erythroid cells and at the same time inhibits its own degradation.[10,123] Moreover, heme synthesis is inherently connected to protein synthesis during erythropoiesis, which is ensured by a sophisticated network composed of a variety of elements.[123,125] Notably, ALAS2 is not the rate-limiting enzyme in erythroid heme synthesis, but synthesis is predominantly dependent on the availability of iron. In case of iron limitation, the final step, i.e. iron insertion, restricts heme synthesis.[122,126] Zinc can substitute for iron forming increased levels of zinc-PPIX in erythrocytes, an initial indicator of iron deficiency.[127] In non-erythroid cells ALAS1 activity is impinged by heme in many ways, for instance, heme represses mitochondrial import of ALAS1 (*cf.* Chapter 2.5).[53,111,123,128,129]

Besides heme synthesis, heme degradation is also a highly coordinated process. In fact, degradation of heme can be accomplished by various chemical and enzymatic mechanisms. The most common form in humans is the HO-catalyzed degradation generating stoichiometric quantities of CO, iron, and biliverdin IXα (Figure 6).[12,130,131] Once heme is bound into a hydrophobic pocket of HO via His25 as the proximal iron ligand, several autocatalytic reactions proceed.[131–134] The reactions depend on the coordinated activity of HO and NADPH-cytochrome P_{450} reductase and require three molecules of O_2 and nicotinamide adenine dinucleotide phosphate (NADPH) each.[131,135] Upon formation of a peroxy intermediate (Fe^{3+}-OOH) the α-*meso*-carbon of the porphyrin scaffold is attacked by the terminal oxygen. The generated α-*meso*-hydroxyheme is converted to α-verdoheme by utilizing O_2 and releasing CO after regiospecific cleavage of the α-methene bridge. Consequently, the iron ion is liberated and biliverdin is formed.[131,135–137] In a subsequent reaction biliverdin reductase (BVR) reduces biliverdin to bilirubin, while oxidizing nicotinamide adenine dinucleotide (NADH) or nicotinamide adenine dinucleotide phosphate (NADPH) depending on the surrounding pH (pH 6.0-7.0, NADH; pH 8.5-8.75, NADPH).[138] Unconjugated bilirubin is released into the blood where it binds to albumin in a 1:1 fashion before being transported to the liver. Once bilirubin undergoes hepatic phase II glucuronidation by uridine diphosphate, the generated mono- or diglucuronides are

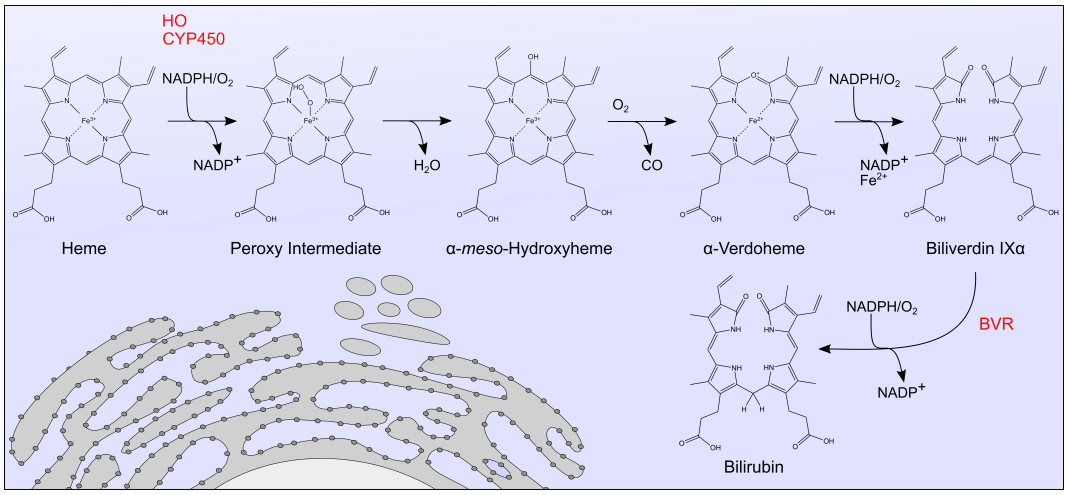

Figure 6. Enzymatic heme degradation via the HO-system. HO is a tail-anchored enzyme located at the smooth ER, however, the reaction takes place in the cytosol. The generated heme degradation products CO, biliverdin, and bilirubin are thought to be bioactive (e.g. anti-oxidant properties). HO, heme oxygenase; CYP_{450}, NADPH-cytochrome P_{450} reductase, BVR, biliverdin reductase.

eliminated via the bile and feces.[136] Some of the other heme degradation products may exhibit physiological functions. CO is a gasotransmitter that shows neuromodulator activity and is suggested to hamper platelet aggregation by activating guanylate cyclase, among other functions.[139–141] Biliverdin and bilirubin are discussed as potent anti-oxidants while the liberated iron is primarily recycled.[136,141,142] Other bioactive products, namely propentdyopents (PDPs) and bilirubin oxidation products (BOXes), may arise upon oxidation of heme. BOXes seem to have a vasoconstrictive effect on cerebral arterioles in addition to other implications. Yet, occurrence, underlying mechanisms, and potential interaction partners are largely unknown and further studies are required to evaluate the physiological role of these molecules.[143–145]

HO enzymes are evolutionary conserved between species. Two HO isoforms, encoded by different genes, differ in reaction rates, primary structure, and molecular weight despite sharing $\sim 42\,\%$ sequence identity.[12,146] An inducible isoform (HO-1) was described in 1968 in the rat and a constitutive isoform (HO-2) was discovered in rat liver in 1986.[12,147,148] The catalytic activity of a third variant (HO-3) seems poor and the physiological relevance of HO-3 remains to be elucidated.[149] Different cell types, species, and individuals are characterized by varying HO expression levels with tissues involved in erythrophagocytosis showing the highest HO activity.[12,134] HO is a tail-anchored enzyme with a hydrophobic sequence stretch embedded in the smooth endoplasmic reticulum (ER) membrane, while the active site is turned towards the cytosol.[150] The enzyme was also detected in the nucleus, the plasma membrane, and the mitochondria, but HO function in these organelles is nebulous.[151–153] Heme

is a regulator of HO-2, which shows poor activity at low heme levels (*cf.* Chapter 2.5). In contrast, HO-1 is active at low heme concentration with rising activity in a heme-dependent manner. Remarkably, maximum HO-2 activity is limited to 10 % of HO-1 activity.[12] HO-1 is rated as promising therapeutic intervention, since the enzyme appears to be of relevance in various pathological conditions and is exquisitely sensitive to all kinds of stimuli, such as hypoxia, heavy metals, H_2O_2, oxidative stress, and heme as such.[141,154–156] Unlike HO-1, HO-2 expression is only induced by a few selected compounds (e.g. opiates, glucocorticoids).[12]

After biosynthesis, heme must be shuttled from the mitochondria to other cellular sites to fulfill its functions and eventually to the cytosol for degradation. It cannot be excluded that synthesized heme intercalates with the mitochondrial membrane, nonetheless an escorted movement via transporters has been proposed.[64] Several proteins that might be involved in intra- and intercellular heme transport have been identified in the last years.[75] Selected representatives will be briefly introduced in the following section.

2.2.2 Intra- and Intercellular Heme Transport

Heme transport and trafficking, related regulatory mechanisms as well as spatio-temporal dynamics remain poorly understood.[75] Only few heme transporters are known to date. A number of examples will be presented hereinafter (Figure 7).

The final step of heme biosynthesis takes place in the mitochondria. Therefore, starting from the mitochondria, heme must be trafficked and compartmentalized in the cell.[92] Feline leukemia virus subgroup C receptor 1b (FLVCR1b), an isoform of the earlier identified plasma membrane heme exporter Feline leukemia virus subgroup C receptor 1a (FLVCR1a), is suggested as a mitochondrial heme exporter, yet it is unknown whether FLVCR1b is located in the inner or outer mitochondrial membrane.[157–159] Due to lipid-like structural features of heme, it is also speculated that mitochondria-associated membranes (MAMs) and mitochondrial-derived vesicles (MDVs) might be involved in heme transport in analogy to lipid transport. MAMs form a connection between the mitochondria and the ER, whereas MDVs are thought to function as transporters from the mitochondria to the peroxisomes and lysosomes (Figure 7). An organelle-directed intracellular heme transport cannot be ruled out, however, there is no experimental proof so far.[75,92]

To attenuate and avert heme-driven cytotoxicity, heme might be loosely associated to proteins in the cytosol that shuttle and/or buffer the porphyrin. Several intracellular heme-binding proteins have been identified, such as glutathione S-transferase (GSH-S-transferase), heme-binding protein 1 (HBP1, SOUL), HBP22, HBP23 (peroxiredoxin-1), fatty acid binding protein (FABP), and glyceraldehyde-3-phosphate dehydrogenase (GAPDH, Figure 7).[75,160–162] Remarkably, the heme-binding affinity of some of these

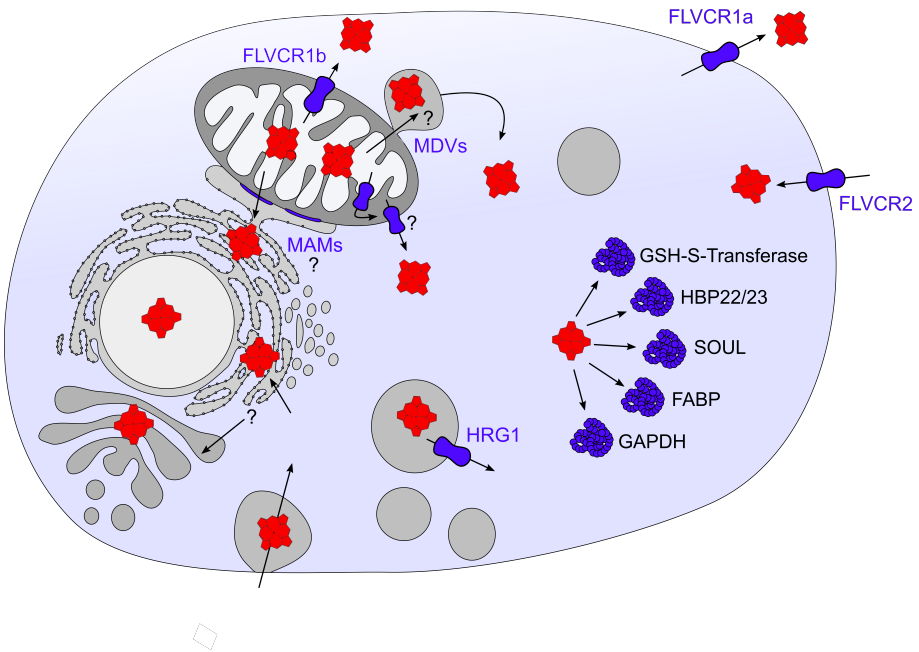

Figure 7. Cellular heme transporters that are currently known or suggested. Full protein names are given in the text. Inspired by Donegan and colleagues.[75] MAMs, Mitochondria-associated membranes; MDVs, mitochondrial-derived vesicles.

proteins is in the nM range, as for example found for HBP22 and HBP23 (26 to 55 nM).[160,161] The metabolic enzyme GAPDH was only recently recognized as an intracellular heme allocator that binds heme via a His53 with a dissociation constant (K_D) of 0.15 µM. It is suggested that a group of proteins within the cell requires GAPDH for heme delivery, whereas another pool obtains heme in a GAPDH-independent fashion.[75,163–165]

Besides intracellular heme transport, some evidence suggest intercellular heme transport. In fact, one third of the dietary iron is absorbed in the form of heme. Therefore, intercellular heme transport as well as cellular heme import is required. The well-known heme scavengers include hemopexin and human serum albumin (HSA), yet, other proteins are thought to facilitate intercellular heme transport (*cf.* Chapter 2.3).[107] Cellular import of heme is also believed to be mediated via transport proteins. The first *bona fide* heme importer, heme-responsive gene 1 protein homolog (HRG1), was identified in *Caenorhabditis elegans* (*C. elegans*), a heme auxotroph and thus a popular model organism to investigate heme trafficking and transport.[166,167] HRG1, a permease, is believed to transport heme from the extracellular space or the endosome-lysosome compartment into the cytoplasm.[107,168] Moreover, HRG1 appears to be involved in heme transport from the phagolysosome to the cytosol during erythrophagocytosis.[106,169] Another protein, heme carrier protein 1 (HCP1), is suggested to function as low-affinity heme importer (Figure 7). Since the protein's

ability to transport folate is at least 10 times higher than to transport heme, the physiological role as heme transporter is controversial.[170–172] Another putative heme importer in mammalian cells is Feline leukemia virus subgroup C cellular receptor family, member 2 (FLVCR2), albeit little is known on the underlying mechanism and the physiological role of this transporter remains to be determined.[107]

Apart from heme importers, a few heme exporters, such as FLVCR1a and ATP-binding cassette super-family G member 2 (ABCG2), have been identified.[157,173] Both proteins appear to export heme more efficiently in the presence of heme scavengers hemopexin or HSA, respectively.[174,175] FLVCR1a is suggested to function as heme exporter during erythrophagocytosis as well as to regulate heme synthesis and heme degradation.[158,176] Different studies indicate that both transporters are not essential for erythropoiesis. Therefore, their physiological function is still a matter of debate and the presence of other heme exporters is assumed.[107] Moreover, multidrug resistance protein 5 (MRP5), which is found in the plasma membrane and endosomal compartments, is suggested to export heme from the cytosol.[177]

Despite the fact that only few heme transporters have been identified and the knowledge gathered is often insufficient, the experimental data obtained in recent years support the concept of a dynamic, exchangeable heme pool. Besides the intracellular labile heme pool, pathological conditions associated with increased breakdown of hemoproteins (e.g. hemolysis) may contribute to the dynamic pool of heme that exhibits alternative functions and affects protein activity. Hemolysis is the most common cause of accelerated hemoprotein breakdown and will thus be explained in more detail in the following chapter.[9,10,95]

2.3 Hemolysis and Heme-Driven Toxicity

Hemolysis, etymologically derived from the ancient Greek words αἷμα (*haíma*, "blood") and λύσις (*lýsis*, "loosening"), describes the lysis of RBCs and the consequent release of their pro-oxidant content, in particular hemoglobin and heme, into the circulation.[84,178,179] Technically, hemolysis takes place at any time since senescent RBCs are continuously removed by the mononuclear phagocyte system (MPS). However, the term hemolysis usually implies a pathophysiological condition if not specified otherwise.[9,10,102] About 10 to 20 % of RBC removal is thought to occur within the circulation.[180] This process is well tolerated by the organism because hemoglobin and heme are sequestered and cleared by an efficient scavenging system of plasma proteins (Figure 8).[9,10,95,181,182] In case of severe hemolysis, the scavenging system can be overwhelmed and cell-free hemoglobin and heme engender inflammation and tissue damage.[183] Hemolysis as such is differentiated into "extravascular hemolysis", which describes the phagocytosis of premature RBCs in the MPS, and "intravascular

hemolysis", which refers to RBC rupture within the circulation.[184,185] Pathological conditions of hereditary, acquired, and iatrogenic nature are associated with hemolysis. Among the causes are mechanical trauma (e.g. vascular alterations, excessive exercise), transfusion reactions, inherited genetic defects (e.g. sickle cell disease (SCD), α- or β-thalassemia), diseases (e.g. malaria infection), bacterial toxins (e.g. hemolysins), ischemia reperfusion, severe sepsis, and autoimmune hemolytic anemias.[18,186–188]

The hemoglobin/heme scavenging system consists of several circulating proteins (Figure 8). Liberated hemoglobin is bound by haptoglobin (estimated K_D of 10^{-15} M), whose plasma levels range from 0.3 to 3 mg/ml.[189] Once the pool of haptoglobin is exhausted, hemoglobin (Fe^{2+}) is oxidized to methemoglobin (Fe^{3+}), which readily releases the heme moiety.[9,10,190] Released heme is scavenged by hemopexin, α_1-microglobulin, HSA, α_1-antitrypsin, α_1-proteinase inhibitor as well as the low-density lipoprotein (LDL) and very low-density lipoprotein (VLDL). Further heme sequestering proteins are likely to be involved, whose nature is yet to be identified.[9,95,182,191–196] It has been suggested that heme is initially bound by LDL and VLDL (K_D 10^{-11} to 10^{-12} M) as well as HSA (K_D 10^{-8} M), before the molecule is transferred to hemopexin. The latter is thought to have the highest heme-binding affinity of any known heme-binding protein ($K_D < 10^{-12}$ M).[9,94,197] Remarkably, LDL and VLDL show faster heme binding kinetics compared to HSA and hemopexin.[191] It is, however, known that heme binding to lipoproteins results in lipid peroxidation and consequently oxidized toxic lipoprotein species. Thus, a quick heme transfer to hemopexin is inevitable to avoid detrimental effects.[9,198] The fact that the HSA plasma concentration is much higher (43 mg/ml) compared to hemopexin (0.6 to 1.2 mg/ml), might explain the initial heme-HSA complex formation.[9] Once heme is bound to hemopexin, it is transported to the liver, absorbed by receptor-mediated endocytosis, and degraded via the HO system.[18,182,198] Noteworthy, binding of neither HSA nor lipoprotein effectively reduces the capability of heme to intercalate into membranes and to act as pro-oxidant, proinflammatory molecule.[95] Even if several hemoglobin/heme scavenging proteins are known, the key players are haptoglobin and hemopexin, respectively, which will be described in more detail henceforth.

Hemoglobin is a tetrameric $(\alpha\beta)_2$ 64 kDa protein present in reduced (Fe^{2+}) form intracellularly. After RBC rupture hemoglobin occurs in a dynamic tetramer-dimer $[(\alpha\beta)_2 - (\alpha\beta)]$ equilibrium intravascularly. The dimer is favored in case of low hemoglobin concentration and ferrous iron (Fe^{2+}). Clearance of cell-free hemoglobin is instantly promoted by haptoglobin.[95] Each haptoglobin molecule binds two hemoglobin dimers (K_D 10^{-15} M) in a non-covalent manner, thereby pushing the intravascular equilibrium of hemoglobin towards dimer formation.[199,200] The formed hemoglobin-haptoglobin complex specifically binds to the cluster of differentiation receptor 163 (CD163) with a K_D of 195 nM on the surface of monocytes and

macrophages.[201,202] Upon internalization the individual parts are degraded by the proteasome and the HO system, respectively. Some studies suggest that CD163-independent elimination of hemoglobin and the haptoglobin-hemoglobin complex is also possible.[95] There are three main haptoglobin phenotypes that are associated with different disease outcomes.[203] Since haptoglobin binding impedes the renal filtration of hemoglobin, it prevents hemoglobin-driven toxicity in the kidneys.[204] The kidney seems to be one of the first targets of free heme and related thereto heme-driven toxicity *in vivo*, although the cause remains to be determined.[9,18]

Heme released from hemoglobin is eventually bound by hemopexin.[9,94,197] The 60 kDa protein consists of two β-propellor domains, resembling two thick discs linked via a 20mer peptide chain in a 90° angle.[192] Upon binding, a stable bis-histidyl complex is formed that is transported to the liver, where it is internalized by receptor-mediated endocytosis.[205] The multi-ligand receptor low-density lipoprotein receptor-related protein 1 (LRP1), alias CD receptor 91 (CD91), was recently discovered as responsible receptor. CD91 is expressed on hepatocytes and macrophages, among others.[206] Internalized heme is degraded via the HO system. Previous studies suggest that hemopexin is secreted back into the plasma upon internalization. Later investigations, however, show lysosomal hemopexin degradation similar to the hemoglobin-haptoglobin clearance system.[10,206,207] Hemopexin is predominantly expressed in the liver, to a lesser extent in the nervous system, and in the kidney.[182]

Hemopexin exhibits a protective role in mouse models and decreased hemopexin levels are associated with various pathological conditions including premature infants, sepsis, severe burns, SCD, and thalassemia.[208–211] Besides heme clearance, a protective effect of hemopexin is attributed to other findings. These include the activation of c-Jun N-terminal kinases (JNKs) and the nuclear factor kappa-light-chain-enhancer (NF-κB), sequestration of CO and NO and thus the inactivation of NOS as well as inhibition of ROS generation.[205,212] It is worth noting that the scavenging proteins do not only mitigate iron-mediated oxidative damage, but reduce host susceptibility to infections by, for example, alleviating the excess of iron for pathogens during hemolysis. The patients concerned often show attenuated immune responses and a concomitant bacterial infection.[20,185] In addition, haptoglobin-hemoglobin- as well as hemopexin-heme-mediated heme degradation might significantly contribute to the iron-recycling machinery.[94]

Haptoglobin and hemopexin have been suggested as promising therapeutics for the treatment of diseases associated with hemolysis. The therapeutic effect of hemopexin is currently tested in pre-clinical trials (e.g. CSL Behring), whereas haptoglobin has been licensed in Japan since 1985 (Japanese Green Cross, now Benesis Corporation) for different conditions (e.g. massive transfusion) that require renal protection from hemoglobin-mediated toxicity. Recent studies suggest that a combined therapy of

haptoglobin and hemopexin might offer synergistic protection.[18,84,95,213,214]

Once the scavengers are exhausted, the deleterious effects of cell-free hemoglobin and heme, both cytotoxic, emerge (Figure 8).[9] For example, severe hemolysis is associated with innate and adaptive immune responses.[215] Cell-free hemoglobin can damage the vascular wall and can overcome the endothelium, which explains hemoglobin occurrence in subendothelial and perivascular spaces as well as the lymph fluid.[213] Heme *per se* is associated with a plethora of negative effects ranging from cell- and tissue-damaging cytotoxicity to its role as alarmin and as potent inflammation trigger (Figure 8).[9,16,213,215] Free heme concentrations of 20 to 350 µM have been reported.[216,217] There is a large body of evidence indicating that the unfettered production of radicals is one of the key mechanisms by which heme-mediated toxicity is driven.[9] The redox-active iron ion of heme enables Fenton chemistry that leads to ROS production and adversely affects cells and tissues. In general, oxidative species cause cellular dysfunction as a consequence of lipid peroxidation, protein peroxidation, and DNA damage.[18,94,218] The reaction of hemoglobin with H_2O_2 yields Fe^{3+}/Fe^{4+}-hemoglobin and reactive radicals. The latter presumably oxidate amino acids in hemoglobin resulting in cross-linking of the protein.[219] Heme can also readily intercalate into cell membranes and other lipid structures due to the molecule's lipophilic nature. In addition, the oxidation of membrane compounds and thus the formation of cytotoxic lipid peroxides are catalyzed by heme. Consequently, membrane permeability is altered, eliciting cell lysis and death. As a result of membrane rupture in combination with ROS formation and concomitant cell damage, heme acts as hemolytic agent, thereby shortening RBC lifespan.[62,94] Heme binding to lipoproteins (e.g. LDL) can induce extensive oxidative modifications of the lipoprotein particles, which subsequently exert severe vascular damage.[213,220] A prominent example is oxidized LDL (LDL_{ox}) that plays a crucial role in the pathogenesis of atherosclerosis.[221] Intracellular, heme causes DNA damage as, for instance, a result of heme-induced DNA nicking followed by DNA degradation (Figure 8).[62,222,223]

The endothelium is the primary tissue compromised by cell-free hemoglobin and heme. Hemolysis directly affects endothelial cells and eventually results in endothelial dysfunction (Figure 8). In chronic hemolytic patients thrombus formation and vaso-occlusion are observed. The effects on endothelial cells are thought to be driven by oxidative stress, inflammatory effects, and reduced NO availability. Activation of the endothelium induced by, for instance, ROS leads to expression of adhesion molecules and consequently to adhesion of RBCs and leukocytes (*cf.* Chapter 2.4.1).[62,84,94,213,215] Extracellular hemoglobin avidly sequesters NO leading to decreased NO availability and eventually NO depletion.[83,224] NO dioxygenation of ferrous hemoglobin (Fe^{2+}) generates nitrate (NO_3^-) and ferric hemoglobin (Fe^{3+}, Figure 8). Moreover, NO can interact directly with the heme iron ion.[95] Both processes

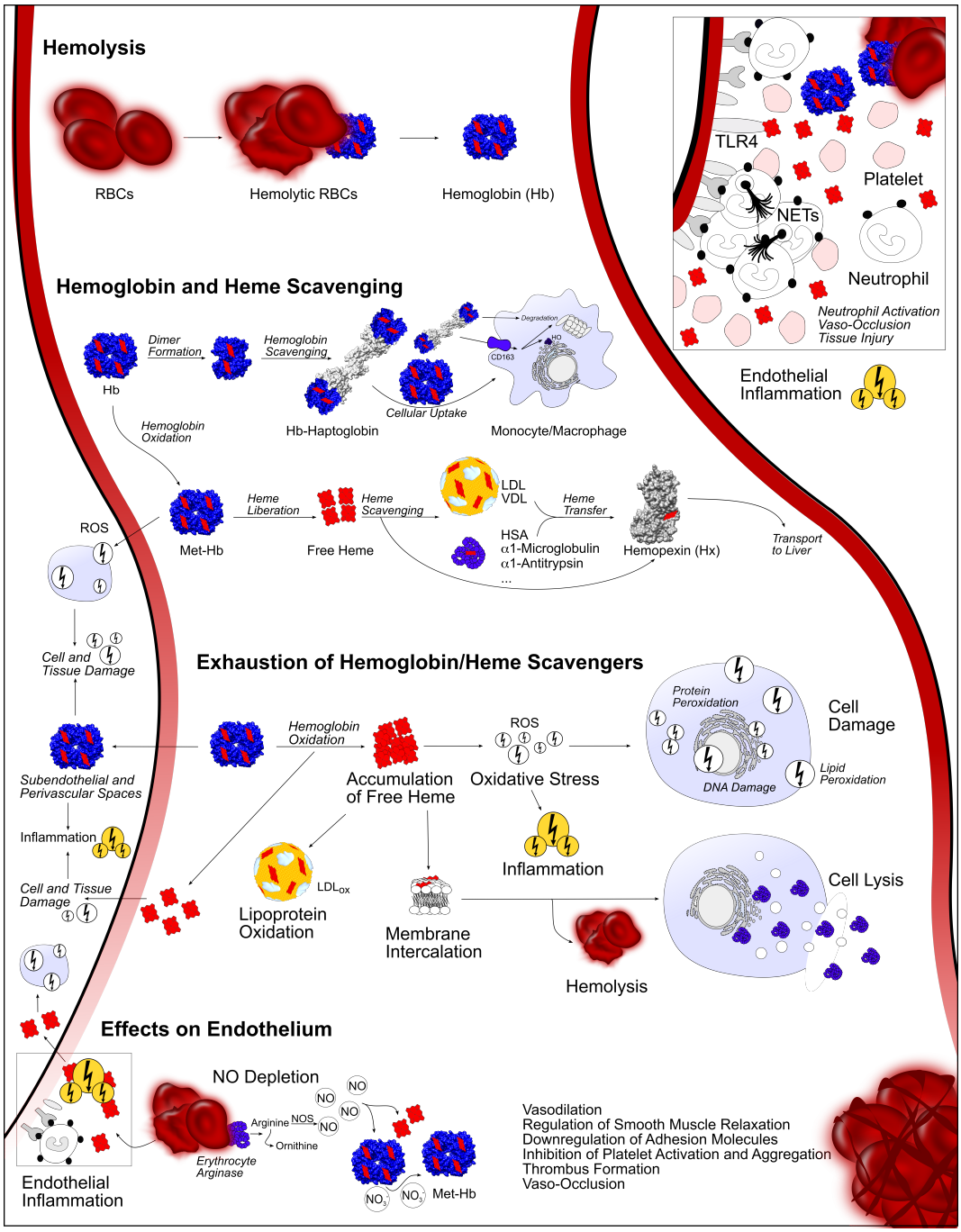

Figure 8. Hemolysis, hemoglobin/heme scavenging, and heme-driven toxicity. Upon hemolysis, cell-free hemoglobin and heme are scavenged by an efficient system of plasma proteins. In case of exhaustion of these proteins, heme-driven toxicity may evoke cell and tissue damage, NO depletion, and inflammation, among other adverse effects. Released heme may trigger endothelial inflammation (box, upper right corner). Moreover, vasodilation, vaso-occlusion, and thrombus formation are associated with elevated heme levels. Abbreviations may be found in the text. Hemoglobin (Hb), PDB 1A3N,[74] Hemopexin (Hx), PDB 1QHU,[192] Haptoglobin (Hp), PDB 4F4O.[200]

result in diminished NO levels, local and systemic, explaining the hypertensive response that often accompanies hemolysis.[95,225] NO is one of the major natural vasodilators. Furthermore, the gas regulates smooth muscle relaxation and vasomotor tone, down-regulates the expression of adhesion molecules, and inhibits the activation and aggregation of platelets.[9,83,84,225] NO diffusing from the endothelium interacts with the heme group of the soluble guanylate cyclase in the smooth muscle and consequently elicits vasodilation.[83,84] Remarkably, Arginase-1, released from ruptured RBCs, reacts with arginine to form ornithine and thereby reduces the substrate availability of the endothelial NOS (*cf.* Chapter 2.1) and as a result NO production.[83]

Heme can also trigger proinflammatory responses and can act as an effector molecule, synergizing for example with toll-like receptor 4 (TLR4) agonists.[226,227] The role of heme in inflammation and as a regulator of proteins is described in chapter 2.4.1 and chapter 2.5, respectively. It is important to note that effects of heme vary in their nature and severity depending on the cell type. Moreover, cells affected by heme may have specific roles for the local and systemic control of heme homeostasis, both in health and disease.[18] Besides hemolysis, other pathological conditions, such as rhabdomyolysis, myolysis, and internal hemorrhage, result in the oxidation of hemoproteins and the subsequent release of heme followed by cell and tissue damage. Whether the scavenging system described is also involved in these conditions remains elusive.[9,18] Due to the omnipresence of the heme molecule in virtually all cells and tissues, elevated heme levels can evoke severe physiological responses. Therefore, heme-associated disorders and diseases are diverse.[9,18,20] A brief overview on associated medical conditions is provided below.

2.4 Heme in Pathophysiology

Various substantial processes are reliant on heme (e.g. oxygen transport, *cf.* Chapter 2.1), which is why disturbances associated with imbalanced heme levels provoke severe pathological consequences (Figure 9). Medical conditions directly or indirectly linked to heme include porphyrias, anemias, hemoglobinopathies (e.g. SCD), brain hemorrhages, infectious diseases (e.g. malaria, leishmaniosis), neurodegenerative diseases (e.g. Parkinson's disease (PD), AD), atherosclerosis, irritant gas inhalation-induced acute lung injury, acute kidney injury, and cancer (e.g. colorectal carcinoma).[15,19,101,228–238] Selected examples of these heme-associated diseases are briefly introduced in the following paragraphs. The experiments performed as part of this work focus on IL-36α and Aβ, which participate in inflammatory processes (IL-36α) and AD (Aβ), respectively. Thus, heme in the context of inflammation and the previously described interaction of heme with Aβ are discussed in sections 2.4.1 and 2.4.2 in more detail.

Since heme is essential for humans, complete failure of heme biosynthesis is lethal.[239] Individuals with partial malfunction of the heme biosynthesis pathway are affected by porphyria or X-linked sideroblastic anemia (XLSA), depending on the affected enzyme and the nature of the dysfunction (*cf.* Chapter 2.2.1).[15,240] Porphyria, a rare panethnic metabolic disorder, can be inherited or acquired and is categorized into hepatic and erythroid porphyria.[15,241] Acquired porphyria is caused by various factors, such as alcohol, smoking, hepatitis C, and HIV infection.[239] The clinical manifestation of the individual porphyria type is usually determined by accumulation of heme precursors.[242] The symptoms of affected patients vary widely with cutaneous photosensitivity and/or neurovisceral disturbances being typical signs.[242] Moreover, porphyria patients can suffer from acute attacks that are often characterized by severe abdominal pain, nausea, vomiting, and constipation.[243] In case of acute attacks heme/hematin infusions and glucose are given as first-in-line treatment in order to downregulate heme synthesis by ALAS inhibition (*cf.* Chapter 2.5).[242,244] No disease-causing mutations of ALAS1 are known in humans, however, a gain of function mutation in ALAS2 has recently been recognized to cause X-linked protoporphyria.[245] In contrast, a loss of function mutation of ALAS2 commonly causes XLSA.[240] Bone marrow sideroblasts, i.e. nucleated erythroblasts characterized by iron accumulation in the mitochondria, are characteristic for XLSA and commonly trigger cytotoxicity and anemia, thereby manifesting clinical symptoms such as fatigue and weakness, among others.[110] The exact molecular mechanism underlying sideroblast formation has not been resolved so far. Protoporphyrin IX deficiency due to diminished ALAS2 activity as well as an increase in mitochondrial iron import have been discussed as causes.[246]

Defects of enzymes responsible for heme degradation and clearance of heme degradation products (e.g. bilirubin) can also trigger a number of diseases.[110,136]

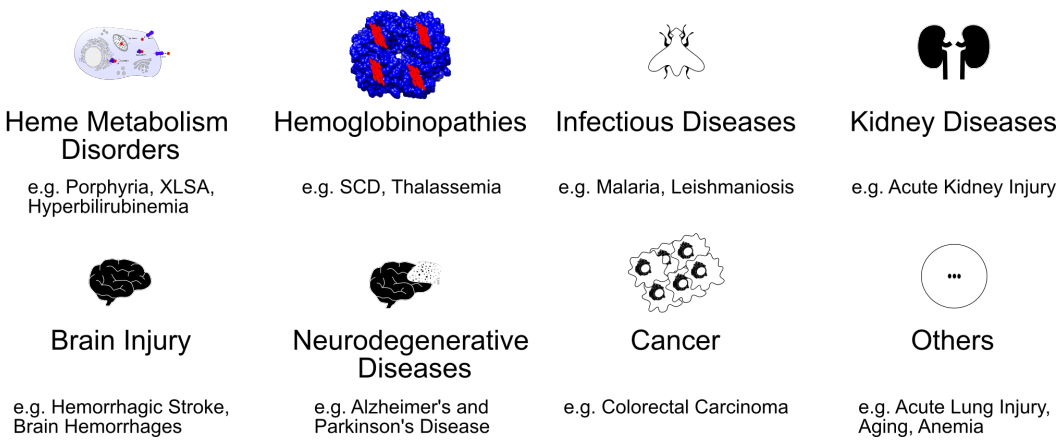

Figure 9. Selection of pathological conditions directly or indirectly associated with heme.[15,19,101,228–238]

The most recognized disease associated with malfunction of heme degradation is hyperbilirubinemia.[110] Hyperbilirubinemia often results in jaundice as a consequence of bilirubin accumulation in the skin. 50 % of all neonates develop jaundice due to low enzymatic activity of UDP-glucuronyl transferase.[110] In adults, hyperbilirubinemia can arise from liver dysfunction, emerging, for instance, from hepatitis infection, tumors or increased hemolysis as observed in hemoglobinopathies (e.g. SCD).[110]

Hemoglobinopathies are inherited defects that hamper the generation of hemoglobin and are thus inevitably linked to heme.[247] Reduced or defective production of both globin chains, i.e. the α- and/or the β-chain, can occur depending on the underlying genetic defect.[247] Hemoglobinopathies are the most common global monogenic disorders, with SCD and thalassemia being the prevalent types.[247,248] According to an estimation of the WHO, more than 330.000 newborns are affected by hemoglobinopathies every year with 83 % sickle cell disorders and 17 % thalassemias.[248] In SCD, a point mutation on chromosome 11 results in the formation of an abnormal β-chain.[9,247,248] RBCs in SCD are characterized by a rigid, sickle-like shape and their susceptibility to lysis.[9,249] Classical SCD symptoms include hemolytic anemia, functional asplenia, episodes of severe pain, and organ damage.[237,248] In thalassemia defects can occur in both globin chains, explaining the classification in α- and β-thalassemia with the latter one having a much higher prevalence.[248] Patients affected by β-thalassemia usually suffer from anemia and require regular blood transfusion and iron-chelation therapy or bone-marrow transplantation. α-Thalassemia is much less common and often results in perinatal death.[247,248] Both SCD and β-thalassemia are usually found in tropical and subtropical areas where they offer a selective advantage to people against potentially lethal malaria infection.[247] Malaria is caused by *Plasmodium* parasites, in particular *Plasmodium falciparum*.[134,232,250] The disease is transmitted from human to human by hematophagous *Anopheles* mosquitoes.[250] Plasmodium infection causes RBC rupture, lysis, and eventually anemia (see below).[134,232] Since malaria parasites require exogenous heme for survival, the parasites digest host RBC hemoglobin.[251] Upon digestion, hemozoin (ferriporphyrin crystals) is generated in order to mitigate the reactivity and toxicity of the digested heme (*cf.* Chapter 2.1).[70,134] Malaria and SCD differ in their etiology, yet both diseases are characterized by RBC rupture and intravascular hemolysis.[16,18,134] SCD and malaria mouse models suggest a role of heme-driven vascular inflammatory reactions in both diseases.[16,18] In addition, hemolytic diseases are suggested to facilitate severe invasive bacterial infection as observed in SCD and malaria patients. Increased nutrient iron-availability upon hemolysis and associated enhanced bacterial outgrowth as well as a direct impact of heme on host immune responses are discussed as causes.[20,185] Hemoglobinopathies, malaria as well as iron deficiency are the most common elicitors for anemia, i.e. the shortage of hemoglobin compared to reference groups depending on age and sex,

among other factors. According to the WHO one third of the global population is affected by anemia, including 800 million women and children.[252] There are three major mechanisms that can cause anemia: ineffective erythropoiesis, hemolysis, and blood loss.[103,252] In children affected by anemia developmental defects are observed, while adults usually show fatigue and poor productivity. Anemia during pregnancy can provoke premature birth, low birth weight as well as maternal, perinatal, and neonatal mortality.[252]

There is raising evidence for a pathological role of heme in the brain.[14,18,19,216] In conditions such as hemorrhagic stroke, intracerebral hemorrhage (ICH), subarachnoid hemorrhage (SAH), and ischemia reperfusion, hemolysis leads to the release of high amounts of cell-free hemoglobin and heme with associated toxicity.[14,19,216,229] In an experimental model of subarachnoid hematoma free heme levels of $> 350\,\mu M$ were observed.[216] Spontaneous ICH causes 15 to 20 % and SAH 7 % of all strokes with the latter having a mortality rate of $> 50\,\%$.[14] Besides acute damage upon cerebral hemolysis, severe damage occurs weeks after the event.[14] This damage is caused by blood products and driven especially by oxidative damage (ROS generation). The observed brain injuries include brain edema, blood-brain barrier disruption, chronic inflammation, and cerebral vasospasm.[14,18,19] Heme has also been proposed to be crucial in the pathogenesis of neurodegenerative diseases, such as PD and AD.[17,19,235,253] Several heme-associated factors and processes are critically discussed in the context of these diseases. Among them are disturbances of the heme metabolism and transport machinery, of heme-regulated processes including ion channel modulation, of the cellular proteostasis, and of mitochondria function as well as heme-driven oxidative stress (*cf.* Chapter 2.4.2).[17,19,235,253]

Besides illness, aging is associated with decreased heme levels as a consequence of reduced ALAS1 activity and increased HO activity.[14] Heme might be the limiting factor in the *de novo* synthesis of CYP_{450}, explaining the higher susceptibility to xenobiotic intoxication and the requirement for reduced drug doses in elderly people. This finding, together with the observation that decreased levels of heme result in premature neuronal cell death, indicates that heme levels are of relevance in the physiological and pathological phenomena of aging.[14,253,254] Apart from the aforementioned medical conditions, heme increasingly emerges as a contributing factor in inflammatory processes.[16] The following section will provide a short description on the current knowledge.

2.4.1 Heme in Inflammation

Heme has an impact on various signaling pathways and immune cells.[9,16,20,215,255] The porphyrin has recently been designated as a 'danger signal' that affects germline encoded pattern recognition receptors (PRRs) and is therefore a 'damage-associated

molecular pattern' (DAMP).[255] DAMPs are biomolecules that initiate noninfectious inflammatory responses in contrast to pathogen-associated molecular patterns (PAMPs) that mediate infectious inflammatory responses. Heme is thought to function as DAMP, whereas hemozoin is discussed as PAMP.[16]

One key element in the defense of viral and bacterial pathogens as well as wound healing is the recruitment of leukocytes to sites of interest.[256] As one of the first in-line defense mechanisms, neutrophils promote inflammation by producing inflammation mediators such as leukotriene B_4 (LTB_4).[16,256] Severe hemolysis triggers tissue damage associated with neutrophil accumulation.[20] Remarkably, heme is able to activate endothelial cells via induction of adhesion molecules such as vascular cell adhesion molecule 1 (VCAM1) and intercellular adhesion molecule 1 (ICAM1) as well as E-selectin and P-selectin (Figure 8).[16,257,258] Furthermore, von Willebrand factor and P-selectin are released from Weibel-Palade bodies after stimulation with heme.[16] Expression of the adhesion molecules allows for neutrophil attachment and migration to the tissue parenchyma once the cells are activated.[16] Heme treatment of human polymorphonuclear neutrophils results in a concentration-dependent oxidative burst, neutrophil activation via protein kinase C (PKC), and ROS formation as well as cytoskeleton reorganization.[259] LTB_4 produced by resident macrophages is suggested to be crucial for neutrophil activation by heme.[260] Heme *per se* can also act as a chemoattractant molecule eliciting neutrophil influx.[259] An unknown G protein-coupled receptor (GPCR) is suggested to be involved in the process since using pertussis toxin, a selective $G\alpha_i$ inhibitor, prevents heme-initiated neutrophil activation.[261] Withal, expression of the proinflammatory cytokine IL-8 is induced upon heme stimulus in the endothelium and in neutrophils.[259,262] Furthermore, spontaneous neutrophil apoptosis is delayed by heme in a HO-1- and ROS-dependent manner *in vitro*, while neutrophil longevity is increased.[263] Neutrophil apoptosis and subsequent phagocytosis are paramount for resolution of inflammation, suggesting that heme aggravates the inflammatory activity of neutrophils.[263,264] The protective effects of heme on neutrophils involve mitogen-activated protein kinases (MAPKs), phosphoinositide 3-kinase (PI_3K) as well as NF-κB activation.[263] The latter proceeds in an NADPH oxidase-dependent manner, since inhibition of extracellular-signaling kinase (ERK), PI_3K or NF-κB leads to deprivation of the anti-apoptotic effect of heme.[263] In humanized SCD mice, heme was shown to trigger the formation of neutrophil extracellular traps (NETs), which are decondensed chromatin fibers associated with granular enzymes that serve as first-line defense against pathogens.[16,265] Besides neutrophils, heme activates macrophages and thereby triggers the production of TNF, keratinocyte-derived chemokine (KC), and IL-1β.[16] In addition, the nucleotide-binding domain and leucine-rich repeat pyrin 3 (NLRP3) containing inflammasome in macrophages is activated by heme via interaction with P2X purinoreceptors.[266]

Consequently, the NLRP3/ASC (Apoptosis-associated speck-like protein containing CARD) inflammasome and the caspase-1 axis are initiated, which results in IL-1β processing and induction in macrophages.[267] Various PAMPs and DAMPs activate TLR4, as for example high-mobility-group-protein B1 (HMGB1), Aβ, and heme.[226,268]

The best-described TLR4 ligand is lipopolysaccharid (LPS) found in the membrane of gram-negative bacteria.[269] Upon extraction of LPS from the membrane, LPS is moved to the heterodimer of TLR4 and the myeloid differentiation factor 2 (MD2) by means of the accessory proteins LPS-binding protein and CD14.[269] Heme interacts with TLR4 and thereby induces myeloid differentiation primary response protein (MyD88) and CD14-dependent responses in mice macrophages.[226,227] Another study showed that TLR4 activation in HEK293 cells is MD2/CD14-dependent at lower heme concentrations (10 μM) and MD2/CD14-independent at higher heme concentrations (50 μM).[227] All studies indicate that the structural properties of heme are crucial for heme-mediated TLR4 activation.[226,227] LPS triggers both MyD88- and TIR-domain-containing adapter-inducing interferon-β (TRIF)-dependent pathways, whereas heme only affects the MyD88-dependent pathway.[16] Activation of MyD88-mediated signaling activates MAPK and NF-κB, which subsequently induces the expression of TNFα and KC.[16,226] Moreover, it was proposed that heme activates endothelial TLR4 followed by Weibel-Palade bodies degranulation, NF-κB activation, and vaso-occlusion.[16] During intracerebral hemorrhage heme is thought to aggravate microglial activation in a TLR4-dependent manner and thus to exacerbate inflammatory injury.[270] Heme can also elicit anti-inflammatory responses.[271] This is at least partially achieved by HO-1 induction and thus by decreased heme concentrations and by increased levels of anti-oxidant heme-degradation products (e.g. CO, bilirubin).[12,272] Moreover, heme was suggested to be a natural negative regulator of the classical complement pathway by directly interacting with the complement component 1q (C1q). Heme binding is also thought to alter the recognition of immunoglobulin G (IgG) and C-reactive protein (CRP).[271] Dipeptiylpeptidase 8 (DPP8), a small peptidase, which is inhibited by heme, is suggested to be involved in T cell activation.[273]

2.4.2 Heme in Alzheimer's Disease

AD was first described as early as 1906 by Alois Alzheimer, yet the underlying etiology has not been clearly identified to date.[275] The last decades of AD research have focused on the 'amyloid hypothesis', a concept regarding Aβ fibrillation and plaque formation as initial event in AD pathogenesis.[276,277] Nowadays, this hypothesis is often considered outdated and AD is recognized as a multifactorial disease.[277–279] According to the World Alzheimer Report 2015, 46.8 million people were affected by dementia in 2015.[280,281] Due to demographic change with an aging society the

numbers are estimated to double by 2035.[280,281] In 2015, 25 to 50 % over age 85, 15 to 20 % over age 75, and 5 to 8 % over age 65 suffered from dementia.[280,281] AD patients show astroglyosis and pervasive neuronal loss, which are associated with episodic memory decline and, in the later course of AD, a progressive loss in cognitive function.[282] Aβ aggregates and fibrils as well as hyper-phosphorylated neurofibrillary tau tangles (NFTs) are major histopathological hallmarks of AD.[14,279] A plurality of physiological abnormalities is observed during disease development including altered cholinergic, dopaminergic, and serotonergic processes as well as oxidative damages based on ROS formation and increased occurrence of metal ions (e.g. copper, iron).[283,284] Since 20 % of the total body dioxygen consumption takes place in the brain, the brain might be particular susceptible to oxidative stress.[281] Another observation made in 90 % of AD-affected people is the progressive destruction of cerebral small blood vessels and microhemorrhages as observed during cerebral amyloid angiopathy (CAA, Figures 10, 11).[285] Moreover, Aβ binds to RBCs and compromises RBC stability.[285] Taken together, these hemolytic events result in micromolar concentrations of free heme.[285] In addition, Aβ was suggested to impair the activity of RBC catalase, thereby increasing H_2O_2 concentrations.[285] Other factors, such as increased cytochrome c release upon neuronal cell damage, have also been proposed to cause accumulation of unbound heme in the brain.[285] In 2006, Atamna and his colleagues discovered peroxidase-active Aβ-heme complexes *in vitro*.[40,101] Other observations have previously linked heme to AD, however, the Aβ-heme interplay represents a strong link between the disease and the porphyrin.[17,253,285–287] The

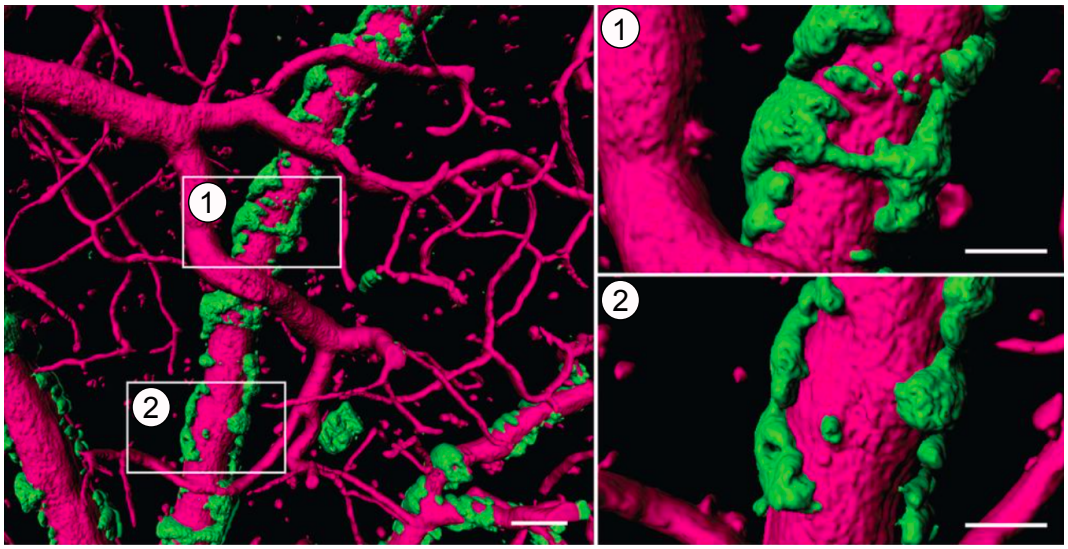

Figure 10. Visualization of vascular amyloid in the brains of mice that overexpress human APP (hAPPJ20 mice, 15 months old). Depicted is the high-resolution 3D rendering generated from *in vivo* multi-photon optical sections (TRITC-Dextran/magenta, vessels and methoxy-XO4/green, Aβ; scale bar 40 µm). Modified from Kimbrough and colleagues.[274]

current knowledge on the complex formed as well as potential physiological effects will be introduced in the following.

Aβ peptides are derived from transmembrane Amyloid-Precursor-Protein (APP). APP can be cleaved by α (cleaves after aa 687), β (cleaves after aa 671), and/or γ (cleaves after aa 711/713) secretase.[288] Among the different cleavage products are Aβ peptides (38 to 43 aa), which are generated by the β- and γ-secretase.[289] Aβ peptides are found in various organelles (e.g. in the multivesicular body and in the mitochondria) as well as in the cytosol and extracellular.[290] The sequence of Aβ is conserved within vertebrates, it is divided into a hydrophilic (Site-H, aa 1 to 17) and a hydrophobic (Site-L, aa 18 to 40/42) part with Site-L being strictly conserved between most vertebrates.[291] Several studies revealed detailed information on the role of distinct residues for the heme-Aβ interaction and the observed pseudo-peroxidase activity.[17,285,291–294] The sequence contains four potential heme coordination sites (His6, Tyr10, His13, His14).[291] Mutational studies implicate heme coordination via His13, which can be replaced by His14 in case of His13 mutation.[17,292] No significant difference of the complex's peroxidase activity was observed for either residue.[292] Arg5 is suggested to facilitate the cleavage of the peroxide O–O bond, while Tyr10 presumably donates an electron.[293,294] When oxidative stress is simulated *in vitro*, Tyr10 is a redox active center that facilitates tyrosine radical formation accompanied by dityrosine linkages.[293,295] Consequently, heme-Aβ complex cross-linking occurs causing increased proteolytic stability, decreased degradation, and further Aβ oligomerization.[295]

Rodents (ro) do not develop AD-like neuropathology despite age-dependent Aβ aggregation. Notably, only three residues of roAβ (Gly5, Phe10, Arg13) deviate from the human sequence (Arg5, Tyr10, His13).[291] roAβ binds heme but the complex formed does not possess any catalytic activity in contrast to the human heme-Aβ complex, supporting a probable role of the three differing residues for AD development.[291] Until now, various studies have come to divergent results and the exact binding stoichiometry, complex structure, and the biochemical mechanisms of the Aβ-heme complex require further analysis.[285]

Several physiological consequences as a result of heme binding to Aβ are discussed.[17,40,101,286,296,297] Among these are, for example, the reduced formation of partially reduced oxygen species (PROS).[17] Moreover, neurotransmitter oxidation is crucial in AD. Serotonin, dopamine, and most likely other compounds serve as substrate for the heme-Aβ complex.[40,286] Furthermore, heme has a stabilizing effect on Aβ and thus decreases aggregation and, at the same time, reduces existing aggregates.[296,297] The intracellular heme pool is thought to be diminished by heme binding to Aβ leading to "functional heme deficiency" and an altered heme metabolism.[101] Increased heme biosynthesis and iron uptake, errors in mitochondrial complex IV as

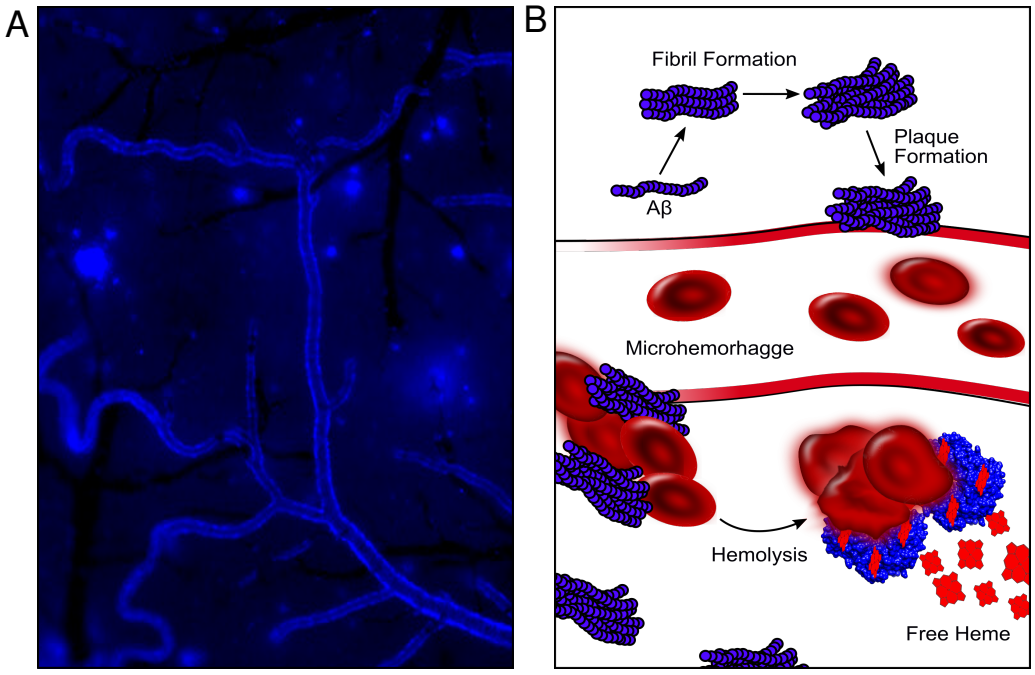

Figure 11. Aβ deposits impair cerebral circulation. (A) Investigation of cerebral amyloid angiopathy (CAA) in a mouse model of AD (Tg2576 mice, 15 months old) revealed substantially progressed CAA deposits in the entire leptomeningeal arteriolar system (congo red derivative fluorescent dye, methoxy-X04, scale bar 50 µM). Modified from Han and colleagues.[298] (B) Aβ plaque formation elicits microhemorrhages as well as RBC rupture followed by the release of free heme.[285]

well as oxidative stress are discussed as corollaries.[40]

Besides heme-Aβ complex formation, further findings link heme to AD.[14,93,299,300] In the postmortem cortex of AD patients the expression of heme biosynthesis enzymes ALAS and PBGD was found to be decreased by 90 % and 60 %, respectively.[14,299] In addition, reduced heme biosynthesis has been associated with neuronal dysfunction.[14] Remarkably, heme is the only source of CO in the brain.[14] Therapeutic strategies aiming at modulation of HO-1 were evaluated as promising in AD and PD models. In fact, upregulation of HO-1 expression is thought to act neuroprotective and anti-inflammatory *in vivo*.[14] Other studies, however, found HO-1 reduction to be neuroprotective, which could be explained by the positive effects of CO.[14,300] Besides, the question remains whether increased HO-1 expression inevitably results in increased HO-1 activity that would consequently lead to a heme phenotype, which is not observed in respective studies.[14,93]

2.5 Heme as Regulator of Mammalian Proteins

For almost 30 years various research groups have contributed to the current knowledge on heme-protein interactions of regulatory nature.[21–24,27–31] Heme-regulated

proteins participate in manifold biological processes, for instance circadian rhythmic, transcription, translation, microRNA (miRNA) processing, protein degradation, ion transport, and signal transduction (Figure 12).[21–24,27–31]

There is no unique mode of action, but the protein's functionality is altered by different mechanisms depending on the individual candidate.[31] In general, transient heme binding can modify a protein's activity and/or stability or result in the formation of a catalytically active heme-peptide/protein complex reminiscent of a heme-peroxidase.[22,29,31,40] Electron-donating side chains of amino acids in HRMs (i.e. His, Cys, Tyr, Met) can serve as heme axial ligand.[28] Besides the coordinating residue, the protein environment is a decisive factor for binding.[26,28,32,79] To allow for a fast association and disassociation of heme, as required for situation-dependent regulation, HRMs have to be readily accessible and are thus predominantly found on the protein's surface.[28,32] Heme-binding affinities in heme-regulated proteins are usually in the range of nanomolar to micromolar.[28,40,273,301,302] The best-known HRM is a cysteine-proline dipeptide motif, designated as CP motif. As the axial ligand, the cysteine residue is essential for binding, while the proline residue alters the structural arrangement of the subsequent amino acids and enhances the binding affinity.[26,28,31,273,303] Other HRMs but the CP motif exist, yet no motif has been found that occurs with equal frequency.[23,54]

The following section (2.5.1) illustrates the fundamental concept of heme-regulation of proteins portrayed by means of selected examples. The focus is on human proteins, although proteins of other organisms, such as yeast transcription factor heme activator protein 1 (HAP1, *Saccharomyces cerevisiae*) and bacterial iron responsive

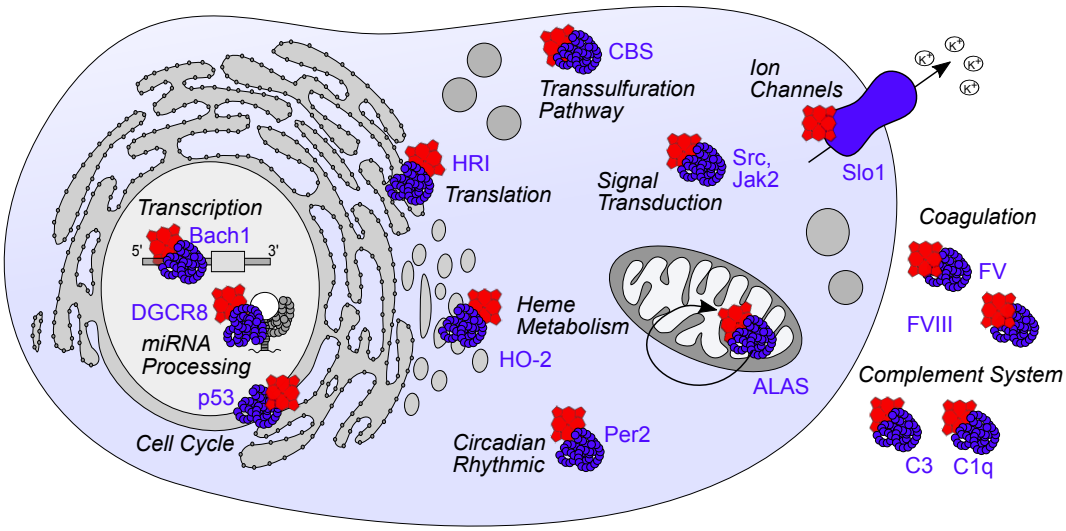

Figure 12. Heme-regulated proteins participate in manifold biological processes. Heme can effect the function and/or stability of intraorganelle, intracellular as well as extracellular proteins.[21–24,27–31]

regulator (Irr, *Bradyrhizobium japonicum*), have contributed tremendously to the present understanding of heme-mediated protein regulation.[304–307] Distinct sequence features and structural aspects of HBMs/HRMs have been identified, yet structural data remain rare.[26,28] A comprehensive systematic peptide-based approach performed by the group of Prof. Diana Imhof (University of Bonn) gave insight into protein sequence requirements, structural features, and eventually allowed for the prediction and verification of previously unknown heme-regulated proteins.[32,34,273,302,303,308,309] Due to the significance of this study for the present work, the findings are summarized in more detail in section 2.5.2.

2.5.1 Heme-Regulated Proteins

The most striking example of a cellular process subject to heme control is the heme metabolism (*cf.* Chapter 2.2.1). In fact, heme synthesis and degradation are governed by heme feedback mechanisms on multiple levels or in other words "heme determines its own fate".[110,111,123,310] The ubiquitously expressed ALAS1 is under negative feedback regulation by heme, whereas ALAS2 is not negatively regulated by heme.[110,310,311] In addition, heme reduces ALAS1 transcription and translation, destabilizes ALAS1 mRNA, and inhibits the transport of the precursor protein to the mitochondria[53,128,129,312–314] The latter results from heme binding to two specific HRMs in the sequence of ALAS1.[314] One of these HRMs is located within the presequence of ALAS1 for mitochondrial translocation and is thus proteolytically cleaved upon mitochondrial import.[314] In the same experimental set-up, mitochondrial transport of ALAS2 does not seem to be impaired by heme despite the fact that the motifs are conserved.[314] In total three CP motifs were identified in ALAS1 and ALAS2.[53,314] Heme binding to the third CP motif, which is present in the mature protein, appears to mediate ALAS1-degradation by the ATP-dependent protease ClpXP (ATP-dependent Clp protease ATP-binding subunit clpX-like, mitochondrial).[315] Moreover, oxidative modifications of ALAS1 are initiated followed by recruitment of another ATP-dependent protease (LONP1).[315] Unlike ALAS1, ALAS2 expression and enzyme activity are tightly linked to iron homeostasis.[316] Thus, iron-free iron regulatory protein 2 (IRP2) binds to an RNA stem-loop element (iron response element, IRE) in the 5'-untranslated region of the ALAS2 mRNA, thereby impeding ALAS2 transcription.[11,316] Bypassing of the IRE-IRP2 system has been discussed to take place during maximal hemoglobinization. One possible explanation is the "kiss and run" hypothesis, which assumes a direct vesicular transport of iron to the mitochondria.[11] IRP2 levels are directly linked to heme levels, because regulatory heme binding to IPR2 mediates oxidation of the protein and thus provokes IRP2 degradation via the ubiquitin-proteasome pathway.[317] Once IRP2 levels decrease, the molecule cannot bind to IREs, thereby allowing for ALAS2 transcription to take

place.[11,111,317] A plethora of other factors are involved in the intricate, accurately planned process of hemoglobinization and RBC differentiation, such as GATA-binding factor 1 (GATA-1), an erythroid-specific transcription factor and major regulator of erythropoiesis which activates ALAS2 expression.[318]

Apart from its own synthesis heme alters its degradation by modulating HO levels and activity.[31,110,123] It is well known that heme *per se* is one of many HO-1 inducers.[154] By the same token, regulatory heme binding to HO-2 is presumed to link the cellular redox state to heme and iron metabolism. Three CP motifs in HO-2 were suggested to act as redox sensor and as such to modulate HO-2 activity.[31,319–321] The sequence of HO-1 does not contain any cysteine residue despite high sequence homology of the two HO isoforms (identical: 55 %, similar: 76 %).[31] Heme binding to the CP motifs is presumed to be independent of the heme interaction with the catalytic core.[31] Some studies indicate that the catalyzed reaction is not directly altered by temporary heme binding, however, further studies are required to clarify the functional nature of the transient heme interactions taking place.[31,320–322] At another level, heme degradation is modulated via transcription regulator protein Bach1 (Bach1), a repressor of oxidative stress-response genes including HO-1.[323] Upon complex formation of Bach1 with small musculoaponeurotic fibrosarcoma (Maf) proteins, the heterodimeric complexes recognize long palindromic DNA sequence stretches designated as Maf recognition elements (MAREs). Binding represses MARE-dependent transcription.[324,325] The interaction of heme and Bach1 obstructs Bach1 binding to MARE sites and facilitates Bach1 export from the nucleus as well as heme-oxidized IRP2 ubiquitin ligase 1 (HOIL1)-mediated ubiquitination and degradation of the protein.[326,327] Thus, high levels of heme enable the expression of Bach1 target genes.[326,327] Besides HO-1, the synthesis of β-globin is subject to Bach-1 control.[328] During erythropoiesis heme regulation of Bach1 guarantees the coordinated generation of the globin chains and heme at transcriptional level.[325] At translational level coordination is assured via heme regulation of eIF2α kinase (HRI) activity, a feedback inhibitor of globin synthesis (Figure 13).[125,329] The inactive precursor of HRI, a homodimer, is believed to bind two heme molecules. Once HRI autophosphorylation occurs, the active autokinase is formed. Upon further HRI autophosphorylation the enzyme's eIF2α activity arises.[125,330,331] Moreover, it was suggested that the activity of fully active HRI can no longer be modulated by heme, but protein degradation occurs instead.[330] In case of high heme levels, two further heme molecules bind to HRI, generating the inactive protein with a total of four heme molecules. Heme also facilitates disulfide formation between HRI subunits.[330] Thus, low heme levels result in HRI activation and subsequently eukaryotic initiation factor (eIF2α) activation via autophosphorylation.[331] eIF2α effectively stops translation initiation.[125]

ALAS1 expression is adjusted in a circadian fashion linking heme biosynthesis

to circadian rhythmic.[332,333] In fact, heme has been indicated to impact several key factors of the circadian machinery (Figure 13).[31,56,333–336] Moreover, circadian oscillations of intracellular heme levels have been described, although the physiological significance of this finding remains to be determined.[335] In humans the suprachiasmatic nucleus, a small region in the hypothalamus, is the central pacemaker of the circadian clock.[337] On the molecular level, core clock proteins act as key factors in maintaining the diurnal cycle via autoregulatory transcription-translation feedback loops.[338] The positive regulators of the loop, circadian locomotor output cycles protein kaput (Clock) and brain and muscle ARNT-like 1 (Bmal1), modulate the expression of the negative regulators period (Per) and cryptochrome (Cry) proteins as well as the nuclear hormone receptors RORα, Rev-Erbα, and Rev-Erbβ.[337,339] A heterodimeric complex of Bmal1 and NPAS2 or Clock activates the transcription of Per, Cry, and Rev-Erb genes via binding to E-box response elements.[337,339] Per and Cry suppress their own transcriptcion by impeding Bmal1-NPAS2/Clock complex formation. Rev-Erbs, on the other hand, repress transcription of Bmal1 and Clock genes.[337,339] Some of the molecular switchboards, which maintain physiological circadian rhythmic, appear to be subject to heme regulation (Figure 13).[31,56,333–336] Heme, independently of its oxidation state (Fe^{2+}, Fe^{3+}), can bind to the PAS domain of Per2 to form a bis-histidyl (Fe^{2+}) or a histidine/cysteine (Fe^{3+}) coordinated complex.[336] In addition, ferric heme but not ferrous heme can bind to a CP motif outside of the PAS domain.[56] Binding results in Per2 degradation independent of the common Casein kinase I epsilon (CKIϵ)-induced degradation.[56] The biological relevance of heme binding to Per2 has been questioned.[336] Furthermore, the DNA-binding capacity of the heme-based sensor NPAS2 was reduced by CO ($> 3\,\mu M$) binding to the heme moiety *in vitro*.[340] Remarkably, NPAS2 mediates ALAS1 transcription, among others.[333] Other proteins that are important in guiding the circadian rhythmic, such as Rev-Erbα and Rev-Erbβ, have also been indicated to be regulated by heme.[31,334,335]

Beyond that, heme is also involved in microRNA (miRNA) processing (Figure 13).[55,341,342] During the maturation of miRNAs a nuclear microprocessor complex consisting of the RNase II Drosha and the DiGeorge critical region 8 (DGCR8) protein is formed that shortens a pri-miRNA into a hairpin-shaped pre-miRNA.[55] Heme was shown to be essential for DGCR8 activity *in vitro*.[342] An inverse CP motif (P351, C352), dimerization, and a tryptophan motif (WW motif) seem to be of importance for the heme-DGCR8 interplay. The dimer is thought to be generated via bis-cysteine complexation of the heme iron by two thiol groups of Cys352 of two DGCR8 molecules.[55,343] A recent study implies that heme binding facilitates bipartite recognition of pri-miRNAs by Drosha and DGCR8, which is thought to assure fidelity of the processing machinery. Furthermore, it was suggested that heme-dependence of pri-miRNA processing varies depending on structural features of

the pri-miRNAs.[344,345]

In addition, the function of ion channels is modulated by heme.[23,54,346–349] One of the most prominent examples is the large-conductance calcium-dependent Slo1 BK channel (Slo1).[54,346] Intracellular heme binding to Slo1 reversibly reduces the frequency of channel opening of Slo1, thus decreasing transmembrane K^+ currents and K^+ influx.[54,346] Furthermore, heme binding to the voltage-gated potassium channel $K_V1.4$ prolongs channel opening by impeding the N-terminal ball-and-chain inactivation mechanism.[347] In cardiac K_{ATP} channels, heme was found to bind to a

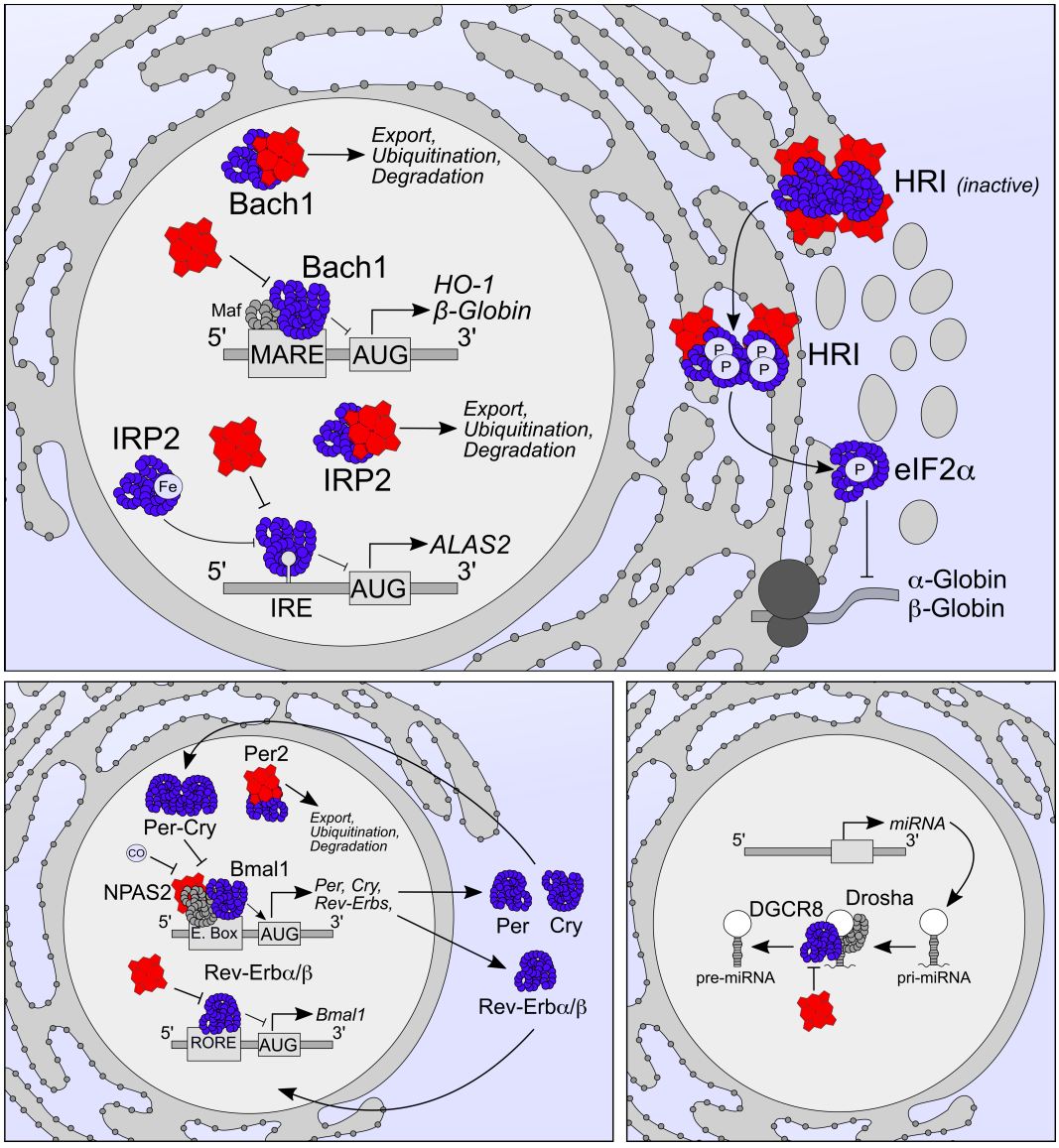

Figure 13. Heme-mediated regulation of proteins exemplified by selected representatives. Among the various proteins that are subject to heme regulation are candidates involved in heme metabolism as well as hemoglobin synthesis (top), circadian rhythmic (lower left), and miRNA processing (lower right). Abbreviations may be found in the text.

$CXXHX_{16}H$ motif in the cytoplasmic regulatory domain, which results in an increased open probability of the channel.[349] The different functional consequences of heme binding to the individual ion channels suggests a more complex role of heme as modulator of ion channels, cellular excitability, and related signaling.[54,346–349]

Another example for a heme-regulated protein is the human cystathionine beta-synthase (CBS).[350–352] CBS catalyzes the generation of cystathionine from homocysteine and serine and is thus essential in homocysteine metabolism.[351] The protein carries a heme group that does not participate in catalysis, however, binding of CO and NO to the heme moiety was found to inhibit the enzyme's activity.[350] In addition, a CP motif present in the intrinsically disordered N-terminus of the protein has been discussed to function as a heme-recruiting motif or as a second, non-canonical heme-binding site.[352]

Furthermore, heme can effect central players of cell growth, proliferation, and survival, which might be of crucial importance for tumor development.[57,353,354] Heme binding to tumor suppressors p53, p63, and p73 is thought to promote nuclear export of the proteins followed by protein degradation. In the event of heme/iron overload associated with ROS formation, the heme interaction with p53 is indicated to further accelerate cell damage.[57,354] This is in agreement with earlier studies, which showed that an artificially induced state of heme deficiency results in increased levels of p53 and cyclin-dependent kinase (CDK) inhibitor p21 in HeLa cells.[353] In the same experimental set-up, heme deficiency was shown to reduce the concentrations of CDK4, CDK1, and cyclin D2. Moreover, the activation of Raf kinase, mitogen-activated protein kinase kinase 1 and 2 (MEK1, MEK2) as well as ERK1 and ERK2, pivotal players of the MAPK signaling pathway, was attenuated. These observations were accompanied by cell growth arrest and apoptosis of the HeLa cells.[353] Heme can also facilitate phosphorylation of the proto-oncogene tyrosine-protein kinase Src (Src), a tyrosine kinase and the first described oncogene that is essentially involved in tumor progression.[355] Phosphorylation of another tyrosine kinase, Janus kinase 2 (JAK2), an enzyme involved in erythropoiesis among many processes, is also modulated by heme.[33,355]

Besides the intracellular and intraorganelle heme-regulated proteins introduced above, extracellular proteins can also be subject to heme regulation as exemplified by complement factor C1q (*cf.* Chapter 2.4.1) and coagulation factors FVIII and FV.[258,271] As a result of heme binding to C1q, activation of the classical complement pathway mediated by CRP and IgG is substantially diminished.[271] At the same time, heme interaction with C3 leads to increased spontaneous hydrolysis followed by overactivation of the alternative complement pathway.[258] During hemolytic events, heme is thought to induce platelet activation and aggregation, yet can also hamper progression of coagulation by inhibiting coagulation factors FVIII and FV, thrombin-

mediated fibrinogen cleavage, and fibrin formation.[258]

The multitude and versatility of the examples presented illustrates how multifarious and sophisticated heme-regulation of proteins is. Due to the intraorganelle as well as intra- and extracellular presence of heme, the porphyrin can intervene in biological processes at various levels.[21–24,27–31] Studies that predict previously unknown heme-regulated proteins based on known HBMs indicate that the activity of a large number of other proteins is regulated by heme.[28,34,79] A peptide-based approach that aimed at predicting heme-regulated proteins is introduced in the following chapter.

2.5.2 Classification and Prediction of Heme-Binding Motifs

Until 2010, sequence features and structural attributes of transient heme-protein interactions were poorly characterized. A global analysis of heme-binding motifs based on peptide sequences was initiated by the group of Prof. Diana Imhof (University of Bonn).[32,34,273,302,303,308,309] The studies aimed at a holistic picture of the molecular basis of regulatory heme-protein interactions. Peptide models had earlier been found to be suitable tools to investigate heme binding.[24,100] The particular advantage of peptides is the comparatively fast and simple examination of a broad spectrum of diverse sequences. The knowledge obtained on peptide level can subsequently be transferred to the protein level.[32,34,273,303,309]

At the outset of the studies, a combinatorial nonapeptide library based on a $X_4(C/H/Y)^0X_4$ motif (X any canonical amino acid and Nle, except for Cys and Met) was designed and synthesized.[34] Histidine, tyrosine, and cysteine were chosen as heme coordination sites, due to their high prevalence in nature. Histidine and tyrosine residues ($\sim$40 % each) dominated over cysteine ($\sim$20 %) as heme axial ligand in the heme-binding sequences. Furthermore, polar amino acids (Glu, Asp, Gln, Asn, Arg, Lys, His, Tyr) and to a lesser extend hydrophobic residues (Leu, Val, Phe, Tyr) at the peptide termini occurred with higher frequency. These amino acids can favor heme binding by interacting with the porphyrin ring. Besides, ancillary heme axial ligands, i.e. histidine and/or tyrosine residues beyond P^0, were found in more than 50 % of the heme-binding peptides.[34] Based on the results HBMs/HRMs were classified by coordinating ligand (His, Tyr, Cys) and presence of additional coordinating residues (His, Tyr, Figure 14). The particular role of CP motifs among HRMs was considered and accounted for two extra classes. Representatives of all eight classes, including library- and literature-derived peptides, were examined intensively using different spectroscopic methods, such as UV/Vis, *resonance* Raman (*r*Raman), *continuous wave* EPR (*cw*EPR), and 2D NMR spectroscopy. Based on expertise gathered from the results of these studies, general conclusions on the molecular basis of heme-peptide/protein complexes could be drawn.[32,34,273,302,303,308,309]

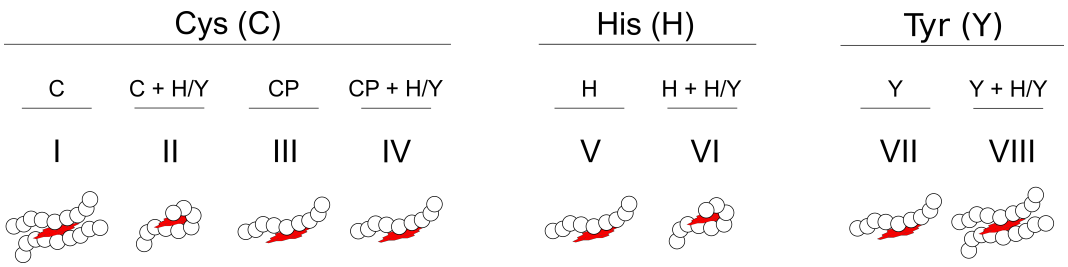

Figure 14. Classification of HBMs/HRMs by coordinating amino acid (His, Tyr, Cys), the presence of additional coordinating residues (His, Tyr), and CP motifs. The cartoons depict structures that were found by NMR spectroscopy of a nonapeptide representative of each class.[32,34,273,302,303,308,309]

The heme-binding mode and heme-binding affinities of all heme-peptide complexes were examined by UV/Vis spectroscopy. Control peptides (e.g. $A_4C^0A_4$ or $A_4C^0P^1A_3$) verified that the sole presence of a coordinating residue is not sufficient for heme binding to occur.[34,99,273,303] For classes I to IV, i.e. cysteine-based peptides, moderate binding affinities with dissociation constants (K_Ds) ranging from $0.40 \pm 0.19\,\mu M$ to $6.36 \pm 2.61\,\mu M$ were determined.[273,303] NMR spectroscopy revealed that CP-based peptides featured a more defined backbone structure than cysteine-only peptides and heme binding increased peptide rigidity. Moreover, the proline residue introduced a peptide bend, causing a turn of the following amino acids away from the porphyrin ring.[273,303] For classes V to VIII, i.e. tyrosine- and histidine-based peptides, no saturation was achieved in the UV/Vis experiments for several peptide-heme complexes, thereby impeding the calculation of K_D values. For the other representatives K_D values ranged from $0.24 \pm 0.17\,\mu M$ to $6.25 \pm 1.44\,\mu M$.[309] The UV/Vis differential spectra of individual complexes (class I to VIII) deviated in intensity, curve shape, and wavelength of maxima, indicating the presence of diverging binding modes. A UV shift to $\sim 370\,nm$ was primarily observed for penta-coordinated heme binding via CP motifs as confirmed by *r*Raman, *cw*EPR, and 2D NMR spectroscopy. A shift to ~ 420 to $430\,nm$ appeared for penta- and hexa-coordinated complexes. Tyrosine-based peptide-heme complexes predominantly emerged in a penta-coordinated fashion, whereas histidine-based peptides formed hexa-coordinated complexes.[309] Hexa-coordinated complexes can form in a sandwich-like conformation (two coordination sites of different peptides) or in a loop-like ('clamp-like') formation (two coordination sites of one peptide, Figure 14). The latter requires a minimal distance of the coordinating residues of two amino acids (e.g. HXXXC).[32,34,273,302,303,308,309]

A global analysis of the investigated peptide sequences suggested that the occurrence of hydrophobic and aromatic residues as well as a positive net charge of the sequence favor heme binding, whereas a negative net charge impairs binding.[34,273,303,308,309] Based on known and identified HBMs, consensus sequences for

the individual coordinating residues were generated and screened against a protein database (ScanProsite, ExPASy Proteomics server). This search revealed numerous potential HBMs in bacterial and human proteins. Besides the motif's primary sequence composition, surface exposure of the motifs was taken into account when protein structures were available. By means of this approach, heme binding to and a functional impact on several bacterial (ferrous iron transport protein B (FeoB), chloramphenicol-acetyltransferase, hemolysin C) and human proteins (DPP8) was proposed and verified.[273,302,303,308,309] Nowadays, an algorithm (SeqD-HBM) offers the computational evaluation of potential HBMs based on the results of the outlined study.[32] In the context of these examinations a potential CP motif (SEGGCPLIL) in the human cytokine IL-36α was identified. Heme binding to the nonapeptide motif in a penta-coordinated fashion was confirmed by UV/Vis spectroscopy, *r*Raman, and 2D NMR spectroscopy.[273] Investigating the heme interaction to and a putative functional impact on IL-36α at the protein level is part of this work. Therefore, the following chapter is intended to introduce the IL-36 family with particular focus on the family member IL-36α.

2.6 A Putative Heme-Regulated Protein: Interleukin-36α

In inflammatory diseases cytokines play a major role upon inflammatory, infectious or immunological challenges.[356] A multi-faceted group, the IL-1 cytokines, triggers pleiotropic effects on immune regulation and inflammatory processes of the innate and adaptive immune system.[356–359] Various autoimmune diseases (e.g. multiple sclerosis, Crohn's disease, rheumatoid arthritis (RA)) are associated with IL-1 members. The cytokines are thus considered an attractive therapeutic target.[357,359,360] At present, ten type-1 transmembrane receptors and eleven IL-1 cytokines have been assigned to the IL-1 family. The latter ones presumably have evolved from a common ancestral gene by gene duplications and share between 13 and 52 % sequence homology.[361,362] The members are designated as follows (alternative names are given in brackets): IL-1α, IL-1β, IL-1Ra (antagonist), IL-18, IL-33, IL-36α (IL-1F6), IL-36β (IL-1F8), IL-36γ (IL-1F9), IL-36Ra (IL-1F5, antagonist), IL-37, and IL-38 (IL-1F10, antagonist).[359,363,364]

IL-36 cytokines are mediators of innate and adaptive immune responses.[363,365–369] Signaling of the IL-36 group is strikingly reminiscent of IL-1α and IL-1β.[365] Thus, IL-36 cytokines bind to the IL-36 receptor (IL-36R, interleukin-1 receptor-like 2), whose extracellular ligand binding moieties appear as three Ig-like domains (D1, D2, D3, Figure 15).[365,369] Recruitment of the co-receptor IL-1R accessory protein (IL-1RacP), shared among IL-1, IL-33, and IL-36, is required for signal transduction to proceed.[365,369,370] Intracellulary, IL-1 receptors exhibit Toll interleukin-1 receptor

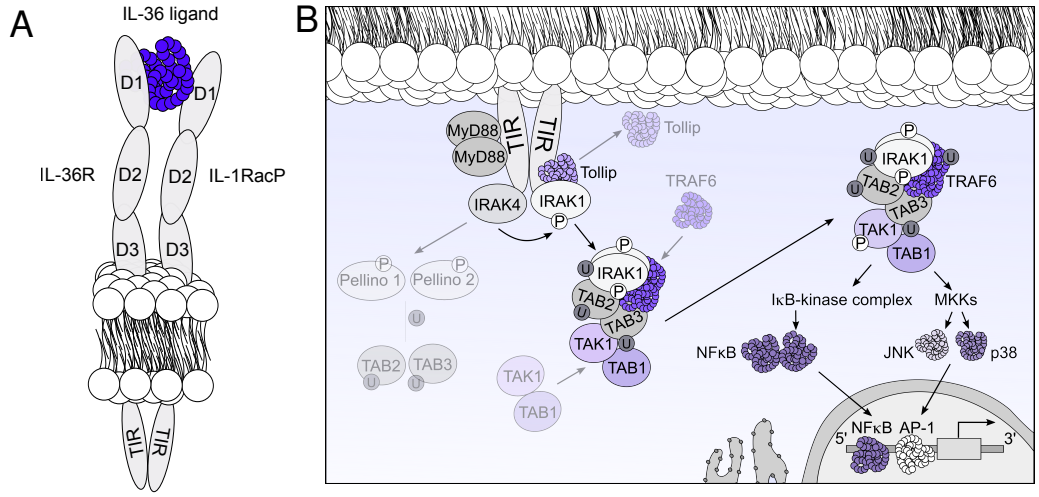

Figure 15. Signaling of IL-36 cytokines. (A) IL-36 ligands bind to a heterodimeric receptor complex, consisting of IL-36R and the accessory protein IL-1RacP. The receptors exhibit IgG (D1-D3) and TIR domains, characteristic for IL-1 family members. (B) Upon receptor binding of an agonistic IL-36 ligand, a complex intracellular signaling cascade is triggered. The portrayed cascade is based on the general findings for IL-1 signaling. Full protein names are given in the text. Inspired by Boraschi and colleagues.[372]

homology regions (TIR domains) that are also found in TLRs.[364,371,372] TIR domains are highly homologous, trigger similar intracellular responses, and are described as alarm receptors of the innate immune system that respond to exogenous (e.g. microbial patterns, TLRs) or endogenous (e.g. IL-1 cytokines, IL-1R) alarm signals.[371,372]

Numerous studies are concerned with the protagonists of the signaling pathway initiated after IL-1 stimulus, a pathway that is complex and multi-layered at every level. The intracellular signaling cascade initiated is shortly introduced in the following, based on a summary of Boraschi *et al.* (Figure 15).[372] Signaling of the juxtamembrane signalosome after generation of the TIR:TIR scaffold starts with a multimeric protein complex, the myddosome.The myddosome is characterized by oligomers of MyD88 and also includes other proteins, such as interleukin-1 receptor associated kinases 2 (IRAK2) and 4 (IRAK4). Upon MyD88-TIR association IRAK4 and subsequently IRAK1 are recruited.[371–373] A conformational change of IRAK1 upon phosphorylation by IRAK4 results in IRAK1 release from the Toll-interacting protein (Tollip) and further phosphorylation. Subsequently, IRAK1 dissociates from MyD88 and is rapidly degraded by the proteasome, thereby restricting its own availability.[371,372,374–376] Indeed, IRAK1 and IRAK4 are able to phosphorylate the ubiquitin ligases pellino 1 and pellino 2, thereby increasing their E3 ubiquitin ligase activity and in turn resulting in TRAF6 and IRAK1 ubiquitination as well as pellino 1 and 2 auto-ubiquitination.[372,377] In the next step, the TNF receptor-associated factor 6 (TRAF6) is recruited to either IRAK1 or IRAK2. Activation of the E3 ubiquitin ligase activity of TRAF6 requires TRAF6 oligomerization.[372,378,379] Consequently, TRAF6 or pellino

1/2 ubiquitinate TAK-1-binding proteins (TABs).[372,380] TABs 1 to 3 are bound to the inactive form of the TGFβ1-activated kinase 1 (TAK1). TAB ubiquitination and a subsequent conformational change liberates TAK1 for auto-phosphorylation and thus activation. By its capacity to phosphorylate several kinases, TAK1 is the first protein of the cascade that amplifies the incoming signal.[372,381] Phosphorylation of the inhibitory κB kinase (IκB) leads to IκB degradation and liberation of an NF-κB dimer. Upon NF-κB release, the transcription factor translocates to the nucleus where it alters gene expression of several genes.[372,382] In addition, mitogen-activated protein kinase (MAPK) phosphorylation results in the activation of downstream effectors, such as activator protein 1 (AP-1) and JNKs.[372] IL-36 cytokines were found to activate various pathways in several cell lines, among them NF-κB, JNK, and/or ERK 1/2. These cellular signals mediate gene expression of growth factors, cytokines, and cytokine receptors, among others.[363,366,369,370,383] In general, the IL-36 stimulus initiates proinflammatory responses via induction of inflammatory mediators such as IL-6 and IL-8.[363]

IL-36 signaling is diminished by binding of IL-36Ra to IL-36R which impedes IL-1RacP recruitment.[366] This mechanism appears to be analogue to IL-1Ra, the natural antagonist of IL-1α and IL-1β. Besides IL-36Ra, IL-38 has also been shown to bind to the IL-36 signaling complex.[384] A direct comparison of the two proteins revealed similar biological responses, however, IL-36Ra is slightly more effective as an IL-36R antagonist. The same study suggested a partial receptor antagonist function of IL-38 and IL-36Ra as well as a potential agonistic function of both proteins at higher concentrations[384] In 2014, the crystal structure of IL-36γ was published.[385] IL-36γ exhibits the characteristic structure of IL-1 cytokines with 12 β-sheets connected via 11 loops that are arranged in a so-called β-trefoil structure.[385] Computational modeling of IL-36γ into the ternary signaling complex revealed an interaction mode known from other IL-1 cytokines, with a direct interplay of the β4/5 and the β11/12 loop with IL-1RacP.[366,385]

IL-36 ligand expression is restricted to selected cell types, whereas its common receptor is more widely expressed. Most predominantly, IL-36 cytokines are expressed in the skin and other epithelial tissues as well as in the esophagus, the lung, the gut, and the brain.[363,366,369] Different cell types are responsible for IL-36 expression including keratinocytes and monocytes/macrophages.[386] The cytokines presumably act extracellularly. Yet, secretion cannot take place via the conventional endoplasmic reticulum/Golgi secretory pathway since, similar to IL-1β, the proteins lack a classical signal sequence.[358] All IL-36 cytokines, like other IL-1 family members, require N-terminal processing to achieve their (full) biological potential.[369,387–389] Artificial truncation of the IL-36 agonistic ligands as part of a deletion analysis increases the biological activity dramatically (1500 to 8000 times), which is accompanied by a rise

in binding affinity of ligand binding to IL-36R (full-length: ∼92-762 nM, truncated: ∼0.007-0.147 nM).[387] Extracellular neutrophil-derived proteases have recently been suggested to be key modulators of IL-1 biological activity.[388,389] These proteases can have activating or inhibiting effects on individual cytokines in the extracellular space. Here, their main function as anti-microbial effectors is only poorly present compared to the function as IL-1-processing enzymes.[389] Henry and colleagues identified cathepsin G, elastase, and proteinase-3, the major neutrophil-derived granule proteases, as IL-36-processing enzymes, which increase IL-36 biological activity ∼500-fold.[388] Different proteases are responsible for the individual members: Cathepsin G and elastase cleave IL-36α after residue Lys3 or Ala4, respectively, Cathepsin G and proteinase-3 truncate IL-36β after Arg5, while IL-36γ is presumably processed via elastase and proteinase-3 after the Val15 residue.[388,389] Small molecule and peptide inhibitors of cathepsin and elastase were suggested as potential future therapeutics of IL-36 activity in inflammatory diseases.[390,391]

IL-36 cytokines have been implicated in autoimmune diseases, especially in skin associated pathological states such as psoriasis, in pulmonary pathologies, and in RA.[363,365,368,369] Patients affected by psoriasis show characteristic plaques, i.e. red, irritated, and flaky skin areas.[392] The pathogenesis of psoriasis remains opaque although intensively investigated. Besides the complex underlying etiology, the multi-factorial causes (e.g. genetic, environmental, immune factors) hamper enlightenment. Psoriasis is frequently accompanied by far-reaching systemic effects, among them cardiovascular comorbidities.[393] Increased IL-1α, IL-1β, and IL-36 transcript levels have been found in lesional psoriasis skin compared to healthy people.[365,369,383,394] In addition, the IL-36 expression correlates positively with levels of phosphorylated p38 and NF-κB, thus strongly suggesting a link between IL-36 expression and p38 MAPK and NF-κB signaling pathways.[394] Treatment with etanercept (TNF inhibitor) significantly reduces IL-36 as well as IL-1α and IL-1β levels in patients, accompanied by a general improvement of the disease state.[395] A particular aggressive, debilitating morbid, potentially lethal form of psoriasis is general pustular psoriasis (GPP).[365,369,396] GPP is characterized by overexpression of many inflammation mediators including the IL-36 ligands.[397] In addition, hypomorphic mutations in the gene *IL-36RN* encoding for IL-36Ra result in frameshift mutations, amino acid substitution or the introduction of a premature stop codon provoking a misfolded, less stable and/or poorly expressed IL-36Ra protein as was found in several GPP patients.[398] It has been proposed to denote this particular form of IL-36Ra scarcity as DITRA ('deficiency of interleukin thirty-six-receptor antagonist').[396] Potentially pathogenic IL-36Ra mutations were found in healthy individuals, too, and the underlying nature of the disease might be more complex, possibly including causative environmental factors.[399]

From 6 % to 20 % of psoriasis patients develop psoriatic arthritis (PsA).[368] IL-36

family members have been found in the synovial membrane of PsA and RA patients.[369] Remarkably, the expression of IL-36α is elevated in the synovial tissue of PsA and RA patients.[400] Furthermore, IL-36α was linked to inflammatory infiltrates and was shown to trigger the expression of IL-6 and IL-8 in synovial fibroblasts (FLS).[400] Treatment with an IL-36 antagonist, however, does not alter the clinical onset and extent of experimental arthritis in RA mouse models. Thus, the role of the IL-36 cytokines in RA remains to be clarified.[368]

The interest in IL-36 cytokines is permanently rising and the cytokines have been implicated in assorted medical conditions. These include allergic contact dermatitis, obesity, systemic lupus erythematosus, pulmonal phenomena (chronic obstructive pulmonary disease, COPD), airway inflammation, mycobacterial, viral and bacterial infection, inflammatory bowel diseases as well as kidney and liver disease.[363,366–369]

3 Motivation

This thesis endeavors to contribute to the understanding of alternative functions of the heme molecule. A pivotal role of the porphyrin is implicated in various medical conditions, among them hemolysis, inflammation, and AD. There is increasing interest in the physiological and pathophysiological effects of biologically available heme, yet there is still a lack of information to draw a comprehensive picture on the underlying molecular processes and mechanisms. This study aims to expand the knowledge on biologically available heme on two levels. On the one hand, there is no established biochemical approach to date that enables quantification of unbound heme in patient samples. A chromogenic test system is to be established and evaluated in view of a potential application as diagnostic tool. On the other hand, missing knowledge on biological effects and mechanisms of action of elevated heme hamper disease understanding as well as adequate treatment. Increased levels of biologically available heme, for example as a consequence of perpetual hemolysis, are associated with inflammatory processes. Recently, the proinflammatory cytokine IL-36α, a member of the IL-1 family, has been suggested to be subject to heme regulation. So far an experimental proof for a heme-IL-36α interplay is missing, it is to be provided as part of this work.

Previous studies demonstrated the possibility to use apo-peroxidases for heme quantification. Based on the finding that Aβ can form catalytically active heme-peptide complexes, the applicability of a set of Aβ-derived and Aβ-independent peptides as well as a suitable assay system are to be tested. Once a convenient peptide candidate is identified, a more detailed analysis of the sequence and structure of the underlying complex is to be performed. Moreover, the general functionality of the assay should be validated using patient samples.

Besides quantification of biologically available heme, identification of potentially heme-regulated proteins is of great interest in order to understand the underlying physiological processes. Over the last few years, numerous intraorganelle, intracellular, and extracellular proteins have been identified whose functions are affected by transient heme binding. Nevertheless, various approaches have indicated a large number of so far unknown heme-regulated proteins. Recent studies revealed a putative heme-

regulatory motif in IL-36α, a cytokine involved in the pathology of RA and psoriasis. In the present thesis, heme binding to the cytokine will be investigated by various spectroscopic methods, including UV/Vis and SPR spectroscopy as well as *resonance* Raman and heteronuclear 3D NMR spectroscopy. The spectroscopic studies aim at providing detailed insight into the structural nature of the suggested interplay. In addition, a possible functional impact of heme on IL-36α will be investigated.

4 Material and Methods

Part of the experiments conducted within the framework of this thesis were performed in cooperation with other laboratories. In an attempt to provide a comprehensive picture of the data, these experimental procedures are epitomized under specification of the respective cooperation partner. Details on these procedures can be found in Wißbrock et al. 2017 and Wißbrock et al. 2019.[99,401] The information on manufacturers of the chemicals, reagents, and solutions that are listed in the following tables, refer to the experiments carried out in the laboratory of Prof. Imhof (University of Bonn). Abbreviations of amino acids and their derivatives follow the revised recommendation of the Nomenclature Committee of IUB (NC-IUB) and the IUPAC-IUB Joint Commission on Biochemical Nomenclature (JCBN).[402] All amino acids were used in their L-configuration.

4.1 Chemicals, Buffers, Solutions, and Media

The pH adjustment of buffers and solutions was done with either 1 M NaOH (Roth) or 1 M HCl (Roth).

Table 1. Chemicals and reagents.

Chemical	Supplier
Solvents	
Aceton	Fisher Scientific
Acetonitrile (*HPLC grade)*	VWR
n-Butanol	Riedel-de Haën
tert-Butanol	Alfa Aesar
Dichloromethane (DCM, *HPLC grade*)	VWR
Diethyl ether	VWR
N,N-Dimethylformamide (DMF, *analytical grade*)	VWR
N,N-Dimethylformamide (DMF, *technical grade*)	VWR
Ethyl acetate	Julius Hoesch
Glacial acetic acid	VWR

Table 1. Chemicals and reagents *(continued)*.

Chemical	Supplier
Hydrochloric acid (HCl, 37 %)	Merck
Isopropanol (*HPLC grade*)	VWR
Methanol (*HPLC grade*)	Fisher Scientific
Phenol	Merck
n-Propanol	Fluka
Pyridine	Alfa Aesar
Trifluoroacetic acid (TFA, Uvasol®, $\geq$ 99.8 %)	Merck
Water (*HPLC grade*)	VWR
Reagents for peptide synthesis	
Acetic anhydride	Fluka
O-(Benzotriazol-1-yl)-*N,N,N',N'*-tetramethyluronium-hexafluorophosphate (HBTU)	Iris Biotech GmbH
N,N-Diisopropylethylamine (DIEA)	Sigma-Aldrich
Ethanedithiol	Sigma-Aldrich
N-Hydroxybenzotriazole (HOBt)	Iris Biotech GmbH
N-Methylimidazole	Fluka
N-methyl-morpholine (NMM)	Sigma-Aldrich
Piperidine	Alfa Aesar
Thioanisole	Alfa Aesar
TFA (95-99 %, *synthesis grade*)	Merck
Amino acid derivatives and resins	
Fmoc-Ala-OH, Fmoc-Arg(Pbf)-OH, Fmoc-Asn(Trt)-OH, Fmoc-Asp(OtBu)-OH, Fmoc-Cys(Trt)-OH, Fmoc-Gln(Trt)-OH, Fmoc-Glu(OtBu)-OH, Fmoc-Gly-OH, Fmoc-His(Trt)-OH, Fmoc-Ile-OH, Fmoc-Leu-OH, Fmoc-Lys(Boc)-OH, Fmoc-Met-OH, Fmoc-Phe-OH, Fmoc-Pro-OH, Fmoc-Ser(tBu)-OH, Fmoc-Thr(tBu)-OH, Fmoc-Trp(Boc)-OH, Fmoc-Tyr(tBu)-OH, Fmoc-Val-OH	ORPEGEN Pharma
Fmoc-Rink amide MBHA resin (0.53 mmol/g)	Iris Biotech GmbH
H-L-Val-2-chlorotrityl resin (0.61 mmol/g)	CBL
Peptide and protein analytics	
Acetic Acid	Sigma Aldrich
Ammoniac (25 %)	Merck
α-Cyano-4-hydroxycinnamic acid	Fluka

Table 1. Chemicals and reagents *(continued).*

Chemical	Supplier
Ethyl acetate	Fluka
Iodoacetamide (IAA)	AppliChem
Ninhydrin	Chemapol
Peptide Calibration Standard	Bruker
Potassium iodide	Laborchemie Apolda
Potassium permanganate ($KMnO_4$)	Fluka
Protein Calibration Standard I	Bruker
Ready to use buffers A–F	Laborservice Onken
Ready to use Reagent R	Laborservice Onken
Sample dilution buffer	Laborservice Onken
TLC plates ADAMANT UV_{254}	Machery-Nagel
o-Tolidine	SERVA
Buffer components	
Ammonium sulfate ($(NH_4)_2SO_4$)	AppliChem
Calcium chloride ($CaCl_2$)	Roth
Citric acid	Fluka
Dipotassium hydrogen phosphate (K_2HPO_4)	Roth
Disodium hydrogen phosphate (Na_2HPO_4)	Roth
Dithiothreitol (DTT)	AppliChem
Ethylenediaminetetraacetic acid (EDTA)	Roth
4-(2-hydroxyethyl)-1-piperazineethanesulfonic acid (Hepes)	Roth
Potassium chloride (KCl)	Roth
Potassium hydrogen phosphate ($KHPO_4$)	Roth
Potassium dihydrogen phosphate (KH_2PO_4)	Roth
Sodium chloride (NaCl)	Roth
Sodium citrate dihydrate	Fluka
Sodium dihydrogen phosphate (NaH_2PO_4)	Roth
Sodium dodecyl sulfate (SDS)	Sigma-Aldrich
Sodium hydroxide (NaOH)	Roth
Sodium hydrogen phosphate ($NaHPO_4$)	Roth
Tricin	AppliChem
Tris(hydroxymethyl)aminomethane (Tris)	Roth
Tris-HCl	Roth

Table 1. Chemicals and reagents *(continued)*.

Chemical	Supplier
Electrophoresis reagents	
Acrylamide, Bisacrylamide	AppliChem
Ammonium persulfate (APS)	AppliChem
Bromophenol blue	Fluka
Coomassie brilliant blue G-250 GelRed	AppliChem
Glutaraldehyde 25 % in water	Merck
Glycerol (water-free, 99 %)	Roth
Glycine	AppliChem
β-Mercaptoethanol (BME)	VWR
Page ruler unstained, Low Range Protein Ladder	Thermo Scientific
Phosphoric acid (85 %)	Fluka
Tetramethylethanediamine (TEMED)	VWR
Proteins	
trInterleukin-36α, CF, $\geq$ 95 %	R&D Systems
trInterleukin-36β, CF, $\geq$ 95 %	R&D Systems
trInterleukin-36γ, CF, $\geq$ 95 %	R&D Systems
Bovine serum albumin (BSA, *Bos taurus*)	Amresco
Low density lipoprotein (LDL, *Homo sapiens*)	Sigma-Aldrich
Lysozyme (*Gallus gallus*)	AppliChem
Thrombin	Sigma-Aldrich
Miscellaneous	
Chloramphenicol	Roth
Isopropyl-β-D-1-thiogalactopyranoside (IPTG)	Sigma-Aldrich
Kanamycin	AppliChem
Lysogeny broth (LB, Lennox) medium	Roth
Biochemical and binding assays	
Hemin	Sigma-Aldrich
Hydrogene peroxide (35 %, H_2O_2)	Merck
Protoporphyrin IX (PPIX)	Frontier Scientific
3‘,3‘,5‘,5‘-Tetramethylbenzidine (TMB)	AppliChem
Thioflavin T (ThT)	Merck
TMB Substrate Kit (Pierce^{TM})	Thermo Scientific

Table 2. Buffers, solutions, and medium.

Buffer	Composition
Recombinant expression	
Dialysis buffer (pH 6.9)[1]	20 mM Tris, 150 mM NaCl, 2 mM DTT
Dialysis buffer (pH 7.4)[2]	50 mM Hepes, 75 mM NaCl, 2 mM DTT
Elution buffer (pH 7.5)[1,2]	50 mM Tris, 300 mM NaCl, 250 mM imidazole, 2 mM BME
Final dialysis buffer, (pH 6.9)[1,2]	20 mM sodium phosphate buffer, 2 mM DTT
Lysis buffer (pH 7.5)[1,2]	50 mM Tris, 300 mM NaCl, 5 mM imidazole, 2 mM BME
SEC buffer (pH 6.9)[1]	10 mM Hepes, 150 mM NaCl, 2 mM BME
SEC buffer (pH 6.9)[2]	20 mM Hepes, 150 mM NaCl, 2 mM BME
Wash buffer (pH 7.5)[1,2]	50 mM Tris, 300 mM NaCl, 10 mM imidazole, 2 mM BME
SDS-PAGE	
Colloidal Coomassie blue staining solution	0.1 % Coomassie brilliant blue G-250, 10 % APS, 10 % phosphoric acid, 20 % methanol
SDS-PAGE running buffer	192 mM glycine, 25 mM Tris, 0.1 % SDS
SDS-PAGE sample buffer (2×, pH 6.8)	150 mM Tris-HCl, 1.2 % (w/v) SDS, 30 % glycerol, 2.15 M BME, 0.0269 mM bromophenol blue
SDS-PAGE tricine cathode buffer	0.1 M tricine, 0.1 M Tris, 0.1 % SDS
Synthesis and analytics	
Matrix solution (MALDI)	α-cyano-4-hydroxycinnamic acid (7 mg/ml) in 50 % acetoniltrile/water with 0.1 % TFA
Reagent K (peptide cleavage)	0.75 g phenol, 0.25 ml ethanedithiol, 0.5 ml thioanisole
o-Tolidine reagent (TLC)	2 parts of saturated *o*-tolidine solution in 2 % glacial acetic acid mixed with 1 part 0.2 % potassium iodide solution
Biochemical and binding assays	
Citrate buffer (pH 5.0)	0.1 M citric acid (pH 5.0), 0.1 M sodium citrate dihydrate
Heme solution	If not stated otherwise, heme was dissolved at 1 mM in 30 mM NaOH and incubated for 30 min in the dark prior to dilution with the respective assay buffer.
Hepes buffer (pH 7.0)	100 mM Hepes
PBS buffer (pH 7.4)	137 mM NaCl, 2.7 mM KCl, 10 mM Na_2HPO_4, 1.8 mM KH_2PO_4
ThT solution (pH 7.4)	0.8 mg ThT/50 ml PBS buffer

[1] Buffer used for the full-length protein.
[2] Buffer used for the truncated protein.

4.2 Solid-Phase Peptide Synthesis (SPPS)

All peptides, except for Aβ40, were synthesized as amides (Fmoc-Rink amide MBHA resin, loading 0.53 mmol/g) using conventional automated Fmoc SPPS. For the synthesis of Aβ40 the initial amino acids Fmoc-Val and Fmoc-Gly were manually introduced onto preloaded H-L-Val-2-chlorotrityl resin (loading 0.61 mmol/g). For manual peptide synthesis the resin was pre-swelled in DMF (20 min) and incubated with a coupling mixture of 0.5 equiv. Fmoc-Val, 4 equiv. HBTU, 4 equiv. HOBt, and 8 equiv. DIEA (in DMF) for 60 min. Following washing of the resin, capping was carried out in a single step using a mixture (100 µl/100 mg resin) of acetic anhydride/N-methylimidazole/DMF (1:2:3, v/v). Subsequent Fmoc deprotection was

Table 3. Protocol of automated SPPS. Volumes are given per 100 mg resin.

Synthesis Step	Action
1st Preparation of the resin	• rinsing with DMF (2500 µl) • rinsing with DCM (1400 µl) • rinsing with DMF (1400 µl) • flushing with air (500 µl) • rinsing with DMF (2500 µl)
2nd Cleavage of the Fmoc group	• 2× 20 % piperidine/DMF (1000 µl), 4 min* • rinsing with DMF (4000 µl) • rinsing with DMF (1400 µl) • flushing with air (300 µl) • 2× rinsing with DMF (2000 µl)
3rd Coupling of amino acids	• coupling: 415 µl HBTU/DMF, 125 µl NMM/DMF (1:1), 10 µl DMF, 420 µl Fmoc-amino acid in DMF, 7 min* • rinsing with DCM (250 µl) • coupling: 415 µl HBTU/DMF, 125 µl NMM/DMF (1:1), 10 µl DMF, 420 µl Fmoc-amino acid in DMF, 8 min* • rinsing with DMF (3000 µl) • rinsing with DMF (1400 µl) • rinsing with DMF (2000 µl)
4th Final Fmoc-cleavage, rinsing of the resin	• 3× Fmoc cleavage with 20 % piperidine/DMF (1000 µl), 10 min each • rinsing with DMF (4000 µl) • rinsing with DMF (1400 µl) • 2× rinsing with DMF (2000 µl) • 4× rinsing with DCM (1400 µl) • 2× flushing with air (4500 µl)

*Reaction times were prolonged after the 8th amino acid.

performed with 20 % piperidine/DMF (1^{st} 5 min, 2^{nd} 15 min). After washing of the resin the following coupling step was accomplished using the same coupling mixture as above with 4 equiv. of Fmoc-Gly instead of 0.5 equiv. Fmoc-Val. After repeating the washing protocol and cleavage of the Fmoc group, the synthesis of Aβ40 was continued automatically as described hereafter. Automated Fmoc SPPS was conducted on an Economy Peptide Synthesizer EPS 221 (Intavis Bioanalytical Instruments AG, Cologne, Germany). For automated SPPS the Fmoc-protected amino acids were dissolved in DMF (0.6 M) and protecting groups were cleaved off by 20 % piperidine/DMF (1^{st} 4 min, 2^{nd} 4 min). 0.6 M HBTU/DMF served as coupling reagent and 50 % NMM/DMF as the base. For conditions of automated SPPS see Table 3. Coupling of all amino acids (steps 2, 3) was performed in a similar manner. Following SPPS the resins were dried *in vacuo*. Consequently, peptide cleavage from the resin and removal of the side chain protecting groups was carried out by treatment of the dry resin with 95 % TFA (1 ml/100 mg resin) and reagent K (150 µl/100 mg resin). The samples were agitated at room temperature for 3 h before the peptides were precipitated in cold diethyl ether. After washing the crude peptides three times with diethyl ether, the peptide-containing pellets were dissolved in 80 % *tert*-butanol and subsequently lyophilized.

4.3 Peptide Purification and Analytics

Semi-preparative HPLC

Peptide purification was accomplished by semi-preparative HPLC on a LC 8A device (Shimadzu, Duisburg, Germany) equipped with a C18 Reversed Phase Eurospher 100 column (250 × 32 mm, 5 µm particle size, 100 Å pore size, KNAUER, Berlin, Germany). Linear elution gradients of solvents A (0.1 % TFA in water) and B (0.1 % TFA in 90 % acetonitrile/water) were employed for peptide elution (Table 4). The flow rate was set to 10 ml/min and the peptides were detected by UV absorbance at 220 nm (A_{220nm}).

Analytical HPLC

Purity of the fractions recovered from semi-preparative HPLC was verified by analytical HPLC using a LC10AT device (Shimadzu, Duisburg, Germany) equipped with a Vydac 218TP54 column (C18 Reversed Phase, 250 × 4.6 mm, 300 Å pore size, 5 µm particle size, Grace Davison Discovery Science, Deerfield, IL, USA). Distinct elution gradients with solvents A (0.1 % TFA in water) and B (0.1 % TFA in acetonitrile) were applied (Table 4). Moreover, the following parameters were employed: flow rate 1 ml/min, detection at A_{220nm}, injection volume 20-400 µl.

LC/ESI Mass Spectrometry

LC/ESI mass spectrometry was carried out on a micrOTOF-Q III instrument (Bruker, Bremen, Germany) coupled to a Dionex UltiMate 3000 LC (Thermo Fisher Scientific GmbH, Dreieich, Germany) in order to confirm peptide identity (Table 4). For liquid chromatography (LC) an EC 100/2 Nucleoshell RP18 column (100×2 mm, 2.7 µm particle size 90 Å pore size) was utilized using 0.1 % acetic acid in water (eluent A) and in acetonitrile (eluent B). 0-60 % eluent B in 12 min with a flow rate of 0.3 ml/min served as gradient. Peptide ionization was achieved by electrospray ionization (ESI). Analysis of the data was conducted by means of the software Data Analysis (version 4.1, Bruker).

Amino Acid Analysis

The peptide content was determined by amino acid analysis (AAA) using an Eppendorf-Biotronik (Hamburg, Germany) Amino Acid Analyzer LC 3000. In advance to the measurements, peptides were hydrolyzed by 6 N HCl at 110 °C for 24 h, evaporated, and the amino acids were subsequently dissolved in sample dilution buffer (Laborservice Onken, Gründau, Germany). Upon chromatographic separation of the amino acids with a cation-exchange column (CK10M, particle size 4 µm, cross linkage 10 %; Mitsubishi Chemical Corporation, Tokyo, Japan), post-column detection at 570 nm and 440 nm was achieved by conversion with ninhydrin reagent. Samples were evaluated in comparison to an amino acid standard (Laborservice Onken, Gründau, Germany) and the calculated peptide contents were subsequently taken into account for concentration determination in the binding studies and the biochemical assays.

Thin-Layer Chromatography

For thin-layer chromatography (TLC) peptides were dissolved in methanol before application onto silica gel plates with a fluorescence indicator (UV_{254}). The following systems were used as mobile phase:

System 1: pyridine/ethyl acetate/glacial acetic acid/water (5:5:1:3, v/v)
System 2: n-butanol/glacial acetic acid/water (48:18:24, v/v)
System 3: 5 % ammonia/isopropanol (3:7, v/v)

Following separation, detection was performed by UV light (254 nm) as well as ninhydrin reagent and heating (0.5 % ninhydrin in aceton). After placing the plates in a chlorine atmosphere for several minutes, they were left on air for complete chlorine evaporation before applying potassium iodide containing *o*-tolidine reagent as second detection agent.

Table 4. Analytical characterization of peptides synthesized in this work.

No.	Sequence	Mass Da[1]	Mass Da[2]	t_R[3]	t_R[4]	$R_{f,1}$[5]	$R_{f,2}$[6]
Aβ40	*see below*[*]	4329.90	4331.55[A]	66.3[D]	22.8[H]	0.58[P]	0.70[Q]
1	AEFRHDSGY	1079.48	540.75[B]	59.2[E]	21.8[I]	0.47[P]	0.20[Q]
2	HDSGYEVHH	1078.46	540.24[B]	50.5[E]	19.6[J]	0.15[P]	0.17[Q]
3	GYEVHHQKL	1108.58	1109.59[A]	61.4[E]	26.7[J]	0.52[P]	0.21[Q]
4	YEVHHQKLV	1150.62	576.32[B]	66.2[E]	26.5[J]	0.52[P]	0.30[Q]
5	RHDSGYEVHH	1235.29	618.29[B]	48.4[F]	23.1[K]	0.10[P]	0.10[Q]
6	DAEFRHDSGYEVHHQKLV	2165.04	2166.36[A]	41.4[F]	21.6[L]	0.22[P]	0.10[Q]
7	AAAAAAAAA	679.18	656.36[x]	48.0[E]	15.0[M]	3.8[6]	-
20	NVNLTSNALLYHYWIAVSHKAPA	2580.36	861.46[C]	65.5[G]	19.1[N]	0.54[R]	0.59[P]
21	NVNLTSNHLLYHYWIAVSAKAPA	2580.36	861.13[C]	60.7[G]	18.4[N]	0.54[R]	0.64[P]
22	NVNLTSNALLYHYWIAVSAKAPA	2514.34	839.46[C]	71.0[G]	20.7[N]	0.56[R]	0.69[P]
23	NVNLTSNHLLYAYWIAVSHKAP	2509.32	837.79[C]	67.3[G]	19.9[N]	0.54[R]	0.63[P]
24	FLFYHSQSG	1083.51	542.77[B]	71.9[E]	20.4 [L]	0.57[R]	0.71[P]
25	FLFYASQSG	1017.49	1018.49[A]	83.3[E]	21.2 [L]	0.66[R]	0.88[P]
26	FLFAHSQSG	991.49	496.75[B]	66.4[E]	17.8 [L]	0.51[R]	0.69[P]
27	FLFAASQSG	925.47	463.74[B]	75.5[E]	19.2 [L]	0.61[R]	0.85[P]
28	SEGGAPLIL	854.49	855.49[A]	65.3[F]	20.6[O]	0.66[R]	0.73[P]
29	SEGGCALIL	860.43	861.43[A]	62.9[F]	21.5[O]	0.57[R]	0.71[P]
30	SEGGAALIL	828.47	829.47[A]	59.7[F]	20.5[O]	0.66[R]	0.73[P]

[*] DAEFRHDSGYEVHHQKLVFFAEDVGSNKGAIIGLMVGGVV

[1] Theoretical molecular mass.

[2] Molecular masses were determined by LC/ESI mass spectrometry as [A][M+H]$^+$, [B][M+2H]$^{2+}$, and [C][M+3H]$^{3+}$. [x]Mass was confirmed as [M+Na]$^+$ by MALDI MS.

[3] Semi-preparative HPLC was performed applying the following gradients: [D]20-70 % eluent B in 120 min, [E]0-50 % eluent B in 120 min, [F]10-60 % eluent B in 120 min, and [G]15-65 % eluent B in 120 min.

[4] For analytical HPLC gradients were chosen as follows: [H]20-60 % eluent B in 40 min, [I]0-30 % eluent B in 30 min, [J]0-40 % eluent B in 40 min, [K]0-50 % eluent B in 50 min, [L]10-50 % eluent B in 40 min, [M]5-55 % eluent B in 60 min, [N]20-50 % eluent B in 30 min, and [O]10-40 % eluent B in 30 min.

[5] TLC analysis was conducted using the following systems as mobile phases: [P]pyridine/acetic ester/acetic acid/water (5:5:1:3, v/v), [Q]25 % ammonia/isopropanol (3:7, v/v), and [R]n-butanol/acetic acid/water (48:18:24, v/v).

[6] TLC of peptide **7** was not successful in any of the applied systems. Thus, the peptide was further characterized by liquid chromatography using an EC 100/2 Nucleoshell RP18 column (100 × 2 mm, 2.7 µm particle size 90 Å pore size) with 0.1 % acetic acid in water (eluent A) and in acetonitrile (eluent B). 0-60 % eluent B in 12 minutes with a flow rate of 0.3 ml/min served as gradient. Retention time is 3.8 min.

4.4 Recombinant Protein Expression

4.4.1 Recombinant Protein Expression of IL-36α and Mutants

To allow for in-depth analysis of the heme interaction with IL-36α, wild-type and mutant IL-36α proteins were recombinantly expressed in *Escherichia coli* (*E. coli*) in cooperation with Dr. Oliver Ohlenschläger (Leibniz Institute on Aging, FLI, Jena, Germany) who also established the required expression protocol. The following mutants were generated as full-length (fl) proteins (aa 1-158) and in their biological active, truncated (tr) form (aa 6-158): Y108S, H109A,C136SP137A, Y108SH109A, Y108SC136SP137A, H109AC136SP137A, and Y108SH109AC136SP137A. Due to the requirement of distinct cleavage sites for thrombin and caspase 3, respectively, the protocol for the full-length proteins differs from the one for the truncated forms. In total, 16 IL-36 proteins were expressed. Caspase 3 was produced in-house at the FLI Jena.

Recombinant Expression of Full-Length IL-36 Proteins

The genes encoding for IL-36α and the protein mutants were inserted into the NdeI/XhoI site of the expression vector pET-28a. Besides the gene of the 158-amino acid protein an N-terminal polyhistidine (His_6) tag and a thrombin cleavage site between the tag and the gene sequence were introduced. Based on this protocol three additional residues (Gly, Ser, His) were N-terminally attached to the full-length IL-36 proteins. After transformation into BL21(DE3) cells (provided in-house, FLI, Jena, Germany), cultures were plated onto kanamycin-containing plates. A single colony was picked and injected into LB medium containing 50 µg/ml kanamycin. Once the optical density at 600 nm (OD_{600}) reached 0.7, the cultures were transferred to 500 ml LB medium. Proteins prepared for NMR studies required nitrogen and carbon labeling, which was achieved by addition of $^{15}NH_4Cl$ and $^{13}C_6$-glucose-containing M9 medium for the primary cultures. Induction of protein expression was achieved by addition of 0.3 mM IPTG for 18 h at 18 °C. Upon cell harvest, cell lysis was performed in lysis buffer utilizing either French press or sonification followed by centrifugation at $10000 \times g$. Ni-NTA agarose resin served for initial purification which was achieved using 10 column volumes of lysis buffer and washing buffer each. After protein elution with 0.25 M imidazole-containing elution buffer, the His_6 tag was cleaved by 5 U thrombin per mg protein at 4 °C overnight. Subsequently, the proteins were concentrated using a 3 kDa Amicon filter (Merck, Darmstadt, Germany) before injection onto a pre-equilibrated 16/60 Hiload S75 size exclusion chromatography column (GE Healthcare Europe GmbH, Freiburg, Germany) in an ÄKTAprime plus (GE Healthcare GmbH, Freiburg, Germany). Pure fractions were combined, concentrated, and dialyzed to

phosphate buffer (final dialysis buffer, pH 6.9). Afterwards, the proteins were either directly used or lyophilized for following experiments.

Recombinant Expression of Truncated IL-36 Proteins

Initial expression steps were similar to full-length IL-36α recombinant protein expression. Instead of a thrombin cleavage site, a caspase 3 cleavage site (DEVD) was inserted into the pET-28a vector. After following the same protocol as before (see above), the tag was cleaved (1 mg caspase 3/40 mg trIL-36α protein) at 4°C overnight in dialysis buffer. Upon an additional Ni-NTA purification step, the cytokines were loaded onto the size exclusion chromatography (SEC) systems previously applied for the full-length protein. Finally, the proteins were dialyzed to phosphate buffer (final dialysis buffer, pH 6.9) and either used directly or lyophilized for later experiments.

4.4.2 SDS-PAGE

Protein purity and identity was confirmed by SDS-PAGE. Resolving gels consisted of 18 % acrylamide/bisacrylamide with 5 % crosslinking dissolved in 0.75 M Tris-HCl (pH 8.4), 0.1 % SDS, 0.1 % APS, and 0.05 % TEMED. Stacking gels comprised 3 % acrylamide/bisacrylamide with 3.3 % crosslinking dissolved in 0.75 M Tris-HCl (pH 8.4), 0.1 % SDS, 0.1 % APS, and 0.1 % TEMED. Samples were mixed 1:1 with SDS-PAGE sample buffer (2×) before application to the gels. Gels ran for 1 h at 45 V and for another 2 to 3 h at 100 V. After gel fixation with 5 % glutaraldehyde for 30 min and washing with water (3× 5 min), samples were stained with colloidal Coomassie blue staining solution over night. Molar masses were determined by comparison with a low range protein ladder (Thermo Fisher Scientific, Dreieich, Germany).

4.4.3 Iodoacetamide Derivatization

To examine the oxidation state of the four cysteine residues in IL-36α, iodoacetamide (IAA), which reacts with free thiol groups, was applied to full-length and truncated IL-36α as follows. 100 µl of IAA in 10 mM phosphate buffer (4 mM) were added to IL-36α (0.05 mM) and gently shaken for 1 h in the dark at room temperature. Samples were subsequently subjected to mass spectrometry.[403]

4.4.4 MALDI Mass Spectrometry

Proteins were dissolved and desalted using C-18 Zip Tip reverse phase chromatography tips (Merck Millipore, Darmstadt, Germany) according to the manufacturer's instructions prior to MALDI analysis. Sample elution from the Zip Tips followed in 10 to 20 µl matrix solution. Subsequently, 2 µl of the eluted solution were spotted onto

the target plate and allowed to dry. Measurements were performed on a Bruker Autoflex III MALDI-TOF/TOF that was calibrated with a Protein Calibration Standard I for proteins up to 20000 Da.

4.5 Binding Assays

4.5.1 UV/Vis Spectroscopy

The heme binding behavior and affinity of various peptides and the IL-36 proteins was investigated by UV/Vis spectroscopy based on a protocol previously established.[34] The heme solution was prepared as described above using Hepes buffer for dilution. Peptides were dissolved at 20 µM in 100 mM Hepes buffer (pH 7.0) and proteins at 5 µM in sodium phosphate buffer (pH 6.9). Subsequently, the solutions were incubated with various heme concentrations (0.4 to 40 µM) under the exclusion of light for 30 min (peptides) or 60 min (proteins), respectively. Measurements were conducted using a Multiskan GO Microplate Spectrophotometer (Thermo Fisher Scientific, Dreieich, Germany). Spectra of isolated individual components (buffer, peptide, heme) were recorded as reference samples. The reference spectra were subtracted from the corresponding spectrum of the heme-peptide/protein complex to create differential spectra. The values of the maximal absorbance difference served for K_D determination by means of an earlier established function that was originally derived from Bogdan and colleagues:[34,404]

$$\Delta A = 0.5 \times \Delta\epsilon \times (C_L + n \times C_P + K_D) - ((C_L + n \times C_P + K_D)^2 - 4 \times C_L \times n \times C_P)^{0.5}.$$

ΔA	Absorbance of the differential spectra at a defined wavelength
C_L	Heme concentration
C_P	Peptide concentration
$\Delta\epsilon$	Difference of the molar extinction coefficients of the complex and heme
K_D	Dissociation constant
n	Possible binding sites of the peptide for heme

Data fitting and K_D calculation were performed using QTiPlot version 0.9.7.8 (Ion Vasilief).

4.5.2 Fluorescence Spectroscopy

IL-36α and trIL-36α (1 µM) were dissolved in sodium phosphate buffer (final dialysis buffer, pH 6.9), whereas control proteins BSA (1 µM) and lysozyme (1 µM) as well as heme were prepared in PBS buffer (pH 7.4). Proteins were incubated for 60 min with

varying heme concentrations (0.1 to 16 µM) under the exclosure of light. Fluorescence intensity was recorded with a fluorescence spectrophotometer FP-8300 (Jasco, Tokyo, Japan) with the following parameters set: excitation at 306 nm, emission at 352 nm, bandwidth 10 nm (extinction) and 20 nm (emission).[302]

4.5.3 Surface Plasmon Resonance Spectroscopy

Heme binding to the commercially available trIL-36 cytokines α, β, γ, full-length IL-36α as well as control proteins BSA and lysozyme was investigated via surface plasmon resonance (SPR) spectroscopy. Measurements were conducted by Biaffin GmbH and Co KG (Kassel, Germany) on a Biacore T200 instrument (GE Healthcare Europe GmbH, Freiburg, Germany) at 25°C. Covalent immobilization of all proteins (Table 5) was carried out by amine coupling on a CM5 sensor chip (GE Healthcare, Solingen, Germany). Depending on the experiment, protein concentration and pH of the acetate buffer varied (Table 5).

Table 5. Immobilization conditions and levels for SPR analysis.

Protein	pH	Concentration [µg/ml]	Immobilization level [RU]
BSA	7.0	2.5	2900
Lysozyme	5.0	2.5	1600
IL-36α	4.0	0.85	1050
trIL-36α	4.0	0.85	1050
trIL-36β	4.0	0.85	937
trIL-36γ	4.0	0.85	320

10 mM Hepes buffer (10 mM Hepes, 150 mM NaCl, 0.05 % Tween 20, pH 7.4) served as running buffer. Proteins were injected on an EDC/NHS activated flow cell unit at 10 µl/ml until the immobilization levels (Table 5) were reached, while an activated/deactivated flow cell served for subtraction of the reference. A series of five consecutive heme injections (0.08 µM, 0.31 µM, 1.25 µM, 5 µM, 20 µM, in running buffer) followed at a flow rate of 30 µl/min using a standard single-cycle kinetics method (Biacore T200 Control Software, GE Healthcare). Surface regeneration was achieved by two injections of 25 mM NaOH/500 mM NaCl. Curves were corrected by subtraction of an injection series of running buffer, which was used for double referencing. A heterogeneous ligand analysis model served for global data fitting.

4.6 Structural Analysis

4.6.1 *Resonance* Raman Spectroscopy

Resonance Raman (*r*Raman) spectroscopy was performed in cooperation with Prof. Dr. Ute Neugebauer (Center for Sepsis Control Care, CSCC, Jena, Germany) using a Horiba Jobin-Yvon LabRam HR 800 Raman spectrometer (Horiba, Kyoto, Japan) connected to a back-illuminated deep-depletion CCD detector (1024 × 256 pixels) cooled by liquid nitrogen. A Coherent Innova 300C ion laser served for excitation of Raman scattering using the krypton line at 413.1 nm. To focus the laser light onto the sample and to collect the 180° backscattered light, the Raman system was attached to an Olympus BX41 upright microscope (Olympus, Tokyo, Japan) with a motorized XY microscope stage and a 20× objective (Olympus UPlanFL N, NA 0.50). The heme solution was prepared using a previously established protocol.[273] Therefore, heme (7.8 mM) was dissolved in 1 M NaOH and incubated for 30 min in the dark. The solution was diluted with water and phosphate buffer (65 mM NaCl, pH 7.0), applied to the lyophilized peptide or protein, and directly neutralized with 1 M HCl to give a final concentration of 400 µM heme and peptide/protein. Incubation followed in the dark at room temperature for 30 min (peptides) and 60 min (proteins), respectively. Samples were centrifuged prior to measurements in order to remove precipitant.

4.6.2 Circular Dichroism Spectroscopy

Circular Dichroism (CD) spectroscopy was performed by Dr. Oliver Ohlenschläger (Leibniz Institute on Ageing, FLI, Jena, Germany) using the CAPITO CD Analysis and Plotting tool as well as the K2D3 algorithm (190 to 240 nm).[405,406]

4.6.3 Nuclear Magnetic Resonance Spectroscopy

Nuclear magnetic resonance (NMR) spectroscopy was conducted by Dr. Oliver Ohlenschläger (Leibniz Institute on Ageing, FLI, Jena, Germany). Bruker Avance III spectrometers (600 and 750 MHz) served for NMR experiments. Proteins were dissolved in phosphate buffer (65 mM NaCl, 5 % D_2O) to give a concentration of 100 µM (trIL-36α) or 140 µM (IL-36α) and incubated with heme or Ga(III)-protoporphyrin IX chloride. [^{1}H, ^{15}N]-HSQC spectra were recorded at 283 K, processed with Topspin (Bruker, Rheinstetten, Germany) and analyzed with XEASY.[407] Upon assignment of the signals, distance constraints were obtained from NOESY spectra (120 ms mixing time). Cross peaks of vicinal and geminal protons served for calibration. Structures (20 %) with the lowest CYANA target functions were chosen as representatives for the NMR solution structure.[408]

Table 6. Structural statistics of the refined NMR solution structure of IL-36α.

Parameter	Value
Total distance restraints	4107
Intra (|i-j|=0)	350
Sequential / short (|i-j|=1)	1158
Medium (1<|i-j|<5)	767
Long range (|i-j|$x \geq 5$)	1832
Hydrogen bond	72
Target function [Å^2]	
After (before) energy minimization	4.13 (4.14)
AMBER physical energies [kcal/mol^{-1}]	
Before energy minimization	-4526 $\pm$ 97
After energy minimization	-5812 $\pm$101
R.M.S.D. [Å] (mean global r.m.s.d. values)	
All heavy atom (residues 10-158)	1.52 $\pm$0.21
Backbone (residues 10-158)	0.74 $\pm$ 0.12
Ramachandran plot [%]	
Residues in most favored regions	69.3
In additionally allowed regions	28.7
In generously allowed regions	1.9
In disallowed regions	0.1

4.6.4 Computational Modeling

Computational Modeling of Heme Binding to Aβ(1-40) and to Peptide 18

Structural modeling was performed by Dr. Oliver Ohlenschläger (Leibniz Institute on Ageing, FLI, Jena, Germany). Details of the applied procedure can be found in Wißbrock et al. 2017.[99] A structure model of Aβ40 was generated based on PDB 1IYT.[409] For structure calculation by CYANA (version 3.97) the angles of the backbone and the side chains were extracted from the PDB structure. Tight angle constraints were determined for residues 8-38 by adding $\pm$ 0.5° to the original angles. The torsion angle of amino acids 1-7 and 39-40 and the side chains of residues expected to be involved in heme binding were not restrained. Since no structure was available for peptide **18** PEP-FOLD, a program that predicts a structure based on the peptide

sequence, was utilized. The best ranked structure was chosen to model heme binding. Heme binding was introduced by 17 additional upper and 13 lower limit distance constraints that defined the metal to Nϵ2 distances and the distance of the porphyrin scaffold. Hδ1/Nδ1 to O2D upper and lower distance limits of 2.0 or 3.0 and 1.8 or 2.8 were applied to consider hydrogen bonding. A ruffled heme (conserved out-of-plane distortion known) residue was used for CYANA structure calculations. Among 100 calculated CYANA structures the best 5 % are depicted (*cf.* Figure 24).

Computational Modeling of IL-36α Protein Mutants

Generation of IL-36α Mutant Structures

Computational modeling of IL-36α and its mutants as well as molecular docking and molecular dynamics (MD) were performed by Ajay Abisheck Paul George (group of Prof. Dr. Diana Imhof, University of Bonn, Germany). The NMR solution structure of wild-type IL-36α was used to generate the structures of the protein mutants using the Mutator plugin of the VMD program (version 1.9.3).[410] At each iteration a single residue was mutated. Whereas serine served to replace tyrosine and cysteine, alanine was chosen as replacement for histidine and proline. The generated structure was energy-minimized by applying a simulated annealing energy-minimization protocol by means of the Yasara molecular modeling and simulation suite (version 18.2.7).[411] Energy minimization of the final mutant structures was performed before they were used for molecular docking and MD simulations.

Molecular Dynamics Simulations

Molecular Dynamics (MD) simulations of IL-36α as well as its seven mutants were conducted utilizing the MD macro in Yasara (Yasara structure version 18.2.7).[302,412] The AMBER99SB-ILDN force field was applied and simulations were run using a 2 fs time step.[413] The AutoSMILES method implemented in Yasara was used to perform force field parameterization of the simulated system. Thereby, assignment of force field parameters to the protoporphyrin by GAFF and AM1-BCC was achieved based on the Fe^{3+} van der Waals (vdW) parameters published by Li and colleagues.[302,414–416] Investigated molecules were placed into a cubic simulation cell, applying a minimal distance of 15 Å from the edge of the box and using a three-point model of water and 0.9 % NaCl.[417] The cut-off for long range was set at 8 Å and periodic boundary conditions were set. The particle-mesh Ewald method was employed to account for long range coulomb interactions.[418] All simulations were conducted in the NPT ensemble at 298 K with the pressure maintained at 1 atm for 200 ns. Molecular graphics and plots were generated by VMD version 1.9.3 and Grace version 5.1.25, respectively.

Molecular Docking Simulations

Yasara and the ensemble docking method were utilized to perform molecular docking simulation for full-length IL-36α as well as its seven mutants.[411,419] Heme (ChemSpider, Royal Society of Chemistry, 16739951) was docked 400 times to a receptor ensemble of 20 high scoring side chain conformations at 298 K that were generated by the software. A total of 8000 runs per docking experiment was conducted. With the exception of H109A, complete search space was applied for docking to all proteins. For H109A the search space was narrowed to a 10 Å radius around H109. Predicted binding energies served to score the results obtained. The final docked complexes were sorted by a clustering method which employs a 5 Å heavy atom RMSD threshold between docked conformations. Subsequently, the top five complexes were selected for further analysis according to the predicted binding energies.

4.7 *In vitro* Assays

4.7.1 Peroxidase Activity Assay

The pseudo-peroxidase activity of various heme-peptide complexes was tested in a TMB/H_2O_2-based chromogenic assay. Peptides (2.1 µM, 4.2 µM, 21 µM, 42 µM) and heme (42 µM) were incubated (1:1) for 30 minutes under light exclosure. TMB (1.66 mM and 163.2 mM) was dissolved in 0.12 N HCl and H_2O_2 (6.5 mM and 163.2 mM) was diluted in either citrate buffer (pH 5) or in PBS buffer (pH 7.4). In addition, a commercially available substrate kit (Thermo Fisher Scientific, Dreieich, Germany) with 1.66 mM TMB and 6.5 mM H_2O_2 was utilized. 10 µl of the sample (buffer, peptide, heme, heme-peptide complex) were added to 200 µl of TMB/H_2O_2 mixture (1:1) in a 96 well plate. TMB oxidation was monitored at 652 nm. All data obtained was evaluated from 100 to 400 s and normalized against the autocatalytic activity of heme only.

4.7.2 Thioflavin Assay

To examine the Aβ40 aggregation potential in the peroxidase assay (see above) Thioflavin (ThT) was used. 22 µl sample (*cf.* Table 7) was added to 1980 µl of ThT solution and vortexed. Subsequently, the fluorescence intensity was recorded with a JASCO FP-8300 fluorescence spectrometer (JASCO Germany GmbH, Gross-Umstadt, Germany) using the following parameters: excitation at 440 nm (slit width 5 nm) and emission at 482 nm (slit width 10 nm).

Table 7. Sample preparation and composition for the ThT assay. Due to fluorescence interferences TMB could not be added (sample 3, 4).

No.	Sample
1	50 μM Aβ (PBS buffer, pH 7.4), 37 °C, 24 h, positive control
2	42 μM Aβ stock solution (PBS buffer, pH 7.4), no incubation
3	42 μM Aβ stock solution (PBS buffer, pH 7.4) added to a mixture of citrate buffer/water to give a concentration of 1 μM
4	42 μM Aβ stock solution (PBS buffer, pH 7.4) incubated with heme (42 μM) for 30 min and added to a mixture of citrate buffer/water to give a concentration of 1 μM

4.7.3 Competition Assay: LDL, Heme, and Aβ

The effect of LDL on the heme-Aβ complex was examined using the peroxidase assay earlier established (*cf.* Chapter 4.7.1, approach II). LDL was dissolved in PBS buffer (pH 7.4) and gently shaken on ice for 24 h, before dilution to 0.44 μM. Concentration determination was conducted by measuring absorbance at 280 nm using 432970 M^{-1} cm^{-1} (ExPASy ScanProsite, without signal peptide) as the molar extinction coefficient. Dilutions of heme and Aβ (44 μM) were prepared in PBS as described above. The three solutions, i.e. LDL, Aβ, and heme, were incubated individually and in varying combinations for 30 min, before addition of the missing compound(s) and immediate application to the peroxidase assay. Due to the addition of a third compound (LDL) the total volume raised to 220 μl. TMB conversion was measured at 652 nm over a period of 15 min.

4.7.4 Cell Tests

The functional impact of heme on trIL-36 proteins was tested on human fibroblast-like synoviocytes (FLS) isolated from knee joints of RA patients. All FLS experiments were performed by Dr. Silke Frey and Dr. Dr. Axel Hueber at the University Hospital Erlangen-Nuremberg (Germany). The local ethics committee approved the research.

Isolation of human FLS

Isolated FLS were stored at 37 °C and 5 % CO_2 in a humidified incubator. Cells were cultured in RPMI and DMEM with 50 U/ml penicillin, 50 μg/ml streptomycin, 0.2 % amphotericin, and 2 % fetal bovine serum at a ratio of 1 to 5. FLS for testing were used at passage levels from 3 to 8.

Stimulation of FLS with trIL-36α and Mutant Proteins

FLS were seeded in a 48 well plate at 100,000 cells/ml in 500 μl culture medium one day before the experiments. Prior to sample application to the cells, trIL-36α proteins

(5.8 nM) were incubated with varying heme concentrations (0.15 µM and 1.5 µM, ratio 1:26 and 1:260) for 60 min under the exclosure of light. Upon incubation, the samples were applied to the cells for either 5 min (analysis of phosphorylation by Western blot) or 24 h (analysis by qRT-PCR, ELISA). For Western blot analysis, samples were loaded onto a reducing 2D gel (10 % SDS polyacrylamide gel) and blotted to a nitrocellulose membrane by a semi-dry blotting technique. 5 % BSA/TBST served as blocking reagent, which was applied for 1 h before the blots were incubated at 4 °C with the respective antibodies (rabbit anti-P-p38, rabbit anti-p38, rabbit anti-GAPDH; Cell Signaling Technology, Danvers, MA, USA) overnight. Following the addition of the secondary antibody (anti-rabbit HRP; Biozol), a Pierce™ ECL Western Blotting Substrate (Thermo Fisher Scientific, Dreieich, Germany) was used for sample detection according to the manufacturer's instruction. In addition, an AlamarBlue assay served for testing cell viability. The experiment was performed according to the manufacturer's instruction (Invitrogen, Carlsbad, CA, USA) and absorbance was recorded at 570 nm and 600 nm.

RNA, cDNA Preparation, and Quantitative RT-PCR

Total RNA from FLS was extracted using peqGold TriFast reagent (Peqlab, Erlangen, Germany) before subsequent first-strand cDNA synthesis using MultiScribe™ MuLV reverse transcriptase (Applied Biosystems, Foster City, CA, USA) according to the manufacturer's instruction. After sample preparation with the SYBR® Select Master Mix (ThermoFisher Scientific, Waltham, MA, USA), quantitative RT-PCR (qRT-PCR) was conducted with an Applied Biosystems 7500 fast-real-time-PCR System (Applied Biosystems, Foster City, CA, USA) to determine relative gene expression. The following primers served for qRT-PCR: GAPDH (fwd 5'-TCCTGTTCGACAGTC-AGCCGC-3', rev 5'-CGCCCAATACGACCAAATCCGT-3'), IL-6 (fwd 5'-AGAGCTGTGCAGATGAGTA-CAA-3', rev 5'-GCGCAGAATGAG-ATGAGTTGTC-3') as well as IL-8 (fwd 5'-AGCACCAG-CCAACTCTCACT-3', rev 5'-CGTTAACTGCATCTGG-CTGA-3'). Samples and the housekeeping gene GAPDH, which functioned as internal control, were tested in duplicates.

Enzyme-linked Immunosorbent Assay (ELISA)

DuoSet ELISA Kits (R&D Systems, Minneapolis, MN, USA) were used for ELISAs of the undiluted supernatant obtained from FLS cell culture according to manufacturer's instructions. The optical density at 450 nm was recorded by a SpectraMax 190 ELISA-Reader (wavelength correction set to 540 nm). Data analysis was performed using Softmax Pro Version 3.0 (both Molecular Devices, Sunnyvale, CA, USA).

4.8 Statistical Analysis, Software, and Bioinformatics

Statistical readout at the University of Erlangen was conducted using Graph Pad Pism 4.00 software (La Jolla, USA). Group differences were considered statistically significant with a p-value less than 0.05. Alignments were carried out using the Clustal Omega webserver. Moreover, the following software was utilized for data evaluation and figure preparation: Microsoft Office programs (Word, Excel, Power Point, all version 16.20), Graph Pad Prism (version 7), Keynote (version 8.2), QTiPlot (version 0.9.7.8), Yasara (version 18.2.7), UCSF Chimera (version 1.13.1), XQuartz (version 2.7.11), and Inkscape (version 0.92.3).

5 Results and Discussion

The results presented in this thesis are based on initial studies performed in a bachelor (2013) and a master thesis (2015).[420,421] To provide a comprehensive description of the results, the findings are reported in their entirety. Moreover, the outcomes of the experiments conducted were summarized in two research articles.[99,401]

5.1 Catalytic Activity of Heme-Peptide Complexes

In 2006, Atamna and colleagues reported on heme binding to Aβ42 and the catalytic activity of the generated heme-Aβ complex (*cf.* Chapter 2.4.2).[40] Several studies suggest that specific residues in Aβ (e.g. Arg5) are crucial for the formation of the catalytically active heme-Aβ complex, yet detailed knowledge is lacking.[17,292–294,422,423] Therefore, one aim of the present work was to further define properties of the heme-Aβ interplay with a focus on specific sequence features and residues. Moreover, the examination of a set of Aβ-independent heme-binding peptides should provide supplemental insight into primary sequence characteristics of catalytically active heme-peptide complexes. In addition to the gain in fundamental knowledge, a heme-peptide complex with high peroxidase activity might be employed in the quantification of biologically available heme in patient samples. This idea is based on the assumption that an apo-peroxidase can bind free and/or labile heme to form the active holoenzmye as was recently shown by different groups.[36,38] Consequently, the level of active holo-peroxidase directly depends on the present concentration of biologically available heme. The method offers two essential advantages. On the one hand, heme concentrations in biological samples are often too low to be quantified by absorbance spectroscopy. The peroxidase activity may be used as signal amplifier and the catalytic activity can readily be analyzed by the conversion of a chromogenic substrate. On the other hand, simple UV/Vis spectroscopy does not allow for differentiation between inert heme in hemoproteins and biologically available heme. In a peroxidase-based system, the monitored substrate conversion exclusively results from the interaction of the apo-peroxidase with the dynamic, exchangeable, non-hemoprotein pool of heme.

Biologically available heme is increasingly discussed in the context of severe diseases. It is essential to quantify heme levels in patient samples in order to collect data that can prospectively be correlated to certain disease states as well as to initiate appropriate therapeutic treatment. First assay systems have been developed in the last years, yet the establishment and optimization of these systems has only just begun. The existing approaches are based on, for instance, genetically encoded fluorescence sensors that are used for intracellular and intraorganelle labile heme quantification or apo-horseradish peroxidase (apo-HRP), which has been applied to test heme levels in cell lysates.[36–39,98] Compared to an apoprotein-based assay, a peptide-based approach is readily manufactured and cost-effective. In an attempt to establish a suitable assay system, heme-binding peptides, including Aβ40, were investigated with regard to their heme-binding behavior and their potential catalytic activity in the following experiments.

5.1.1 Heme Binding to Aβ and Aβ-Derived Peptides

UV/Vis spectroscopy is frequently utilized to investigate heme binding to peptides and proteins.[24,30,34,100,273,303,336] Due to the particular electronic properties of heme and structurally-related molecules, the porphyrin is characterized by a specific absorption spectrum.[424–426] The experimental data and empirical classification of more than forty different porphyrins by Stern and his colleagues enabled M. Gouterman to introduce a four-orbital model for porphyrins in the 1960ies.[425,426] According to the model, each metal porphyrin is characterized by four bands, two so-called B and Q bands each.[425] For heme the intensive B band at around 400 nm, the Soret band, is of special interest.[48] A shift of the Soret band as well as concomitant changes of spectral features upon complex formation of heme with another molecule are frequently used to investigate heme-peptide/protein interactions (*cf.* Chapter 2.5.2).[24,30,34,100,273,303,336] Consequently, heme binding to Aβ40 and six Aβ-derived peptides was investigated by UV/Vis spectroscopy using a previously established experimental set-up.[34,273]

The sequence of Aβ is divided into a hydrophilic part (site-H) comprising residues 1 to 17 and a lipophilic part (site-L) consisting of residues 18 to 40/42 (Figure 16).[291] Two predominant forms of Aβ, Aβ40 and Aβ42, differ in the two C-terminal residues alanine and isoleucine that are absent in Aβ40.[427] Since neither of the two can function as heme axial ligand and all potential heme-coordinating residues are located in the N-terminal site-H of Aβ, a similar heme-binding mode of both Aβ variants is likely. Therefore, and also due to the significantly lower level of aggregation compared to Aβ42, Aβ40 was chosen for the studies performed herein.[428] Four potential heme coordination sites (His6, Tyr10, His13, His14) are present in Aβ. Hence, four nonapeptides (**1-4**) each including one potential heme axial ligand

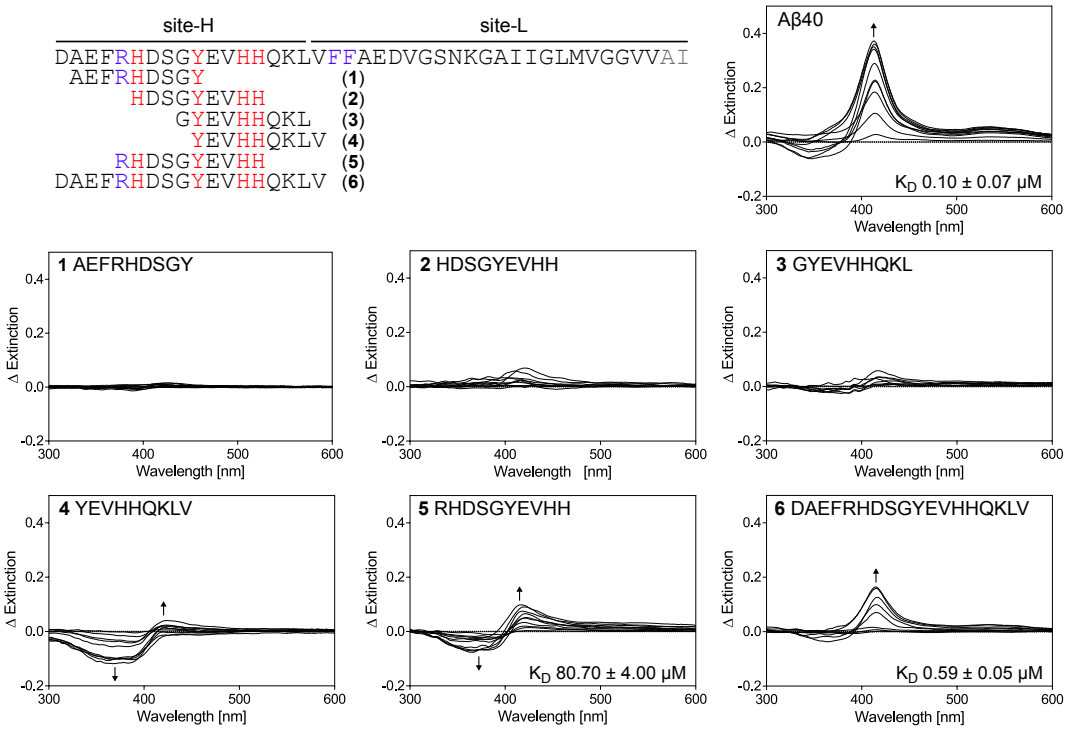

Figure 16. Peptide sequence and UV/Vis differential spectra of (heme-incubated) Aβ and Aβ-derived peptides **1-6**. Coloring of the Aβ sequence is as follows: residues present in Aβ42 in grey, potential heme coordination sites in red, residues that have been suggested to impact heme binding and/or the catalytic activity but cannot function as axial ligand in blue. Modified from Wißbrock et al. 2017.[99]

at central position (P^0), a decapeptide including Arg5 (**5**), and an 18mer peptide (**6**) were synthesized using conventional Fmoc SPPS (Figure 16). The 18mer peptide represents site-H of Aβ, i.e. all four potential heme axial ligands as well as two C-terminal phenylalanines that had earlier been suggested to support heme binding through aromatic π-π interactions.[297]

The following discussion of the results is based on the calculated differential spectra which are received upon subtracting the UV/Vis spectra of the controls (heme, peptide, buffer) from the UV/Vis spectrum of the heme-peptide complex. The differential spectrum of heme-incubated Aβ40 is characterized by a bathochromic shift of the Soret band to ∼414 nm, thereby confirming heme binding to Aβ40 (Figure 16).[99] The calculated K_D value of 0.10 ± 0.07 µM is in good agreement with earlier studies of Atamna and colleagues (K_D 0.14 ± 0.06 µM).[291] According to the best fit possible, at least two heme molecules bind to one molecule of Aβ40. Studies published so far report a 1:1 or 1:2 (Aβ to heme) stoichiometry, yet a recent publication suggests a 2:1 mode based on a computational model.[285,291,297,423] These contradictory results may be due to different experimental set-ups, however, further studies are required to draw an unambiguous conclusion regarding the binding stoichiometry.

For peptide **1** and **2** no change of absorbance was observed, thereby indicating that neither of the two peptides binds heme (Figure 16). Consequently, His6 and Tyr10 are unlikely to function as heme axial ligand in Aβ. In contrast, a maximum at ∼416 nm for peptide **3** and ∼421 nm for peptide **4** suggests heme binding to both sequences. The UV/Vis differential spectra shows only minor changes in absorbance, rendering determination of the dissociation constants impossible. Peptide **5** binds heme with low affinity (K_D 80.70 ± 4.00 µM, λ_{max} ∼421 nm), whereas a K_D value of 0.59 ± 0.05 µM (λ_{max} ∼415 nm) was determined for peptide **6** (Figure 16). It can thus be reasonably assumed that His13 or His14 is the heme-coordinating residue in Aβ, which is consistent with previous findings from other studies.[292] The great difference in affinity between peptides **5**, **6**, and Aβ40 indicates a significant impact of residues 1-4 (DAEF) and/or residues 17/18 (FF) for heme binding to Aβ40. It should be noted that negatively charged residues (Asp1, Glu3) hamper heme binding, whereas aromatic amino acids such as phenylalanine (Phe3, Phe17, Phe18) can support the interaction (e.g. by π-stacking).[297,303,309] Peptides **2** and **5** only differ in the N-terminal arginine present in decapeptide **5**. Thus, the divergent differential spectra suggest that Arg5 in Aβ40 is important for heme binding to the peptide. In contrast to Aβ40, Aβ-derived peptides **5** and **6** bind heme in equimolar quantities. This finding indicates that the interaction of a second heme molecule with Aβ40 is realized by the peptide's site-L, despite the absence of a heme-coordinating residue.[99]

5.1.2 A Chromogenic Assay for Testing the Catalytic Activity of Heme-Peptide Complexes

Heme catalyzes Fenton-type reactions while generating hydroxyl radicals and oxidizing a substrate.[86] Once the heme moiety in peroxidases reacts with H_2O_2, the peroxide is reduced to water.[86] At the same time, Compound I, presumably an oxoferryl porphyrin-π-cationic radical, is generated.[86] In two consecutive one-electron reactions Compound I is reduced to the native enzyme, while Compound II (oxoferryl heme $PorFe^{4+}$=O) is formed as an intermediate and peroxidase substrate oxidation takes place (two one-electron oxidations).[86] 3,3',5,5'-Tetramethylbenzidine (TMB) is often applied as a chromogenic peroxidase substrate. The benzidine has been used to examine the catalytic activity of various heme-peptide complexes herein. TMB is oxidized to either a blue-colored charge-transfer complex (one electron) or a yellow diimine product (two electrons, Figure 17).[429] The oxidation can be monitored at 370 or 652 nm (charge transfer complex) and 450 nm (diimine), respectively.[429]

To assess the catalytic activity of various heme-peptide complexes, a commercially available TMB-based test kit served as the starting point for the optimization of a convenient chromogenic assay. The kit included an aqueous TMB solution and H_2O_2 diluted in citrate buffer. Within the performed experiments, generation of the blue-

colored charge transfer complex was measured at 652 nm. For reasons of simplicity the charge-transfer complex is referred to as oxidized TMB (TMB_{ox}) henceforth. In an effort to examine pH dependence and to determine suitable substrate concentrations, three different assay conditions were tested: (I) the commercial TMB substrate kit (1.66 mM TMB, 6.5 mM H_2O_2, pH 5.0 in citrate buffer, Thermo Scientific), (II) an in-house citrate buffer-based system (1.66 mM TMB, 163.2 mM H_2O_2, pH 5.0), and (III) an in-house phosphate buffer-based system (20.8 mM TMB, 163.2 mM H_2O_2, pH 7.4).[99] In the following, the different approaches will be referred to their Roman numerals. To test the individual assay systems, 1 µM was chosen as heme concentration since labile heme levels in healthy cells are estimated to be <1 µM. Moreover, HO-1 is thought to be induced at heme concentrations >1 µM, which would result in heme degradation (*cf.* Chapter 2.2.1).[93] Taking into account all measurements, a linear conversion of the chromogenic substrate occurred within 100 to 400 seconds of measuring time, which was consequently chosen as time range for all samples.[99]

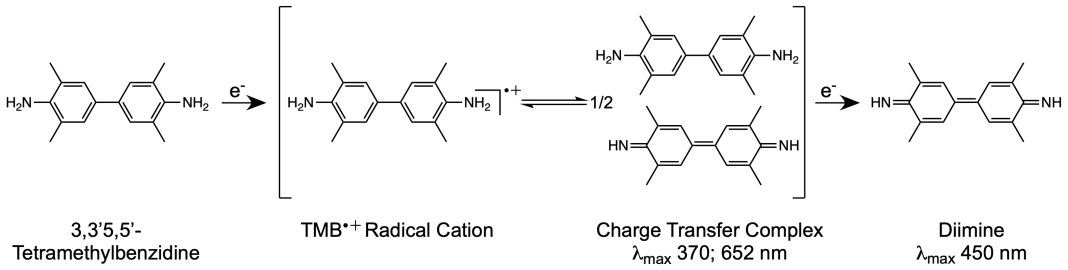

Figure 17. Oxidation reaction of 3,3',5,5'-tetramethylbenzidine (TMB) according to Stefan and colleagues.[429]

The Fenton reaction proceeds in acidic conditions. Notwithstanding, neutral approach III aimed at simulating physiological conditions, as a neutral pH is preferred when testing heme concentrations in patient samples. As anticipated, the data of approaches I-III demonstrate a clear pH dependency (Figure 18). Increasing the concentration of TMB from 1.66 mM (I, II) to 20.8 mM (III) and of H_2O_2 from 1.66 mM (I) to 163.2 mM (II, III) led to the formation of detectable quantities of TMB_{ox} in approach III, although these were significantly lower compared to approach I and II. The H_2O_2 concentration in approach II is ∼25-fold higher than in approach I, which increases the amount of TMB_{ox} formed in 400 seconds (I, $A_{652nm} \sim 0.06$; II, $A_{652nm} \sim 0.15$).

A deviating substrate conversion was recorded when the solutions of approach I, i.e. the commercial substrate kit, were prepared in an in-house protocol (approach I*). Comparing the activity of heme in approach I versus I*, reveals a decrease in activity of ∼40 % in approach I* (Figure 18). Based on two observations, it may be hypothesized that this finding is a result of stabilizers used in the H_2O_2

solution of the manufactured kit. Firstly, mass spectrometry of the H_2O_2 solution revealed additional compounds in the fluid whose nature could not be unambiguously determined.[99] Secondly, H_2O_2 solutions in citrate buffer (I*, II) prepared during the course of the experiments were not stable for more than 10 minutes. This finding further suggests the presence of stabilizers in the commercial H_2O_2 solution, which comes in a ready-to-go format. It is important to keep this observation in mind, in particular as heme-peptide complex formation might be altered by the occurrence of additional compounds.[99]

5.1.3 Pseudo-Peroxidase Activity of Aβ and Aβ-Derived Peptides

In an attempt to study the impact of individual residues in Aβ on the catalytic activity of the heme-Aβ complex, the peroxidase activity of heme-incubated Aβ40 as well as Aβ-derived peptides **1-6** was tested in approach I to III (Figures 18, 19). Since Aβ fibril formation is known to occur more efficiently in acidic conditions than at neutral pH, the acidic pH of approach I and II might evoke Aβ fibrillation.[430] Thus, the aggregation level of Aβ40 was analyzed in a thioflavin T (ThT) fluorescence assay prior to the chromogenic peroxidase assay (Figure 19). Interaction of the benzothiazole salt ThT with β-sheet rich structures leads to a substantial increase in fluorescence intensity, which can be monitored at ∼480 nm. ThT has been widely used to examine the formation of Aβ aggregates.[431] An artificially generated positive control (50 µM Aβ40, 37°C, 24 hours) verified the suitability of the assay. Neither in the Aβ stock solution nor in the acidic preparations with Aβ or the heme-Aβ complex, formation of larger Aβ40 aggregates occurred (Figure 19). Consequently,

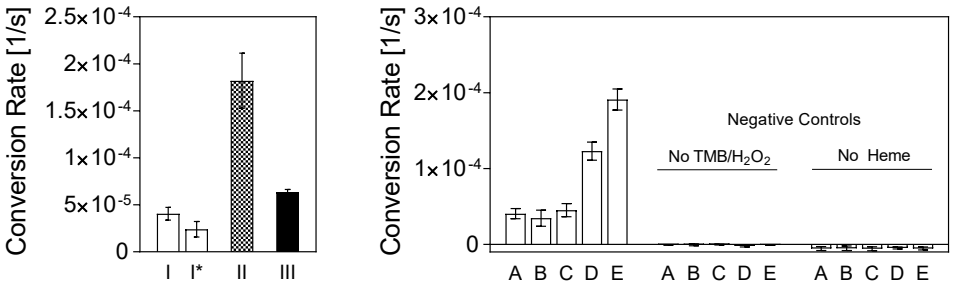

Figure 18. Catalytic activity of heme and the heme-Aβ40 complex in approach I to III. Substrate conversion was analyzed using 1 µM heme (I*, in-house-prepared solutions of I, left panel). Various concentrations of Aβ40 (A = 0 µM, B = 0.05 µM, C = 0.1 µM, D = 0.5 µM, E = 1 µM) were incubated with heme (1 µM) and tested in approach I (right panel). The activity of the heme-Aβ complex increased in a peptide-concentration dependent manner. No substrate conversion was observed for the negative controls. Modified from Wißbrock et al. 2017.[99]

higher aggregates of Aβ40 can be excluded, whereas low molecular weight aggregates are not detected by ThT and can therefore not be excluded.[99]

To evaluate the effect of Aβ and Aβ-derived sequences, a constant concentration of heme (1 µM) was incubated with varying peptide concentrations (0.1 to 1 µM) for 30 minutes before application to the chromogenic assay systems. As a general trend, a peptide concentration-dependent increase in activity was observed for the investigated heme-peptide complexes (Figure 18). All data obtained were normalized against the activity of heme only (100 %) and thus represent a direct comparison of heme and the respective heme-peptide complex.[99]

For Aβ40 a minimal peptide concentration of 0.05 µM is required to obtain a detectable amount of TMB_{ox} (Figure 18). Complex formation of heme and Aβ40 significantly increases the catalytic activity to ∼500 % (I, II) and ∼170 % (III, Figure 19). These results further support the pH dependency of the proceeding reaction (*cf.* Chapter 5.1.2). Heme-complexes with peptides **1-6** show a significantly reduced activity compared to Aβ40. Peptide **1** has no substantial effect on the catalytic activity of heme. With the exception of peptide **3** (∼265 %, II), the activity of the other peptides is in the range of ∼110 to 180 % in acidic conditions (I, II). Peptides **1-6** are anticipated to be structurally more flexible and might, in addition, lack secondary structure elements compared to the full-length, conformationally more restricted Aβ40 peptide, which is thought to adopt a helical structure (*cf.* Chapter 5.1.6). Missing secondary structure elements might serve as explanation for the loss of affinity and activity of all Aβ-derived peptides compared to full-length Aβ40.

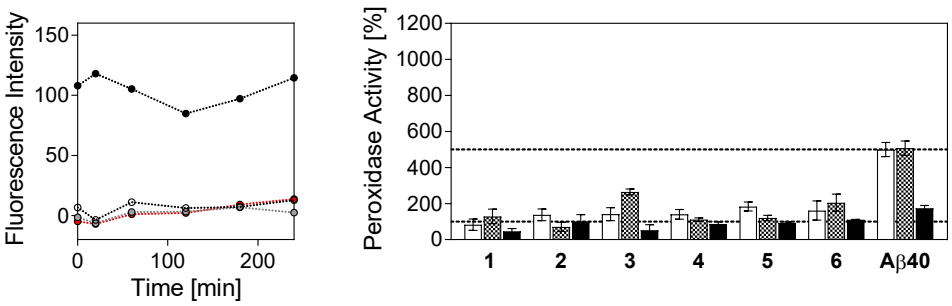

Figure 19. Catalytic activity of Aβ40 and Aβ-derived peptides. Initially, the aggregation state of Aβ40 was analyzed by a ThT fluorescence-based assay mimicking the acidic conditions of the peroxidase assay. Samples are denoted as follows: positive control (black circle), 42 µM Aβ (open circle), 1 µM Aβ (grey circle), and 1 µM heme-Aβ complex (red circle). Except for the positive control, no high molecular Aβ40 aggregates were formed (left panel). Afterwards, the catalytic activity of heme-incubated Aβ40 and peptides **1-6** (1:1, 1 µM) was determined in approach I to III (*cf.* Figure 18). All data are normalized against the activity of heme only (100 %, dashed line). The dashed line at 500 % reflects the activity of the heme-Aβ40 complex. Modified from Wißbrock et al. 2017.[99]

Taking the binding data into account, no effect for non-heme binding peptides **1** and **2** was expected. Peptides **3** to **5** are weak heme binders and a modest effect on the autocatalytic activity of heme is conceivable. 18mer peptide **6** comprises site-H of Aβ, including all putative heme-coordinating residues. Nevertheless, the peroxidase-activity of the heme-peptide complex is considerably decreased compared to the heme-Aβ complex. Remarkably, the determined heme-binding affinity of peptide **6** is not dramatically lower than the affinity of Aβ40. However, whereas Aβ40 was shown to bind at least two heme molecules, peptide **6** only interacts with one heme molecule according to the best fit possible. The acquired data indicate that site-L of Aβ is of major importance for the catalytic activity in the heme-Aβ complex. This finding is consistent with previous studies that report a minor peroxidase activity of site-H of Aβ.[295] In summary, the available data offer initial pointers to sequence requirements (e.g. length, secondary structure elements) for the formation of a catalytically active heme-peptide complex. A further insight on sequence features was provided in the following by investigating the activity of various non Aβ-derived peptides.[99]

5.1.4 Pseudo-Peroxidase Activity of Heme-Binding Peptides

In the subsequent experiments, heme-binding peptides **7-19** from previous studies were investigated with regard to a putative catalytic activity in complex with heme (Table 8, Figure 20).[99] Peptide candidates were selected that differed in coordination site, sequence composition, and peptide length. Initially, four negative controls, i.e. non-heme-binding nonapeptides (**7-10**), consisting of either only alanine residues (A_9) or a central (P^0) coordinating amino acid (His, Tyr, Cys) surrounded by alanines ($\pm A_4$), were tested in approach II. The lack of binding capacity correlates with the finding that peptides **7-10** do not have a substantial effect on the autocatalytic activity of heme (Figure 20).[99] Afterwards, heme-binding peptides **11-19** were tested in approach I to III. As expected, the substrate conversion in approach III is again significantly lower compared to approach I and II. The heme-binding affinity of peptides **11-19** was determined in earlier studies (Table 8). In general, no direct correlation between binding capacity and catalytic activity was observed. As for the heme-Aβ complex, a rise in peptide concentration (0.01 to 1 μM) leads to an increase of substrate conversion in a peptide concentration-dependent fashion. As anticipated, the highest substrate conversion occurs in approach II using 1 μM of heme and peptide each. Based on the original idea to identify a heme-peptide complex with the highest possible catalytic activity that can be applied in a heme detection kit, the following discussion focuses on the data obtained in this set-up (approach II, 1 μM heme/peptide).[99]

Initially, cysteine-based peptides were investigated. Incubation of heme with the nonapeptides **11** and **12** engenders a decrease of the heme's autocatalytic activity

to ∼80-90 % in approach II. A substrate conversion < 100 % might result from a heme-peptide interaction that leads to the formation of an inactive complex. The peroxidase activity of the 23mer heme-peptide **17** complex reaches ∼200 % in all approaches (Figure 20).[99]

Table 8. Heme-binding peptides studied in the peroxidase assay.[34,99,273,303,309]

No.	Sequence	UV [nm]	K_D [μM]
Aβ40	see below[1]	414	0.10 ± 0.0
1	AEFRHDSGY	-	n.b.
2	HDSGYEVHH	-	n.b.
3	GYEVHHQKL	416	n.p.
4	YEVHHQKLV	421	n.p.
5	RHDSGYEVHH	421	80.70 ± 4.00
6	DAEFRHDSGYEVHHQKLV	415	0.59 ± 0.05
7	AAAAAAAAA	-	n. b.
8	AAAAYAAAA[34,309]	-	n.b.
9	AAAACAAAA[34,303]	-	n.b.
10	AAAAHAAAA[34,309]	-	n.b.
11	AIRRCSTFQ[303]	432	0.50 ± 0.20
12	TPILCPFHL[273,303]	368	0.60 ± 0.41
		415	2.03 ± 1.38
13	FKAAHKHVR[309]	421	0.99 ± 0.21
14	AAHYHTYER[309]	417	0.83 ± 0.33
15	WELDYFQWK[309]	376	n.sat.
16	HPFPYIWKA[34,309]	423	0.33 ± 0.25
17	SGGLPAPSDFKCPIKEEIAITSG[34,273]	369	1.42 ± 0.24
18	NVNLTSNHLLYHYWIAVSHKAPA[34]	419	5.28 ± 0.95
19	VRMDTLAHVLYYPQKPLVTTRSM[34]	430	0.51 ± 0.72
20	NVNLTSNALLYHYWIAVSHKAPA	416	3.00 ± 1.19
21	NVNLTSNHLLYHYWIAVSAKAPA	416	1.89 ± 0.72
22	NVNLTSNALLYHYWIAVSAKAPA	414	0.88 ± 0.94
23	NVNLTSNHLLYAYWIAVSHKAP[2]	416	19.84 ± 4.11

n.b., not binding; n.p., not possible; n.sat., not saturated

[1] DAEFRHDSGYEVHHQKLVFFAEDVGSNKGAIIGLMVGGVV

[2] Due to technical difficulties, the C-terminal alanine residue is not included in the sequence. The residue is not expected to impact heme binding or the catalytic activity. Therefore peptide **23** was used as such.

Nonapeptides **13**, **14**, and 23mer peptide **18** represent His-based peptides. For peptides **13** and **14**, both strong heme binders (**13**: K_D 0.99 ± 0.21 μM, **14**: K_D 0.83 ± 0.33 μM[309]), a minor increase in activity is observed (**13**: ∼195 %, **14** ∼150 %).[99]

The complex of 23mer peptide **18** and heme exhibits a catalytic activity of >1000 % in approach II. Within the studies performed as part of this work, peptide **18** is the candidate with the highest potential even if compared to the heme-Aβ40 complex (∼ 500 %, Figure 20).[99] Peptide **18** is characterized by a central histidine residue (His12) and two distal histidine residues (His8, His19), a feature well known from various heme peroxidases. The role of these His residues is discussed below (*cf.* Chapter 5.1.5).

At last, a group of Tyr-based heme-binding peptides was analyzed (Figure 20). Nonapeptide **15** shows a similar effect as the Cys- and His-based nonapeptides. As such, the heme-peptide complex exhibits an activity of ∼ 140 to 195 %. Among the investigated nonapeptides, peptide **16**, a strong heme binder (K_D 0.33 ± 0.25 μM), displays the highest increase in activity (∼ 325 %). Analyzing the peptide sequence (HPFPYIWKA) reveals the presence of several amino acids that might support the formation of a catalytically active heme-peptide complex as, for instance, the distal His and the Trp residue.[99] Distal His residues in heme peroxidases are suggested to be important for the activation of H_2O_2, while Trp residues are thought to facilitate electron transfer.[432,433] As peptide **18** also exhibits distal His residues, the potential impact of these residues for the catalytic activity was further analyzed by means of alanine mutants of peptide **18** later on (*cf.* Chapter 5.1.5). The Tyr-based 23mer peptide **19** exhibits a peroxidase activity of 200 % in complex with heme and was thus regarded as a less potential candidate.[99]

Taken all data into account, peptide **18** is the most promising candidate, which was therefore investigated in more detail (*cf.* Chapter 5.1.5). The results obtained for all Aβ-derived and Aβ-independent peptides suggest that a distinct peptide length ($10 < Xaa < 25$; Xaa, amino acid) favors the formation of a catalytically active heme-peptide complex.[99] It might be assumed that specific secondary structure

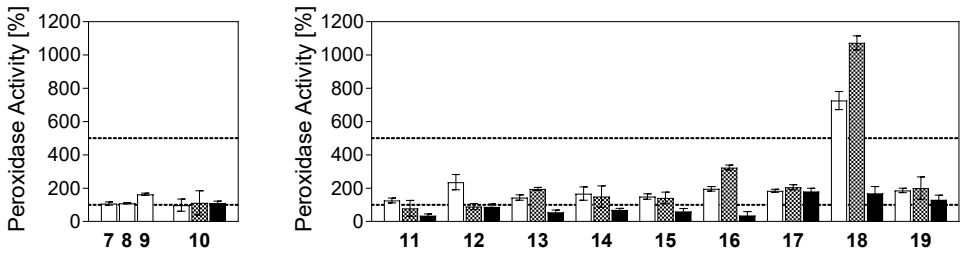

Figure 20. Catalytic activity of heme-incubated peptides **1-19** (1:1, 1 μM) in approach I to III (*cf.* Figure 18). Negative controls **7-9** were tested in approach I only. All data are normalized against the activity of heme only (100 %, dashed line). The dashed line at 500 % reflects the activity of the Aβ40-heme complex. Modified from Wißbrock et al. 2017.[99]

elements are required, however, further studies are inevitable to shed light on the structural nature of the heme-peptide complexes as well as the underlying reaction mechanism. Prior to the structural investigations, the role of the distal histidines for the catalytic activity was initially investigated by alanine mutation of peptide **18**.

5.1.5 Mutational Analysis of Peptide 18

The complex of peptide **18** and heme has a catalytic activity significantly higher than the heme-Aβ40 complex.[99] The sequence of peptide **18** is derived from the human fatty acyl-CoA reductase.[273] Remarkably, the protein occurs in the peroxisome, an organelle characterized by an acidic environment and high levels of H_2O_2. The protein is located in the peroxisomal membrane, however, the sequence stretch of interest reaches into the peroxisomal lumen.[434] It is well known that heme is present in the peroxisome and it would thus be interesting to study a potential heme interaction and catalytic activity on the protein level prospectively.[435] Since the protein is not commercially available and, moreover, is a transmembrane protein, studies on the protein level could not be performed as part of this work.

Two distal His residues (His8, His19) and a central His residue (His12), which is assumed to function as the heme axial ligand, are present in the sequence of peptide **18**.[99] Since distal histidines are believed to be involved in the O-O bond cleavage of H_2O_2 in heme peroxidases, a putative functional role of these histidines in peptide **18** was investigated by mutational analysis (Figure 21, 22).[436] The following Ala mutants of peptide **18** were synthesized by standard Fmoc SPPS: H8A (**20**), H19A (**21**), H8A/H19A (**22**), and H12A (**23**). A dramatic loss of binding affinity

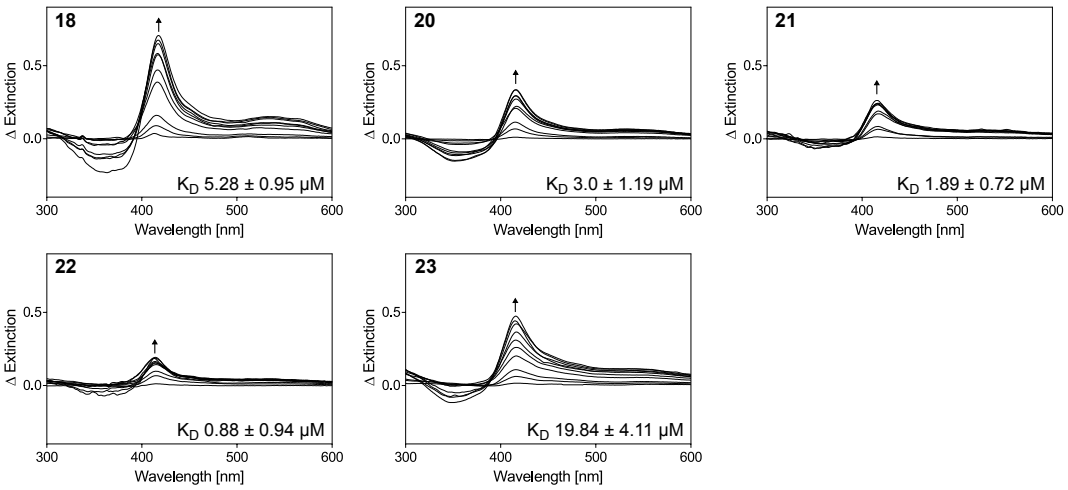

Figure 21. Heme binding to peptide **18** and mutants. UV/Vis differential spectra of heme-incubated peptides **18** and **20-23**. Peptide sequences can be found in Table 8. Modified from Wißbrock et al. 2017.[99]

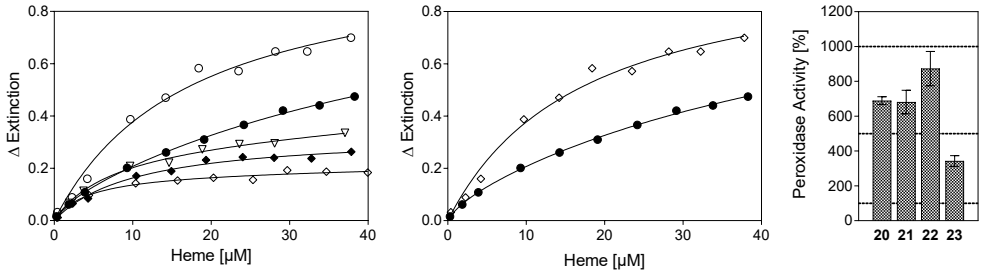

Figure 22. Mutational analysis of peptide **18**. Change of absorbance at ∼416 nm of heme-incubated peptides **18** and **20-23** as well as of peptide **18** directly compared to peptide **23** as used for K_D determination. Samples are denoted as follows: **18** (open circle), **20** (open triangle), **21** (black circle), **22** (open diamond), and **23** (black diamond, left and middle panel). Moreover, the catalytic activity of mutant peptides **20-23** was determined in approach II (*cf.* Figure 18, 1 μM, right panel). Modified from Wißbrock et al. 2017.[99]

(K_D 19.84 ± 4.11 μM, λ ∼416 nm) is observed for peptide **23** (H12A) compared to wild-type peptide **18** (K_D 5.28 ± 0.95 μM, λ∼416 nm, Figures 21, 22). Hence, the His12 residue is likely to function as heme coordination site in wild-type peptide **18**. Moreover, according to the best fit possible, two peptide molecules bind to one heme molecule. Mutation of one or both distal His residue(s) in peptides **20-22** results in a slight affinity increase in the range of 0.88 to 3.0 μM. One might assume that the presence of both distal His residues leads to a competitive situation of the side chains, which, in turn, results in a decrease in affinity. It is worth noting that the impact of individual amino acids on heme binding and the catalytic activity of the formed complex might also be of structural nature (*cf.* Chapter 5.1.6).[99]

Subsequently, the pseudo-peroxidase activity of all heme-peptide **18** mutant complexes was examined using the earlier established protocol (*cf.* Chapter 5.1.2).[99] A decrease of the catalytic activity is observed for all peptide **18** mutants (Figure 22). The activity of peptide **20-22** is in the range of 700 to 800 %, whereas peptide **18** shows an activity of >1000 % in complex with heme. The catalytic activity of peptide **23** is substantially decreased, which is likely a result of the significantly attenuated binding affinity for heme. The data obtained indicate that the central His residue in peptide **18** functions as heme axial ligand, while the distal His residues appear to be involved in heme binding, yet not implicitly assigned to an exclusive role.[99]

5.1.6 Structural Analysis of Aβ and Peptide 18 in Complex with Heme

A preference for sequences longer than 10 residues for a heme-peptide complex with high catalytic activity was observed during the prior examination of heme-binding peptides (*cf.* Chapters 5.1.3, 5.1.4).[99] A rationale for a minimum sequence length

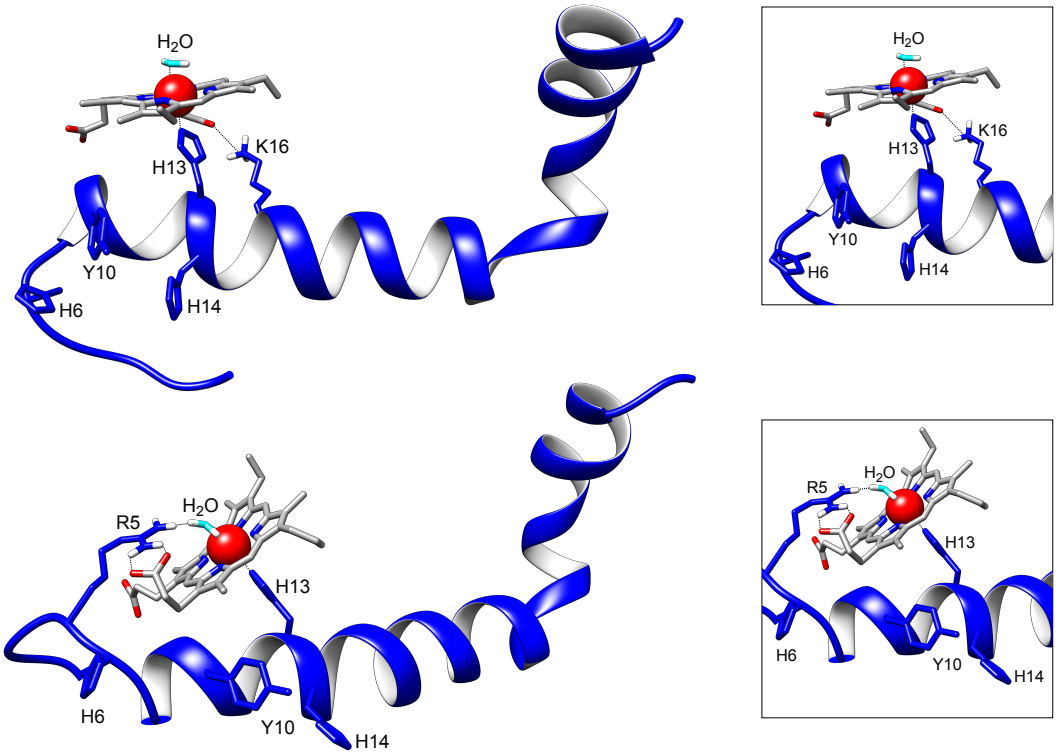

Figure 23. *In silico* modeling of heme binding to Aβ40. Relevant amino acids are labeled. Heme coordination via His13 can be supported by an H-bond donated from the side chain of either Lys16 or Arg5. Modified from Wißbrock et al. 2017.[99]

may be the presence of specific secondary structure elements that cannot be formed by shorter peptide sequences. Since Aβ40 and peptide **18** are the most promising candidates tested, detailed structural analysis of the heme-peptide complexes is of

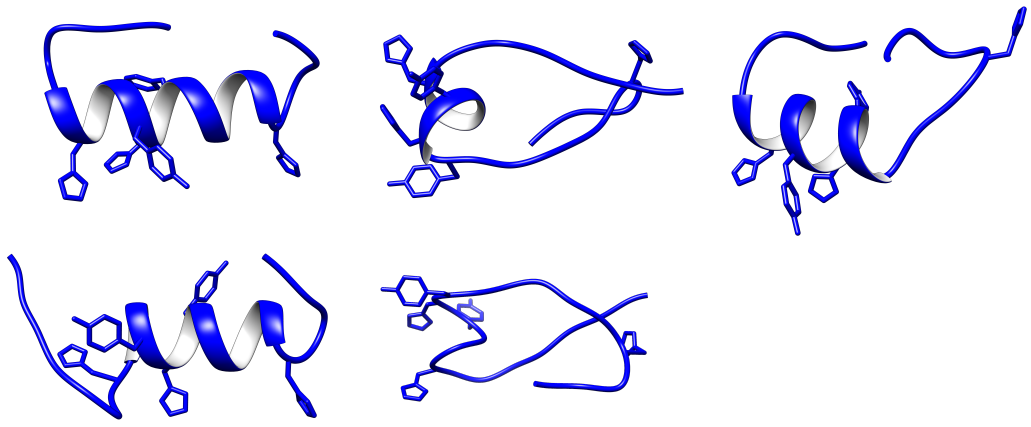

Figure 24. The five best clusters of peptide **18** as determined by *de novo* structure prediction using PEP-FOLD. Modified from Wißbrock et al. 2017.[99]

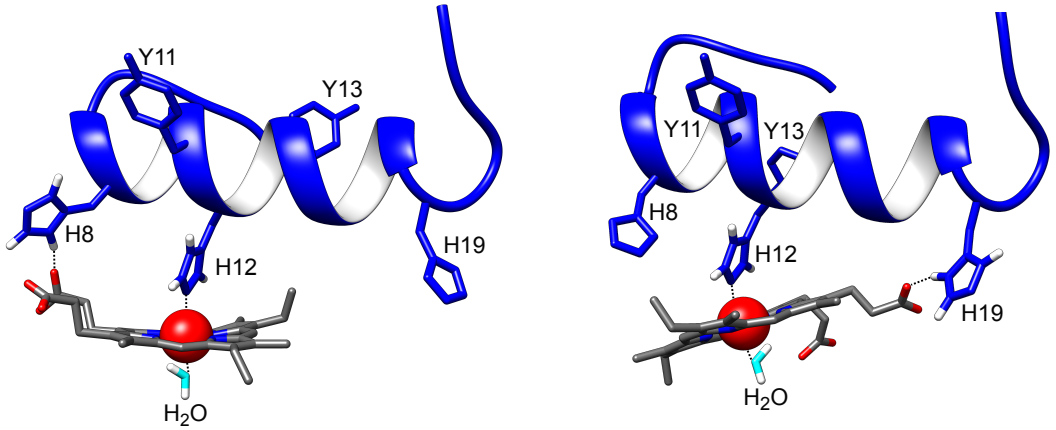

Figure 25. *In silico* modeling of heme binding to peptide **18**. Relevant amino acids are labeled. Heme coordination via His12 can be supported by an H-bond donated from the side chain of either His8 (left) or His19 (right). Modified from Wißbrock et al. 2017.[99]

great interest. Due to poor solubility of both peptides, pure and in complex with heme, NMR analysis was unfeasible and computational modeling was carried out by Dr. Oliver Ohlenschläger (FLI, Jena, Germany) instead.[99] Previous studies have documented that the structure of Aβ is strongly dependent on the experimental set-up.[409,437,438] Only a small fraction of Aβ is characterized by a defined secondary structure in aqueous solution, whereas the main part of the peptide is present as a random coil.[437] In an environment that mimics the lipidic surrounding of membranes, a helical structure between residues 8 or 15 to 24/25 and 28 to 36/38 was found.[409,437,438]

The experimental data obtained by UV/Vis spectroscopy confirmed heme binding to Aβ via His13/14 (*cf.* Chapter 5.1.1).[99] Modeling of heme binding to Aβ40 (PDB 1IYT[409]) indicates that heme coordination via His13 can be supported by H-bond formation (Figure 23). Thus, the ϵ-amino proton from the side chain of the Lys16 residue may donate an H-bond to one of the propionate side chains. Besides, the guanidinium protons of the Arg5 side chain may generate an H-bond to the propionate side chains. The latter provides a stronger binding network. Moreover, a water molecule might serve as sixth ligand of the hexacoordinated heme-Aβ complex as previously suggested (Figure 23).[99,423]

To get an impression of the structural features of the heme-peptide **18** complex, the peptide structure was modeled *de novo* using the software PEP-FOLD, since there was no structure available (Figure 24).[99,439,440] Mutational analysis strongly suggests that heme binding to peptide **18** takes place via His12 (*cf.* Chapter 5.1.5). This residue is located in an α-helical-like sequence stretch according to the best clusters of the calculated folds (Figure 24). Sheet and coil prediction were determined for other segments of the peptide sequence. The best-ranked fold was utilized for modeling

heme binding as earlier performed for Aβ40. Modeling confirms heme coordination to His12 (Figure 25). In addition, H-bonds that strengthen the interaction are donated from either His8 or His19, respectively (Figure 25). Furthermore, a water molecule might serve as sixth ligand to form the hexacoordinated complex that can easily be replaced by a second coordinating residue from the same or another peptide chain.[99]

5.1.7 Assessment of the Assay Using Human CSF Specimen

One of the aims of this work was to establish a heme/peptide-based approach that might prospectively be developed and applied for the diagnostic quantification of biologically available heme in patient samples such as CSF, urine, and plasma. In an effort to test the basic applicability of the technique for biological samples, first studies with human CSF were conducted in the most promising experimental set-up (approach II, peptide **18**). CSF samples were kindly provided by Prof. Dr. Albert Becker (University Hospital Bonn, Germany). In the context of this work only a small sample size could be examined. Thus, the data obtained can merely provide a first idea and testing of a large number of biological samples in the future is essential to further validate the applicability of the system.[99]

Remarkably, addition of human CSF to the substrate mixture (without heme) shows no significant effect in eight of ten patient samples, while two samples (2, 8) display increased substrate conversion activity (Figure 26). The applied CSF was a clear fluid in all cases and no obvious elevation of blood components (e.g. hemoglobin, heme) as in the case of, for instance, cerebral bleeding was visible with naked eye. Besides heme *per se*, other factors, such as an increase in iron, are also expected to catalyze the Fenton reaction in the chromogenic assay system. Therefore, a detailed analysis is required to qualitatively and quantitatively assess the composition of the CSF. One option is to carry out a comprehensive mass spectrometry analysis, however, time-consuming optimization, sufficient sample amounts as well as analytical standards are needed. Therefore, the nature of the underlying reaction could not be clarified within the framework of this preliminary investigation.

When applying heme and the heme-peptide **18** complex (1 to 9 μM heme) to the substrate mixture, a clear heme-concentration dependence was recorded that confirms the general functionality of the assay system (Figure 26). As anticipated, compared to heme, a higher substrate conversion occurs when the heme-peptide complex is deployed. To address the question whether the use of peptide **18** is beneficial for the quantification of heme in CSF, heme, peptide, and CSF were incubated for 30 minutes in a 1:1:2 ratio (v/v). Pre-incubation of peptide **18** and heme is required to observe complex formation in the presence of CSF, i.e. no comparable catalytic activity is monitored when heme, peptide, and CSF are incubated at the same time. When CSF is added to the preformed complex, a significant increase of substrate conversion

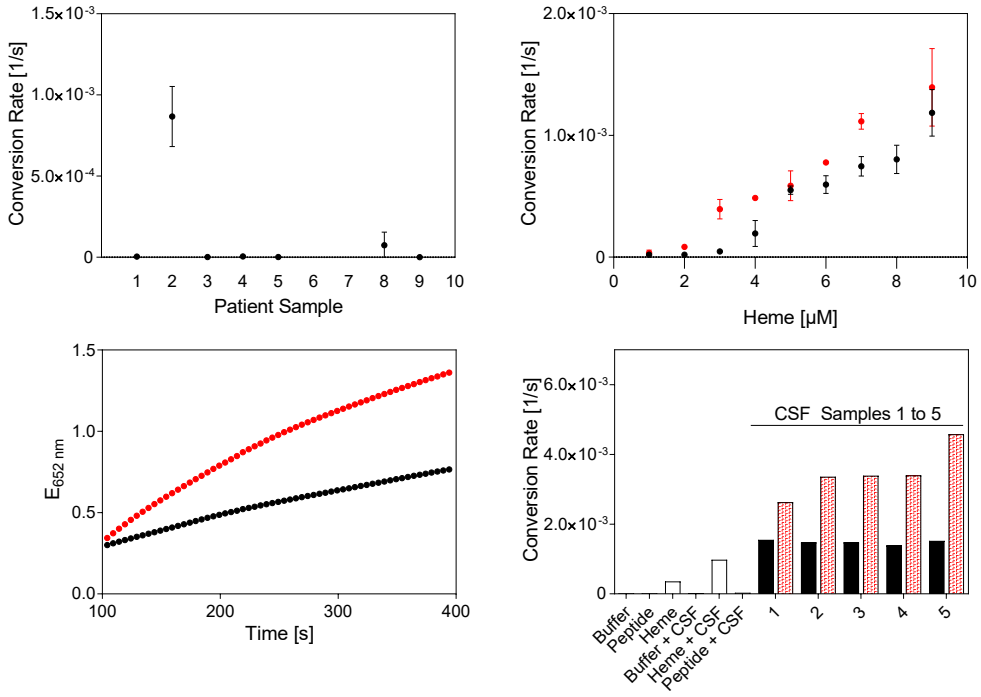

Figure 26. Assessment of the established chromogenic assay using human CSF specimen. Application of CSF (only) to approach II revealed increased substrate conversion in the case of samples 2 and 8, while no effect was observed for all other samples (top, left). A clear heme-concentration dependence was observed when various concentrations of heme (black, 1-9 µM) and the heme-peptide **18** complex (red, constant peptide concentration of 1 µM) were applied to approach II (top, right). Adding CSF to heme (black) or the preformed heme-peptide **18** complex (red) resulted in increased TMB oxidation (bottom, left). The activity of the heme-peptide **18** complex (black bars) was compared to the catalytic activity observed for the mixture of CSF (samples 1 to 5) and the heme-peptide **18** complex (bottom, right). A significant increase in activity is observed in the case of all tested CSF samples (1-5). Due to sample limitations measurements were only performed once.

proceeds compared to CSF only (Figure 26). However, due to sample limitation, the measurements have to be regarded as preliminary results. Notably, a substantial increase of substrate turnover in the presence of the heme-peptide complex is found for all samples.

The data obtained suggest that the heme-peptide **18** complex is a promising tool for the quantification of biologically available heme in patient samples. A clear heme concentration-dependence is apparent and an increase in substrate conversion is observed after complex application to CSF. Whether this increase is a result of complex formation between biologically available heme present in the CSF and peptide **18** needs to be clarified in future experiments.

5.1.8 Impact of Lipoprotein LDL on the Heme-Aβ Complex

Lipid peroxidation associated with increased levels of LDL_{ox} is frequently observed in AD patients. To date it is not clear whether lipid peroxidation is a primary phenomenon or an epiphenomenon in AD.[281,441] Remarkably, various findings link LDL_{ox} to heme and Aβ.[10,19] For example, it is well known that heme is able to interact with lipoproteins and can cause oxidation of LDL particles (*cf.* Chapter 2.3).[10,19] In addition, it was observed that about 5 % of Aβ added to plasma samples seem to bind to distinct lipoproteins (e.g. LDL, HDL).[442] Furthermore, increased concentrations of LDL in AD are associated with elevated Aβ42 levels independent of the crucial apoE genotype.[443]

To examine a potential interference of heme-Aβ complex formation in the presence of LDL and consequently an impact of LDL on the pseudo-peroxidase activity of the heme-Aβ complex, a chromogenic assay was performed based on the earlier established experimental set-up (*cf.* Chapter 5.1.2, Figure 27). In individual samples LDL was added to both Aβ and heme before and after heme-Aβ complex formation.[99] For the experiments a molar ratio of 1:100 of LDL to Aβ, heme or the heme-Aβ complex was chosen because highly differing molar ratios for the heme-LDL interplay had earlier been published.[99,444] It is conceivable that more than one heme molecule may interact with one LDL particle due to the large discrepancy in molecular size of LDL and heme (Figure 28). By measuring the catalytic activity of the samples, several conclusions on the interaction of LDL, Aβ, and heme could be drawn.[99]

Initially, all three compounds were added to the TMB/H_2O_2 substrate mixture immediately after mixing ($t_{1\,min}$) and upon 30 minutes of incubation ($t_{30\,min}$). Compared to the heme-Aβ complex the resulting TMB conversion is significantly reduced at $t_{1\,min}$ and $t_{30\,min}$ (Figure 27). This observation might be a consequence of heme

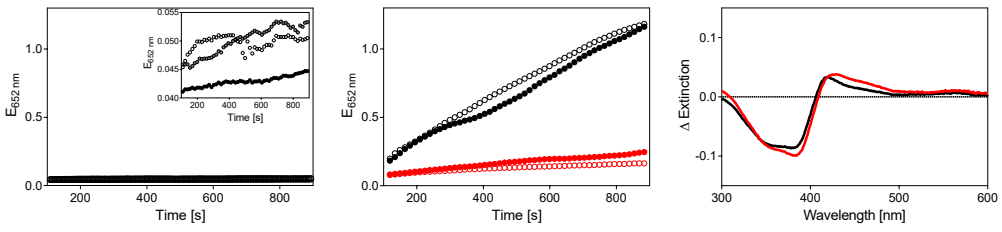

Figure 27. Impact of LDL on the heme-Aβ40 complex. No catalytic activity was observed for the controls, i.e. buffer (white open circle), LDL (grey open circle) as well as Aβ40 and LDL (black circle, left panel). The heme-Aβ40 complex (black open circle) was stable in the presence of LDL (black circle, middle panel). When Aβ40 was applied to a pre-incubated mixture of LDL and heme (red circle), the monitored activity resembled the activity of heme only (red open circle, middle panel). Differential spectra of heme-incubated LDL (λ_{max} ∼ 429 nm, red) and the heme-Aβ complex (λ_{max} ∼ 420 nm, black).

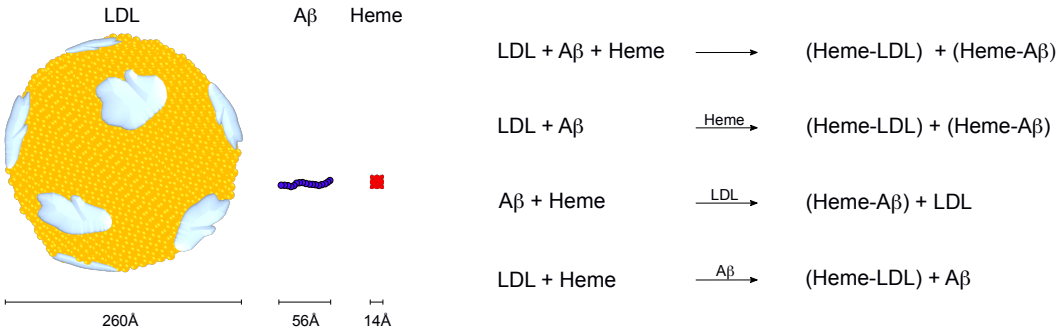

Figure 28. Interplay of LDL, heme, and Aβ40. Molecular size of LDL, Aβ40, and heme (left). The monitored catalytic activity suggests that the occurence of heme-Aβ and heme-LDL complexes is dependent on the order of component addition (right). Compounds added after an initial incubation of 30 minutes are given on the arrows. Brackets indicate the presumed heme-binding scenario based on the catalytic activity observed. Modified from Wißbrock et al. 2017.[99]

binding to both molecules, LDL and Aβ, resulting in reduced levels of the catalytically active heme-Aβ species. When Aβ and heme were preincubated (30 minutes) before addition of LDL, the catalytic activity measured resembles the activity of the heme-Aβ complex. It might thus be concluded that the heme-Aβ complex is stable in the presence of LDL for at least 15 minutes (Figure 27). It is also possible that the heme-Aβ complex as such interacts with LDL, forming a trimeric complex that maintains the catalytic activity of the dimeric heme-Aβ complex. In the performed experiments, LDL does not seem to be capable of scavenging the heme moiety from Aβ. When heme is added to a solution of preincubated Aβ and LDL, the resulting activity suggests a situation similar to the first scenario when all three compounds are added at the same time. Presumably, no stable complex of LDL and Aβ is formed, which would have impeded heme binding to either compound (Figure 28). Substrate conversion indicates, however, that a portion of the catalytically active heme-Aβ complex is generated. When heme and LDL were preincubated before applying Aβ, an activity similar to heme only is monitored, which suggests that no heme-Aβ complex is formed. These findings suggest that complexes of LDL and heme as well as Aβ and heme are stable with respect to the third component. Summarizing the above, it can be said that an interplay of the three molecules can occur. *In vivo*, time, order, and level of occurrence of the three molecules may determine the nature of the formed complexes and consequently decide whether catalytically active complexes are present.[99]

The analysis of the catalytic activity of various heme-peptide complexes gave insight into sequence requirements for catalytically active heme-peptide complexes. Based on the optimized assay system and the identification of peptide **18** as a suitable

candidate with high catalytic activity in complex with heme, a promising set-up was established. The approach might prospectively be developed into a diagnostic tool. Moreover, further characterization of the heme-Aβ complex gave insight into sequence features as well as a possible interplay of LDL, heme, and Aβ.

5.2 Analysis of a Putative Heme-IL-36α Interaction

Beyond heme quantification in patient samples, it is a prime concern to examine physiological effects of elevated heme levels to ensure adequate medical treatment. For that reason there is a continuous search for proteins regulated by heme. The human proinflammatory cytokine IL-36α was predicted to be regulated by heme in previous studies.[273] Moreover, an IL-36α-derived nonapeptide, more precisely a CP motif, was shown to bind heme (*cf.* Chapter 2.5.2).[273] A series of prior experiments aimed at verifying heme binding to IL-36α on the protein level, however, these studies were not successful due to the limitation of the experimental set-up on the one hand and high expenses of the commercially available protein on the other hand.[420,421] In addition to other experimental methods, recombinant protein expression of IL-36α was therefore established in cooperation with Dr. Oliver Ohlenschläger, Dr. Nishit Goradia, and Amit Kumar (Leibniz Institute on Aging, FLI, Jena, Germany) within the scope of this work, which allowed for working with higher protein quantities. After a global IL-36 sequence analysis, heme binding to all agonistic IL-36 family members was confirmed. Various spectroscopic methods (SPR, UV/Vis, fluorescence, *r*Raman, 3D NMR spectroscopy) and *in vitro* cell tests provided insight into the molecular processes taking place upon heme binding to IL-36α. The spectroscopic analysis was further supported by computational modeling of wild-type and mutated IL-36α proteins in complex with heme. The results gathered during these studies will be discussed in the following sections.

5.2.1 SPR Analysis of Heme-Incubated IL-36 Cytokines

Inspired by the studies of Karnaukhova et al.,[195] heme binding to the truncated (tr) agonistic IL-36 family members was initially investigated using an SPR-based approach.[401] SPR is a label-free, optical technique based on the eponymous physical phenomenon. In short, evanescent waves are formed in the metallic film as a result of photon induction. When photons excite surface plasmons, a change in the refraction angle is detected. Once the optical density of the sample placed on the metal is altered (e.g. complex formation) the resonance angle shifts. This effect is used for protein interaction studies.[445–447]

Biaffin GmbH & Co KG (Kassel) conducted the SPR experiments using commercially available trIL-36α, trIL-36β, and trIL-36γ (R&D Systems, Minneapolis, MN, USA). The proteins were covalently immobilized on a CM5 sensor chip via amine coupling. BSA and lysozyme were included as control proteins as described by others (Figure 29).[57,401] BSA, which served as positive control, shows a significant effect upon incubation with heme, thereby confirming heme binding to the protein. In contrast, only a minor effect is found for lysozyme, which was thus

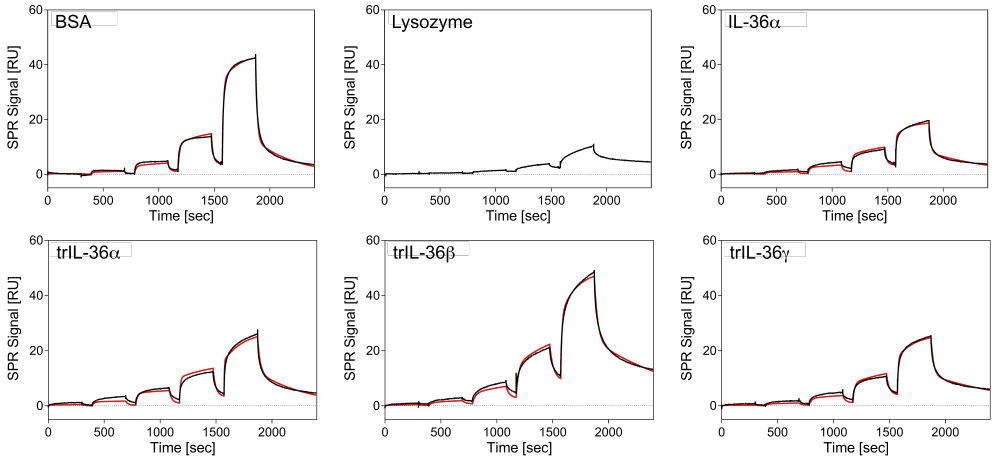

Figure 29. SPR spectra of control proteins BSA and lysozyme as well as agonistic IL-36α cytokines, trIL-36α, trIL-36β, and trIL-36γ after consecutive injection of 80 nM to 20 µM heme. A kinetic titration (single cycle kinetics) method was applied (fits are displayed in red). Modified from Wißbrock et al. 2019.[401]

assessed as negative control. The putative heme interaction with the IL-36 cytokines was investigated using a similar experimental set-up. SPR analysis demonstrates heme binding to trIL-36α (6-158), trIL-36β (5-157), and trIL-36γ (18-169, Figure 29). The observed interactions appear to follow a biphasic binding profile. A fit according to a 1:1 Langmuir binding model did not reveal satisfying results, whereas a global heterogenous ligand model was convenient for data evaluation. This model assumes two independent binding events on two different protein sites. This is in good agreement with the theoretical sequence analysis that suggests at least two possible HRMs in all agonistic family members (*cf.* Chapter 5.2.2). Binding to the IL-36 protein recombinantly expressed in *E. coli* (*cf.* Chapter 5.2.4) was confirmed at a later stage (Figure 29). A slighty faster heme-binding kinetic was observed for trIL-36α compared to the full-length protein. Both proteins exhibit comparable heme-binding affinities, ranging from 4 to 13 µM and from 3 to 10 µM for the individual binding events. In fact, heme binding to all trIL-36 proteins is characterized by comparable affinity (Table 11).[401]

5.2.2 Sequence Analysis and Evaluation of IL-36 Cytokines

Sequence analysis and assessment of the agonistic IL-36 cytokines, namely IL-36α, IL-36β, and IL-36γ, revealed potential HBMs in all proteins (Figure 30, Table 9). It is worth noting that members of the IL-36 cytokine family share 31 to 57 % sequence identity as shown by sequence alignment using Clustal Omega (Figure 31, Table 10).[449] The most prevalent heme-coordinating amino acids, Cys, Tyr, and His, were

considered as potential axial ligand.[401] Earlier studies unveiled characteristic sequence features of HBMs (*cf.* Chapter 2.5.2): A positive net charge, aromatic residues, and additional coordination sites favor heme binding based on the nonapeptide sequence surrounding the axial ligand.[30,32,34,273,303,308] Furthermore, transient heme binding requires HBMs to be exposed on the protein's surface.[32] Therefore, the protein structure of IL-36γ (PDB 4IZE)[385] was considered for HBM elucidation. No structure for IL-36β has yet been published, while the structure of IL-36α was obtained as part of this work and was thus incorporated for HBM evaluation.[401,450]

The sequence of IL-36α (158 aa) contains ten possible heme coordination sites ($\mathbf{m}_{1-10}$), considering Tyr, His, and Cys residues (*cf.* Figure 30, Table 9). The four Cys residues occur in the reduced form as demonstrated by iodoacetamide derivatization and subsequent MALDI-MS analysis and are thus available for coordination to the heme iron (Figure 32).[401] The previously identified CP motif ($\mathbf{m}_{10}$)[273] represents a

IL-36α
MEKALKIDTPQQGSIQDIN**H**RVWVLQDQTLIAVPRKDRMSPVTIALIS**C**R**H**VETLEKDRG
NPI**Y**LGLNGLNL**C**LM**C**AKVGDQPTLQLKEKDIMDL**Y**NQPEPVKSFLF**Y**H**S**QSGRNSTFES
VAFPGWFIAVSSEGG**C**PLILTQELGKANTTDFGLTMLF

IL-36β (isoform 1)
MNPQREAAPKS**Y**AIRDSRQMVWVLSGNSLIAAPLSRSIKPVTL**H**LIA**C**RDTEFSDKEKGN
MV**Y**LGIKGKDL**C**LF**C**AEIQGKPTLQLKLQGSQDNIGKDT**C**WKLVGI**H**T**C**INLDVRES**C**FM
GTLDQWGIGVGRKKWKSSFQ**HHH**LRKKDKDFSSMRTNIGMPGRM

IL-36β (isoform 2)
MNPQREAAPKS**Y**AIRDSRQMVWVLSGNSLIAAPLSRSIKPVTL**H**LIA**C**RDTEFSDKEKGN
MV**Y**LGIKGKDL**C**LF**C**AEIQGKPTLQLKEKNIMDL**Y**VEKKAQKPFLFF**H**NKEGSTSVFQSV
S**Y**PGWFIATSTTSGQPIFLTKERGITNNTNF**Y**LDSVE

IL-36γ (isoform 1)
MRGTPGDADGGGRAVYQSM**C**KPITGTINDLNQQVWTLQGQNLVAVPRSDSVTPVTVAVIT
CK**Y**PEALEQGRGDPI**Y**LGIQNPEM**C**L**Y**CEKVGEQPTLQLKEQKIMDL**Y**GQPEPVKPFLF**Y**
RAKTGRTSTLESVAFPDWFIASSKRDQPIILTSELGKS**Y**NTAFELNIND

IL-36γ (isoform 2)
MRGTPGDADGGGRAVYQSITVAVIT**C**K**Y**PEALEQGRGDPI**Y**LGIQNPEM**C**L**Y**CEKVGEQP
TLQLKEQKIMDL**Y**GQPEPVKPFLF**Y**RAKTGRTSTLESVAFPDWFIASSKRDQPIILTSEL
GKS**Y**NTAFELNIND

IL-36Ra (antagonist)
MVLSGAL**C**FRMKDSALKVL**Y**L**H**NNQLLAGGL**H**AGKVIKGEEISVVPNRWLDASLSPVILG
VQGGSQ**C**LSCGVGQEPTLTLEPVNIMEL**Y**LGAKESKSFTF**Y**RRDMGLTSSFESAA**Y**PGWF
L**C**TVPEADQPVRLTQLPENGGWNAPITDFYFQQCD

Figure 30. Protein sequences of IL-36 family members. Sequences were derived from Uniprot.[448] Potential coordinating residues (in bold) and potential HBMs (in red) are highlighted. Residues depicted in grey are proteolytically cleaved in the biologically active cytokine species.[448]

Table 9. Evaluation of HBMs in IL-36 family members. Motifs $\mathbf{m}_1$-$\mathbf{m}_6$ in both isoforms of IL-36β are identical, thus only deviating motifs in isoform 2 are listed. In IL-36γ residues 19-54 are replaced by an isoleucine residue resulting in a shifted but otherwise similar sequence of both proteins.[448] $\mathbf{m}_1$ is different and $\mathbf{m}_2$ is missing in isoform 2. For reasons of simplicity motif numbering is similar in both isoforms.[401]

	Interleukin-36α				Interleukin-36β					Interleukin-36γ				
No.	Pos.	Sequence	Cha.	Pot.	No.	Pos.	Sequence	Cha.	Pot.	No.	Pos.	Sequence	Cha.	Pot.
$\mathbf{m}_1$	H20	QDIN**H**RVWV	0/+1*	-	$\mathbf{m}_1$	Y12	APKS**Y**AIRD	+1	-	$\mathbf{m}_1$	Y16#	GRAV**Y**QSM**C**	+1	+
$\mathbf{m}_2$	C49	ALIS**C**R**H**VE	0/+1*	-	$\mathbf{m}_2$	H44	PVTL**H**LIA**C**	0/+1*	-	$\mathbf{m}_2$	C20*	**Y**QSM**C**KPIT	+1	+
$\mathbf{m}_3$	H51	IS**C**R**H**VETL	0/+1*	-	$\mathbf{m}_3$	C48	**H**LIA**C**RDTE	-1/+0*	-	$\mathbf{m}_3$	C61/26	AVIT**C**K**Y**PE	0	-
$\mathbf{m}_4$	Y64	GNPI**Y**LGLN	0	-	$\mathbf{m}_4$	Y63	GNMV**Y**LGIK	+1	-	$\mathbf{m}_4$	Y63/28	IT**C**K**Y**PEAL	0	-
$\mathbf{m}_5$	C73	GLNL**C**LM**C**A	0**	-	$\mathbf{m}_5$	C72	GKDL**C**LF**C**A	0	-	$\mathbf{m}_5$	Y76/41	GDPI**Y**LGIQ	-1	-
$\mathbf{m}_6$	C76	L**C**LM**C**AKVG	+1**	-	$\mathbf{m}_6$	C75	L**C**LF**C**AEIQ	-1	-	$\mathbf{m}_6$	C85/50	NPEM**C**L**YC**E	-2	-
$\mathbf{m}_7$	Y96	IMDL**Y**NQPE	-2	-	$\mathbf{m}_7$	C100	GKDT**C**WKLV	+1	-	$\mathbf{m}_7$	Y87/52	EM**C**L**YC**EKV	-1	-
$\mathbf{m}_8$	Y108	SFLF**YH**SQS	0/+1*	+	$\mathbf{m}_8$	H107	LVGI**HTC**IN	0/+1*	-	$\mathbf{m}_8$	C88/53	M**C**L**YC**EKVG	0	-
$\mathbf{m}_9$	H109	FLF**YH**SQSG	0/+1*	+	$\mathbf{m}_9$	C109	GI**H**T**C**INLD	-1/+0*	-	$\mathbf{m}_9$	Y108/73	IMDL**Y**GQPE	-2	-
$\mathbf{m}_{10}$	C136	SEGG**CP**LIL	-1	+	$\mathbf{m}_{10}$	C118	VRES**C**FMGT	0	-	$\mathbf{m}_{10}$	Y120/97	PFLF**Y**RAKT	+2	+
					$\mathbf{m}_{11}$	H141	SSFQ**HHH**LR	+1/+4*	+	$\mathbf{m}_{11}$	Y159/136	LGKS**Y**NTAF	+1	+
					$\mathbf{m}_{12}$	H142	SFQ**HHH**LRK	+2/+5*	+					
					$\mathbf{m}_{13}$	H143	FQ**HHH**LRKK	+3/+6*	+					
							Isoform 2					Isoform 2		
					$\mathbf{m}_7$	Y95	MDL**Y**VEKKA	0	-	$\mathbf{m}_1$	Y16#	GRAV**Y**QSIT	+1	+
					$\mathbf{m}_8$	H108	FLFF**H**NKEG	0	+					
					$\mathbf{m}_9$	Y123	QSVS**Y**PGWF	0	-					
					$\mathbf{m}_{10}$	Y153	NTNF**Y**LDSV	-1	-					

Pos., Position; Cha., Charge; Pot., Heme-Binding Potential.
* Histidine has no charge when acting as heme axial ligand.
** Solitary cysteines are generally poor or ineffective heme binders.
\# Removed in active cytokine species.

Figure 31. Sequence alignment of the IL-36 family. Alignment was performed using Clustal Omega.[449] The suggested YH and CP motif and the corresponding sequence stretches in the other IL-36 family members are marked in red. Modified from Wißbrock et al. 2019.[401]

promising HBM based on the general prevalence of CP motifs in heme-regulated proteins, despite the negative net charge (-1).[79]

Moreover, a Tyr-His-based motif (YH motif; $\mathbf{m}_8$, $\mathbf{m}_9$) of particular interest was identified. The occurrence of two putative coordinating residues and the aromatic phenylalanines argue in favor of heme binding.[30,401] Heme coordination via both Tyr and His is conceivable and was thus addressed in subsequent studies.[401]

All other motifs are classified as less probable due to the following reasons: Motifs $\mathbf{m}_1$-$\mathbf{m}_5$ have no charge or a single positive charge, bearing in mind that histidines are neutral when serving as heme axial ligand. With the exception of one tryptophan in $\mathbf{m}_1$ there are no aromatic residues present in $\mathbf{m}_1$-$\mathbf{m}_7$. $\mathbf{m}_7$ is further excluded due to the negative net charge (-2). Moreover, solitary cysteines were shown to be generally poor or ineffective heme binders ($\mathbf{m}_5$, $\mathbf{m}_6$).[303,401] Consequently, the later in-depth analysis of the heme-IL-36α complex focused on the CP and YH motif as potential HBMs.[401]

Subsequently, potential HBMs in IL-36β and IL-36γ (two isoforms each) were classified deploying the same criteria (Figure 30, Table 9). In IL-36β thirteen (isoform 1), respectively, ten (isoform 2) potential coordination sites exist. Among the first six motifs in IL-36β ($\mathbf{m}_1$-$\mathbf{m}_6$), which are identical in both isoforms, are two Tyr-based motifs ($\mathbf{m}_1$, $\mathbf{m}_4$) that might function as HBM based on the net charge of the sequence. The three consecutive histidines (His141-143) in IL-36β, together with two phenylalanines ($\mathbf{m}_{11}$-$\mathbf{m}_{13}$), and a multiple positive charge in isoform 1 appear auspicious. In both isoforms of IL-36γ a Cys-based ($\mathbf{m}_2$) and three Tyr-based ($\mathbf{m}_1$, $\mathbf{m}_{10}$, $\mathbf{m}_{11}$) motifs are rated as promising sequence stretches, however, experimental

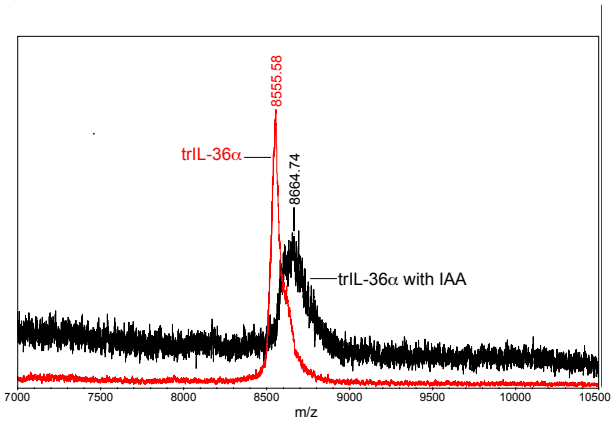

Figure 32. Mass spectrum of trIL-36α after iodoacetamide (IAA) derivatization. All four cysteines present in IL-36α are in the reduced state as confirmed by MALDI-MS.

examination is required for a more accurate assessment. $\mathbf{m}_1$ is not present in the proteolytically truncated trIL-36γ.[401]

The CP motif in IL-36α is unique within the IL-36 family, despite sequence identities ranging from 31 to 57 % for IL-36 cytokines (Figure 31, Table 10). The corresponding proline is conserved in all IL-36 cytokines, whereas the cysteine is only present in IL-36α. The second motif of interest in IL-36α, the YH motif, is not conserved as such, yet either the His or the Tyr residue is found in all family members. Based on the unique occurrence of the CP motif in IL-36α, this cytokine was chosen for in-depth analysis. Consequently, the proposed YH and CP motif were initially investigated on the peptide level.

Table 10. Sequence identity of IL-36 family members. Alignment was performed using Clustal Omega.[401,449] Values are expressed as percentage.

	IL-36α	IL-36β	IL-36β (2)	IL-36γ	IL-36γ (2)	IL-36Ra
IL-36α	100	31.82	45.22	55.41	57.38	32.21
IL-36β	31.82	-	62.34	28.76	24.58	19.18
IL-36β (2)	45.22	62.34	-	43.59	43.80	32.89
IL-36γ	55.41	28.76	43.59	-	99.25	30.41
IL-36γ (2)	57.38	24.58	43.80	99.25	-	35.40
IL-36Ra	32.21	19.18	32.89	30.41	35.40	-

5.2.3 Heme Binds to IL-36α-Derived Nonapeptides

Heme binding to the two proposed IL-36α-derived HBMs was examined on the nonapeptide level using the protocol previously described for Aβ40 (Figure 33).[401] Previous studies of the 9mer CP motif revealed a shift of the Soret band to ∼366 nm with a dissociation constant of 3.75 ± 0.77 µM.[273] A shift of the Soret band to ∼370 nm has earlier been shown to be characteristic for pentacoordinated binding of heme to CP motifs.[273,303]

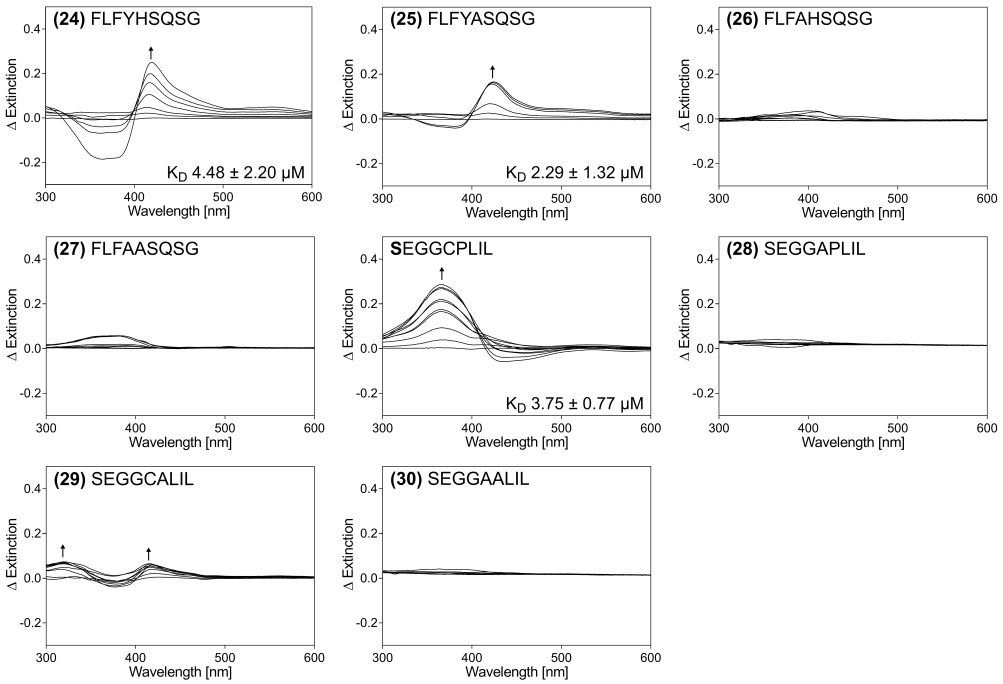

Figure 33. UV/Vis differential spectra of heme-incubated peptides **24-30**. The spectrum of the CP motif (SEGGCPLIL) was derived from previous studies.[273] Modified from Wißbrock et al. 2019.[401]

Incubating the suggested YH motif (peptide **24**) with heme implies a 1:1 interaction with a shift of the Soret band to ~ 415 nm and a dissociation constant of 4.48 ± 2.20 µM (Figure 33). Hence, heme binding to the two putative motifs was verified on the peptide level.[273,401] Alanine mutants of both motifs were created with single and double Cys, Pro, Tyr, and His mutations (peptides **25-30**). Remarkably, no heme binding is found in case of the Tyr to Ala mutation in peptides **26** and **27**, pointing towards Tyr as the axial ligand of heme (Figure 33). In contrast, Tyr-based peptide **25** binds heme with a K_D value of 2.29 ± 1.32 µM and a shift to ~ 418 nm, a UV/Vis shift earlier associated with Tyr-based heme coordination in the presence of additional coordinating residues in close proximity to the coordinating tyrosine.[30,401] According to the best fit possible, a 1:1 heme-peptide complex is present. The different curve shape of the differential spectra of peptides **24** and **25** indicates an impact of the Tyr and His residue on heme binding in wild-type peptide **24**.[401]

As anticipated, loss of the Cys residue prevents an interaction (peptides **28**, **30**), whereas Pro mutation (peptide **29**) leads to a significantly altered UV/Vis differential spectrum with maxima a ~ 319 nm and ~ 419 nm (Figure 33). K_D determination is not possible due to the low change in absorbance. The differential spectra implies heme binding, however, the pronounced difference in curve shape indicates a structurally

altered complex compared to the wild-type peptide. Therefore, the significant role of proline for heme binding to CP motifs was once again confirmed.[273,401] Based on the data obtained from the peptide study, Tyr108 and Cys136 are proposed as heme coordination sites in wild-type IL-36α with His109 and Pro137 having a supporting effect on the heme interaction taking place. To investigate heme binding on the protein level, recombinant protein expression of IL-36α and corresponding mutant proteins was performed in the following.[401]

5.2.4 Recombinant Protein Expression of IL-36α and Variants

With the aim to produce protein amounts sufficient for in-depth analysis of heme binding to IL-36α via fluorescence, UV/Vis, *r*Raman, and 3D NMR spectroscopy, recombinant protein expression of IL-36α and IL-36α protein mutants was performed in *E.coli* in cooperation with Dr. Oliver Ohlenschläger (FLI, Jena, Germany). The residues suggested to be involved in heme binding were mutated individually and in combination (Y108S, H109A, C136S, P137A). For reasons of simplicity the mutant proteins will be further referred to as the residue(s) mutated (e.g. Y108S) without the cytokine designation (IL-36α) being specified. The following mutant proteins were generated: Y108S, H109A,C136SP137A, Y108SH109A, Y108SC136SP137A, H109AC136SP137A, and Y108SH109AC136SP137A. Full-length and truncated cytokine species were expressed giving a total number of 16 protein variants. Successful protein expression of the proteins was confirmed by MALDI-MS (*data not shown*) and SDS-PAGE (Figure 34).[401]

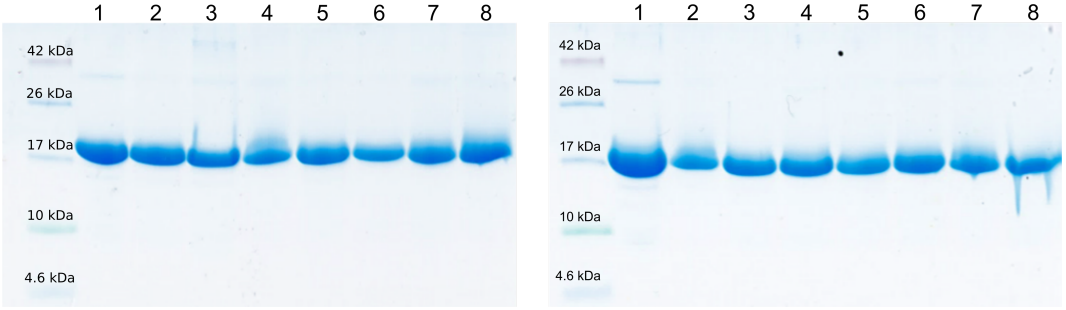

Figure 34. SDS-PAGE of recombinantly expressed IL-36α cytokines (coomassie blue-stained 18 % reducing gel). Molecular weight markers are indicated. The proteins are organized as follows (full-length, left; truncated, right): 1) wild-type, 2) Y108S, 3) H109A, 4) C136SP137A, 5) Y108SH109A, 6) Y108SC136SP137A, 7) H109AC136SP137A, and 8) Y108SH109AC136SP137A. Modified from Wißbrock et al. 2019.[401]

5.2.5 Fluorescence Quenching Confirms Heme Binding to IL-36α

Heme binding to the recombinantly expressed wild-type IL-36α proteins was initially confirmed by SPR (*cf.* Chapter 5.2.1) and fluorescence spectroscopy.[401] Fluorescence

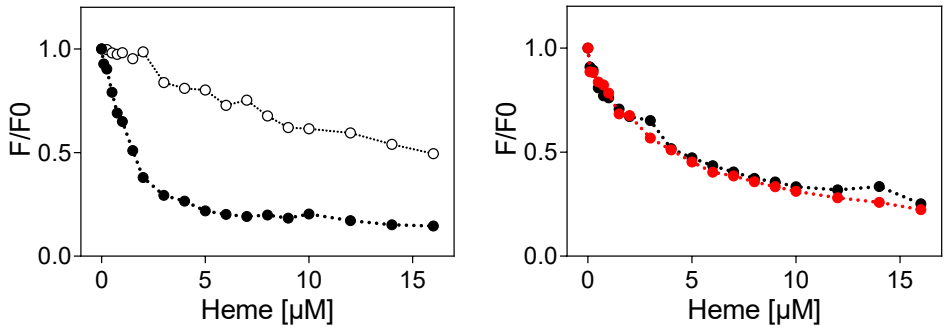

Figure 35. Fluorescence intensity of heme-incubated control proteins BSA (black circle, left) and lysozyme (open circle, left) as well as full-length (black, right) and trIL-36α (red, right). Shown is the quotient of the fluorescence intensity of the heme-incubated protein (F0) and the pure protein (λ_{ex} 306 nm, λ_{em} 352 nm). Modified from Wißbrock et al. 2019.[401]

spectroscopy is a widely used method to study proteins and bioactive peptides. The technique can give insight into conformational changes, intermolecular interactions, and protein dynamics.[451–454] Heme binding to a protein results in quenching of the protein's intrinsic fluorescence.[57,455] In case of complex formation dynamic and static quenching are apparent and can be detected in a non-linear decrease of fluorescence intensity. When no interaction takes place, a linear decrease of fluorescence intensity is observed as a consequence of solely dynamic quenching.[456]

The fluorescence emission of control proteins BSA and lysoyzme as well as full-length and truncated IL-36α was monitored as a function of the applied heme concentration (Figure 35). The fluorescence data display a clear quenching effect that correlated with the applied heme concentration in case of all examined proteins. As expected, a linear decrease of fluorescence intensity is found for the heme-incubated negative control lysozyme. In contrast, heme binding to BSA is confirmed as demonstrated by the non-linear decrease in fluorescence intensity, verifying the suitability of the applied system (Figure 35). Heme binding to IL-36α and trIL-36α is shown according to the non-linear decrease of fluorescence intensity (Figure 35). The quenching effects of both proteins appear similar, suggesting an analogous binding mode of both IL-36α species.[401]

5.2.6 UV/Vis Spectroscopy Reveals Heme Binding to IL-36α via a YH and a CP Motif

In an effort to investigate heme binding to IL-36α in more detail, UV/Vis spectroscopy was applied to wild-type IL-36α and the seven protein variants using the experimental set-up earlier described (*cf.* Chapter 5.2.3).[401] Spectra of the heme-incubated positive (BSA) and negative (lysozyme) controls were also included (Figure 36). Heme binding

to BSA is observed, however, due to missing saturation no binding affinity can be estimated. Analysis of the differential spectrum of lysozyme reveals the occurrence of a broad band, which was earlier associated with unspecific heme binding.[302,401] Together with the data obtained during SPR analysis, an unspecific interaction of heme and lysozyme is plausible.[401]

The differential spectra of heme-incubated IL-36α shows a hypsochromic and a bathochromic shift to ∼369 nm and ∼416 nm (Figure 37).[401] A shift to ∼370 nm is characteristic for heme-protein interactions via CP motifs.[273,303] Hence, the obtained spectrum strongly indicates involvement of the proposed C136P137 motif. The maximum at ∼416 nm further suggests the presence of a second binding event, thereby supporting the findings of the SPR analysis (*cf.* Chapter 5.2.1). According to the best fit possible, both maxima are treated as separate binding events, assuming 1:1 stoichiometry. Dissociation constants (K_Ds) were determined as 3.63 ± 2.67 µM and 11.50 ± 3.06 µM, respectively, indicating moderate binding. No interaction takes place, when heme is replaced with PPIX, which verifies the pivotal role of the metal ion for the interaction (Figure 37).[401] To test whether time-dependent heme binding to IL-36α can be monitored by UV/Vis spectroscopy, IL-36α was incubated in a 1:1 and a 1:2 molar ratio with heme (5, 10 µM). UV/Vis spectra were recorded in intervals of 30 seconds up to 10 minutes over a time period of 60 minutes. Comparison of the first (30 seconds) and the last differential spectrum (60 minutes) reveals only minor differences for both molecular ratios, indicating that heme-IL-36α complex formation occurs within the first 30 seconds upon heme addition (Figure 36). Due to the fast kinetic, further information on, for instance, disparate binding kinetics of the two binding events or a recruitment mechanism cannot be acquired from these experiments.

Subsequently, heme binding to the IL-36α mutants was investigated (Figure 37). The proposed heme-binding sites in IL-36α were mutated both individually

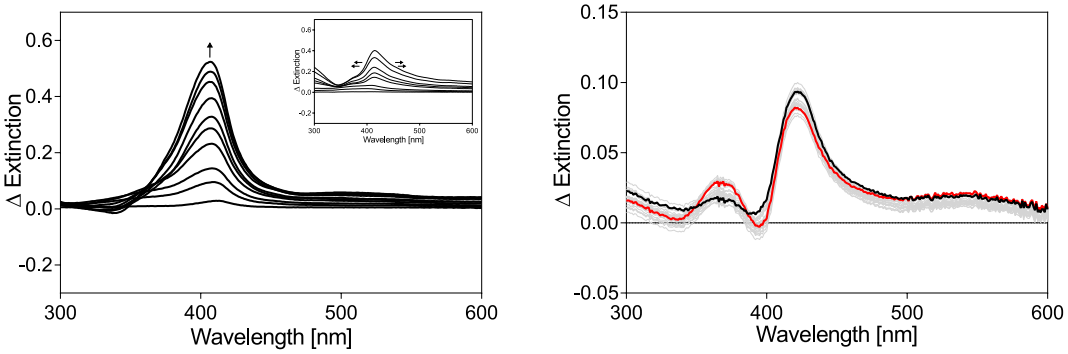

Figure 36. UV/Vis differential spectra of control proteins BSA[401] (left panel) and lysozyme[401] (inset, left panel) as well as the time-dependent measurement of heme binding to IL-36α (30 s in black, 60 min in red, right panel).

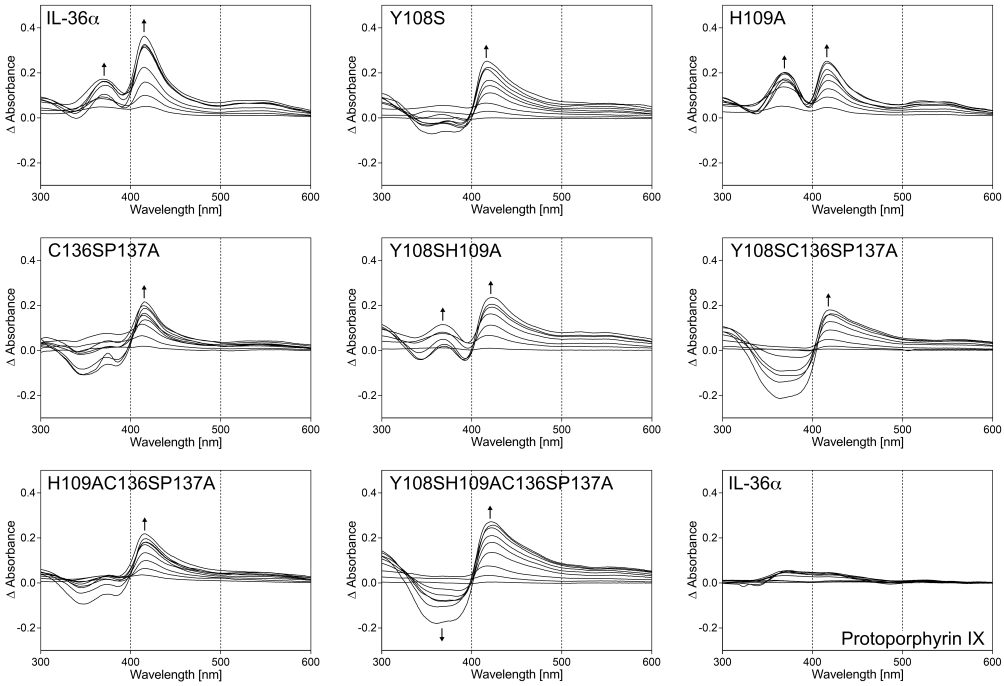

Figure 37. UV/Vis differential spectra of heme-incubated IL-36α and protein variants. Dashed lines mark the wavelengths 400 and 500 nm, respectively. PPIX was included as a negative control. Modified from Wißbrock et al. 2019.[401]

and collectively (*cf.* Chapter 5.2.4). It is worth noting that the differential spectra of all heme-incubated IL-36α variants deviate from the wild-type spectrum, thus strongly indicating that all four proposed residues are involved in heme binding to IL-36α (Figure 37).[401] The spectrum of the Y108S mutant displays one maximum at ∼418 nm, whereas no band occurs at ∼370 nm, suggesting an aberrant binding mode of heme compared to IL-36α. One explanation for the disappearance of the shift at ∼370 nm might be a cooperative binding mode of the two interaction sites. Thereby, mutation of Y108 would affect heme binding at C136. The significant loss of binding affinity (K_D 30.69 ± 7.49 µM) portends a substantial role of Y108 for heme binding in wild-type IL-36α. In contrast, the differential spectra of IL-36α and the H109A mutant resemble one another closely, which suggests a minor role of H109 in heme binding. In fact, the spectrum of H109A is the closest to the wild-type cytokine among all variants with identical maxima (∼369 nm, ∼416 nm) and binding affinities of 0.77 ± 0.53 µM and 10.35 ± 3.16 µM, respectively (Figure 37). The small rise in binding affinity from 3.63 ± 2.67µM (wild-type) to 0.77 ± 0.53 µM (H109A), supports the assumption of a minor impact of H109 on heme binding. In the case of mutation of either Y108 or H109, the adjacent residue may function as the coordinating ligand. Further studies (e.g. NMR spectroscopy, *cf.* Chapter 5.2.9) were required and

conducted in the following to define the role of Y108 and H109 unequivocally.[401] The disappearance of the shift at ∼369 nm in the C136SP137A mutant strongly insinuates that the CP motif is substantially involved in heme binding to IL-36α. Moreover, the maximum at ∼415 nm (K_D 12.69 ± 4.43 µM) shows no significant deviation from the wild-type protein, suggesting a CP motif-independent binding event. The spectrum of the heme-incubated Y108SH109A protein shows both maxima, yet the maximum at ∼368 nm is less distinct than for IL-36α and calculation of a K_D value is not feasible (Figure 37). For the second maximum a K_D value of 13.64 ± 4.69 µM was determined.[401]

Table 11. Spectroscopic data of heme-IL-36α complex formation. The table summarizes the binding data obtained from SPR, UV/Vis, and *r*Raman spectroscopy.[401]

Protein	SPR K_{D1} [µM]	SPR K_{D2} [µM]	nUV K_{D1} [µM]	Soret K_{D2} [µM]	Raman c.s.
trIL-36α	12.7 9.3	3.0 4.4	n.d.	n.d.	n.d.
trIL-36β	10.0 13.9	4.1 3.7	n.d.	n.d.	n.d.
trIL-36γ	8.9 15.9	5.3 4.1	n.d.	n.d.	n.d.
IL-36α	6.1 4.4	10.2 7.1	2.69 ± 1.15 ∼369 nm	11.50 ± 3.06 ∼416 nm	5c
Y108S	n.d.	n.d.	-	30.69 ± 7.49 ∼418 nm	5c
H109A	n.d.	n.d.	0.77 ± 0.53 ∼ 369 nm	10.35 ± 3.16 ∼416 nm	5c
C136SP137A	n.d.	n.d.	-	12.69 ± 4.43 ∼415 nm	5c*
Y108SH109A	n.d.	n.d.	n.p. ∼368 nm	13.64 ± 4.69 ∼420 nm	5c
Y108SC136SP137A	n.d.	n.d.	-	15.17 ± 4.35 ∼419 nm	5c
H109AC136SP137A	n.d.	n.d.	-	13.29 ± 3.12 ∼417 nm	5c
Y108SH109AC136SP137A	n.d.	n.d.	-	14.23 ± 3.82 ∼421 nm	5c*

nUV, nearUV; c.s., coordination state.; n.d., not determined; n.p., not possible

* Negligible indication of hexacoordination.

In the following, heme binding to variants Y108SC136SP137A, H109AC136SP137A, and Y108SH109AC136SP137A was analyzed (Figure 37). The spectrum as well

as the heme binding affinity of H109AC136SP137A is comparable to the spectrum of the C136SP137A mutant, consistent with a minor role of H109 for heme binding. The two protein variants Y108SC136SP137A and Y108SH109AC136SP137A seem to bind heme in a similar manner according to the UV/Vis spectra. Both spectra are characterized by a pronounced minimum at $\sim 370\,\text{nm}$. There is no information regarding the structural nature of heme-peptide/protein complexes that show a minimum in the UV/Vis differential spectra so far. Therefore, no further interpretation is permitted here.[401] In addition to the minimum, the spectra of both heme-incubated proteins exhibit maxima at $\sim 419\,\text{nm}$ (K_D $15.17 \pm 4.35\,\mu\text{M}$) and $\sim 421\,\text{nm}$ (K_D $14.23 \pm 3.82\,\mu\text{M}$), respectively. Therefore, contrary to expectations, heme binds to the quadruple mutant, which proposes the presence of a further binding site in IL-36α.[401] A strong broadening of the maximum at $\sim 420\,\text{nm}$, as found for all Y108 variants, points towards an unspecific heme interaction with Y108SH109AC136SP137A (Figure 37).[32,302,401] Furthermore, it should be noted that mutation of four residues might have a substantial influence on the protein's structure which might result in altered heme bining.[401]

In conclusion, altered UV/Vis spectra were observed in case of all protein mutants and a role of the C136(P137) motif as well as Y108, and H109 for heme binding in wild-type IL-36α appear likely.[401] The obtained spectra indicate heme coordination via C136 and Y108 with H109 as a replacement for Y108 in case of mutation. In the following, the structure of the heme-IL-36α complex was initially examined by *r*Raman and 3D NMR spectroscopy, before subsequent computer-based modeling experiments provided further insight into heme binding to the mutant proteins.[401]

5.2.7 *Resonance* Raman Spectroscopy Discloses a Pentacoordinated Heme-IL-36α Complex

In an attempt to unravel the coordination state of the iron ion in the heme-IL-36α complex, *resonance* Raman (*r*Raman) spectroscopy was performed in cooperation with the group of Prof. Dr. Ute Neugebauer (IPHT, Jena, Germany) based on a previously established protocol.[273,303,309,401] Unlike *non-resonance* Raman spectroscopy, *r*Raman utilizes the amplification of specific vibrational frequencies to allow for high quality spectra of samples with concentrations in the micromolar range. The Soret band of heme (400 nm) served as excitation frequency and the allowed electronic π-π^* transitions of the porphyrin were monitored. In the event of a heme-protein interaction, changed vibrational heme frequencies occur as a result of an altered porphyrin structure. These changes are used to determine the coordination state of the iron ion in the formed complexes.[273,303,309,457–460]

Heme exhibits several characteristic stretching bands in the high frequency region (1200 to $1700\,\text{cm}^{-1}$). These bands (ν_3, ν_2, ν_{10}, ν_4) are distinctive for the heme iron

oxidation state (ν_4) as well as the heme iron coordination and spin state (ν_3, ν_2, ν_{10}). The ν_4 band is typical for Fe^{3+} heme. Ligation of a strong π-electron donor results in a shift from 1375 cm^{-1} to lower wavenumbers. In addition, ν_4 is a marker for electron density, enabling porphyrin "breathing" and giving information on the heme iron ligand interplay. To distinguish between penta- and hexacoordinated heme-peptide/protein complexes, the ν_3 band is of particular interest. A hexacoordinated heme complex, often a low-spin configuration, results in a ν_3 shift to higher wavenumbers. The ν_2 band is not sensitive to neither the coordination state nor the oxidation state of the heme iron. In case of a hexacoordinated heme complex, the band shifts to higher (hexacoordinated low-spin) and lower (hexacoordinated high-spin) wavenumbers. Due to only minimal splitting of the d-orbitals, there is no observable pentacoordinated low-spin heme iron and the low-spin state is only found in case of hexacoordination. Usually, bands of the lower frequency region (350 to 1200 cm^{-1}) appear much weaker compared to the higher frequency region (1200 to 1700 cm^{-1}). In heme the iron is usually found in a 'domed shape', meaning that the iron protrudes from the porphyrin plane. In case of hexacoordination, the interaction of two axial ligands from either side pushes the iron back into the planar porphyrin ring. This change of the position of the iron ion can be recorded in an enhancement of the ν_7 band, the dominant heme band in the lower frequency region.[273,303,309,457–461]

*r*Raman spectroscopy was performed for heme complexes with IL-36α-derived peptides **24**, **25**, and **29** as well as IL-36α and the proteins mutants (Figure 38, 39, Table 11). No shift of the ν_3 band occurs in the case of heme-incubated peptide **24**, suggesting a pentacoordinated complex (Figure 38).[401] The spectrum does, however, suggest that ν_3 and ν_2 are less distinct than ν_4, which implies the presence of a small

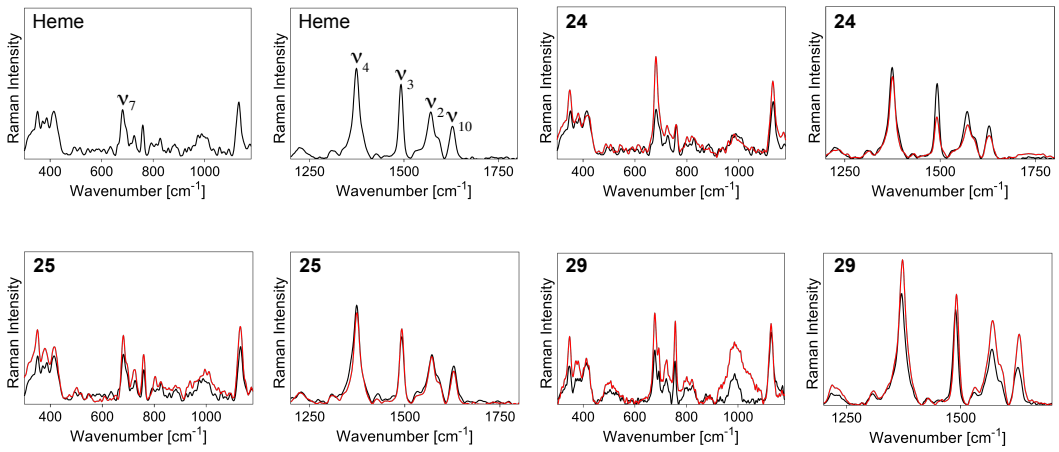

Figure 38. Raman spectra of heme (black) and heme-incubated peptides **24**, **25**, and **29** (red). The wavenumber fingerprint region of interest was assigned with the prominent normal-mode frequencies for heme: ν_7 (681 cm^{-1}), ν_4 (1374 cm^{-1}), ν_3 (1492 cm^{-1}), ν_2 (1571 cm^{-1}), and ν_{10}(1628 cm^{-1}). Modified from Wißbrock et al. 2019.[401]

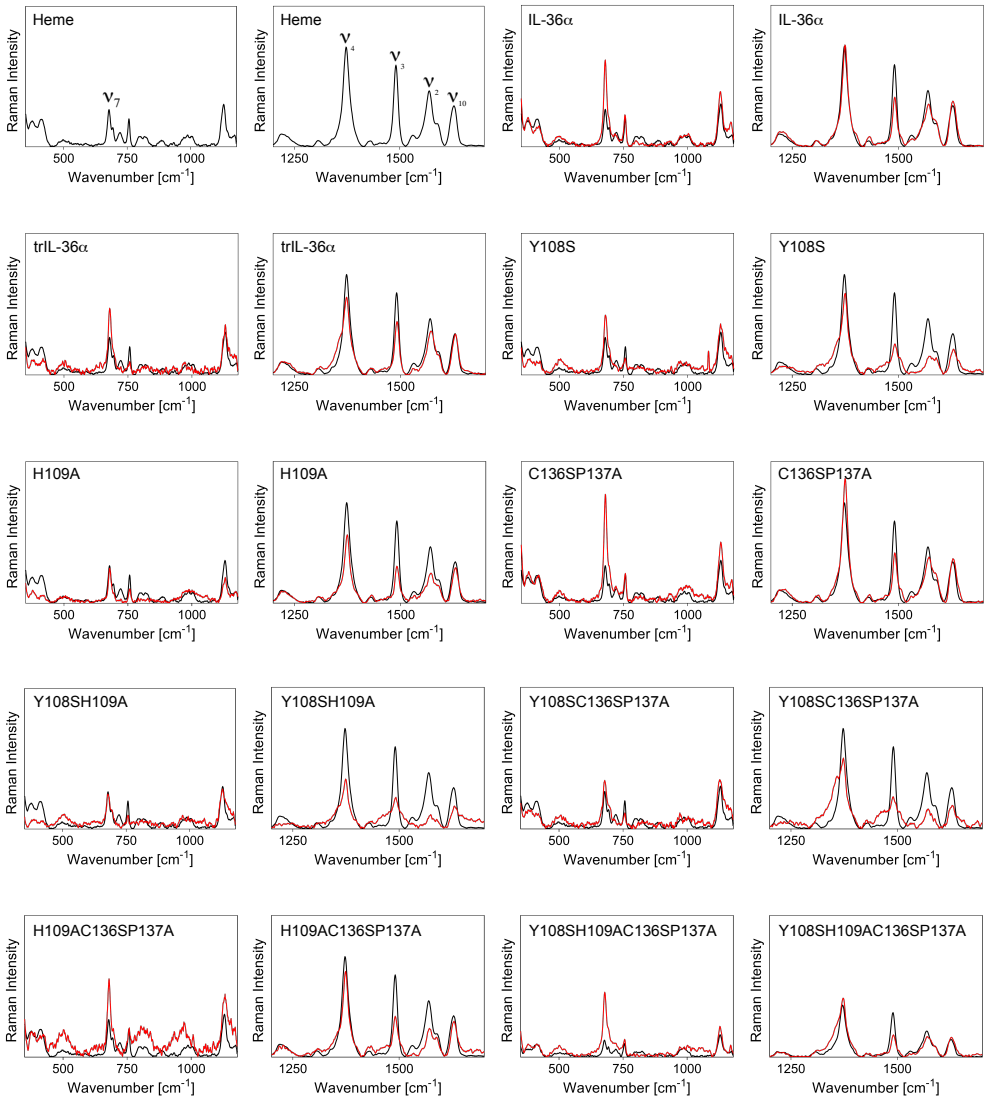

Figure 39. Raman spectra of heme (black) and heme-incubated IL-36α proteins (red). The wavenumber fingerprint region of interest was assigned with the prominent normal-mode frequencies for heme: ν_7 (681 cm^{-1}), ν_4 (1374 cm^{-1}), ν_3 (1492 cm^{-1}), ν_2 (1571 cm^{-1}), and ν_{10} (1628 cm^{-1}). Modified from Wißbrock et al. 2019.[401]

quantity of a planar hexacoordinated complex.[303,401] Heme complexes with both peptide **25** and peptide **29** are found to be pentacoordinated, with the spin- and coordination-state sensitive ν_3 band at around 1492 cm^{-1} and only minor alterations in the prominent normal mode frequencies (Figure 38).[401]

Subsequently, the coordination state of the heme-incubated IL-36α proteins was examined.[401] In general, the obtained signals for the proteins are weaker compared to the peptide-based measurements conducted as part of this work and also to earlier studies on heme-binding peptides.[303,309,401] The heme-IL-36α complex predominantly

appears as a pentacoordinated complex. The spin- and coordination state-sensitive ν_3 is found around 1492 cm^{-1}. In addition, only a marginal shoulder around 1508 cm^{-1} and a minor increase in intensity of ν_7 (around 681 cm^{-1}) are observed (Figure 39). In accordance with the findings from UV/Vis spectroscopy, the Raman spectrum of the H109A variant is most similar to wild-type IL-36α, revealing a pentacoordinated heme-protein complex. Despite the presence of a pentacoordinated heme-protein complex, a decrease in intensity of ν_3 and ν_2 is observed upon mutation of Y108, which is supported by the findings on the peptide level. The ν_3 is characterized by a weak shoulder at around 1504 cm^{-1} for distinct C136SP137A variants. At the same time, the intensity of ν_3 and ν_2 is decreased and ν_7 (around 681 cm^{-1}) as well as the oxidation state marker band ν_4 (around 1374 cm^{-1}) are increased, possibly implying the existence of a small fraction of hexacoordinated complex (Figure 39).[401]

SPR and UV/Vis data suggest heme binding to IL-36α in a 2:1 stoichiometry. Both heme iron ions seem to be predominantly present in a pentacoordinated fashion. Ensuing studies with circular dichroism (CD) and 3D NMR spectroscopy revealed further structural details.

5.2.8 Circular Dichroism Suggests Irregular Structural Elements in IL-36α

In an attempt to get an impression of the secondary structure of IL-36α, circular dichroism (CD) spectroscopy was employed by Dr. O. Ohlenschläger (FLI, Jena, Germany). The CAPITO (CD Analysis and Plotting tool)[405] and K2D3[406] algorithms served for detailed analysis of the CD spectrum.

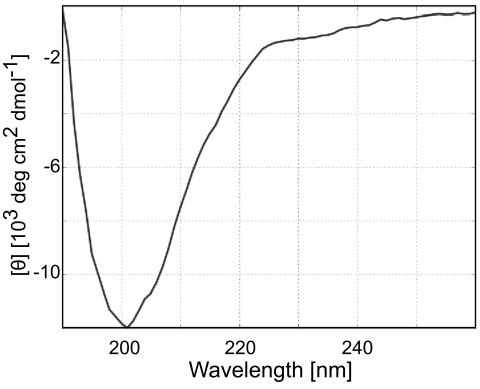

Figure 40. CD spectrum of IL-36α. The negative band at 203 nm suggests a predominantly disordered structure. Modified from Wißbrock et al. 2019.[401]

The CAPITO algorithm utilizes far-UV CD spectra that have been associated with tertiary structures. These structures are deposited in the Protein Circular Dichroism Data Bank (PCDDB) repository.[405] The algorithm of K2D3 (190-240 nm) is based

on the standard pattern recognition algorithm k-nearest neighbors, an approach commonly used for classification and regression.[406] The circular dichroism pattern of IL-36α, with a negative band at 203 nm, points towards a disordered structure (Figure 40).[401] According to the analysis provided by both algorithms, the secondary structure of the cytokine comprises of 50 to 70 % irregular structural elements, whereas α-helixes (10 %) and β-sheets (20 to 35 %) are less present (Table 12).[401]

Table 12. CD analysis of IL-36α and trIL-36α.[401]

Protein	Analysis Tool	α-Helix	β-Sheet	Irregular
IL-36α	CAPITO	10-13 %	30-35 %	50-60 %
IL-36α	K2D3	9.8 %	19.7 %	70.5 %
trIL-36α	CAPITO	10-13 %	32-37 %	51-59 %
trIL-36α	K2D3	8.5 %	19.5 %	72 %

5.2.9 Structural Analysis of IL-36α and the Heme-IL-36α Complex by NMR Spectroscopy

Subsequently, heteronuclear 3D NMR spectroscopy of truncated and full-length IL-36α as well as the heme-bound protein was performed by Dr. O. Ohlenschläger (FLI, Jena, Germany).[401] All NMR experiments for ^{1}H, ^{15}N, and ^{13}C chemical shift assignments were acquired using ^{15}N and ^{13}C labeled IL-36α variants (Figure 41).[401,450] A total of 4107 NOE constraints were analyzed and calculated to determine the structure of IL-36α (Figure 41, 42).[401] The detailed structural analysis was previously published (Table 6).[450]

IL-36α forms a β-trefoil structure characteristic for IL-1 cytokines (Figure 43).[401,462] The β-trefoil comprises 14 β-strands in three β-sheets (XIV-I-IV-V-VI-VII-X-XI-XII-XIII, II-III, VIII-IX), which are linked via short helical elements (one α-helix and two 3_{10} helices). Eleven loops are responsible for connecting the 14 β-strands. Among these, five show higher structural disorder (Pro34-Met39 (loop 3), Lys79-Gln82 (loop 6), Ser112-Asn115 (loop 8), Glu133-Gly135 (loop 10), Leu144-Ala147 (loop 11)) as a consequence of elevated dynamics. The putative heme-coordinating residue Cys136 is located directly after loop 10 (Glu133-Gly135), a more flexible loop that connects β-strands VII and VIII of the first β-sheet (Figure 43). Starting from Pro10 to Phe158, IL-36α adopts a predominantly folded, rigid structure. In contrast, the [^{15}N,^{1}H]-heteronuclear NOE data suggest a very flexible N-terminus (Met1-Thr9, Figure 42).[401,450] No major deviations are observed between the [^{15}N,^{1}H]-HSQC spectra of IL-36α and trIL-36α (Figure 41). In fact, despite the missing five N-terminal amino acids in trIL-36α, the NMR fingerprint appears almost similar. Consequently,

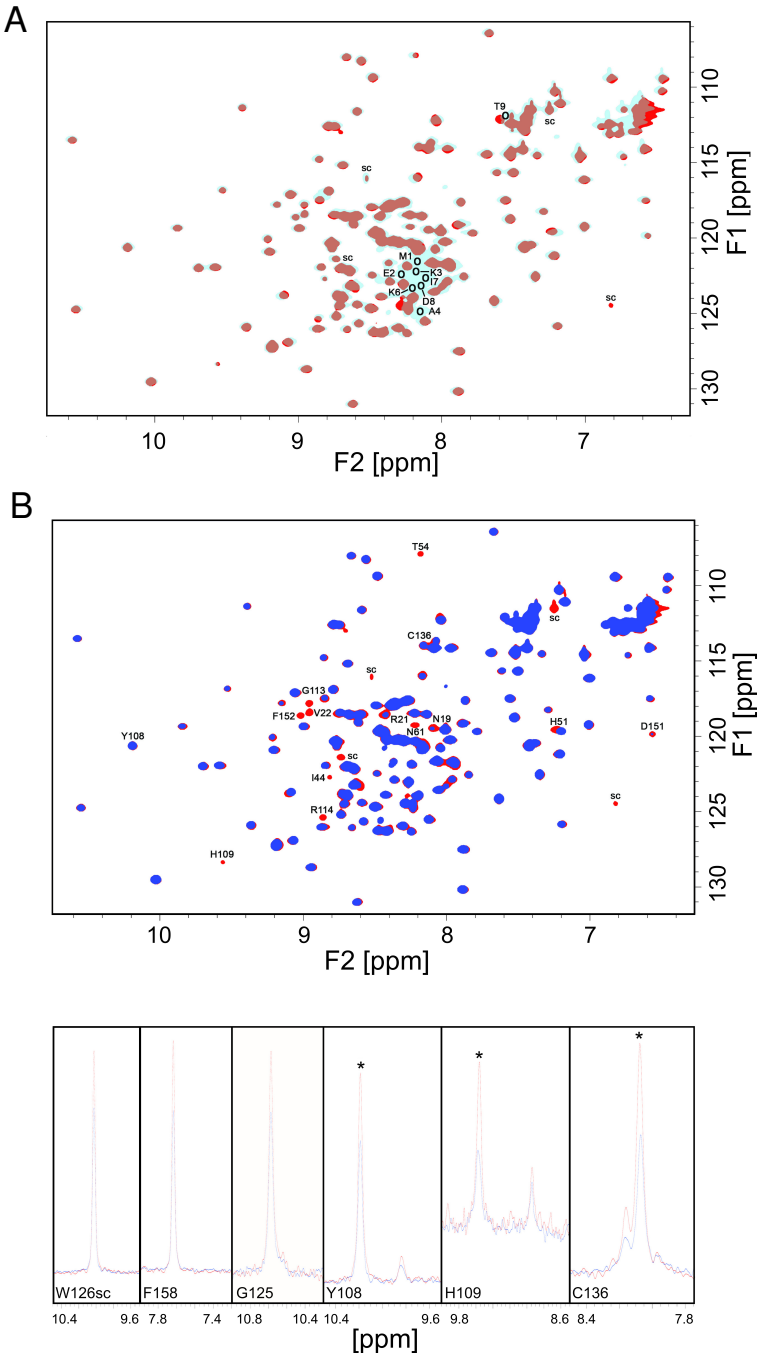

Figure 41. Structural analysis of free and heme-bound IL-36α. **(A)** Comparison of the [^{15}N,^{1}H]-HSQC spectra of full-length (cyan) and truncated IL-36α (red). Missing or shifted signals are circled in black (sc, side chain signal). **(B)** Top: Superposition of the [^{15}N,^{1}H]-HSQC spectra of free (red) and heme-bound (blue) trIL-36α. For residues Asn19, Arg21, Val22, Ile44, His51, Thr54, Asn61, His109, Gly113, Arg114, Asp151, Phe152 (sc, side chain signal) a substantial decrease in signal intensity was observed. Bottom: Moderate changes of the signal intensities affect the suggested coordinating amino acids Tyr108 and Cys136 when compared to His109 (relevant cross peaks marked by *). To allow for comparison of the uniform drop in signal intensities as a result of the solvent paramagnetic effect, traces of residues Phe158 and Gly125, which are not affected by heme binding, as well as the side chain signal of W126 are provided. Modified from Wißbrock et al. 2019.[401]

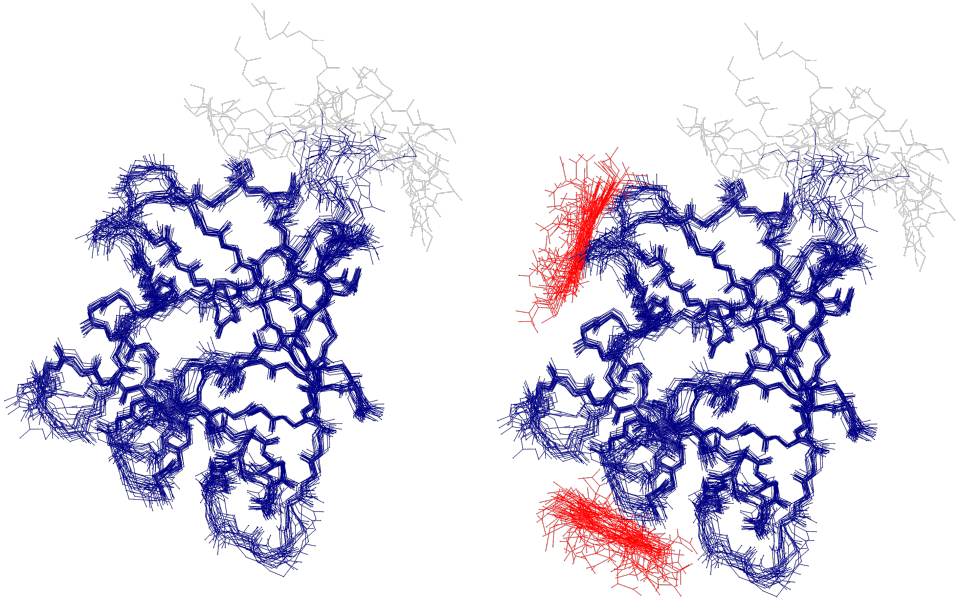

Figure 42. Stereoview of the 20 best energy-minimized conformers of IL-36α and the heme-IL-36α complex. The flexible N-terminal residues (Met1-Leu5) are colored in grey. Modified from Wißbrock et al. 2019.[401]

truncation of the cytokine does not seem to alter the general 3D fold of the protein, which further supports the anticipated similar binding mode of both cytokine species.[401]

The X-ray structure of another IL-36 family member, IL-36γ, was recently published.[385] IL-36γ shares the IL-1 characteristic β-trefoil structure as well as 67 % sequence homology (with 57 % identity) with IL-36α (Table 10). Remarkably, superimposition of the structure of IL-36α and family member IL-36γ (PDB 4IZE[385]) reveals a root-mean-square deviation (RMSD) of 1.63 Å based on the backbone atoms of Pro10 to Phe158 when excluding the loop regions (Figure 44).[401,450]

Subsequently, NMR spectra of heme-incubated IL-36α were recorded and [^{15}N,^{1}H]-HSQC NMR cross peak intensities were superimposed with the earlier obtained spectra of the pure protein (Figure 41). No change in the structural scaffold is observed for heme-incubated IL-36α (Figure 45). Yet, the signal intensities of various residues are decreased: Asn19, Arg21, Val22, Ile44, His51, Thr54, Asn61, Tyr108, His109, Gly113, Arg114, Cys136, Asp151, Phe152 (Figure 41). Moreover, Cys136 and Tyr108 appear as heme-coordinating residues, while the signal of His109 disappears at the given threshold. It is worth noting that neighboring residues may be subject to stronger effects due to smaller distances of the amide hydrogens and the metallic center, as implemented by the HN of the *de facto* interacting ligand. Because of the well-known disadvantageous of heme for NMR spectroscopy, spectra of Ga^{3+}-protoporphyrin were also recorded. Comparable signal attenuations verify a similar binding situation

as earlier found for heme.[401,450]

5.2.10 Computational Modeling of IL-36α and its Protein Variants

Recombinant expression of isotope-labeled IL-36α variants in M9 medium as required for NMR analysis was not successful. Hence, *in silico* computational modeling was conducted to determine the protein structure of the IL-36α mutants as well as to simulate heme binding to IL-36α and its variants. Molecular docking and molecular dynamics (MD) simulations were performed by Ajay Abisheck Paul George (group of Prof. Dr. Diana Imhof, University of Bonn, Germany) based on the NMR structures of the free and heme-bound IL-36α protein (*cf.* Chapter 5.2.9).[401]

Over the course of the molecular dynamics simulation of IL-36α and the mutant proteins, equilibration is reached after ∼150 ns simulation time according to the time evolution of the backbone RMSD (Figure 46). With the initial structure (NMR data) as reference, fluctuations in IL-36α yield a general RMSD deviation of 3.34 Å, which is primarily caused by the C- and N-terminal residues (∼8 Å from mean positions). The high flexibility of the N-terminal residues is also quantitatively characterized by the high RMSF values found for the N-terminal region (Figure 46). Comparing the solvent accessible surface area (SASA) of IL-36α and its mutants reveals a decrease of the values for the Y108SH109A mutant, while an increase is observed for the C136SP137A mutants (Figure 47). No major deviation is monitored for the remaining mutants compared to the wild-type protein (Figure 47). The respective change of the SASA values is conceivable since replacing residues with higher or lower mean SASA values, respectively, is expected to have a general effect on the protein's solvent accessible

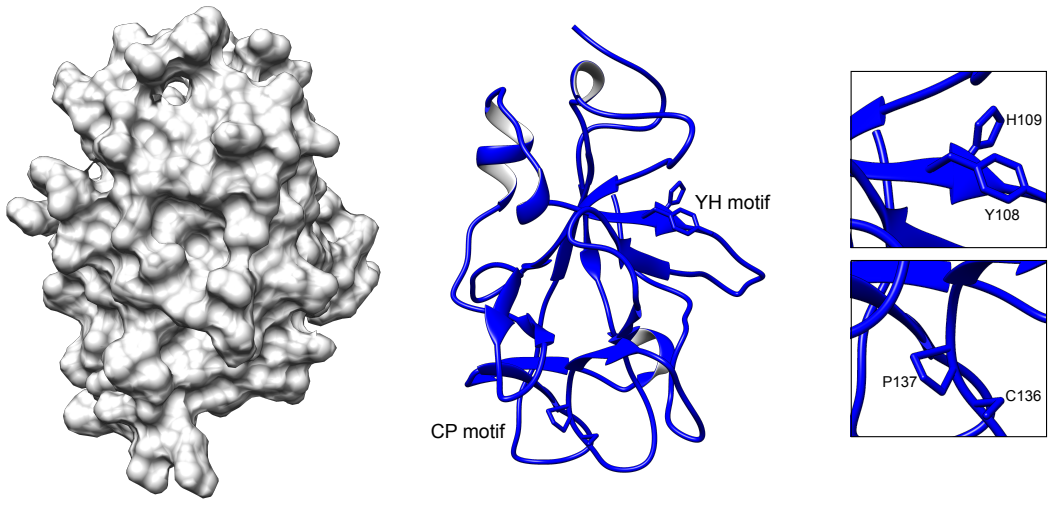

Figure 43. Structure of IL-36α. 3D schematic representations of IL-36α as surface (left) and ribbon diagram (middle) as well as close-ups (right) of the potential heme-binding sites. Modified from Wißbrock et al. 2019.[401]

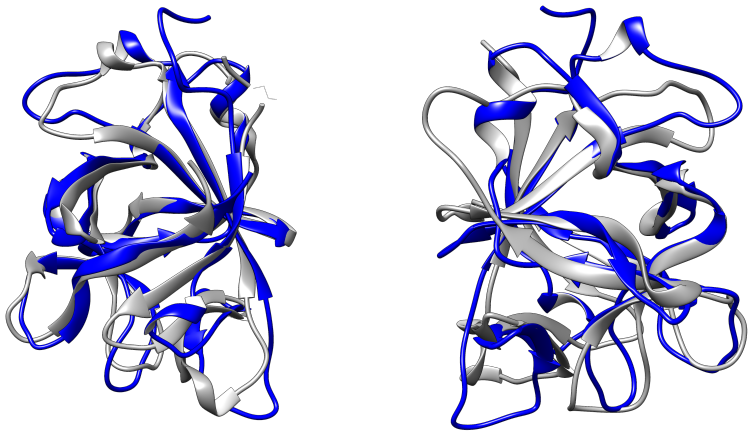

Figure 44. Superimposition of IL-36α (blue) and the crystal structure of IL-36γ (grey, PDB 4IZE,[385] left) as well as of IL-1β (grey, PDB3O4O,[463] right). Modified from Wißbrock et al. 2019.[401]

surface area (Tyr46 Å^2, His54 Å^2, Cys17 Å^2, Ala28 Å^2, Ser39 Å^2). Superimposition of the C_α atoms of wild-type IL-36α and the final frame from MD simulations of the mutant proteins indicates no major changes of the protein scaffolds (Figure 48).[401]

Molecular docking of heme to IL-36α as predicted by the Vina docking algorithm supports the experimental data.[401,464] Accordingly, the top two heme-IL-36α complexes feature heme coordination via C136 and Y108, respectively. For heme coordination via C136, the iron ion is placed 2.72 Å from the sulfur atom of C136.

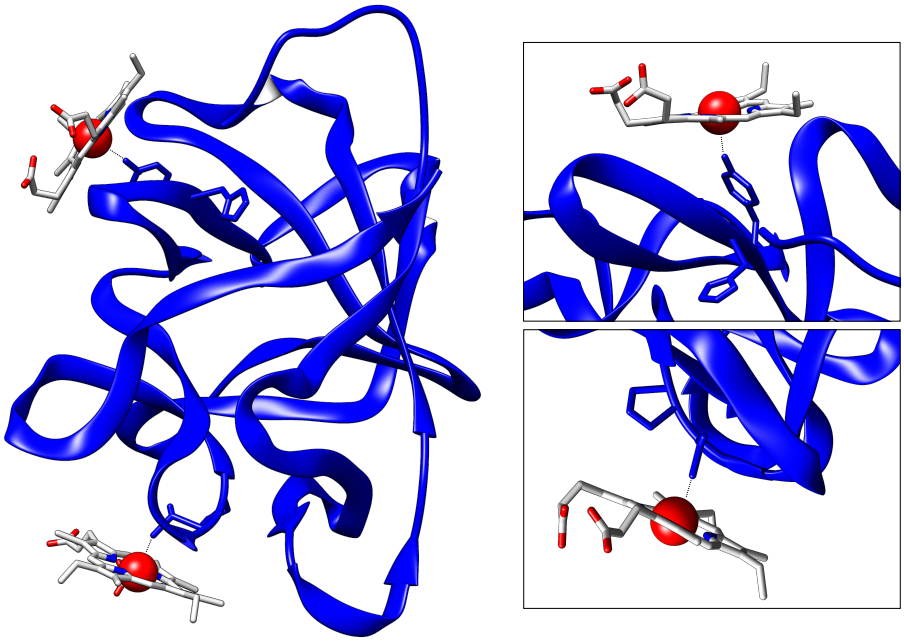

Figure 45. Structure of the heme-IL-36α complex. Modified from Wißbrock et al. 2019.[401]

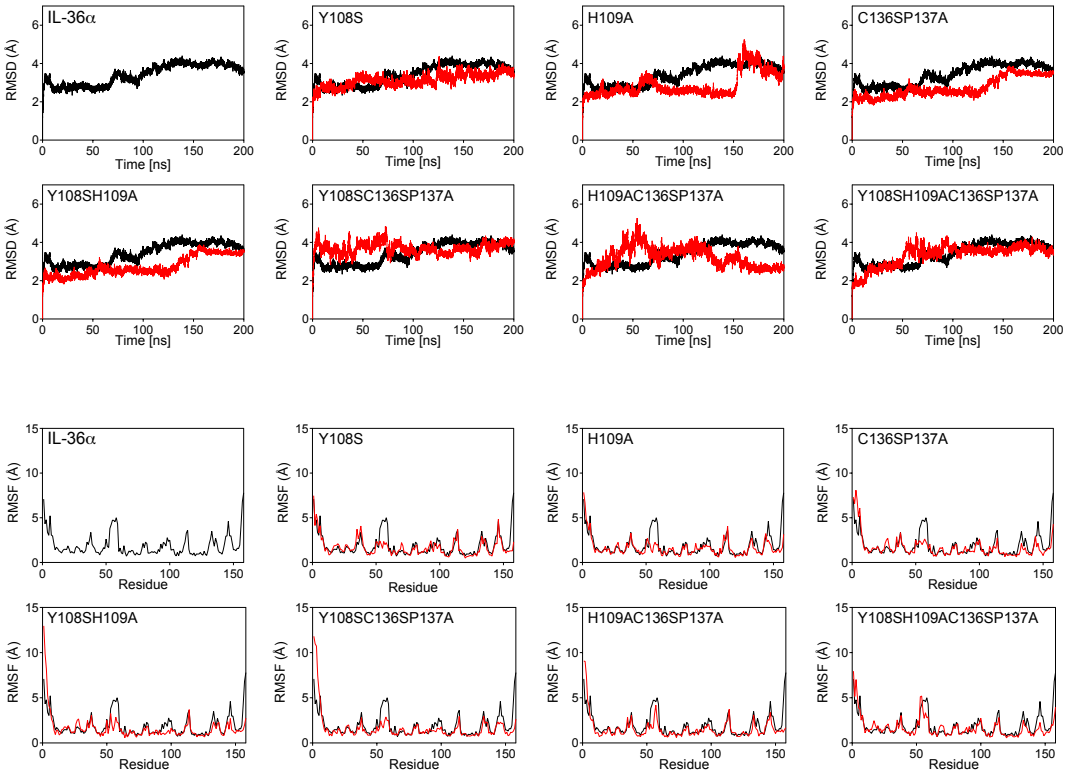

Figure 46. Backbone root-mean-square deviation (RMSD, top) and root-mean-square fluctuation (RMSF) per residue (bottom) of IL-36α and its mutant proteins.

Stabilizing interactions of surrounding amino acids foster the interplay, among the residues are Thr29, Ile31, Ala32, Val33, Pro34, Ser132, Glu133, Gly134, Gly135, Pro137, Leu138, Ile139, and Asn148. In case of heme coordination via Y108, the heme iron ion is 2.32 Å away from the oxygen atom of Y108 and again several other residues are involved, among them are Asp58, Arg59, His109, Ser110, Ser112, Thr117, and Phe127. Remarkably, heme binding to C136 appears to be a prerequisite for a stable interaction via Y108. This observation might result from the conformational

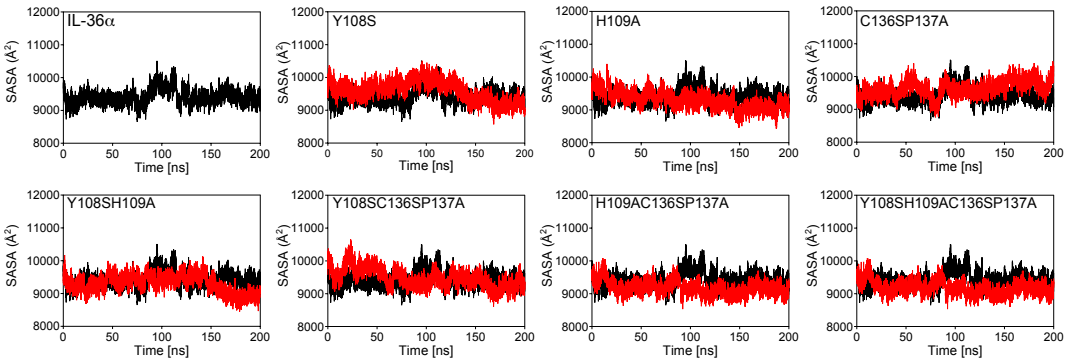

Figure 47. Time evolution of the solvent accessible surface area (SASA) of IL-36α and its mutant proteins.

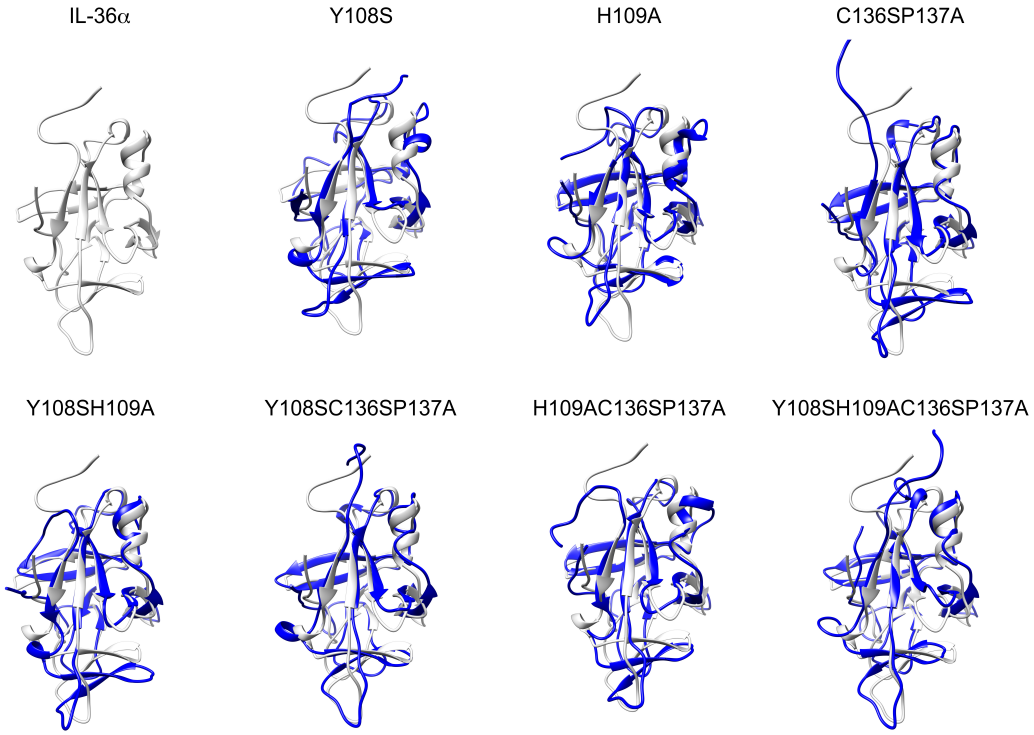

Figure 48. *In silico* models of the IL-36α mutant proteins. Structural models (blue) were generated based on the NMR structure of IL-36α (grey). Modified from Wißbrock et al. 2019.[401]

flexibility of loop 6 (Lys79-Gln82) and 10 (Glu133-Gly135) as well as parts of loop 3 (Pro34-Met39), which is reduced upon heme binding to C136 (*cf.* Chapter 5.2.9). Consequently, the overall flexibility of IL-36α is decreased and binding to Y108 is supported. Heme binding to Y108 is also observed in the absence of C136P137, however, the porphyrin dislocates much faster (5 ns vs. 150 ns). Unlike docking heme to C136 and Y108, docking heme to H109 requires restriction of the docking search space. Besides, heme promptly dislocates from the protein during the simulation of the docked complex. Hence, in agreement with the UV/Vis studies (*cf.* Chapter 5.2.6), a heme interaction via H109 appears less likely.[401]

Besides heme binding to the proposed motifs, an additional interaction is observed for all IL-36α variants. This interplay is characterized by heme binding to Ser104 as found by a 2.42 Å distance from the heme iron ion to the oxygen atom of the serine residue. No coordinative bond is formed, yet an interplay involving the porphyrin's electrostatic and hydrophobic features is conceivable. This finding might explain the UV/Vis differential spectrum of the Y108SH109AC136SP137A mutant which indicates heme binding to the protein despite the absence of the two suggested coordinating residues.[401]

5.2.11 Impact of Heme Binding on IL-36α Receptor Binding

In order to get an impression of whether IL-36α receptor binding takes place and, moreover, whether heme binding to IL-36α impacts the interaction with the receptor, computational modeling studies were performed by Dr. O. Ohlenschläger (FLI, Jena, Germany). The crystal structure of IL-1β bound to the ectodomains (D1 or D3) of IL-1 receptor type II (IL-1RII) and IL-1RAcP (PDB 3O4O[463]) was utilized for modeling (Figure 49).[401]

Initially, the NMR-structure of IL-36α was superimposed on the structure of IL-1β (Figure 44).[401] IL-1β and IL-36α share 32.71 % sequence identity (Table 10). Excluding loop areas, an RMSD of 2.15 Å (IL-36α residues 10-15, 20-28, 29-34, 42-49, 60-87, 101-143, 149-158) ensures similar backbone folds of the two cytokines.

Simulating receptor binding of full-length IL-36α reveals that the first five residues (Met1-Leu5) cannot enter a V-shaped cleft in the third domain (D3) of IL-1RII near residues Trp260 and Gly280, although the sequence stretch is characterized by high structural flexibility (Figure 49). As opposed to the full-length protein, the biologically active species (trIL-36α) is missing Met1-Leu5. Remarkably, the remaining residues of trIL-36α, i.e. Lys6 to Thr9 of the protein chain, are able to enter the V-shaped cleft. Hence, these sterical clashes of the full-length protein and the receptor might

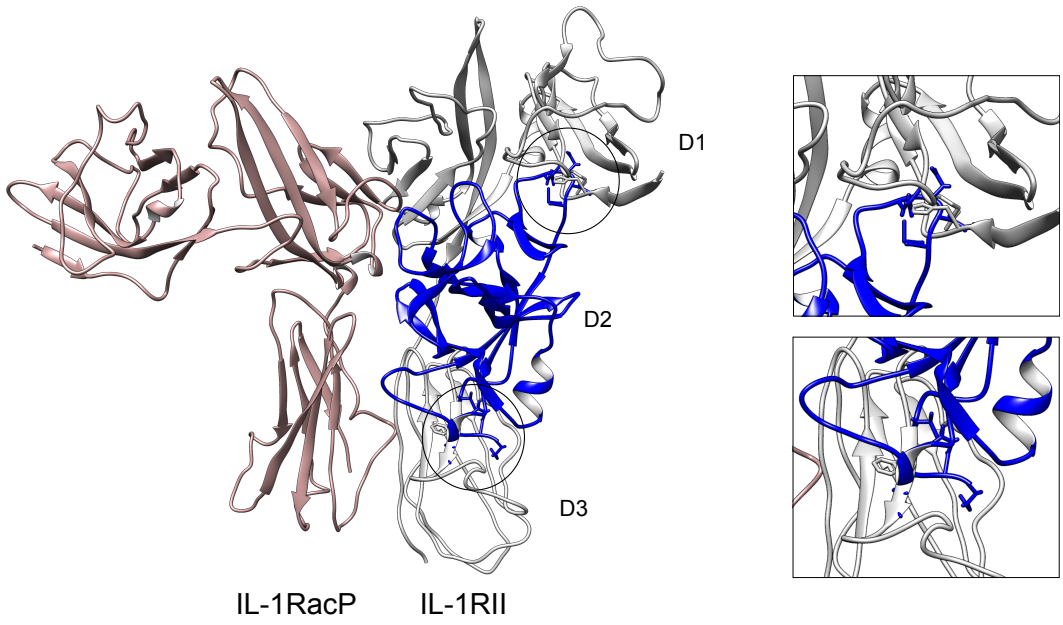

Figure 49. Superimposed structure of IL-36α (blue) and the heterodimeric IL-1β receptor complex (IL-1RacP in rosy brown, IL-1RII in grey, PDB3O4O[463]). The receptor domains D1 to D3 are labeled. The circles mark the areas of molecular clashes between IL-36α and IL-1RII, which are also depicted as close-ups on the right side. Modified from Wißbrock et al. 2019.[401]

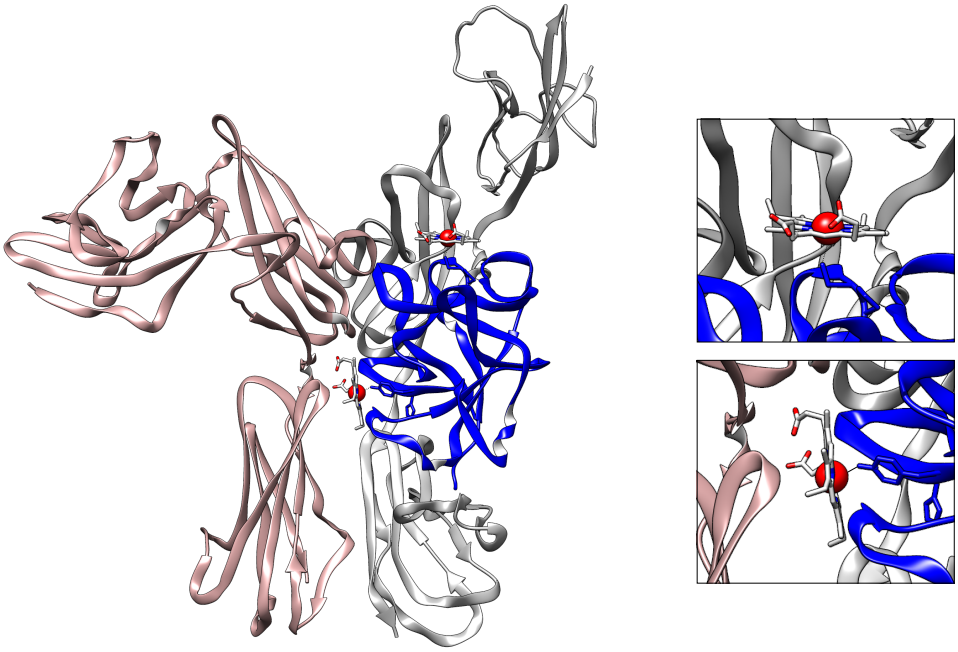

Figure 50. Superimposed structure of the heme-IL-36α complex and the IL-1β receptor complex (PDB3O4O[463]). Heme-binding sites are presented as close-ups on the right side. Coloring as in Figure 49. Modified from Wißbrock et al. 2019.[401]

explain the requirement for proteolytic activation of the cytokine. This is further supported by the collision of the N-terminal five residues with residues from the D3 domain of the receptor. In addition, a flexible loop area (Lys36 -Met39) of IL-36α clashes with residues His21 to Arg24 of domain D1 (Figure 49).

D1 and D2 are linked via a rotatable chain (E114-T116) that facilitates reposition of D1. Thereby, van der Waals interactions between the cytokine and the receptor are impeded. Moreover, domain rotation may destroy an H-bond between D1 and D2 (Arg27Hη12/22-Y125Oη). D3 is connected to D2 via a short sequence stretch including residues Arg214 to Thr222. Accommodation of IL-36α in D3 does not require major domain rotation. Heme binding to IL-36α increases the overall gross shape of the molecule and might thus further induce sterical clashes, in particular considering D1 of IL-1RII and the linker between D2 and D3 of IL-1RAcP (Figure 50.[401]

5.2.12 Heme Modulates IL-36-Mediated Signaling

Previous studies have shown that IL-36 cytokines affect the cytokine production of synovial fibroblast-like synoviocytes (FLS) *in vitro*. IL-36 treatment of FLS isolated from RA patients resulted in induction of the proinflammatory mediators IL-6 and IL-8.[400,465]

In an effort to examine a putative functional impact of heme binding to trIL-36α,

cell tests were performed by Dr. Silke Frey and Dr. Dr. Axel Hueber (University Hospital Erlangen, Germany). Therefore, isolated FLS were incubated with either trIL-36α or the preformed heme-trIL-36α complex for 24 hours.[401] trIL-36α (5.8 nM) and heme were tested in a 1:26 and 1:260 molar ratio (0.15 , 1.5 µM heme). These concentrations were chosen in consideration of previous studies, since serum albumin present in the medium readily binds and scavenges heme.[226,401] After 24 hours, the expression of IL-6 and IL-8 was quantified on the mRNA level by qRT-PCR. Furthermore, the levels of IL-6 and IL-8 were determined in the cell culture supernatant by ELISA.[401] Heme did not adversely affect cell viability under the given conditions as confirmed by live/dead staining using the AlamarBlue assay (Figure 52).[401,466]

The data gained by qRT-PCR correlate with the results from ELISA. As anticipated, IL-36α induced IL-6 and IL-8 expression in FLS, whereas heme alone did not have any effect (Figure 51). Cell treatment with the heme-trIL-36α complex resulted in significantly reduced induction of IL-6 and IL-8 expression compared to trIL-36α. To further verify the effect of the heme-trIL-36α complex on the intracellular signal

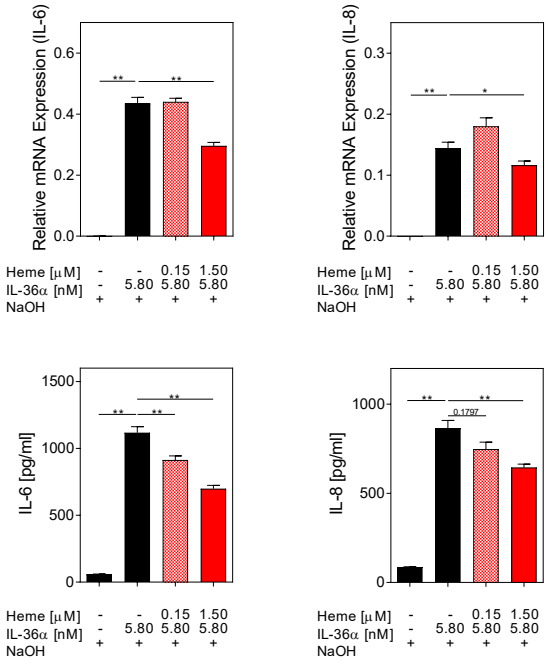

Figure 51. Biological testing of trIL-36α. Fibroblast-like synoviocytes (FLS) isolated from RA patients were treated with IL-36α, heme, and the heme-IL-36α complex for 24 h. Relative mRNA expression of IL-6 and IL-8, normalized to GAPDH, was quantified by real time PCR (top). In addition, the concentration of IL-6 and IL-8 in the cell culture supernatant was determined by ELISA (bottom). One representative experiment (n = 6) of two independent experiments is depicted. Values are means + SEM. Statistical analysis was carried out using Mann-Whitney Test Bonferroni corrected with *$p < 0.05$ and **$p < 0.01$. Modified from Wißbrock et al. 2019.[401]

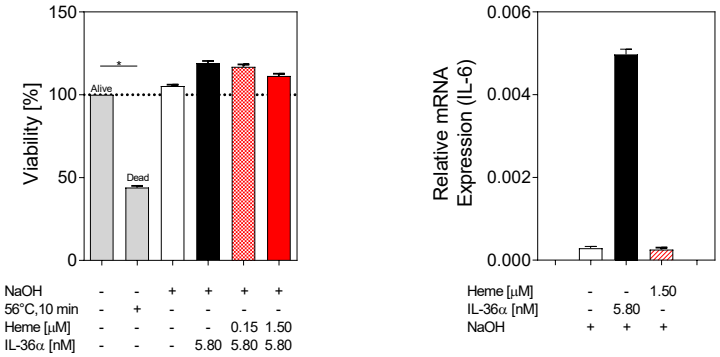

Figure 52. Effect of heme on cell viability of FLS as well as on IL-6 induction. Cell viability of FLS isolated from RA patients upon treatment with IL-36α, heme, and the heme-IL-36α complex for 24 h (left). Cell viability of FLS was tested using the AlamarBlue assay (Invitrogen, Carlsbad, CA, USA). Statistical analysis for samples with decreased cell viability was conducted using the Wilcoxon matched-pairs signed rank test with $^*p < 0.05$. Values are means + SEM ($n = 6$). Relative mRNA expression of IL-6, normalized to GAPDH, upon heme incubation of FLS for 24 h was quantified by real time PCR (right, *cf.* Figure 51). Modified from Wißbrock et al. 2019.[401]

cascade that is initiated by trIL-36α, p38 mitogen-activated protein kinase (p38) was chosen as a suitable intracellular marker.[401] Activation of p38 MAP kinase is achieved by combined phosphorylation at Thr180 and Tyr182.[467] Western Blot analysis of both p38 and phosphorylated p38 confirm the impairing effect of heme binding to trIL-36α on trIL-36α signaling (Figure 53).[401]

The SPR analysis suggests that heme also binds to the other IL-36 agonistic cytokines, trIL-36β and trIL-36γ. Thus, a possible functional effect of heme binding to trIL-36β and trIL-36γ was investigated using the same FLS-based cell assay. Heme binding impaired IL-36 signaling of all IL-36 agonistic cytokines as found by

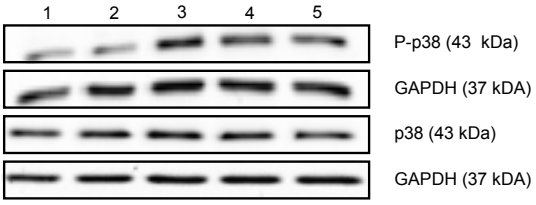

Figure 53. Effect of heme on IL-36α-induced intracellular signaling in FLS. FLS isolated from RA patients were treated with IL-36α, heme, and the heme-IL-36α complex for 5 min. Numbering is as follows: 1) control, 2) 1.5 µM heme, 3) 5.8 nM IL-36α, 4) 0.15 µM heme, 5.8 nM IL-36α (pre-incubated), and 5) 1.5 µM heme, 5.8 nM IL-36α (pre-incubated). Western blot analysis followed after sample separation by a reducing 2D gel electrophoresis. For experimental details see Chapter 4.7.4. One representative (of $n = 4$) Western blot for phosphorylated p38 (P-p38) and p38 with respective GAPDH loading control is shown. Modified from Wißbrock et al. 2019.[401]

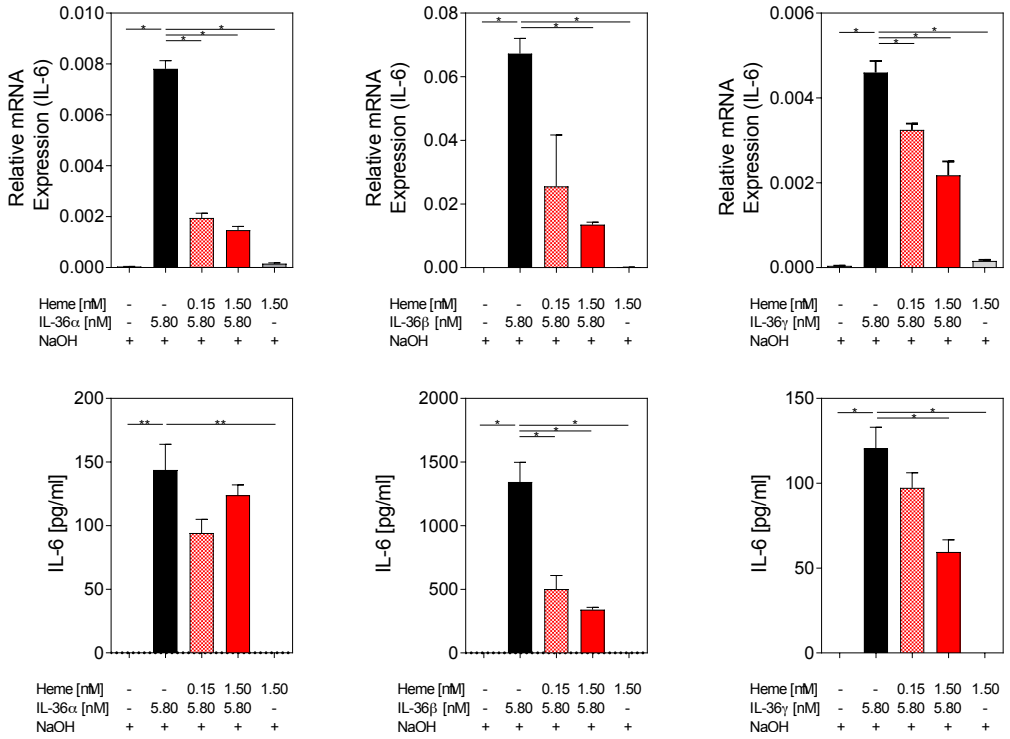

Figure 54. Biological testing of agonistic IL-36 cytokines. FLS were treated with trIL-36α, trIL-36β, trIL-36γ, heme, and the respective heme-complexes for 24 h. Relative mRNA expression of IL-6 and IL-8, normalized to GAPDH, was quantified by real time PCR (top). In addition, the concentration of IL-6 and IL-8 in the cell culture supernatant was determined by ELISA (bottom). One representative experiment (n = 5) of two independent experiments is depicted. Values are means + SEM. Statistical analysis was carried out using the Mann-Whitney Test Bonferroni corrected with *$p < 0.05$ and **$p < 0.01$. Modified from Wißbrock et al. 2019.[401]

significantly reduced levels of IL-6 compared to the respective (pure) IL-36 cytokine (Figure 54).

To elucidate the impact of the suggested binding motifs, the seven trIL-36α mutants were incubated with heme in the same experimental set-up as described above. A significant reduction of the IL-6 expression in FLS was observed for all protein mutants compared to wild-type trIL-36α (Figure 55). Only mutant C136P137 showed residual activity on FLS. Thus, the data indicate that the site-directed mutation of residues Y108, H109, C136, and P137 has a significant effect on the protein's functionality. This might be a result of major structural rearrangements resulting in a different protein fold and consequently in an alteration of the protein's biological activity. The results attained by molecular modeling and docking studies (*cf.* Chapter 5.2.10) oppose this hypothesis, since no major structural rearrangements of the mutant proteins were found. Yet, experimental proof is missing and further

studies are needed to rule out this opportunity. In addition, the mutated residues (Y108, H109, C136, and P137) might be crucial for the IL-36α receptor interplay. This observation is supported by the fact that the cytokine variant without a mutation of Y108 and/or H109, is the sole protein with residual biological activity, despite a substantial decrease in signaling compared to wild-type IL-36α. Therefore, the sequence stretch around Y108H109 might exhibit a pivotal role for the interaction between IL-36α with the receptor complex.[401]

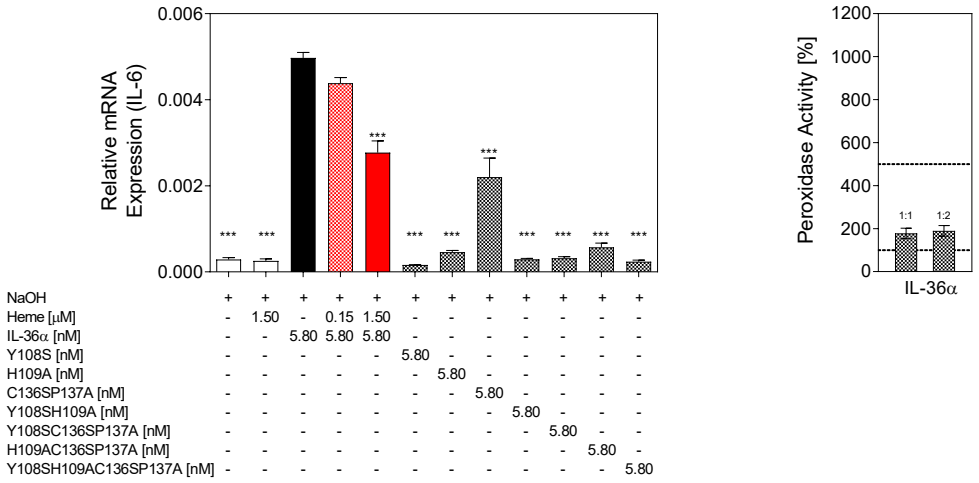

Figure 55. Biological testing of IL-36α mutant cytokines as well as analysis of the catalytic activity of the heme-IL-36α complex. FLS were treated with trIL-36α and mutant proteins for 24 h (left panel). Relative mRNA expression of IL-6 and IL-8, normalized to GAPDH, was quantified by real time PCR (n = 3). Values are means + SEM. Statistical analysis was performed using One-Way Anova Test Dunnet corrected with *$p < 0.05$ and **$p < 0.01$ and ***$p < 0.0001$ for comparisons with recombinant trIL-36α. In addition, the catalytic activity of the heme-IL-36α complex (1μM, 1:1 and 1:2 protein:heme ratio) was tested in approach II (*cf.* Figure 18, Chapter 5.1.2, right panel).

5.2.13 Peroxidase Activity of the Heme-IL-36α Complex

The pseudo-peroxidase activity of heme-peptide/protein complexes has been associated with the cytotoxic activities of heme, in particular with ROS formation.[17,40] The most prominent example is Aβ that was found to have a significant catalytic activity in complex with heme (*cf.* Chapter 2.4.2).[40] To test whether IL-36α has an impact on the autocatalytic activity of heme, the chromogenic assay introduced earlier was performed (*cf.* Chapter 5.1.2). IL-36α was tested for its activity upon incubation with heme in a ratio of 1:1 and 1:2. No increase of activity higher than 200 % was observed for the heme-IL-36α complex (Figure 55). Therefore, the heme-IL-36α complex does not possess a relevant catalytic activity under the conditions tested.

The performed experiments demonstrate heme binding to the proinflammatory cytokine IL-36α. The structural characterization of the formed complex indicates binding of two heme molecules to different sites on the surface of IL-36α. Moreover, the *in vitro* cell assays suggest diminished IL-36 signaling upon heme binding.

6 Conclusions

Heme is a versatile and vital molecule which is entangled in a plethora of biological processes. Beyond that, a crucial role of the metalloporphyrin emerges in assorted pathological conditions. In light of this, a thorough analysis of the underlying principles of all of its functions is pivotal for the understanding of diseases in question as well as future treatment strategies. This thesis is dedicated to the realm of heme, in particular to the field of biologically available heme. In the first instance, the pseudo-peroxidase activity of heme-binding peptides was examined with regard to a potential application as diagnostic tool for quantification of heme in patient samples. Besides determining heme concentrations in body fluids, it is a major concern to identify physiological components affected by elevated heme levels as frequently encountered in disorders associated with hemolysis. Hence, IL-36α, a potentially heme-regulated protein, was investigated herein with respect to heme binding as well as the structural and functional impact of the respective interaction.

Despite increasing interest in sensitive heme quantification assays, there are only a few promising approaches available to date. In an attempt to identify a peptide candidate that can be deployed as apo-peroxidase in a heme quantification assay, the potential pseudo-peroxidase activity of Aβ-derived and Aβ-independent heme-peptide complexes was analyzed. Examination of these peptides demonstrated that a substantial catalytic activity is not exclusive to the heme-Aβ complex but also exists for distinct heme-peptide complexes. The studies imply the requirement for distinct residues in the primary sequence as well as for a minimal peptide sequence length (at least 10 to 25 amino acids) for the formation of a catalytically active heme-peptide complex. Moreover, binding of the porphyrin to the peptide is a prerequisite, however, there is no direct correlation between the binding affinity and the extent of catalytic activity. Notably, the requirement of an acidic pH for the Fenton reaction to proceed was once again observed during the performed experiments. The necessity for an acidic environment must be considered when evaluating the physiological relevance of *in vitro* findings and also with regard to a putative impact on components of patient samples (e.g. proteins).[99]

For the heme-Aβ complex, heme coordination via His13/His14 was confirmed,

which is in good agreement with other studies.[99,292] Moreover, the peptide seems to interact with at least two heme molecules, with one interaction being mediated via the lipophilic part (site-L) of the peptide despite the absence of heme-coordinating residues. Characterization and comparison of the two peptides with the highest catalytic activity in complex with heme, Aβ40 (500 %) and 23mer peptide **18** (>1000 %), revealed heme coordination via a histidine residue in both complexes (Figure 56). Furthermore, H-bond formation of the propionate carboxylic function with a distal basic residue occurs in either complex according to molecular modeling studies.[99] The Arg5 residue in Aβ is suggested to substantially contribute to the pseudo-peroxidase activity.[293] Since no arginine is present in peptide **18**, one might assume that another basic residue resumes this function (e.g. Lys16). In addition, Aβ and peptide **18** exhibit one (Tyr10, Aβ) or two (Tyr11, Tyr13, peptide **18**) tyrosine residues in close proximity to the coordinating residue as well as one (His5, Aβ) or two (His8, His19, peptide **18**) distal histidine residues, which might support the reaction progress.[99] The latter is a sequence feature that is well known from heme peroxidases.[436] Alanine mutation of the histidines in peptide **18** individually and in combination shows, however, that these residues have only a minor effect on the catalytic activity. Hence, the presence of a distal histidine residue is not pivotal for a catalytic activity to occur. Furthermore, the modeling studies indicate helical structural elements in both peptide chains. This finding, together with the observation that a minimal sequence length seems to be required, indicate that the presence of secondary structural elements might favor the generation of a catalytically active complex. The observation that all truncated Aβ peptides exhibit a substantially decreased pseudo-peroxidase activity in complex with heme compared to Aβ40 further supports this hypothesis.[99] Besides basic research, the experiments aimed at the identification of a peptide, which can prospectively be applied in a diagnostic test kit. Peptide **18** is a promising candidate. In comparison to Aβ, the physico-chemical properties (e.g. solubility) of peptide **18** are more convenient for an application as tool. Furthermore, the sequence is 17 amino acids shorter which would make an industrial synthesis less expensive compared to Aβ. Initial experiments with the heme-peptide **18** complex and human CSF verify a heme-concentration dependent substrate conversion and thus the general applicability of the established biochemical approach. Future studies with a large number of samples as well as body fluids of different nature will have to be performed to evaluate accuracy, stability, and broader applicability of the test system. It is worth noting that the development of a peroxidase-based biochemical approach is highly desirable for several reasons. The assay offers a simply applicable, cost-effective experimental set-up for the quantification of biologically available heme which – in contrast to other methods – is also suitable for less developed countries (e.g. for malaria patients in subtropical areas).[99]

Heme and Aβ are known to interact with a number of molecules *in vivo*. One of these molecules is the lipoprotein LDL, a compound elevated in AD patients, which readily binds heme.[9,443] Indeed, analyzing the impact of LDL on the catalytic activity of the heme-Aβ complex reveals a competitive situation of Aβ and LDL for heme binding. Neither Aβ nor LDL is able to scavenge the heme moiety from a preformed complex with the other component under the given experimental conditions. Yet, when all three components are present at the same time, equal amounts of the heme-Aβ and the heme-LDL complex seem to be generated. Thus, location, time, and concentration of the three molecules determine the nature of the complexes formed and, in turn, the occurrence of catalytically active heme-Aβ species. Consequently, the physiological effects derived from heme-Aβ complex formation (e.g. neurotransmitter oxidation) might also depend on the present level of LDL.[99]

In conclusion, these studies show that peptides can form catalytically active complexes with heme dependent on the occurrence of distinct residues and presumably the existence of secondary structural elements. These complexes are promising tools for the diagnostic quantification of biologically available heme in body fluids. *In vivo*, the presence of additional components might impact the formation of catalytically active complex species and related physiological effects as exemplified by the interplay of heme, Aβ, and LDL.[99]

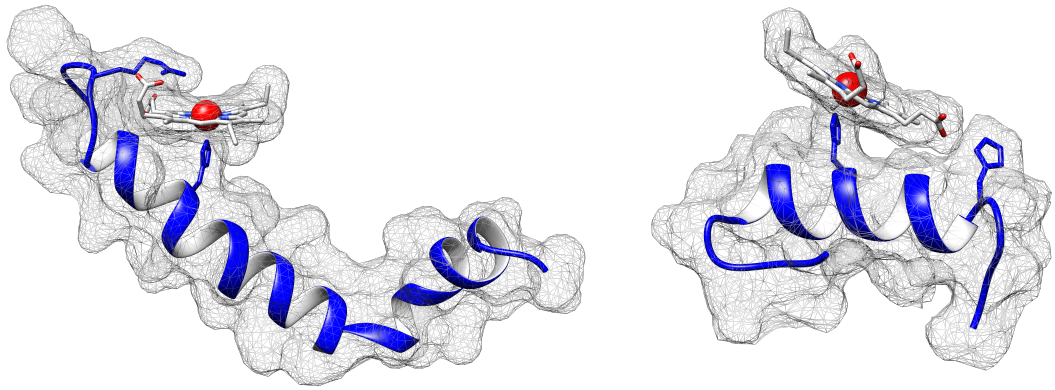

Figure 56. Heme-peptide complexes as pseudo-peroxidases. 3D structures of the two peptides with the highest catalytic activity in complex with heme, Aβ40 (500%) and 23mer peptide **18** (>1000%). Heme coordination via a histidine residue as well as H-bond formation via a distal basic residue is observed in both complexes. Modified from Wißbrock et al. 2017.[99]

Beyond the diagnostic quantification of heme, the elucidation of physiological consequences of elevated heme levels is of great interest. The regulation of protein function and stability is essential for the porphyrin's mode of operation and it is thus of great interest to identify heme-regulated proteins. The proinflammatory cytokine IL-36α has earlier been suggested to be a heme-regulated protein.[273] Heme binding to

IL-36α as well as the family members IL-36β and IL-36γ was shown in this work.[401] A biphasic binding profile with two individual interaction sites is evident for all three cytokines. Moreover, binding affinities with dissociation constants in the micromolar range were determined for either binding event. Heme-IL-36 complex formation results in diminished biological activity as indicated by decreased production of the proinflammatory cytokines IL-6 and IL-8 in cell tests.[401]

The detailed analysis of the heme-IL-36α interplay reveals binding of the porphyrin involving residues Y108H109 and C136P137. Residues Y108 and C136 are thought to function as heme axial ligands, while H109 and P137 seem to assist heme binding. Moreover, an additional interaction site, potentially non-specific, is assumed according to UV/Vis spectroscopy and molecular docking experiments. *r*Raman and 3D NMR spectroscopy insinuated the presence of a penta-coordinated heme-IL-36α complex.[401] This finding confirms earlier studies, which found that heme binding via CP-based and Y-based motifs emerged almost exclusively (CP motifs) or predominantly (Y motifs) in a penta-coordinated fashion.[273,303,309] Comparison of the 3D NMR results of the full-length with the truncated IL-36α cytokine portends no major structural alterations between the proteins. Computational docking of IL-36α to the X-ray structure of the heterodimeric receptor complex of IL-1RII and IL-1RacP shows that the structurally flexible N-terminal region (Met1 to Leu5) provokes sterical clashes between the cytokine and the receptor. This may explain the demand for proteolytic processing of the full-length protein. In accordance with the NMR results, SPR and fluorescence spectroscopy suggest a similar heme-binding mode of full-length and truncated cytokine variants. Heme binding to IL-36α further increases the steric demand in regions close to the IL-1RII domain D1 and the linker between IL-1RAcP domains D2 and D3 according to molecular docking studies. Whether heme binding inhibits IL-36 receptor binding or the recruitment of IL-1RacP after IL-36α receptor binding could not be clarified within these studies (Figure 57). It was shown, however, that heme binding to IL-36α significantly reduces the generation of the proinflammatory cytokines IL-6 and IL-8 in FLS isolated from RA patients, thereby eliciting an anti-inflammatory effect. Testing the impact of the individual binding sites on the biological activity was not feasible, due to the loss of biological activity in all variants with exception of the C136SP137A mutant. Computational modeling of mutated IL-36α variants indicates no major structural rearrangements upon mutation that may explain this loss in activity. Thus, one might hypothesize that the sequence stretch surrounding the Y108H109 motif is essential for IL-36α receptor binding.[401] Indeed, earlier studies by others have shown that point mutations can significantly alter IL-36 receptor binding and even change agonistic and antagonistic features of the ligand.[385]

As the current data is limited to *in vitro* studies, it is undisputedly necessary

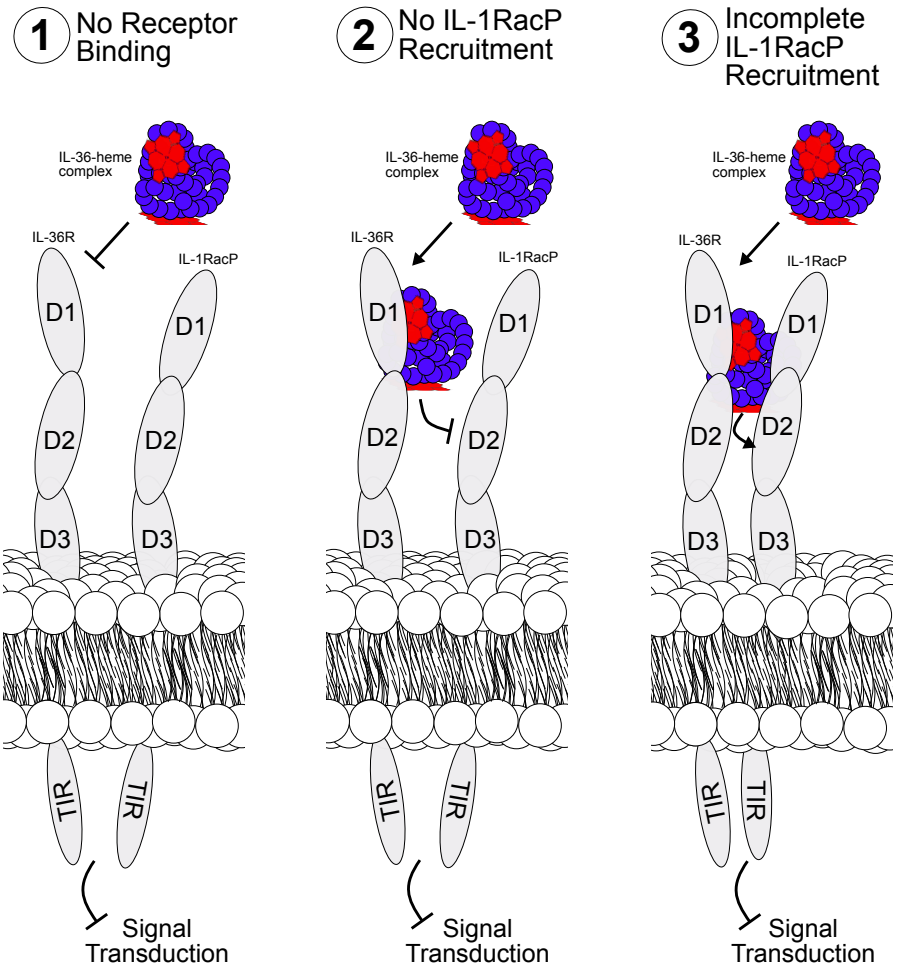

Figure 57. Different scenarios that may explain the decreased biological activity of IL-36 agonistic cytokines observed upon heme binding. IL-36-heme complex formation may prevent IL-36 receptor binding (1) or in case of receptor binding it may circumvent (2) or impair (3) recruitment of IL-1RacP. Modified from Wißbrock et al. 2019.[401]

to prospectively perform *in vivo* experiments to verify the biological significance of the obtained data. Notwithstanding, one might make an effort to put the findings into a physiological context. Heme is commonly described as a proinflammatory molecule based on the porphyrin's toxicity as well as interactions with specific proteins (e.g. TLR4).[9,16] The current study suggests that heme binding diminishes the proinflammatory stimulus of the IL-36 agonistic ligands.[401] Remarkably, heme is suggested to act as endogenous negative-feedback regulator of the complement factor C1q.[271] Heme binding to C1q leads to inhibition of the classical complement pathway and thus prevents inflammatory responses. In this context, heme might function as part of a rescue system that is initiated in case of, for example, cell damage upon heme release.[271] Whether a similar rescue system might explain the anti-inflammatory effect observed for heme binding to the IL-36 cytokines remains elusive. IL-36 cytokines

were only identified two decades ago. Therefore, the knowledge on these proteins is restricted and discussing specific heme-related physiological scenarios would be notional.

Remarkably, sequence analysis of other IL-1 family members revealed HBMs of interest in several candidates, such as IL-1Ra, IL-33, and IL-1β. This observation might enable development towards a more general concept of heme as a regulator of cytokine function. In other proteins, such as IL-18, no suitable sequences were identified, reducing the probability of heme binding. Further studies, such as an analysis of the potential motifs on the peptide level, have to be performed to verify the heme binding capacity of these sequence stretches.[401]

In the course of the studies performed, IL-36α was identified as a heme-binding protein, which was previously unknown. The detailed spectroscopic investigation provided structural data of the interaction taking place. To find out whether the underlying concept is not restricted to IL-36 cytokines but plays a more general role in inflammatory processes, future studies should address possible heme interactions with other IL-1 family members that might be subject to heme regulation.[401]

The present work contributes to the understanding of the alternative functions of heme. Based on the characterization of the catalytic activity of various heme-peptide complexes, an assay system was established, which might prospectively be developed into a diagnostic tool. Beyond that, binding of heme to the proinflammatory cytokine IL-36α was proven. The interaction results in a decrease of IL-36α-mediated signaling. Moreover, the structural investigations of the heme-protein complex does not only afford detailed insight into the interaction taking place, but contributes to the rare structural characterization of transient heme-protein complexes. While many questions remain to be addressed, one thing is certain. The complex properties, the numerous functions, and the presence in the blood render heme an essential molecule for life. After all, Goethe's Mephisto proved to be right: "Blood is a very special juice".

Bibliography

[1] J. W. von Goethe. Faust. Der Tragödie erster Teil. **1808**, Verse 1740.

[2] B. Hayes. Five quarts: A personal and natural history of blood. *Random House Trade Paperbacks* **2006**.

[3] A. D'Alessandro, L. Zolla. Proteomic analysis of red blood cells and the potential for the clinic: What have we learned so far? *Expert Review of Proteomics* **2017**, *14*, 243–252.

[4] I. U. Heinemann, M. Jahn, D. Jahn. The biochemistry of heme biosynthesis. *Archives of Biochemistry and Biophysics* **2008**, *474*, 238–251.

[5] P. Ponka. Cell biology of heme. *The American Journal of the Medical Sciences* **1999**, *318*, 241–256.

[6] M. Paoli, J. Marles-Wright, A. Smith. Structure-function relationships in heme-proteins. *DNA and Cell Biology* **2002**, *21*, 271–280.

[7] V. Jeney, J. Balla, A. Yachie, Z. Varga, G. M. Vercellotti, J. W. Eaton, G. Balla. Pro-oxidant and cytotoxic effects of circulating heme. *Blood* **2002**, *100*, 879–887.

[8] T. L. Poulos. The Janus nature of heme. *Natural Product Reports* **2007**, *24*, 504–510.

[9] R. Larsen, Z. Gouveia, M. P. Soares, R. Gozzelino. Heme cytotoxicity and the pathogenesis of immune-mediated inflammatory diseases. *Frontiers in Pharmacology* **2012**, *3*, 77.

[10] D. Chiabrando, F. Vinchi, V. Fiorito, S. Mercurio, E. Tolosano. Heme in pathophysiology: a matter of scavenging, metabolism and trafficking across cell membranes. *Frontiers in Pharmacology* **2014**, *5*, 61.

[11] I. Hamza, H. A. Dailey. One ring to rule them all: Trafficking of heme and heme synthesis intermediates in the metazoans. *Biochimica et Biophysica Acta* **2012**, *1823*, 1617–1632.

[12] F. A. D. T. G. Wagener, H.-D. Volk, D. Willis, N. G. Abraham, M. P. Soares, G. J. Adema, C. G. Figdor. Different faces of the heme-heme oxygenase system in inflammation. *Pharmacological Reviews* **2003**, *55*, 551–571.

[13] N. Wijayanti, N. Katz, S. Immenschuh. Biology of heme in health and disease. *Current Medicinal Chemistry* **2004**, *11*, 981–986.

[14] T. Chernova, A. G. Smith. Role of heme in brain functions, Dr. Jekyll or Mr. Hyde? *in Heme biology: The secret life of heme in regulating diverse biological processes* **2011**, 85–126.

[15] H. Puy, L. Gouya, J. C. Deybach. Porphyrias. *The Lancet* **2010**, *375*, 924–937.

[16] F. F. Dutra, M. T. Bozza. Heme on innate immunity and inflammation. *Frontiers in Pharmacology* **2014**, *5*, 115.

[17] C. Ghosh, M. Seal, S. Mukherjee, S. Ghosh Dey. Alzheimer's disease: A heme-Aβ perspective. *Accounts of Chemical Research* **2015**, *48*, 2556–2564.

[18] S. Immenschuh, V. Vijayan, S. Janciauskiene, F. Gueler. Heme as a target for therapeutic interventions. *Frontiers in Pharmacology* **2017**, *8*, 146.

[19] D. Chiabrando, V. Fiorito, S. Petrillo, E. Tolosano. Unraveling the role of heme in neurodegeneration. *Frontiers in Neuroscience* **2018**, *12*, 712.

[20] R. Martins, S. Knapp. Heme and hemolysis in innate immunity: adding insult to injury. *Current Opinion in Immunology* **2018**, *50*, 14–20.

[21] L. Zhang. Heme biology: The secret life of heme in regulating diverse biological processes. *World Scientific* **2011**.

[22] T. Kühl, D. Imhof. Regulatory FeII/III heme: The reconstruction of a molecule's biography. *ChemBioChem* **2014**, *15*, 2024–2035.

[23] S. Hou, M. F. Reynolds, F. T. Horrigan, S. H. Heinemann, T. Hoshi. Reversible binding of heme to proteins in cellular signal transduction. *Accounts of Chemical Research* **2006**, *39*, 918–924.

[24] J. Igarashi, M. Murase, A. Iizuka, F. Pichierri, M. Martinkova, T. Shimizu. Elucidation of the heme binding site of heme-regulated eukaryotic initiation factor 2α kinase and the role of the regulatory motif in heme sensing by spectroscopic and catalytic studies of mutant proteins. *Journal of Biological Chemistry* **2008**, *283*, 18782–18791.

[25] J. Igarashi, K. Kitanishi, M. Martinkova, M. Murase, A. Iizuka, T. Shimizu. The roles of thiolate-heme proteins, other than the P450 cytochromes, in the regulation of heme-sensor proteins. *Acta Chimica Slovenica* **2008**, *55*, 67–74.

[26] Y. Li, L. Zhang. The chemical and structural bases of heme recognition: Binding interactions of heme with proteins and peptides. *in Heme biology: The secret life of heme in regulating diverse biological processes* **2011**, 161–196.

[27] T. Shimizu. Binding of cysteine thiolate to the Fe(III) heme complex is critical for the function of heme sensor proteins. *Journal of Inorganic Biochemistry* **2012**, *108*, 171–177.

[28] L. Hannibal, D. J. Stuehr. Non-canonical heme-binding proteins. *in Handbook of Porphyrin Science* **2012**, *30*, 55–102.

[29] H. M. Girvan, A. W. Munro. Heme sensor proteins. *Journal of Biological Chemistry* **2013**, *288*, 13194–13203.

[30] H. H. Brewitz, G. Hagelueken, D. Imhof. Structural and functional diversity of transient heme binding to bacterial proteins. *Biochimica et Biophysica Acta (BBA) - General Subjects* **2016**, *1861*, 683–697.

[31] A. S. Fleischhacker, E. L. Carter, S. W. Ragsdale. Redox regulation of heme oxygenase-2 and the transcription factor, Rev-Erb, through heme regulatory motifs. *Antioxidants & Redox Signaling* **2017**, *29*, 1841–1857.

[32] A. Wißbrock, A. A. Paul George, H. H. Brewitz, T. Kühl, D. Imhof. The molecular basis of transient heme-protein interactions: Analysis, concept and implementation. *Bioscience Reports* **2019**, BSR20181940.

[33] L. Zhang, A. Arvey, D. P. Huynh, C. Leslie. The vast potential of heme in regulating biological processes: A global perspective. *in Heme biology: The secret life of heme in regulating diverse biological processes* **2011**, 139–159.

[34] T. Kühl, N. Sahoo, M. Nikolajski, B. Schlott, S. H. Heinemann, D. Imhof. Determination of hemin-binding characteristics of proteins by a combinatorial peptide library approach. *ChemBioChem* **2011**, *12*, 2846–2855.

[35] P. R. Sinclair, N. Gorman, J. M. Jacobs. Measurement of heme concentration. *Current Protocols in Toxicology* **1999**, *8*, 8.3.

[36] H. Atamna, M. Brahmbhatt, W. Atamna, G. A. Shanower, J. M. Dhahbi. ApoHRP-based assay to measure intracellular regulatory heme. *Metallomics* **2015**, *7*, 309–321.

[37] D. A. Hanna, R. M. Harvey, O. Martinez-Guzman, X. Yuan, B. Chandrasekharan, G. Raju, F. W. Outten, I. Hamza, A. R. Reddi. Heme dynamics and trafficking factors revealed by genetically encoded fluorescent heme sensors. *Proceedings of the National Academy of Sciences of the United States of America* **2016**, *113*, 7539–7544.

[38] X. Yuan, N. Rietzschel, H. Kwon, A. B. Walter Nuno, D. A. Hanna, J. D. Phillips, E. L. Raven, A. R. Reddi, I. Hamza. Regulation of intracellular heme trafficking revealed by subcellular reporters. *Proceedings of the National Academy of Sciences of the United States of America* **2016**, *113*, E5144–E5152.

[39] A. Wißbrock, D. Imhof. A tough nut to crack: Intracellular detection and quantification of heme in malaria parasites by a genetically encoded protein sensor. *ChemBioChem* **2017**, *18*, 1561–1564.

[40] H. Atamna, K. Boyle. Amyloid-beta peptide binds with heme to form a peroxidase: relationship to the cytopathologies of Alzheimer's disease. *Proceedings of the National Academy of Sciences of the United States of America* **2006**, *103*, 3381–3386.

[41] A. Van Leeuwenhoek. More microscopical observations made by the same M. Leewenhoeck, and promised in numb. 97. Of these tracts; communicated in his letters of August 15. 1673 and of April 7. 1674. *Philosophical Transactions of the Royal Society of London* **1674**, *9*, doi.org/10.1098/rstl.1674.0010.

[42] J. M. S. Pearce. Malpighi and the discovery of capillaries. *European Neurology* **2007**, *58*, 253–255.

[43] S. I. Hajdu. The discovery of blood cells. *Annals of Clinical & Laboratory Science* **2003**, *33*, 237–238.

[44] F. L. Hünefeld. Der Chemismus in der thierischen Organization. *F. A. Brockhaus, Leipzig* **1840**.

[45] F. Hoppe-Seyler. Medicinisch-chemische Untersuchungen: aus dem Laboratorium für angewandte Chemie zu Tübingen. *A. Hirschwald, Berlin* **1866**.

[46] H. J. H. Fenton. On a new reaction of tartaric acid. *Chemistry News* **1876**, *33*, 190.

[47] H. J. H. Fenton. Oxidation of tartaric acid in presence of iron. *Journal of the Chemical Society* **1894**, *65*, 899–910.

[48] J.-L. Soret. Analyse spectrale: Sur le spectre d'absorption du sang dans la partie violette et ultra-violette. *Comptes rendus de l'Académie des sciences* **1883**, *97*, 1269–1270.

[49] H. Fischer, K. Zeile. Synthese des Hämatoporphyrins, Protoporphyrins und Hämins. *Justus Liebigs Annalen der Chemie* **1929**, *468*, 98–116.

[50] Nobel Prize Organisation. *Retrieved February 4* **2019**, www.nobelprize.org.

[51] D. W. Green, V. M. Ingram, M. F. Perutz, W. L. Bragg. The structure of haemoglobin. IV. Sign determination by the isomorphous replacement method. *Proceedings of the Royal Society of London. Series A, Mathematical and Physical Sciences* **1954**, *225*, 287–307.

[52] J. C. Kendrew, G. Bodo, H. M. Dintzis, R. G. Parrish, H. Wyckoff, D. C. Phillips. A three-dimensional model of the myoglobin molecule obtained by X-ray analysis. *Nature* **1958**, *181*, 662–666.

[53] J. T. Lathrop, M. P. Timko. Regulation by heme of mitochondrial protein transport through a conserved amino acid motif. *Science* **1993**, *259*, 522–525.

[54] X. D. Tang, R. Xu, M. F. Reynolds, M. L. Garcia, S. H. Heinemann, T. Hoshi. Haem can bind to and inhibit mammalian calcium-dependent Slo1 BK channels. *Nature* **2003**, *425*, 531–535.

[55] M. Faller, M. Matsunaga, S. Yin, J. A. Loo, F. Guo. Heme is involved in microRNA processing. *Nature Structural & Molecular Biology* **2007**, *14*, 23–29.

[56] J. Yang, K. D. Kim, A. Lucas, K. E. Drahos, C. S. Santos, S. P. Mury, D. G. S. Capelluto, C. V. Finkielstein. A novel heme-regulatory motif mediates heme-dependent degradation of the circadian factor period 2. *Molecular and Cellular Biology* **2008**, *28*, 4697–4711.

[57] J. Shen, X. Sheng, Z. Chang, Q. Wu, S. Wang, Z. Xuan, D. Li, Y. Wu, Y. Shang, X. Kong, L. Yu, L. Li, K. Ruan, H. Hu, Y. Huang, L. Hui, D. Xie, F. Wang, R. Hu. Iron metabolism regulates p53 signaling through direct heme-p53 interaction and modulation of p53 localization, stability, and function. *Cell Reports* **2014**, *7*, 180–193.

[58] NCBI Resource Coordinators. Database resources of the National Center for Biotechnology Information. *Nucleic Acids Research* **2018**, *46*, D8–D13.

[59] L. Zhang. Introduction. *in Heme biology: The secret life of heme in regulating diverse biological processes* **2011**, 1–6.

[60] A. R. Battersby. Tetrapyrroles: The pigments of life. *Natural Product Reports* **2000**, *17*, 507–526.

[61] A. D. McNaught, A. Wilkinson. IUPAC. Compendium of chemical terminology (Gold Book). *Blackwell Scientific Publications, Oxford* **1997**, 2nd ed.

[62] S. Kumar, U. Bandyopadhyay. Free heme toxicity and its detoxification systems in human. *Toxicology Letters* **2005**, *157*, 175–188.

[63] K. T. Sawicki, H.-C. Chang, H. Ardehali. Role of heme in cardiovascular physiology and disease. *Journal of the American Heart Association* **2015**, *4*, e001138–e001138.

[64] T. Korolnek, I. Hamza. Like iron in the blood of the people: the requirement for heme trafficking in iron metabolism. *Frontiers in Pharmacology* **2014**, *5*, 126.

[65] M. E. Gillam, G. A. Hunter, G. C. Ferreira. The ultimate step of heme biosynthesis: Orchestration between iron trafficking and porphyrin synthesis. *in Handbook of Porphyrin Science* **2014**, *26*, 129–189.

[66] K. M. T. Oliveira, M. Trsic. Comparative theoretical study of the electronic structures and electronic spectra of Fe(2+)-, Fe(+3)-porphyrin and free base porphyrin. *Journal of Molecular Structure: THEOCHEM* **2001**, *539*, 107–117.

[67] C. J. Reedy, B. R. Gibney. Heme protein assemblies. *Chemical Reviews* **2004**, *104*, 617–650.

[68] S. Severance, I. Hamza. Trafficking of heme and porphyrins in metazoa. *Chemical Reviews* **2009**, *109*, 4596–4616.

[69] T. J. Egan. Physico-chemical aspects of hemozoin (malaria pigment) structure and formation. *Journal of Inorganic Biochemistry* **2002**, *91*, 19–26.

[70] L. M. Coronado, C. T. Nadovich, C. Spadafora. Malarial hemozoin: From target to tool. *Biochimica et Biophysica Acta (BBA) - General Subjects* **2014**, *1840*, 2032–2041.

[71] R. G. Kranz, C. Richard-Fogal, J.-S. Taylor, E. R. Frawley. Cytochrome c biogenesis: mechanisms for covalent modifications and trafficking of heme and for heme-iron redox control. *Microbiology and Molecular Biology Reviews* **2009**, *73*, 510–528.

[72] D. P. Barupala, S. P. Dzul, P. J. Riggs-Gelasco, T. L. Stemmler. Synthesis, delivery and regulation of eukaryotic heme and Fe-S cluster cofactors. *Archives of Biochemistry and Biophysics* **2016**, *592*, 60–75.

[73] A. S. Tsiftsoglou, A. I. Tsamadou, L. C. Papadopoulou. Heme as key regulator of major mammalian cellular functions: Molecular, cellular, and pharmacological aspects. *Pharmacology & Therapeutics* **2006**, *111*, 327–345.

[74] J. R. H. Tame, B. Vallone. The structures of deoxy human haemoglobin and the mutant Hb Tyrα42His at 120 K. *Acta Crystallographica Section D Biological Crystallography* **2000**, *56*, 805–811.

[75] R. K. Donegan, C. M. Moore, D. A. Hanna, A. R. Reddi. Handling heme: The mechanisms underlying the movement of heme within and between cells. *Free Radical Biology and Medicine* **2018**, *133*, 88–100.

[76] R. Beri, R. Chandra. Chemistry and biology of heme effect of metal salts, organometals, and metalloporphyrins on heme synthesis and catabolism, with special reference to clinical implications and interactions with cytochrome P-450. *Drug Metabolism Reviews* **1993**, *25*, 49–152.

[77] P. B. Danielson. The cytochrome P450 superfamily: Biochemistry, evolution and drug metabolism in humans. *Current Drug Metabolism* **2002**, *3*, 561–597.

[78] M. M. Rahaman, A. C. Straub. The emerging roles of somatic globins in cardiovascular redox biology and beyond. *Redox Biology* **2013**, *1*, 405–410.

[79] T. Li, H. L. Bonkovsky, J.-T. Guo. Structural analysis of heme proteins: implications for design and prediction. *BMC Structural Biology* **2011**, *11*, doi: 10.1186/1472–6807–11–13.

[80] G. Battistuzzi, M. Bellei, C. A. Bortolotti, M. Sola. Redox properties of heme peroxidases. *Archives of Biochemistry and Biophysics* **2010**, *500*, 21–36.

[81] M.-A. Gilles-Gonzalez, G. Gonzalez. Signal transduction by heme-containing PAS-domain proteins. *Journal of Applied Physiology* **2004**, *96*, 774–783.

[82] J. Tejero, J. Santolini, D. J. Stuehr. Fast ferrous heme-NO oxidation in nitric oxide synthases. *FEBS Journal* **2009**, *276*, 4505–4514.

[83] G. J. Kato, J. G. Taylor 6th. Pleiotropic effects of intravascular hemolysis on vascular homeostasis. *British Journal of Haematology* **2010**, *148*, 690–701.

[84] F. Vinchi, E. Tolosano. Therapeutic approaches to limit hemolysis driven endothelial dysfunction: Scavenging free heme to preserve vasculature homeostasis. *Oxidative Medicine and Cellular Longevity* **2013**, *2013*, 396527.

[85] A. T. Smith, N. C. Veitch. Substrate binding and catalysis in heme peroxidases. *Current Opinion in Chemical Biology* **1998**, *2*, 269–278.

[86] I. I. Vlasova. Peroxidase activity of human hemoproteins: Keeping the fire under control. *Molecules* **2018**, *23*, 2561.

[87] B. Chance. The nature of electron transfer and energy coupling reactions. *FEBS Letters* **1972**, *23*, 3–20.

[88] F. P. Guengerich, T. L. MacDonald. Mechanisms of cytochrome P-450 catalysis. *The FASEB Journal* **1990**, *4*, 2453–2459.

[89] R. J. Mailloux, X. Jin, W. G. Willmore. Redox regulation of mitochondrial function with emphasis on cysteine oxidation reactions. *Redox Biology* **2013**, *2*, 123–139.

[90] S. Yoshikawa, K. Shinzawa-Itoh, R. Nakashima, R. Yaono, E. Yamashita, N. Inoue, M. Yao, M. J. Fei, C. P. Libeu, T. Mizushima, H. Yamaguchi, T. Tomizaki, T. Tsukihara. Redox-coupled crystal structural changes in bovine heart cytochrome c oxidase. *Science* **1998**, *280*, 1723–1729.

[91] G. W. Bushnell, G. V. Louie, G. D. Brayer. High-resolution three-dimensional structure of horse heart cytochrome c. *Journal of Molecular Biology* **1990**, *214*, 585–595.

[92] A. R. Reddi, I. Hamza. Heme mobilization in animals: A metallolipid's journey. *Accounts of Chemical Research* **2016**, *49*, 1104–1110.

[93] S. Sassa. Why heme needs to be degraded to iron, biliverdin IXalpha, and carbon monoxide? *Antioxidants & Redox Signaling* **2004**, *6*, 819–824.

[94] D. Chiabrando, E. Tolosano, F. Vinchi, V. Fiorito. Haptoglobin and hemopexin in heme detoxification and iron recycling, acute phase proteins - regulation and functions of acute phase proteins. *in Acute Phase Proteins - Regulation and Functions of Acute Phase Proteins* **2011**, doi: 10.5772/18241.

[95] D. J. Schaer, F. Vinchi, G. Ingoglia, E. Tolosano, P. W. Buehler. Haptoglobin, hemopexin, and related defense pathways-basic science, clinical perspectives, and drug development. *Frontiers in Physiology* **2014**, *5*, 415.

[96] A. A. Khan, J. G. Quigley. Control of intracellular heme levels: Heme transporters and heme oxygenases. *Biochimica et Biophysica Acta - Molecular Cell Research* **2011**, *1813*, 668–682.

[97] Z. Gouveia, A. R. Carlos, X. Yuan, F. Aires-da Silva, R. Stocker, G. J. Maghzal, S. S. Leal, C. M. Gomes, S. Todorovic, O. Iranzo, S. Ramos, A. C. Santos, I. Hamza, J. Gonçalves, M. P. Soares. Characterization of plasma labile heme in hemolytic conditions. *The FEBS Journal* **2017**, *284*, 3278–3301.

[98] Y. Song, M. Yang, S. V. Wegner, J. Zhao, R. Zhu, Y. Wu, C. He, P. R. Chen. A genetically encoded FRET sensor for intracellular heme. *ACS Chemical Biology* **2015**, *10*, 1610–1615.

[99] A. Wißbrock, T. Kühl, K. Silbermann, A. J. Becker, O. Ohlenschläger, D. Imhof. Synthesis and evaluation of Amyloid β-derived and Amyloid β-independent enhancers of the peroxidase-like activity of heme. *Journal of Medicinal Chemistry* **2017**, *60*, 373–385.

[100] L. Zhang, L. Guarente. Heme binds to a short sequence that serves a regulatory function in diverse proteins. *The EMBO Journal* **1995**, *14*, 313–320.

[101] H. Atamna, W. H. Frey. A role for heme in Alzheimer's disease: heme binds amyloid beta and has altered metabolism. *Proceedings of the National Academy of Sciences of the United States of America* **2004**, *101*, 11153–11158.

[102] T. Korolnek, I. Hamza. Macrophages and iron trafficking at the birth and death of red cells. *Blood* **2015**, *125*, 2893–2897.

[103] J. Chung, C. Chen, B. H. Paw. Heme metabolism and erythropoiesis. *Current Opinion in Hematology* **2012**, *19*, 156–162.

[104] S. Warule, J. B. Shital Bidkar, G. Dama. Loaded erythrocyte: A review article. *World Journal of Pharmaceutical Research* **2017**, *6*, 154–173.

[105] D. Bratosin, J. Mazurier, J. P. Tissier, J. Estaquier, J. J. Huart, J. C. Ameisen, D. Aminoff, J. Montreuil. Cellular and molecular mechanisms of senescent erythrocyte phagocytosis by macrophages. A review. *Biochimie* **1998**, *80*, 173–195.

[106] C. White, X. Yuan, P. J. Schmidt, E. Bresciani, T. K. Samuel, D. Campagna, C. Hall, K. Bishop, M. L. Calicchio, A. Lapierre, D. M. Ward, P. Liu, M. D. Fleming, I. Hamza. HRG1 is essential for heme transport from the phagolysosome of macrophages during erythrophagocytosis. *Cell Metabolism* **2013**, *17*, 261–270.

[107] X. Yuan, M. D. Fleming, I. Hamza. Heme transport and erythropoiesis. *Current Opinion in Chemical Biology* **2013**, *17*, 204–211.

[108] I. Solar, U. Muller-Eberhard, Y. Shviro, N. Shaklai. Long-term intercalation of residual hemin in erythrocyte membranes distorts the cell. *Biochimica et Biophysica Acta (BBA) - Biomembranes* **1991**, *1062*, 51–58.

[109] M. Knutson, M. Wessling-Resnick. Iron metabolism in the reticuloendothelial system. *Critical Reviews in Biochemistry and Molecular Biology* **2003**, *38*, 61–88.

[110] L. Zhang, R. Sessoms. Heme biosynthesis and degradation: What happens when it goes Haywire? *in Heme biology: The secret life of heme in regulating diverse biological processes* **2011**, 7–31.

[111] R. S. Ajioka, J. D. Phillips, J. P. Kushner. Biosynthesis of heme in mammals. *Biochimica et Biophysica Acta (BBA) - Molecular Cell Research* **2006**, *1763*, 723–736.

[112] G. Layer, D. Jahn, E. Deery, A. D. Lawrence, M. J. Warren. Biosynthesis of heme and vitamin B12. *Comprehensive Natural Products II* **2010**, *7*, 445–499.

[113] N. Kresge, R. D. Simoni, R. L. Hill. A pathway for heme biosynthesis: the work of David Shemin. *The Journal of Biological Chemistry* **2006**, *281*, e28.

[114] H. A. Dailey, T. A. Dailey, S. Gerdes, D. Jahn, M. Jahn, M. R. O'Brian, M. J. Warren. Prokaryotic heme biosynthesis: Multiple pathways to a common essential product. *Microbiology and Molecular Biology Reviews* **2017**, *81*, e00048–16.

[115] G. Layer, J. Reichelt, D. Jahn, D. W. Heinz. Structure and function of enzymes in heme biosynthesis. *Protein Science* **2010**, *19*, 1137–1161.

[116] M. Sachar, K. E. Anderson, X. Ma. Protoporphyrin IX: the Good, the Bad, and the Ugly. *Journal of Pharmacology and Experimental Therapeutics* **2016**, *356*, 267–275.

[117] G. A. Hunter, G. C. Ferreira. Molecular enzymology of 5-Aminolevulinate synthase, the gatekeeper of heme biosynthesis. *Biochimica et Biophysica Acta (BBA) - Proteins and Proteomics* **2011**, *1814*, 1467–1473.

[118] M. Bayeva, A. Khechaduri, R. Wu, M. A. Burke, J. A. Wasserstrom, N. Singh, M. Liesa, O. S. Shirihai, N. B. Langer, B. H. Paw, H. Ardehali. ATP-binding cassette B10 regulates early steps of heme synthesis. *Circulation Research* **2013**, *113*, 279–287.

[119] A. Seguin, N. Takahashi-Makise, Y. Y. Yien, N. C. Huston, J. C. Whitman, G. Musso, J. A. Wallace, T. Bradley, H. A. Bergonia, M. D. Kafina, M. Matsumoto, K. Igarashi, J. D. Phillips, B. H. Paw, J. Kaplan, D. M. Ward. Reductions in the mitochondrial ABC transporter Abcb10 affect the transcriptional profile of heme biosynthesis genes. *Journal of Biological Chemistry* **2017**, *292*, 16284–16299.

[120] P. C. Krishnamurthy, G. Du, Y. Fukuda, D. Sun, J. Sampath, K. E. Mercer, J. Wang, B. Sosa-Pineda, K. G. Murti, J. D. Schuetz. Identification of a mammalian mitochondrial porphyrin transporter. *Nature* **2006**, *443*, 586–589.

[121] K. L. Proulx, S. I. Woodard, H. A. Dailey. In situ conversion of coproporphyrinogen to heme by murine mitochondria: Terminal steps of the heme biosynthetic pathway. *Protein Science* **1993**, *2*, 1092–1098.

[122] P. Ponka, H. M. Schulman. Regulation of heme biosynthesis: Distinct regulatory features in erythroid cells. *Stem Cells* **1993**, *11*, 24–35.

[123] K. Furuyama, K. Kaneko, P. D. Vargas. Heme as a magnificent molecule with multiple missions: Heme determines its own fate and governs cellular homeostasis. *The Tohoku Journal of Experimental Medicine* **2007**, *213*, 1–16.

[124] D. F. Bishop, A. S. Henderson, K. H. Astrin. Human delta-aminolevulinate synthase: Assignment of the housekeeping gene to 3p21 and the erythroid-specific gene to the X chromosome. *Genomics* **1990**, *7*, 207–214.

[125] J. J. Chen. Regulation of protein synthesis by the heme-regulated eIF2alpha kinase: relevance to anemias. *Blood* **2007**, *109*, 2693–2699.

[126] T. Rutherford, G. G. Thompson, M. R. Moore. Heme biosynthesis in Friend erythroleukemia cells: control by ferrochelatase. *Proceedings of the National Academy of Sciences of the United States of America* **1979**, *76*, 833–836.

[127] R. F. Labbé, H. J. Vreman, D. K. Stevenson. Zinc protoporphyrin: A metabolite with a mission. *Clinical Chemistry* **1999**, *45*, 2060–2072.

[128] M. Yamamoto, N. Hayashi, G. Kikuchi. Evidence for the transcriptional inhibition by heme of the synthesis of δ-aminolevulinate synthase in rat liver. *Biochemical and Biophysical Research Communications* **1982**, *105*, 985–990.

[129] M. Yamamoto, N. Hayashi, G. Kikuchi. Translational inhibition by heme of the synthesis of hepatic δ-aminolevulinate synthase in a cell-free system. *Biochemical and Biophysical Research Communications* **1983**, *115*, 225–231.

[130] E. Nagababu, J. M. Rifkind. Heme degradation by reactive oxygen species. *Antioxidants & Redox Signaling* **2004**, *6*, 967–978.

[131] G. Kikuchi, T. Yoshida, M. Noguchi. Heme oxygenase and heme degradation. *Biochemical and Biophysical Research Communications* **2005**, *338*, 558–567.

[132] L. Lad, D. J. Schuller, H. Shimizu, J. Friedman, H. Li, P. R. Ortiz de Montellano, T. L. Poulos. Comparison of the heme-free and -bound crystal structures of human heme oxygenase-1. *Journal of Biological Chemistry* **2003**, *278*, 7834–7843.

[133] D. J. Schuller, A. Wilks, P. R. Ortiz de Montellano, T. L. Poulos. Crystal structure of human heme oxygenase-1. *Nature Structural Biology* **1999**, *6*, 860–867.

[134] S. Shibahara, T. Kitamuro, K. Takahashi. Heme degradation and human disease: Diversity is the soul of life. *Antioxidants & Redox Signaling* **2002**, *4*, 593–602.

[135] Y. Liu, P. R. Ortiz de Montellano. Reaction intermediates and single turnover rate constants for the oxidation of heme by human heme oxygenase-1. *Journal of Biological Chemistry* **2000**, *275*, 5297–5307.

[136] S. W. Ryter, R. M. Tyrrell. The heme synthesis and degradation pathways: Role in oxidant sensitivity. Heme oxygenase has both pro- and antioxidant properties. *Free Radical Biology and Medicine* **2000**, *28*, 289–309.

[137] A. Wilks, G. Heinzl. Heme oxygenation and the widening paradigm of heme degradation. *Archives of Biochemistry and Biophysics* **2014**, *544*, 87–95.

[138] M. D. Maines, G. M. Trakshel. Purification and characterization of human biliverdin reductase. *Archives of Biochemistry and Biophysics* **1993**, *300*, 320–326.

[139] M. D. Maines. The heme oxygenase system: a regulator of second messenger gases. *Annual Review of Pharmacology and Toxicology* **1997**, *37*, 517–554.

[140] H. P. Kim, S. W. Ryter, A. M. K. Choi. CO as a cellular signaling molecule. *Annual Review of Pharmacology and Toxicology* **2006**, *46*, 411–449.

[141] M. P. Soares, F. H. Bach. Heme oxygenase-1: From biology to therapeutic potential. *Trends in Molecular Medicine* **2009**, *15*, 50–58.

[142] T. Jansen, A. Daiber. Direct antioxidant properties of bilirubin and biliverdin. Is there a role for biliverdin reductase? *Frontiers in Pharmacology* **2012**, *3*, 30.

[143] A. Joerk, R. A. Seidel, S. G. Walter, A. Wiegand, M. Kahnes, M. Klopfleisch, K. Kirmse, G. Pohnert, M. Westerhausen, O. W. Witte, K. Holthoff. Impact of heme and heme degradation products on vascular diameter in mouse visual cortex. *Journal of the American Heart Association* **2014**, *3*, e001220.

[144] M. Ritter, R. A. Seidel, P. Bellstedt, B. Schneider, M. Bauer, H. Görls, G. Pohnert. Isolation and identification of intermediates of the oxidative bilirubin degradation. *Organic Letters* **2016**, *18*, 4432–4435.

[145] R. A. Seidel, T. Claudel, F. A. Schleser, N. K. Ojha, M. Westerhausen, S. Nietzsche, C. Sponholz, F. Cuperus, S. M. Coldewey, S. H. Heinemann, G. Pohnert, M. Trauner, M. Bauer. Impact of higher-order heme degradation products on hepatic function and hemodynamics. *Journal of Hepatology* **2017**, *67*, 272–281.

[146] A. Wilks. Heme oxygenase: Evolution, structure, and mechanism. *Antioxidants & Redox Signaling* **2002**, *4*, 603–614.

[147] R. Tenhunen, H. S. Marver, R. Schmid. The enzymatic conversion of heme to bilirubin by microsomal heme oxygenase. *Proceedings of the National Academy of Sciences of the United States of America* **1968**, *61*, 748–775.

[148] M. D. Maines, G. M. Trakshel, R. K. Kutty. Characterization of two constitutive forms of rat liver microsomal heme oxygenase. Only one molecular species of the enzyme is inducible. *Journal of Biological Chemistry* **1986**, *261*, 411–419.

[149] W. K. Mccoubrey, T. J. Huang, M. D. Maines. Isolation and characterization of a cDNA from the rat brain that encodes hemoprotein heme oxygenase-3. *European Journal of Biochemistry* **1997**, *247*, 725–732.

[150] Y. Gottlieb, M. Truman, L. A. Cohen, Y. Leichtmann-Bardoogo, E. G. Meyron-Holtz. Endoplasmic reticulum anchored heme-oxygenase 1 faces the cytosol. *Haematologica* **2012**, *97*, 1489–1493.

[151] Q. Lin, S. Weis, G. Yang, Y.-H. Weng, R. Helston, K. Rish, A. Smith, J. Bordner, T. Polte, F. Gaunitz, P. A. Dennery. Heme oxygenase-1 protein localizes to the nucleus and activates transcription factors important in oxidative stress. *Journal of Biological Chemistry* **2007**, *282*, 20621–20633.

[152] H. P. Kim, X. Wang, F. Galbiati, S. W. Ryter, A. M. Choi. Caveolae compartmentalization of heme oxygenase-1 in endothelial cells. *The FASEB Journal* **2004**, *18*, 1080–1089.

[153] P. K. Waltz, B. Kautza, J. Luciano, M. Dyer, D. B. Stolz, P. Loughran, M. D. Neal, J. L. Sperry, M. R. Rosengart, B. S. Zuckerbraun. Heme oxygenase-2 localizes to mitochondria and regulates hypoxic responses in hepatocytes. *Oxidative Medicine and Cellular Longevity* **2018**, *2018*, 2021645.

[154] S. Immenschuh, G. Ramadori. Gene regulation of heme oxygenase-1 as a therapeutic target. *Biochemical Pharmacology* **2000**, *60*, 1121–1128.

[155] D. Morse, A. M. K. Choi. Heme oxygenase-1 the "emerging molecule" has arrived. *American Journal of Respiratory Cell and Molecular Biology* **2002**, *27*, 8–16.

[156] S. W. Ryter, A. M. K. Choi. Targeting heme oxygenase-1 and carbon monoxide for therapeutic modulation of inflammation. *Translational Research* **2016**, *167*, 7–34.

[157] J. G. Quigley, Z. Yang, M. T. Worthington, J. D. Phillips, K. M. Sabo, D. E. Sabath, C. L. Berg, S. Sassa, B. L. Wood, J. L. Abkowitz. Identification of a human heme exporter that is essential for erythropoiesis. *Cell* **2004**, *118*, 757–766.

[158] S. B. Keel, R. T. Doty, Z. Yang, J. G. Quigley, J. Chen, S. Knoblaugh, P. D. Kingsley, I. De Domenico, M. B. Vaughn, J. Kaplan, J. Palis, J. L. Abkowitz. A heme export protein is required for red blood cell differentiation and iron homeostasis. *Science* **2008**, *319*, 825–828.

[159] D. Chiabrando, S. Marro, S. Mercurio, C. Giorgi, S. Petrillo, F. Vinchi, V. Fiorito, S. Fagoonee, A. Camporeale, E. Turco, G. R. Merlo, L. Silengo, F. Altruda, P. Pinton, E. Tolosano. The mitochondrial heme exporter FLVCR1b mediates erythroid differentiation. *Journal of Clinical Investigation* **2012**, *122*, 4569–4579.

[160] S.-c. Iwahara, H. Satoh, D. X. Song, J. Webb, A. L. Burlingame, Y. Nagae, U. Muller-Eberhard. Purification, characterization, and cloning of a heme-binding protein (23 kDa) in rat liver cytosol. *Biochemistry* **1995**, *34*, 13398–13406.

[161] S. Taketani, Y. Adachi, H. Kohno, S. Ikehara, R. Tokunaga, T. Ishii. Molecular characterization of a newly identified heme-binding protein induced during differentiation of urine erythroleukemia cells. *The Journal of Biological Chemistry* **1998**, *273*, 31388–31394.

[162] S. Immenschuh, C. Nell, S. I. Iwahara, N. Katz, U. Muller-Eberhard. Gene regulation of HBP 23 by metalloporphyrins and protoporphyrin IX in liver and hepatocyte cultures. *Biochemical and Biophysical Research Communications* **1997**, *231*, 667–670.

[163] R. Chakravarti, K. S. Aulak, P. L. Fox, D. J. Stuehr. GAPDH regulates cellular heme insertion into inducible nitric oxide synthase. *Proceedings of the National Academy of Sciences of the United States of America* **2010**, *107*, 18004–18009.

[164] E. A. Sweeny, A. B. Singh, R. Chakravarti, O. Martinez-Guzman, A. Saini, M. M. Haque, G. Garee, P. D. Dans, L. Hannibal, A. R. Reddi, D. J. Stuehr. Glyceraldehyde-3-phosphate dehydrogenase is a chaperone that allocates labile heme in cells. *The Journal of Biological Chemistry* **2018**, *293*, 14557–14568.

[165] A. S. Fleischhacker, S. W. Ragsdale. An unlikely heme chaperone confirmed at last. *The Journal of Biological Chemistry* **2018**, *293*, 14569–14570.

[166] A. U. Rao, L. K. Carta, E. Lesuisse, I. Hamza. Lack of heme synthesis in a free-living eukaryote. *Proceedings of the National Academy of Sciences of the United States of America* **2005**, *102*, 4270–4275.

[167] J. Sinclair, I. Hamza. Lessons from bloodless worms: Heme homeostasis in C. elegans. *BioMetals* **2015**, *28*, 481–489.

[168] A. Rajagopal, A. U. Rao, J. Amigo, M. Tian, S. K. Upadhyay, C. Hall, S. Uhm, M. K. Mathew, M. D. Fleming, B. H. Paw, M. Krause, I. Hamza. Haem homeostasis is regulated by the conserved and concerted functions of HRG-1 proteins. *Nature* **2008**, *453*, 1127–1131.

[169] C. Delaby, C. Rondeau, C. Pouzet, A. Willemetz, N. Pilard, M. Desjardins, F. Canonne-Hergaux. Subcellular localization of iron and heme metabolism related proteins at early stages of erythrophagocytosis. *PLoS ONE* **2012**, *7*, e42199.

[170] M. Shayeghi, G. O. Latunde-Dada, J. S. Oakhill, A. H. Laftah, K. Takeuchi, N. Halliday, Y. Khan, A. Warley, F. E. McCann, R. C. Hider, D. M. Frazer, G. J. Anderson, C. D. Vulpe, R. J. Simpson, A. T. McKie. Identification of an intestinal heme transporter. *Cell* **2005**, *122*, 789–801.

[171] A. Qiu, M. Jansen, A. Sakaris, S. H. Min, S. Chattopadhyay, E. Tsai, C. Sandoval, R. Zhao, M. H. Akabas, I. D. Goldman. Identification of an intestinal folate transporter and the molecular basis for hereditary folate malabsorption. *Cell* **2006**, *127*, 917–928.

[172] S. Le Blanc, M. D. Garrick, M. Arredondo. Heme carrier protein 1 transports heme and is involved in heme-Fe metabolism. *American Journal of Physiology-Cell Physiology* **2012**, *302*, 1780–1785.

[173] P. Krishnamurthy, J. D. Schuetz. The ABC transporter Abcg2/Bcrp: Role in hypoxia mediated survival. *BioMetals* **2005**, *18*, 349–358.

[174] Z. Yang, J. D. Philips, R. T. Doty, P. Giraudi, J. D. Ostrow, C. Tiribelli, A. Smith, J. L. Abkowitz. Kinetics and specificity of Feline Leukemia Virus Subgroup C Receptor (FLVCR) export function and its dependence on hemopexin. *Journal of Biological Chemistry* **2010**, *285*, 28874–28882.

[175] P. Krishnamurthy, D. D. Ross, T. Nakanishi, K. Bailey-Dell, S. Zhou, K. E. Mercer, B. Sarkadi, B. P. Sorrentino, J. D. Schuetz. The stem cell marker Bcrp/ABCG2 enhances hypoxic cell survival through interactions with heme. *Journal of Biological Chemistry* **2004**, *279*, 24218–24225.

[176] F. Vinchi, G. Ingoglia, D. Chiabrando, S. Mercurio, E. Turco, L. Silengo, F. Altruda, E. Tolosano. Heme exporter FLVCR1a regulates heme synthesis and degradation and controls activity of cytochromes P450. *Gastroenterology* **2014**, *146*, 1325–1338.

[177] T. Korolnek, J. Zhang, S. Beardsley, G. L. Scheffer, I. Hamza. Control of metazoan heme homeostasis by a conserved multidrug resistance protein. *Cell Metabolism* **2014**, *19*, 1008–1019.

[178] M. Diab. Lexicon of Orthopaedic Etymology. *Harwood Academic Publishers* **1999**, 144, 186.

[179] G. Gordh. A Dictionary of Entomology, 2nd Edition. *Emerald Group Publishing Limited* **2001**, 662.

[180] L. Garby, W. D. Noyes. Studies on hemoglobin metabolism. I. The kinetic properties of the plasma hemoglobin pool in normal man. *The Journal of Clinical Investigation* **1959**, *38*, 1479–1483.

[181] M. J. Nielsen, H. J. Møller, S. K. Moestrup. Hemoglobin and heme scavenger receptors. *Antioxidants & Redox Signaling* **2010**, *12*, 261–273.

[182] E. Tolosano, S. Fagoonee, N. Morello, F. Vinchi, V. Fiorito. Heme scavenging and the other facets of hemopexin. *Antioxidants & Redox Signaling* **2010**, *12*, 305–320.

[183] A. Smith, R. J. McCulloh. Hemopexin and haptoglobin: allies against heme toxicity from hemoglobin not contenders. *Frontiers in Physiology* **2015**, *6*, 187.

[184] F. Rapido. The potential adverse effects of haemolysis. *Blood Transfusion* **2017**, *15*, 218–221.

[185] H. Zhong, K. Yazdanbakhsh. Hemolysis and immune regulation. *Current Opinion in Hematology* **2018**, *25*, 177–182.

[186] S. Bhakdi, H. Bayley, A. Valeva, I. Walev, B. Walker, U. Weller, M. Kehoe, M. Palmer. Staphylococcal alpha-toxin, streptolysin-O, and Escherichia coli hemolysin: prototypes of pore-forming bacterial cytolysins. *Archives of Microbiology* **1996**, *165*, 73–79.

[187] C. Guillaud, V. Loustau, M. Michel. Hemolytic anemia in adults: main causes and diagnostic procedures. *Expert Review of Hematology* **2012**, *5*, 229–241.

[188] K. Orf, A. J. Cunnington. Infection-related hemolysis and susceptibility to Gram-negative bacterial co-infection. *Frontiers in Microbiology* **2015**, *6*, 666.

[189] A. P. Levy, R. Asleh, S. Blum, N. S. Levy, R. Miller-Lotan, S. Kalet-Litman, Y. Anbinder, O. Lache, F. M. Nakhoul, R. Asaf, D. Farbstein, M. Pollak, Y. Z. Soloveichik, M. Strauss, J. Alshiek, A. Livshits, A. Schwartz, H. Awad, K. Jad, H. Goldenstein. Haptoglobin: Basic and clinical aspects. *Antioxidants & Redox Signaling* **2010**, *12*, 293–304.

[190] H. F. Bunn, J. H. Jandl. Exchange of heme among hemoglobins and between hemoglobin and albumin. *Journal of Biological Chemistry* **1968**, *243*, 465–475.

[191] Y. I. Miller, N. Shaklai. Kinetics of hemin distribution in plasma reveals its role in lipoprotein oxidation. *Biochimica et Biophysica Acta (BBA) - Molecular Basis of Disease* **1999**, *1454*, 153–164.

[192] M. Paoli, B. F. Anderson, H. M. Baker, W. T. Morgan, A. Smith, E. N. Baker. Crystal structure of hemopexin reveals a novel high-affinity heme site formed between two β-propeller domains. *Nature Structural Biology* **1999**, *6*, 926–931.

[193] M. Allhorn, T. Berggård, J. Nordberg, M. L. Olsson, B. Åkerström. Processing of the lipocalin α1-microglobulin by hemoglobin induces heme-binding and heme-degradation properties. *Blood* **2002**, *99*, 1894–1901.

[194] E. Karnaukhova, S. S. Krupnikova, M. Rajabi, A. I. Alayash. Heme binding to human alpha-1 proteinase inhibitor. *Biochimica et Biophysica Acta (BBA) - General Subjects* **2012**, *1820*, 2020–2029.

[195] E. Karnaukhova, S. Rutardottir, M. Rajabi M., L. W. Rosenlöf, A. I. Alayash, B. Åkerström. Characterization of heme binding to recombinant α1-microglobulin. *Frontiers in Physiology* **2014**, *5*, 465.

[196] S. Janciauskiene, S. Tumpara, M. Wiese, S. Wrenger, V. Vijayan, F. Gueler, R. Chen, K. Madyaningrana, R. Mahadeva, T. Welte, S. Immenschuh, J. Chorostowska-Wynimko.

Alpha1-antitrypsin binds hemin and prevents oxidative activation of human neutrophils: putative pathophysiological significance. *Journal of Leukocyte Biology* **2017**, *102*, 1127–1141.

[197] W. T. Morgan, H. Heng Liem, R. P. Sutor, U. Muller-Eberhard. Transfer of heme from heme-albumin to hemopexin. *Biochimica et Biophysica Acta (BBA) - General Subjects* **1976**, *444*, 435–445.

[198] P. Ascenzi, A. Bocedi, P. Visca, F. Altruda, E. Tolosano, T. Beringhelli, M. Fasano. Hemoglobin and heme scavenging. *IUBMB Life* **2005**, *57*, 749–759.

[199] S. K. Lim, B. Ferraro, K. Moore, B. Halliwell. Role of haptoglobin in free hemoglobin metabolism. *Redox Report* **2001**, *6*, 219–227.

[200] C. B. F. Andersen, M. Torvund-Jensen, M. J. Nielsen, C. L. P. De Oliveira, H. P. Hersleth, N. H. Andersen, J. S. Pedersen, G. R. Andersen, S. K. Moestrup. Structure of the haptoglobin-haemoglobin complex. *Nature* **2012**, *489*, 456–459.

[201] M. Kristiansen, J. H. Graversen, C. Jacobsen, O. Sonne, H. J. Hoffman, S. K. Law, S. K. Moestrup. Identification of the haemoglobin scavenger receptor. *Nature* **2001**, *409*, 198–201.

[202] J. H. Graversen, M. Madsen, S. K. Moestrup. CD163: A signal receptor scavenging haptoglobin-hemoglobin complexes from plasma. *International Journal of Biochemistry and Cell Biology* **2002**, *34*, 309–314.

[203] I. K. Quaye. Haptoglobin, inflammation and disease. *Transactions of the Royal Society of Tropical Medicine and Hygiene* **2008**, *102*, 735–742.

[204] S. Fagoonee, J. Gburek, E. Hirsch, S. Marro, S. K. Moestrup, J. M. Laurberg, E. I. Christensen, L. Silengo, F. Altruda, E. Tolosano. Plasma protein haptoglobin modulates renal iron loading. *American Journal of Pathology* **2005**, *166*, 973–983.

[205] P. Ascenzi, M. Fasano. Heme-hemopexin: A 'chronosteric' heme-protein. *IUBMB Life* **2008**, *59*, 700–708.

[206] V. Hvidberg, M. B. Maniecki, C. Jacobsen, P. Højrup, H. J. Møller, S. K. Moestrup. Identification of the receptor scavenging hemopexin-heme complexes. *Blood* **2005**, *106*, 2572–2579.

[207] A. Smith, R. C. Hunt. Hemopexin joins transferrin as representative members of a distinct class of receptor-mediated endocytic transport systems. *European Journal of Cell Biology* **1990**, *53*, 234–245.

[208] U. Muller-Eberhard, J. Javid, H. H. Liem, A. Hanstein, M. Hanna. Plasma concentrations of hemopexin, haptoglobin and heme in patients with various hemolytic diseases. *Blood* **1968**, *32*, 811–815.

[209] T. Lin, D. Maita, S. R. Thundivalappil, F. E. Riley, J. Hambsch, L. J. Van Marter, H. A. Christou, L. Berra, S. Fagan, D. C. Christiani, H. S. Warren. Hemopexin in severe inflammation and infection: Mouse models and human diseases. *Critical Care* **2015**, *19*, 166–173.

[210] R. Larsen, R. Gozzelino, V. Jeney, L. Tokaji, F. A. Bozza, A. M. Japiassú, D. Bonaparte, M. M. Cavalcante, Â. Chora, A. Ferreira, I. Marguti, S. Cardoso, N. Sepúlveda,

A. Smith, M. P. Soares. A central role for free heme in the pathogenesis of severe sepsis. *Science Translational Medicine* **2010**, *2*, 51–71.

[211] F. Vinchi, L. De Franceschi, A. Ghigo, T. Townes, J. Cimino, L. Silengo, E. Hirsch, F. Altruda, E. Tolosano. Hemopexin therapy improves cardiovascular function by preventing heme-induced endothelial toxicity in mouse models of hemolytic diseases. *Circulation* **2013**, *127*, 1317–1329.

[212] J. D. Eskew, R. M. Vanacore, L. Sung, P. J. Morales, A. Smith. Cellular protection mechanisms against extracellular heme: Heme-hemopexin, but not free heme, activates the N-terminal c-Jun kinase. *Journal of Biological Chemistry* **1999**, *274*, 638–648.

[213] D. J. Schaer, P. W. Buehler, A. I. Alayash, J. D. Belcher, G. M. Vercellotti. Hemolysis and free hemoglobin revisited: Exploring hemoglobin and hemin scavengers as a novel class of therapeutic proteins. *Blood* **2013**, *121*, 1276–1284.

[214] J. Chen-Roetling, S.-K. Ma, Y. Cao, A. Shah, R. F. Regan. Hemopexin increases the neurotoxicity of hemoglobin when haptoglobin is absent. *Journal of Neurochemistry* **2018**, *145*, 464–473.

[215] M. P. Soares, M. T. Bozza. Red alert: Labile heme is an alarmin. *Current Opinion in Immunology* **2016**, *38*, 94–100.

[216] P. B. Letarte, K. Lieberman, K. Nagatani, R. A. Haworth, G. B. Odell, T. A. Duff. Hemin: levels in experimental subarachnoid hematoma and effects on dissociated vascular smooth-muscle cells. *Journal of Neurosurgery* **1993**, *79*, 252–255.

[217] C. D. Reiter, X. Wang, J. E. Tanus-Santos, N. Hogg, R. O. Cannon III, A. N. Schechter, M. T. Gladwin. Cell-free hemoglobin limits nitric oxide bioavailability in sickle-cell disease. *Nature Medicine* **2002**, *8*, 1383–1389.

[218] J. M. Gutteridge, A. Smith. Antioxidant protection by haemopexin of haem-stimulated lipid peroxidation. *Biochemical Journal* **1988**, *256*, 861–865.

[219] F. Vallelian, T. Pimenova, C. P. Pereira, B. Abraham, M. G. Mikolajczyk, G. Schoedon, R. Zenobi, A. I. Alayash, P. W. Buehler, D. J. Schaer. The reaction of hydrogen peroxide with hemoglobin induces extensive α-globin crosslinking and impairs the interaction of hemoglobin with endogenous scavenger pathways. *Free Radical Biology and Medicine* **2008**, *45*, 1150–1158.

[220] N. Grinshtein, V. V. Bamm, V. A. Tsemakhovich, N. Shaklai. Mechanism of Low-Density Lipoprotein Oxidation by Hemoglobin-Derived Iron. *Biochemistry* **2003**, *42*, 6977–6985.

[221] T. Kita, N. Kume, M. Minami, K. Hayashida, T. Murayama, H. Sano, H. Moriwaki, H. Kataoka, E. Nishi, H. Horiuchi, H. Arai, M. Yokode. Role of Oxidized LDL in Atherosclerosis. *Annals of the New York Academy of Sciences* **2006**, *947*, 199–206.

[222] R. L. Aft, G. C. Mueller. Hemin-mediated DNA strand scission. *Journal of Biological Chemistry* **1983**, *258*, 12069–12072.

[223] S.-i. Ishikawa, S. Tamaki, M. Ohata, K. Arihara, M. Itoh. Heme induces DNA damage and hyperproliferation of colonic epithelial cells via hydrogen peroxide produced by

heme oxygenase: A possible mechanism of heme-induced colon cancer. *Molecular Nutrition & Food Research* **2010**, *54*, 1182–1191.

[224] J. S. Olson, E. W. Foley, C. Rogge, A.-L. Tsai, M. P. Doyle, D. D. Lemon. No scavenging and the hypertensive effect of hemoglobin-based blood substitutes. *Free Radical Biology and Medicine* **2004**, *36*, 685–697.

[225] R. RP, L. Bell, P. Hillmen, G. MT. The clinical sequelae of intravascular hemolysis and extracellular plasma hemoglobin: A novel mechanism of human disease. *Journal of the American Medical Association* **2005**, *293*, 1653–1662.

[226] R. T. Figueiredo, P. L. Fernandez, D. S. Mourao-Sa, B. N. Porto, F. F. Dutra, L. S. Alves, M. F. Oliveira, P. L. Oliveira, A. V. Graça-Souza, M. T. Bozza. Characterization of heme as activator of Toll-like receptor 4. *Journal of Biological Chemistry* **2007**, *282*, 20221–20229.

[227] M. Piazza, G. Damore, B. Costa, T. L. Gioannini, J. P. Weiss, F. Peri. Hemin and a metabolic derivative coprohemin modulate the TLR4 pathway differently through different molecular targets. *Innate Immunity* **2010**, *17*, 293–301.

[228] K. E. Anderson, S. S. Sassa, D. F. Bishop, R. J. Desnick. Disorders of heme biosynthesis: X-linked sideroblastic anemia and the porphyrias. *in The online metabolic and molecular bases of inherited disease* **2001**, doi: 10.1036/ommbid.153.

[229] K. R. Wagner, F. R. Sharp, T. D. Ardizzone, A. Lu, J. F. Clark. Heme and iron metabolism: Role in cerebral hemorrhage. *Journal of Cerebral Blood Flow & Metabolism* **2003**, *23*, 629–652.

[230] V. M. Hodges, S. Rainey, T. R. Lappin, A. P. Maxwell. Pathophysiology of anemia and erythrocytosis. *Critical Reviews in Oncology/Hematology* **2007**, *64*, 139–158.

[231] M. J. Tracz, J. Alam, K. A. Nath. Physiology and pathophysiology of heme: Implications for kidney disease. *Journal of the American Society of Nephrology* **2007**, *18*, 414–420.

[232] A. Ferreira, J. Balla, V. Jeney, G. Balla, M. P. Soares. A central role for free heme in the pathogenesis of severe malaria: the missing link? *Journal of Molecular Medicine* **2008**, *86*, 1097–1111.

[233] E. Nagy, J. W. Eaton, V. Jeney, M. P. Soares, Z. Varga, Z. Galajda, J. Szentmiklósi, G. Méhes, T. Csonka, A. Smith, G. M. Vercellotti, G. Balla, J. Balla. Red cells, hemoglobin, heme, iron and atherogenesis. *Arteriosclerosis, Thrombosis, and Vascular Biology* **2010**, *30*, 1347–1353.

[234] C. Huynh, X. Yuan, D. C. Miguel, R. L. Renberg, O. Protchenko, C. C. Philpott, I. Hamza, N. W. Andrews. Heme uptake by Leishmania amazonensis is mediated by the transmembrane protein LHR1. *PLoS Pathogens* **2012**, *8*, e1002795.

[235] J. Freed, L. Chakrabarti. Defining a role for hemoglobin in Parkinson's disease. *NPJ Parkinson's disease* **2016**, *2*, 16021.

[236] S. Aggarwal, A. Lam, S. Bolisetty, M. A. Carlisle, A. Traylor, A. Agarwal, S. Matalon. Heme attenuation ameliorates irritant gas inhalation-induced acute lung injury. *Antioxidants & Redox Signaling* **2016**, *24*, 99–112.

[237] G. J. Kato, M. H. Steinberg, M. T. Gladwin. Intravascular hemolysis and the pathophysiology of sickle cell disease. *Journal of Clinical Investigation* **2017**, *127*, 750–760.

[238] S. M. Gamage, L. Dissabandara, A. K. Y. Lam, V. Gopalan. The role of heme iron molecules derived from red and processed meat in the pathogenesis of colorectal carcinoma. *Critical Reviews in Oncology/Hematology* **2018**, *126*, 121–128.

[239] V.-M. S. Ramanujam, K. E. Anderson. Porphyria Diagnostics-Part 1: A brief overview of the porphyrias. *Current Protocols in Human Genetics* **2015**, *86*, 17.20.1–17.20.26.

[240] M. Cazzola, L. Malcovati. Diagnosis and treatment of sideroblastic anemias: from defective heme synthesis to abnormal RNA splicing. *Hematology ASH Education Program* **2015**, *2015*, 19–25.

[241] U. Gross, G. F. Hoffmann, M. O. Doss. Erythropoietic and hepatic porphyrias. *Journal of Inherited Metabolic Disease* **2000**, *23*, 641–661.

[242] H. Manceau, L. Gouya, H. Puy. Acute hepatic and erythropoietic porphyrias: From ALA synthases 1 and 2 to new molecular bases and treatments. *Current Opinion in Hematology* **2017**, *24*, 198–207.

[243] H. Thadani, A. Deacon, T. Peters. Diagnosis and management of porphyria. *British Medical Journal* **2000**, *320*, 1647–1651.

[244] M. Balwani, R. J. Desnick. The porphyrias: Advances in diagnosis and treatment. *Blood* **2012**, *120*, 4496–4504.

[245] S. D. Whatley, S. Ducamp, L. Gouya, B. Grandchamp, C. Beaumont, M. N. Badminton, G. H. Elder, S. A. Holme, A. V. Anstey, M. Parker, A. V. Corrigall, P. N. Meissner, R. J. Hift, J. T. Marsden, Y. Ma, G. Mieli-Vergani, J.-C. Deybach, H. Puy. c-Terminal deletions in the ALAS2 gene lead to gain of function and cause X-linked dominant protoporphyria without anemia or iron cverload. *American Journal of Human Genetics* **2008**, *83*, 408–414.

[246] K. Kaneko, Y. Kubota, K. Nomura, H. Hayashimoto, T. Chida, N. Yoshino, M. Wayama, K. Ogasawara, Y. Nakamura, I. Tooyama, K. Furuyama. Establishment of a cell model of X-linked sideroblastic anemia using genome editing. *Experimental Hematology* **2018**, *65*, 57–68.e2.

[247] H. Cario. Hemoglobinopathies - genetically diverse, clinically complex, and globally relevant. *Memo - Magazine of European Medical Oncology* **2018**, *11*, 235–240.

[248] B. Modell, M. Darlison. Global epidemiology of haemoglobin disorders and derived service indicators. *Bulletin of the World Health Organization* **2008**, *86*, 480–487.

[249] H. F. Bunn. Pathogenesis and treatment of sickle cell disease. *New England Journal of Medicine* **1997**, *337*, 762–769.

[250] E. Meibalan, M. Marti. Biology of malaria transmission. *Cold Spring Harbor Perspectives in Medicine* **2017**, *7*, a025452.

[251] D. E. Goldberg, P. A. Sigala. Plasmodium heme biosynthesis: To be or not to be essential? *PLoS Pathogens* **2017**, *13*, e1006511.

[252] Geneva: World Health Organization. Nutritional anaemias: tools for effective prevention and control. **2017**, CC BY–NC–SA 3.0 IGO.

[253] H. Atamna, D. W. Killilea, A. N. Killilea, B. N. Ames. Heme deficiency may be a factor in the mitochondrial and neuronal decay of aging. *Proceedings of the National Academy of Sciences of the United States of America* **2002**, *99*, 14807–14812.

[254] H. Atamna. Heme, iron, and the mitochondrial decay of ageing. *Ageing Research Reviews* **2004**, *3*, 303–318.

[255] B. Wegiel, C. J. Hauser, L. E. Otterbein. Heme as a danger molecule in pathogen recognition. *Free Radical Biology and Medicine* **2015**, *89*, 651–661.

[256] S. de Oliveira, E. E. Rosowski, A. Huttenlocher. Neutrophil migration in infection and wound repair: going forward in reverse. *Nature Reviews Immunology* **2016**, *16*, 378–391.

[257] F. A. Wagener, E. Feldman, T. de Witte, N. G. Abraham. Heme induces the expression of adhesion molecules ICAM-1, VCAM-1, and E selectin in vascular endothelial cells. *Proceedings of the Society for Experimental Biology and Medicine* **1997**, *216*, 456–463.

[258] L. T. Roumenina, J. Rayes, S. Lacroix-Desmazes, J. D. Dimitrov. Heme: Modulator of plasma systems in hemolytic diseases. *Trends in Molecular Medicine* **2016**, *22*, 200–213.

[259] A. V. Graça-Souza, M. A. B. Arruda, M. S. De Freitas, C. Barja-Fidalgo, P. L. Oliveira. Neutrophil activation by heme: Implications for inflammatory processes. *Blood* **2002**, *99*, 4160–4165.

[260] A. P. T. Monteiro, C. S. Pinheiro, T. Luna-Gomes, L. R. Alves, C. M. Maya-Monteiro, B. N. Porto, C. Barja-Fidalgo, C. F. Benjamim, M. Peters-Golden, C. Bandeira-Melo, M. T. Bozza, C. Canetti. Leukotriene B4 mediates neutrophil migration induced by heme. *The Journal of Immunology* **2011**, *186*, 6562–6567.

[261] B. N. Porto, L. S. Alves, P. L. Fernández, T. P. Dutra, R. T. Figueiredo, A. V. Graça-Souza, M. T. Bozza. Heme induces neutrophil migration and reactive oxygen species generation through signaling pathways characteristic of chemotactic receptors. *Journal of Biological Chemistry* **2007**, *282*, 24430–24436.

[262] R. Natarajan, B. J. Fisher, A. A. Fowler. Hypoxia inducible factor-1 modulates hemin-induced IL-8 secretion in microvascular endothelium. *Microvascular Research* **2007**, *73*, 163–172.

[263] M. A. Arruda, A. G. Rossi, M. S. de Freitas, C. Barja-Fidalgo, A. V. Graça-Souza. Heme inhibits human neutrophil apoptosis: involvement of phosphoinositide 3-kinase, MAPK, and NF-kappaB. *Journal of Immunology* **2004**, *173*, 2023–2030.

[264] A. Ortega-Gómez, M. Perretti, O. Soehnlein. Resolution of inflammation: an integrated view. *EMBO Molecular Medicine* **2013**, *5*, 661–674.

[265] G. Chen, D. Zhang, T. A. Fuchs, D. Manwani, D. D. Wagner, P. S. Frenette. Heme-induced neutrophil extracellular traps contribute to the pathogenesis of sickle cell disease. *Blood* **2014**, *123*, 3818–3827.

[266] Q. Li, W. Fu, J. Yao, Z. Ji, Y. Wang, Z. Zhou, J. Yan, W. Li. Heme Induces IL-1β Secretion Through Activating NLRP3 in Kidney Inflammation. *Cell Biochemistry and Biophysics* **2014**, *69*, 495–502.

[267] F. F. Dutra, L. S. Alves, D. Rodrigues, P. L. Fernandez, R. B. de Oliveira, D. T. Golenbock, D. S. Zamboni, M. T. Bozza. Hemolysis-induced lethality involves inflammasome activation by heme. *Proceedings of the National Academy of Sciences of the United States of America* **2014**, *111*, E4110–E4118.

[268] G. Y. Chen, G. Nuñez. Sterile inflammation: sensing and reacting to damage. *Nature Reviews Immunology* **2010**, *10*, 826–837.

[269] K. Miyake. Roles for accessory molecules in microbial recognition by Toll-like receptors. *Journal of Endotoxin Research* **2006**, *12*, 195–204.

[270] S. Lin, Q. Yin, Q. Zhong, F.-L. Lv, Y. Zhou, J.-Q. Li, J.-Z. Wang, B.-y. Su, Q.-W. Yang. Heme activates TLR4-mediated inflammatory injury via MyD88/TRIF signaling pathway in intracerebral hemorrhage. *Journal of Neuroinflammation* **2012**, *9*, 46.

[271] L. T. Roumenina, M. Radanova, B. P. Atanasov, K. T. Popov, S. V. Kaveri, S. Lacroix-Desmazes, V. Frémeaux-Bacchi, J. D. Dimitrov. Heme interacts with C1q and inhibits the classical complement pathway. *Journal of Biological Chemistry* **2011**, *286*, 16459–16469.

[272] R. Gozzelino, V. Jeney, M. P. Soares. Mechanisms of Cell Protection by Heme Oxygenase-1. *Annual Review of Pharmacology and Toxicology* **2010**, *50*, 323–354.

[273] T. Kühl, A. Wißbrock, N. Goradia, N. Sahoo, K. Galler, U. Neugebauer, J. Popp, S. H. Heinemann, O. Ohlenschläger, D. Imhof. Analysis of Fe(III) heme binding to cysteine-containing heme-regulatory motifs in proteins. *ACS Chemical Biology* **2013**, *8*, 1785–1793.

[274] I. F. Kimbrough, S. Robel, E. D. Roberson, H. Sontheimer. Vascular amyloidosis impairs the gliovascular unit in a mouse model of Alzheimer's disease. *Brain* **2015**, *138*, 3716–3733.

[275] A. Alzheimer. Über eine eigenartige Erkrankung der Hirnrinde. *Allgemeine Zeitschrift fur Psychiatrie und Psychisch-gerichtliche Medizin* **1907**, *64*, 146–148.

[276] J. Hardy, D. Allsop. Amyloid deposition as the central event in the aetiology of Alzheimer's disease. *Trends in Pharmacological Sciences* **1991**, *12*, 383–388.

[277] F. Kametani, M. Hasegawa. Reconsideration of amyloid hypothesis and tau hypothesis in Alzheimer's disease. *Frontiers in Neuroscience* **2018**, *12*, 25.

[278] J. Hardy. The amyloid hypothesis for Alzheimer's disease: A critical reappraisal. *Journal of Neurochemistry* **2009**, *110*, 1129–1134.

[279] K. Iqbal, I. Grundke-Iqbal. Alzheimer's disease, a multifactorial disorder seeking multitherapies. *Alzheimer's & Dementia* **2010**, *6*, 420–424.

[280] M. Prince, A. Wimo, M. Guerchet, G. Ali, Y. Wu, M. Prina. World Alzheimer Report 2015. The global impact of dementia. An analysis of prevalence, incidence, cost and trends. *Alzheimer's Disease International (ADI), London* **2015**.

[281] C. Cheignon, M. Tomas, D. Bonnefont-Rousselot, P. Faller, C. Hureau, F. Collin. Oxidative stress and the amyloid beta peptide in Alzheimer's disease. *Redox Biology* **2018**, *14*, 450–464.

[282] L. M. Osborn, W. Kamphuis, W. J. Wadman, E. M. Hol. Astrogliosis: An integral player in the pathogenesis of Alzheimer's disease. *Progress in Neurobiology* **2016**, *144*, 121–141.

[283] X. Zhu, B. Su, X. Wang, M. A. Smith, G. Perry. Causes of oxidative stress in Alzheimer disease. *Cellular and Molecular Life Sciences* **2007**, *64*, 2202–2210.

[284] K. Hirao, G. M. Pontone, G. S. Smith. Molecular imaging of neuropsychiatric symptoms in Alzheimer's and Parkinson's disease. *Neuroscience & Biobehavioral Reviews* **2015**, *49*, 157–170.

[285] J. Flemmig, M. Zámocký, A. Alia. Amyloid β and free heme: bloody new insights into the pathogenesis of Alzheimer's disease. *Neural Regeneration Research* **2018**, *13*, 1170–1174.

[286] H. Atamna. Heme binding to Amyloid-beta peptide: mechanistic role in Alzheimer's disease. *Journal of Alzheimer's disease* **2006**, *10*, 255–266.

[287] E. Chiziane, H. Telemann, M. Krueger, J. Adler, J. Arnhold, A. Alia, J. Flemmig. Free heme and amyloid-β: A fatal liaison in Alzheimer's disease. *Journal of Alzheimer's Disease* **2018**, *61*, 963–984.

[288] M. Goedert, M. G. Spillantini. A century of Alzheimer's disease. *Science* **2006**, *314*, 777–781.

[289] G. Thinakaran, E. H. Koo. Amyloid precursor protein trafficking, processing, and function. *The Journal of Biological Chemistry* **2008**, *283*, 29615–29619.

[290] F. M. LaFerla, K. N. Green, S. Oddo. Intracellular amyloid-β in Alzheimer's disease. *Nature Reviews Neuroscience* **2007**, *8*, 499–509.

[291] H. Atamna, W. H. Frey, N. Ko. Human and rodent amyloid-beta peptides differentially bind heme: Relevance to the human susceptibility to Alzheimer's disease. *Archives of Biochemistry and Biophysics* **2009**, *487*, 59–65.

[292] D. Pramanik, S. G. Dey. Active site environment of heme-bound Amyloid β peptide associated with Alzheimer's disease. *Journal of the American Chemical Society* **2011**, *133*, 81–87.

[293] N. Lu, J. Li, R. Tian, Y. Y. Peng. Key roles of Arg(5), Tyr(10) and His residues in Aβ-heme peroxidase: relevance to Alzheimer's disease. *Biochemical and Biophysical Research Communications* **2014**, *452*, 676–681.

[294] N. Lu, J. Li, R. Tian, Y.-y. Peng. Key Roles for Tyrosine 10 in Aβ-Heme Complexes and Its Relevance to Oxidative Stress. *Chemical Research in Toxicology* **2015**, *28*, 365–372.

[295] C. L. Thiabaud G., Pizzocaro S., Garcia-Serres R., Latour J. M., Monzani E. Heme binding induces dimerization and nitration of truncated β-Amyloid peptide Aβ16 under oxidative stress. *Angewandte Chemie International Edition* **2013**, *52*, 8041–8044.

[296] Q. Bao, Y. Luo, W. Li, X. Sun, C. Zhu, P. Li, Z.-X. Huang, X. Tan. The mechanism for heme to prevent Aβ(1-40) aggregation and its cytotoxicity. *Journal of Biological Inorganic Chemistry* **2011**, *16*, 809–816.

[297] C. Yuan, Z. Gao. Aβ interacts with Both the Iron Center and the Porphyrin Ring of Heme: Mechanism of Heme's Action on Aβ Aggregation and Disaggregation. *Chemical Research in Toxicology* **2013**, *26*, 262–269.

[298] B. H. Han, M.-l. Zhou, F. Abousaleh, R. P. Brendza, H. H. Dietrich, J. Koenigsknecht-Talboo, J. R. Cirrito, E. Milner, D. M. Holtzman, G. J. Zipfel. Cerebrovascular dysfunction in amyloid precursor protein transgenic mice: contribution of soluble and insoluble Amyloid-β peptide, partial restoration via γ-secretase inhibition. *The Journal of Neuroscience* **2008**, *28*, 13542–13550.

[299] B. E. Dwyer, M. A. Smith, S. L. Richardson, G. Perry, X. Zhu. Down-regulation of aminolevulinate synthase, the rate-limiting enzyme for heme biosynthesis in Alzheimer's disease. *Neuroscience Letters* **2009**, *460*, 180–184.

[300] H. M. Schipper, A. Gupta, W. A. Szarek. Suppression of Glial HO-1 Activitiy as a Potential Neurotherapeutic Intervention in AD. *Current Alzheimer Research* **2009**, *6*, 424–430.

[301] M. Miksanova, J. Igarashi, M. Minami, I. Sagami, S. Yamauchi, H. Kurokawa, T. Shimizu. Characterization of heme-regulated eIF2alpha kinase: Roles of the N-terminal domain in the oligomeric state, heme binding, catalysis, and inhibition. *Biochemistry* **2006**, *45*, 9894–9905.

[302] S. Peherstorfer, H. H. B. Brewitz, A. A. Paul George, A. Wißbrock, J. M. Adam, L. Schmitt, D. Imhof. Insights into mechanism and functional consequences of heme binding to hemolysin-activating lysine acyltransferase HlyC from Escherichia coli. *Biochim Biophys Acta* **2018**, *1862*, 1964–1972.

[303] H. H. Brewitz, T. Kühl, N. Goradia, K. Galler, J. Popp, O. Neugebauer, Ute Ohlenschläger, D. Imhof. Role of the chemical environment beyond the coordination site: Structural insight into Fe(III) protoporphyrin binding to cysteine-based heme-regulatory protein motifs. *ChemBioChem* **2015**, *16*, 2216–2224.

[304] T. Hon, A. Hach, H. C. Lee, T. Cheng, L. Zhang. Functional analysis of heme regulatory elements of the transcriptional activator Hap1. *Biochemical and Biophysical Research Communications* **2000**, *273*, 584–591.

[305] M. J. Hickman, F. Winston. Heme levels switch the function of Hap1 of Saccharomyces cerevisiae between transcriptional activator and transcriptional repressor. *Molecular and Cellular Biology* **2007**, *27*, 7414–7424.

[306] Z. Qi, I. Hamza, M. R. O'Brian. Heme is an effector molecule for iron-dependent degradation of the bacterial iron response regulator (Irr) protein. *Proceedings of the National Academy of Sciences of the United States of America* **1999**, *96*, 13056–13061.

[307] J. Yang, K. Ishimori, M. R. O'Brian. Two heme binding sites are involved in the regulated degradation of the bacterial iron response regulator (Irr) protein. *Journal of Biological Chemistry* **2005**, *280*, 7671–7676.

[308] E. Schubert, N. Florin, F. Duthie, H. H. Brewitz, T. Kühl, D. Imhof, G. Hagelueken, O. Schiemann. Spectroscopic studies on peptides and proteins with cysteine-containing heme regulatory motifs (HRM). *Journal of Inorganic Biochemistry* **2015**, *148*, 49–56.

[309] H. Brewitz, N. Goradia, E. Schubert, K. Galler, T. Kühl, B. Syllwasschya, J. Popp, U. Neugebauer, G. Hagelueken, O. Schiemann, O. Ohlenschläger, D. Imhof. Heme interacts with histidine- and tyrosine-based protein motifs and inhibits enzymatic activity of chloramphenicol acetyltransferase from E. coli. *Biochimica et Biophysica Acta (BBA) - General Subjects* **2016**, *1860*, 1343–1353.

[310] P. Ponka. Tissue-specific regulation of iron metabolism and heme synthesis: Distinct control mechanisms in erythroid cells. *Blood* **1997**, *89*, 1–25.

[311] D. Chiabrando, S. Mercurio, E. Tolosano. Heme and erythropoieis: more than a structural role. *Haematologica* **2014**, *99*, 973–983.

[312] K. Yamauchi, N. Hayashi, G. Kikuchi. Translocation of delta-aminolevulinate synthase from the cytosol to the mitochondria and its regulation by hemin in the rat liver. *Journal of Biological Chemistry* **1980**, *255*, 1746–1751.

[313] J. W. Hamilton, W. J. Bement, P. R. Sinclair, J. F. Sinclair, J. A. Alcedo, K. E. Wetterhahn. Heme regulates hepatic 5-aminolevulinate synthase mRNA expression by decreasing mRNA half-life and not by altering its rate of transcription. *Archives of Biochemistry and Biophysics* **1991**, *289*, 387–392.

[314] S. Munakata, H., Sun, J. Y., Yoshida, K., Nakatani, T., Honda, E., Hayakawa, N. Furuyama, K., Hayashi. Role of the heme regulatory motif in the heme-mediated inhibition of mitochondrial import of 5-aminolevulinate synthase. *Journal of Biochemistry* **2004**, *136*, 233–238.

[315] Y. Kubota, K. Nomura, Y. Katoh, R. Yamashita, K. Kaneko, K. Furuyama. Novel mechanisms for heme-dependent degradation of ALAS1 protein as a component of negative feedback regulation of heme biosynthesis. *The Journal of Biological Chemistry* **2016**, *291*, 20516–20529.

[316] R. S. Eisenstein. Iron regulatory proteins and the molecular control of mammalian iron metabolism. *Annual Review of Nutrition* **2000**, *20*, 627–662.

[317] H. Ishikawa, M. Kato, H. Hori, K. Ishimori, T. Kirisako, F. Tokunaga, K. Iwai. Involvement of heme regulatory motif in heme-mediated ubiquitination and degradation of IRP2. *Molecular Cell* **2005**, *19*, 171–181.

[318] N. Tanimura, E. Miller, K. Igarashi, D. Yang, J. N. Burstyn, C. N. Dewey, E. H. Bresnick. Mechanism governing heme synthesis reveals a GATA factor/heme circuit that controls differentiation. *EMBO Reports* **2016**, *17*, 249–265.

[319] T. J. Huang, W. K. McCoubrey, M. D. Maines. Heme oxygenase-2 interaction with metalloporphyrins: function of heme regulatory motifs. *Antioxidants & Redox Signaling* **2001**, *3*, 685–696.

[320] L. Yi, S. W. Ragsdale. Evidence that the heme regulatory motifs in heme oxygenase-2 serve as a thiol/disulfide redox switch regulating heme binding. *Journal of Biological Chemistry* **2007**, *282*, 21056–21067.

[321] A. S. Fleischhacker, A. Sharma, M. Choi, A. M. Spencer, I. Bagai, B. M. Hoffman, S. W. Ragsdale. The C-terminal heme regulatory motifs of heme oxygenase-2 are redox-regulated heme binding sites. *Biochemistry* **2015**, *54*, 2709–2718.

[322] W. K. McCoubrey, T. J. Huang, M. D. Maines. Heme oxygenase-2 is a hemoprotein and binds heme through heme regulatory motifs that are not involved in heme catalysis. *Journal of Biological Chemistry* **1997**, *272*, 12568–12574.

[323] J. Sun, H. Hoshino, K. Takaku, O. Nakajima, A. Muto, H. Suzuki, S. Tashiro, S. Takahashi, S. Shibahara, J. Alam, M. M. Taketo, M. Yamamoto, K. Igarashi. Hemoprotein Bach1 regulates enhancer availability of heme oxygenase-1 gene. *EMBO Journal* **2002**, *21*, 5216–5224.

[324] H. Kurokawa, H. Motohashi, S. Sueno, M. Kimura, H. Takagawa, Y. Kanno, M. Yamamoto, T. Tanaka. Structural basis of alternative DNA recognition by Maf transcription factors. *Molecular and Cellular Biology* **2009**, *29*, 6232–6244.

[325] X. Zhang, J. Guo, X. Wei, C. Niu, M. Jia, Q. Li, D. Meng. Bach1: function, regulation, and involvement in disease. *Oxidative Medicine and Cellular Longevity* **2018**, 1347969.

[326] K. Ogawa, J. Sun, S. Taketani, O. Nakajima, C. Nishitani, S. Sassa, N. Hayashi, M. Yamamoto, S. Shibahara, H. Fujita, K. Igarashi. Heme mediates derepression of Maf recognition element through direct binding to transcription repressor Bach1. *EMBO Journal* **2001**, *20*, 2835–2843.

[327] Y. Zenke-Kawasaki, Y. Dohi, Y. Katoh, T. Ikura, M. Ikura, T. Asahara, F. Tokunaga, K. Iwai, K. Igarashi. Heme induces ubiquitination and degradation of the transcription factor Bach1. *Molecular and Cellular Biology* **2007**, *27*, 6962–6971.

[328] K. Igarashi, H. Hoshino, A. Muto, N. Suwabe, S. Nishikawa, H. Nakauchi, M. Yamamoto. Multivalent DNA binding complex generated by small Maf and Bach1 as a possible biochemical basis for β-globin locus control region complex. *Journal of Biological Chemistry* **1998**, *273*, 11783–11790.

[329] A. P. Han, C. Yu, L. Lu, Y. Fujiwara, C. Browne, G. Chin, M. Fleming, P. Leboulch, S. H. Orkin, J. J. Chen. Heme-regulated eIF2alpha kinase (HRI) is required for translational regulation and survival of erythroid precursors in iron deficiency. *EMBO Journal* **2001**, *20*, 6909–6918.

[330] M. Rafie-Kolpin, A.-P. Han, J.-J. Chen. Autophosphorylation of threonine 485 in the activation loop is essential for attaining eIF2α kinase activity of HRI. *Biochemistry* **2003**, *42*, 6536–6544.

[331] J.-J. Chen, R. N. Suragani. Heme-regulated eIF2α kinase in translation and erythropoiesis. *in Heme biology: The secret life of heme in regulating diverse biological processes* **2011**, 55–84.

[332] B. Zheng, U. Albrecht, K. Kaasik, M. Sage, W. Lu, S. Vaishnav, Q. Li, Z. S. Sun, G. Eichele, A. Bradley, C. C. Lee. Nonredundant roles of the mPer1 and mPer2 genes in the mammalian circadian clock. *Cell* **2001**, *105*, 683–694.

[333] K. Kaasik, C. Chi Lee. Reciprocal regulation of haem biosynthesis and the circadian clock in mammals. *Nature* **2004**, *430*, 467–471.

[334] S. Raghuram, K. R. Stayrook, P. Huang, P. M. Rogers, A. K. Nosie, D. B. McClure, L. L. Burris, S. Khorasanizadeh, T. P. Burris, F. Rastinejad. Identification of heme

as the ligand for the orphan nuclear receptors REV-ERBα and REV-ERBβ. *Nature Structural & Molecular Biology* **2007**, *14*, 1207–1213.

[335] P. M. Rogers, L. Ying, T. P. Burris. Relationship between circadian oscillations of Rev-erbα expression and intracellular levels of its ligand, heme. *Biochemical and Biophysical Research Communications* **2008**, *368*, 955–958.

[336] M. V. Airola, J. Du, J. H. Dawson, B. R. Crane. Heme binding to the mammalian circadian clock protein period 2 is non-specific. *Biochemistry* **2010**, *49*, 4327–4338.

[337] M. H. Hastings, E. S. Maywood, M. Brancaccio. Generation of circadian rhythms in the suprachiasmatic nucleus. *Nature Reviews Neuroscience* **2018**, *19*, 453–469.

[338] J. S. Takahashi. Molecular components of the circadian clock in mammals. *Diabetes, Obesity & Metabolism* **2015**, *17*, 6–11.

[339] J. S. Takahashi. Transcriptional architecture of the mammalian circadian clock. *Nature Reviews Genetics* **2016**, *18*, 164–179.

[340] E. M. Dioum, J. Rutter, J. R. Tuckerman, G. Gonzalez, M. A. Gilles-Gonzalez, S. L. McKnight. NPAS2: A gas-responsive transcription factor. *Science* **2002**, *298*, 2385–2387.

[341] I. Barr, A. T. Smith, R. Senturia, Y. Chen, B. D. Scheidemantle, J. N. Burstyn, F. Guo. DiGeorge critical region 8 (DGCR8) is a double-cysteine-ligated heme protein. *Journal of Biological Chemistry* **2011**, *286*, 16716–16725.

[342] S. H. Weitz, M. Gong, I. Barr, S. Weiss, F. Guo. Processing of microRNA primary transcripts requires heme in mammalian cells. *Proceedings of the National Academy of Sciences of the United States of America* **2014**, *111*, 1861–1866.

[343] H. M. Girvan, J. M. Bradley, M. R. Cheesman, J. R. Kincaid, Y. Liu, K. Czarnecki, K. Fisher, D. Leys, S. E. J. Rigby, A. W. Munro. Analysis of heme iron coordination in DGCR8: The heme-binding component of the microprocessor complex. *Biochemistry* **2016**, *55*, 5073–5083.

[344] A. C. Partin, T. D. Ngo, E. Herrell, B.-C. Jeong, G. Hon, Y. Nam. Heme enables proper positioning of Drosha and DGCR8 on primary microRNAs. *Nature Communications* **2017**, *8*, 1737.

[345] T. Nguyen, J. Park, T. Dang, Y.-G. Choi, V. Kim. Microprocessor depends on hemin to recognize the apical loop of primary microRNA. *Nucleic Acids Research* **2018**, *46*, 5726–5736.

[346] F. T. Horrigan, S. H. Heinemann, T. Hoshi. Heme regulates allosteric activation of the Slo1 BK channel. *The Journal of General Physiology* **2005**, *126*, 7–21.

[347] N. Sahoo, N. Goradia, O. Ohlenschläger, R. Schönherr, M. Friedrich, W. Plass, R. Kappl, T. Hoshi, S. H. Heinemann. Heme impairs the ball-and-chain inactivation of potassium channels. *Proceedings of the National Academy of Sciences of the United States of America* **2013**, *110*, E4036–E4044.

[348] M. Burton, S. Kapetanaki, N. Davies, J. Mitcheson, R. Schmid, P. Moody, E. Raven, N. Storey. The molecular basis for heme modulation of KATP channels. *Biophysical Journal* **2015**, *108*, 2197–PosB334.

[349] M. J. Burton, S. M. Kapetanaki, T. Chernova, A. G. Jamieson, P. Dorlet, J. Santolini, P. C. E. Moody, J. S. Mitcheson, N. W. Davies, R. Schmid, E. L. Raven, N. M. Storey. A heme-binding domain controls regulation of ATP-dependent potassium channels. *Proceedings of the National Academy of Sciences of the United States of America* **2016**, *113*, 3785–3790.

[350] C. L. Weeks, S. Singh, P. Madzelan, R. Banerjee, T. G. Spiro. Heme regulation of human cystathionine beta-synthase activity: Insights from fluorescence and Raman spectroscopy. *Journal of the American Chemical Society* **2009**, *131*, 12809–12816.

[351] K.-H. Jhee, W. D. Kruger. The role of cystathionine β-synthase in homocysteine metabolism. *Antioxidants & Redox Signaling* **2005**, *7*, 813–822.

[352] A. Kumar, A. Wißbrock, N. Goradia, P. Bellstedt, R. Ramachandran, D. Imhof, O. Ohlenschläger. Heme interaction of the intrinsically disordered N-terminal peptide segment of human cystathionine-β-synthase. *Scientific Reports* **2018**, *8*, 2474.

[353] W. Ye, L. Zhang. Heme controls the expression of cell cycle regulators and cell growth in HeLa cells. *Biochemical and Biophysical Research Communications* **2004**, *315*, 546–554.

[354] J. Shen, X. Sheng, Z. Chang, Q. Wu, D. Xie, F. Wang, R. Hu. The heme-p53 interaction: Linking iron metabolism to p53 signaling and tumorigenesis. *Molecular & Cellular Oncology* **2014**, *3*, e965642–e965642.

[355] X. Yao, P. Balamurugan, A. Arvey, C. Leslie, L. Zhang. Heme controls the regulation of protein tyrosine kinases Jak2 and Src. *Biochemical and Biophysical Research Communications* **2010**, *403*, 30–35.

[356] J. M. Zhang, J. An. Cytokines, inflammation, and pain. *International Anesthesiology Clinics* **2007**, *45*, 27–37.

[357] C. A. Dinarello. Immunological and inflammatory functions of the interleukin-1 family. *Annual Review of Immunology* **2009**, *27*, 519–550.

[358] J. E. Sims, D. E. Smith. The IL-1 family: Regulators of immunity. *Nature Reviews Immunology* **2010**, *10*, 89–102.

[359] C. Garlanda, C. A. Dinarello, A. Mantovani. The Interleukin-1 Family: Back to the Future. *Immunity* **2013**, *39*, 1003–1018.

[360] J. J. O'Shea, A. Ma, P. Lipsky. Cytokines and autoimmunity. *Nature Reviews Immunology* **2002**, *2*, 37–45.

[361] D. E. Smith, B. R. Renshaw, R. R. Ketchem, M. Kubin, K. E. Garka, J. E. Sims. Four new members expand the interleukin-1 superfamily. *Journal of Biological Chemistry* **2000**, *275*, 1169–1175.

[362] E. Dunn, J. E. Sims, M. J. H. Nicklin, L. A. J. O'Neill. Annotating genes with potential roles in the immune system: Six new members of the IL-1 family. *Trends in Immunology* **2001**, *22*, 533–536.

[363] M. S. Gresnigt, F. L. Van de Veerdonk. Biology of IL-36 cytokines and their role in disease. *Seminars in Immunology* **2013**, *25*, 458–465.

[364] C. A. Dinarello. Overview of the interleukin-1 family of ligands and receptors. *Seminars in Immunology* **2013**, *25*, 389–393.

[365] J. Towne, J. Sims. IL-36 in psoriasis. *Current Opinion in Pharmacology* **2012**, *12*, 486–490.

[366] C. Gabay, J. E. Towne. Regulation and function of interleukin-36 cytokines in homeostasis and pathological conditions. *Journal of Leukocyte Biology* **2015**, *97*, 645–652.

[367] L. E. Jensen. Interleukin-36 cytokines may overcome microbial immune evasion strategies that inhibit interleukin-1 family signaling. *Science Signaling* **2017**, *10*, eaan3589.

[368] M. Hahn, S. Frey, A. J. Hueber. The novel Interleukin-1 cytokine family members in inflammatory diseases. *Current Opinion in Rheumatology* **2017**, *29*, 208–213.

[369] E. Y. Bassoy, J. E. Towne, C. Gabay. Regulation and function of interleukin-36 cytokines. *Immunological Reviews* **2018**, *281*, 169–178.

[370] J. E. Towne, K. E. Garka, B. R. Renshaw, G. D. Virca, J. E. Sims. Interleukin (IL)-1F6, IL-1F8, and IL-1F9 signal through IL-1Rrp2 and IL-1RAcP to activate the pathway leading to NF-κB and MAPKs. *Journal of Biological Chemistry* **2004**, *279*, 13677–13688.

[371] S. Akira, K. Takeda. Toll-like receptor signalling. *Nature Reviews Immunology* **2004**, *4*, 499–511.

[372] D. Boraschi, P. Italiani, S. Weil, M. U. Martin. The family of the interleukin-1 receptors. *Immunological Reviews* **2018**, *281*, 197–232.

[373] S. Akira, S. Sato. Toll-like receptors and their signaling mechanisms. *Scandinavian Journal of Infectious Diseases* **2003**, *35*, 555–562.

[374] C. Kollewe, A.-C. Mackensen, D. Neumann, J. Knop, P. Cao, S. Li, H. Wesche, M. U. Martin. Sequential autophosphorylation steps in the interleukin-1 receptor-associated kinase-1 regulate its availability as an adapter in interleukin-1 signaling. *Journal of Biological Chemistry* **2004**, *279*, 5227–5236.

[375] P. G. Motshwene, M. C. Moncrieffe, J. G. Grossmann, C. Kao, M. Ayaluru, A. M. Sandercock, C. V. Robinson, E. Latz, N. J. Gay. An oligomeric signaling platform formed by the Toll-like receptor signal transducers MyD88 and IRAK-4. *Journal of Biological Chemistry* **2009**, *284*, 25404–25411.

[376] R. Ferrao, H. Zhou, Y. Shan, Q. Liu, Q. Li, D. E. Shaw, X. Li, H. Wu. IRAK4 dimerization and trans-autophosphorylation are induced by myddosome assembly. *Molecular Cell* **2014**, *55*, 891–903.

[377] P. N. Moynagh. The roles of Pellino E3 ubiquitin ligases in immunity. *Nature Reviews Immunology* **2014**, *14*, 122–131.

[378] H. Ye, J. R. Arron, B. Lamothe, M. Cirilli, T. Kobayashi, N. K. Shevde, D. Segal, O. K. Dzivenu, M. Vologodskaia, M. Yim, K. Du, S. Singh, J. W. Pike, B. G. Darnay, Y. Choi, H. Wu. Distinct molecular mechanism for initiating TRAF6 signalling. *Nature* **2002**, *418*, 443–447.

[379] V. Baud, Z.-G. Liu, B. Bennett, N. Suzuki, Y. Xia, M. Karin. Signaling by proinflammatory cytokines: Oligomerization of TRAF2 and TRAF6 is sufficient for JNK

and IKK activation and target gene induction via an amino-terminal effector domain. *Genes & Development* **1999**, *13*, 1297–1308.

[380] S. Strickson, C. H. Emmerich, E. T. H. Goh, J. Zhang, I. R. Kelsall, T. Macartney, C. J. Hastie, A. Knebel, M. Peggie, F. Marchesi, J. S. C. Arthur, P. Cohen. Roles of the TRAF6 and Pellino E3 ligases in MyD88 and RANKL signaling. *Proceedings of the National Academy of Sciences of the United States of America* **2017**, *114*, 3481–3489.

[381] Y. Hirata, M. Takahashi, T. Morishita, T. Noguchi, A. Matsuzawa. Post-translational modifications of the TAK1-TAB complex. *International Journal of Molecular Sciences* **2017**, *18*, 205.

[382] M. Karin, Y. Ben-Neriah. Phosphorylation meets ubiquitination: The control of NF-κB activity. *Annual Review of Immunology* **2000**, *18*, 621–663.

[383] R. Debets, J. C. Timans, B. Homey, S. Zurawski, T. R. Sana, S. Lo, J. Wagner, G. Edwards, T. Clifford, S. Menon, J. F. Bazan, R. a. Kastelein. Two novel IL-1 family members, IL-1 delta and IL-1 epsilon, function as an antagonist and agonist of NF-kappa B activation through the orphan IL-1 receptor-related protein 2. *Journal of Immunology* **2001**, *167*, 1440–1446.

[384] F. L. van de Veerdonk, A. K. Stoeckman, G. Wu, A. N. Boeckermann, T. Azam, M. G. Netea, L. A. B. Joosten, J. W. M. van der Meer, R. Hao, V. Kalabokis, C. A. Dinarello. IL-38 binds to the IL-36 receptor and has biological effects on immune cells similar to IL-36 receptor antagonist. *Proceedings of the National Academy of Sciences of the United States of America* **2012**, *109*, 3001–3005.

[385] S. Günther, E. J. Sundberg. Molecular determinants of agonist and antagonist signaling through the IL-36 receptor. *Journal of Immunology* **2014**, *193*, 921–930.

[386] F. L. van de Veerdonk, M. G. Netea. New insights in the immunobiology of IL-1 family members. *Frontiers in Immunology* **2013**, *4*, 167.

[387] J. E. Towne, B. R. Renshaw, J. Douangpanya, B. P. Lipsky, M. Shen, C. A. Gabel, J. E. Sims. Interleukin-36 (IL-36) ligands require processing for full agonist (IL-36α, IL-36β, and IL-36γ) or antagonist (IL-36Ra) activity. *Journal of Biological Chemistry* **2011**, *286*, 42594–42602.

[388] C. M. Henry, G. P. Sullivan, D. M. Clancy, I. S. Afonina, D. Kulms, S. J. Martin. Neutrophil-derived proteases escalate inflammation through activation of IL-36 family cytokines. *Cell Reports* **2016**, *14*, 708–722.

[389] D. M. Clancy, G. P. Sullivan, H. B. Moran, C. M. Henry, E. P. Reeves, N. G. McElvaney, E. C. Lavelle, S. J. Martin. Extracellular neutrophil proteases are efficient regulators of IL-1, IL-33, and IL-36 cytokine activity but poor effectors of microbial killing. *Cell Reports* **2018**, *22*, 2937–2950.

[390] G. P. Sullivan, P. B. Davidovich, S. Sura-Trueba, E. Belotcerkovskaya, C. M. Henry, D. M. Clancy, A. Zinoveva, T. Mametnabiev, A. V. Garabadzhiu, S. J. Martin. Identification of small-molecule elastase inhibitors as antagonists of IL-36 cytokine activation. *FEBS Open Bio* **2018**, *8*, 751–763.

[391] G. P. Sullivan, C. M. Henry, D. M. Clancy, T. Mametnabiev, E. Belotcerkovskaya, P. Davidovich, S. Sura-Trueba, A. V. Garabadzhiu, S. J. Martin. Suppressing IL-36-driven inflammation using peptide pseudosubstrates for neutrophil proteases. *Cell Death and Disease* **2018**, *9*, 378.

[392] M. Murphy, P. Kerr, J. M. Grant-Kels. The histopathologic spectrum of psoriasis. *Clinics in Dermatology* **2007**, *25*, 524–528.

[393] W.-H. Boehncke. Etiology and pathogenesis of psoriasis. *Rheumatic Disease Clinics* **2015**, *41*, 665–675.

[394] Q. He, H. X. Chen, W. Li, Y. Wu, S. J. Chen, Q. Yue, M. Xiao, J. W. Li. IL-36 cytokine expression and its relationship with p38 MAPK and NF-κB pathways in psoriasis vulgaris skin lesions. *Journal of Huazhong University of Science and Technology - Medical Science* **2013**, *33*, 594–599.

[395] A. Johnston, X. Xing, A. M. Guzman, M. Riblett, C. M. Loyd, N. L. Ward, C. Wohn, E. P. Prens, F. Wang, L. E. Maier, S. Kang, J. J. Voorhees, J. T. Elder, J. E. Gudjonsson. IL-1F5, -F6, -F8, and -F9: A novel IL-1 family signaling system that is active in psoriasis and promotes keratinocyte antimicrobial peptide expression. *Journal of Immunology* **2011**, *186*, 2613–2622.

[396] S. Marrakchi, P. Guigue, B. R. Renshaw, A. Puel, X.-Y. Pei, S. Fraitag, J. Zribi, E. Bal, C. Cluzeau, M. Chrabieh, J. E. Towne, J. Douangpanya, C. Pons, S. Mansour, V. Serre, H. Makni, N. Mahfoudh, F. Fakhfakh, C. Bodemer, J. Feingold, S. Hadj-Rabia, M. Favre, E. Genin, M. Sahbatou, A. Munnich, J.-L. Casanova, J. E. Sims, H. Turki, H. Bachelez, A. Smahi. Interleukin-36-receptor antagonist deficiency and generalized pustular psoriasis. *The New England Journal of Medicine* **2011**, *365*, 620–628.

[397] A. Johnston, X. Xing, L. Wolterink, D. H. Barnes, Z. Q. Yin, L. Reingold, J. M. Kahlenberg, P. W. Harms, J. E. Gudjonsson. IL-1 and IL-36 are dominant cytokines in generalized pustular psoriasis. *Journal of Allergy and Clinical Immunology* **2017**, *140*, 109–120.

[398] M. Tauber, E. Bal, X. Y. Pei, M. Madrange, A. Khelil, H. Sahel, A. Zenati, M. Makrelouf, K. Boubridaa, A. Chiali, N. Smahi, F. Otsmane, B. Bouajar, S. Marrakchi, H. Turki, E. Bourrat, M. Viguier, Y. Hamel, H. Bachelez, A. Smahi. IL36RN mutations affect protein expression and function: A basis for genotype-phenotype correlation in pustular diseases. *Journal of Investigative Dermatology* **2016**, *136*, 1811–1819.

[399] F. Capon. IL36RN mutations in generalized pustular psoriasis: Just the tip of the iceberg. *Journal of Investigative Dermatology* **2013**, *133*, 2503–2504.

[400] S. Frey, A. Derer, M.-E. Messbacher, D. L. P. Baeten, S. Bugatti, C. Montecucco, G. Schett, A. J. Hueber. The novel cytokine interleukin-36α is expressed in psoriatic and rheumatoid arthritis synovium. *Annals of the Rheumatic Diseases* **2013**, *72*, 1569–1574.

[401] A. Wißbrock, N. B. Goradia, A. Kumar, A. A. Paul George, T. Kühl, P. Bellstedt, R. Ramachandran, P. Hoffmann, K. Galler, J. Popp, U. Neugebauer, K. Hampel, B. Zimmermann, S. Adam, M. Wiendl, G. Krönke, I. Hamza, S. H. Heinemann, S. Frey,

A. J. Hueber, O. Ohlenschläger, D. Imhof. Structural insights into heme binding to IL-36α proinflammatory cytokine. *Scientific Reports* **2019**, *9(1)*, doi: 10.1038/s41598–019–53231–0.

[402] J. H. Jones. Abbreviations and symbols in peptide science: A revised guide and commentary. *Journal of Peptide Science* **2006**, *12*, 1–12.

[403] P. Heimer, T. Schmitz, C. A. Bäuml, D. Imhof. Synthesis and structure determination of μ-conotoxin PIIIA isomers with different disulfide connectivities. *Journal of Visualized Experiments* **2018**, *140*, doi: 10.3791/58368.

[404] A. Pîrnău, M. Bogdan. Investigation of the interaction between naproxen and human serum albumin. *Romanian Journal of Biophysics* **2008**, *18*, 49–55.

[405] C. Wiedemann, P. Bellstedt, M. Görlach. CAPITO - A web server-based analysis and plotting tool for circular dichroism data. *Bioinformatics* **2013**, *29*, 1750–1757.

[406] C. Louis-Jeune, M. A. Andrade-Navarro, C. Perez-Iratxeta. Prediction of protein secondary structure from circular dichroism using theoretically derived spectra. *Proteins: Structure, Function, and Bioinformatics* **2012**, *80*, 374–381.

[407] C. Bartels, T. Xia, M. Billeter, P. Guntert, K. Wuthrich. The program XEASY for computer-supported NMR spectral analysis of biological macromolecules. *Journal of Biomolecular NMR* **1995**, *6*, 1–10.

[408] T. Herrmann, P. Guntert, K. Wuthrich. Protein NMR structure determination with automated NOE-identification in the NOESY spectra using the new software ATNOS. *Journal of Biomolecular NMR* **2002**, *24*, 171–189.

[409] O. Crescenzi, S. Tomaselli, R. Guerrini, S. Salvadori, A. M. D'Ursi, P. A. Temussi, D. Picone. Solution structure of the Alzheimer amyloid beta-peptide (1-42) in an apolar microenvironment: Similarity with a virus fusion domain. *European Journal of Biochemistry* **2002**, *269*, 5642–5648.

[410] W. Humphrey, A. Dalke, K. Schulten. VMD: Visual Molecular Dynamics. *Journal of Molecular Graphics* **1996**, *14*, 33–38.

[411] E. Krieger, G. Vriend. YASARA View - molecular graphics for all devices - from smartphones to workstations. *Bioinformatics* **2014**, *30*, 2981–2982.

[412] E. Krieger, G. Vriend. New ways to boost molecular dynamics simulations. *Journal of Computational Chemistry* **2015**, *36*, 996–1007.

[413] K. Lindorff-Larsen, S. Piana, K. Palmo, P. Maragakis, J. L. Klepeis, R. O. Dror, D. E. Shaw. Improved side-chain torsion potentials for the Amber ff99SB protein force field. *Proteins: Structure, Function and Bioinformatics* **2010**, *78*, 1950–1958.

[414] J. M. Wang, R. M. Wolf, J. W. Caldwell, P. a. Kollman, D. a. Case. Development and testing of a general amber force field. *J. Comput. Chem.* **2004**, *25*, 1157–1174.

[415] A. Jakalian, D. B. Jack, C. I. Bayly. Fast, efficient generation of high-quality atomic charges. AM1-BCC model: II. Parameterization and validation. *Journal of Computational Chemistry* **2002**, *23*, 1623–1641.

[416] P. Li, L. F. Song, K. M. Merz. Parameterization of highly charged metal ions using the 12-6-4 LJ-type nonbonded model in explicit water. *Journal of Physical Chemistry B* **2015**, *119*, 883–895.

[417] W. L. Jorgensen, J. Chandrasekhar, J. D. Madura, R. W. Impey, M. L. Klein. Comparison of simple potential functions for simulating liquid water. *The Journal of Chemical Physics* **1983**, *79*, 926–935.

[418] U. Essmann, L. Perera, M. L. Berkowitz, T. Darden, H. Lee, L. G. Pedersen. A smooth particle mesh Ewald method. *The Journal of Chemical Physics* **1995**, *103*, 8577–8593.

[419] E. M. Novoa, L. R. De Pouplana, X. Barril, M. Orozco. Ensemble docking from homology models. *Journal of Chemical Theory and Computation* **2010**, *6*, 2547–2557.

[420] A. Wißbrock. Sind Thrombomodulin und Interleukin-36α potentielle Interaktionspartner von Häm/Hämin? *Bachelor thesis, Pharmaceutical Institute, University of Bonn* **2012**.

[421] A. Wißbrock. Untersuchungen zur transienten Interaktion von Hämin mit potentiell Häm-bindenden Proteinen. *Master thesis, Pharmaceutical Institute, University of Bonn* **2015**.

[422] Y. Zhou, J. Wang, L. Liu, R. Wang, X. Lai, M. Xu. Interaction between Amyloid-β peptide and heme probed by electrochemistry and atomic force microscopy. *ACS Chemical Neuroscience* **2013**, *4*, 535–539.

[423] D. Pramanik, C. Ghosh, S. Mukherjee, S. G. Dey. Interaction of amyloid β peptides with redox active heme cofactor: Relevance to Alzheimer's disease. *Coordination Chemistry Reviews* **2013**, *257*, 81–92.

[424] A. Pichon. Ionic self-assembly: Porphyrins pair up. *Nature Chemistry* **2010**, *2*, 611.

[425] M. Gouterman. Spectra of porphyrins. *Journal of Molecular Spectroscopy* **1961**, *6*, 138–163.

[426] M. Gouterman, G. H. Wagniere, L. C. Snyder. Spectra of porphyrins: Part II. Four orbital model. *Journal of Molecular Spectroscopy* **1963**, *11*, 108–127.

[427] A. Rauk. The chemistry of Alzheimer's disease. *Chemical Society Reviews* **2009**, *38*, 2698–2715.

[428] A. Vandersteen, E. Hubin, R. Sarroukh, G. De Baets, J. Schymkowitz, F. Rousseau, V. Subramaniam, V. Raussens, H. Wenschuh, D. Wildemann, K. Broersen. A comparative analysis of the aggregation behavior of amyloid-β peptide variants. *FEBS Letters* **2012**, *586*, 4088–4093.

[429] L. Stefan, F. Denat, D. Monchaud. Insights into how nucleotide supplements enhance the peroxidase-mimicking DNAzyme activity of the G-quadruplex/hemin system. *Nucleic Acids Research* **2012**, *40*, 8759–8772.

[430] Y. Su, P. T. Chang. Acidic pH promotes the formation of toxic fibrils from beta-amyloid peptide. *Brain Research* **2001**, *893*, 287–291.

[431] M. Groenning. Binding mode of Thioflavin T and other molecular probes in the context of amyloid fibrils-current status. *Journal of Chemical Biology* **2010**, *3*, 1–18.

[432] T. Matsui, S. I. Ozaki, E. Liong, G. N. Phillips, Y. Watanabe. Effects of the location of distal histidine in the reaction of myoglobin with hydrogen peroxide. *Journal of Biological Chemistry* **1999**, *274*, 2838–2844.

[433] J. Colin, B. Wiseman, J. Switala, P. C. Loewen, A. Ivancich. Distinct role of specific tryptophans in facilitating electron transfer or as [Fe(IV)=O Trp•] intermediates in the peroxidase reaction of bulkholderia pseudomallei catalase-peroxidase: A multifrequency EPR spectroscopy investigation. *Journal of the American Chemical Society* **2009**, *131*, 8557–8563.

[434] M. Honsho, S. Asaoku, K. Fukumoto, Y. Fujiki. Topogenesis and homeostasis of Fatty acyl-CoA reductase 1. *Journal of Biological Chemistry* **2013**, *288*, 34588–34598.

[435] O. Soga, H. Kinoshita, M. Ueda, A. Tanaka. Evaluation of peroxisomal heme in yeast. *The Journal of Biochemistry* **1997**, *121*, 25–28.

[436] J. Zhao, V. De Serrano, R. Dumarieh, M. Thompson, R. A. Ghiladi, S. Franzen. The role of the distal histidine in H2O2 activation and heme protection in both peroxidase and globin functions. *The Journal of Physical Chemistry B* **2012**, *116*, 12065–12077.

[437] M. Coles, W. Bicknell, A. A. Watson, D. P. Fairlie, D. J. Craik. Solution Structure of Amyloid β-Peptide(1-40) in a Water-Micelle Environment. *Biochemistry* **1998**, *37*, 11064–11077.

[438] J. Jarvet, J. Danielsson, P. Damberg, M. Oleszczuk, A. Gräslund. Positioning of the Alzheimer Aβ(1-40) peptide in SDS micelles using NMR and paramagnetic probes. *Journal of Biomolecular NMR* **2007**, *39*, 63–72.

[439] P. Thévenet, Y. Shen, J. Maupetit, F. Guyon, P. Derreumaux, P. Tufféry. PEP-FOLD: an updated de novo structure prediction server for both linear and disulfide bonded cyclic peptides. *Nucleic Acids Research* **2012**, *40*, 288–293.

[440] Y. Shen, J. Maupetit, P. Derreumaux, P. Tufféry. Improved PEP-FOLD approach for peptide and miniprotein structure prediction. *Journal of Chemical Theory and Computation* **2014**, *10*, 4745–4758.

[441] A. Kontush. Lipid peroxidation and Alzheimer's disease: Key role of Amyloid-β. *OCL - Oilseeds and fats, Crops and Lipids* **2006**, *13*, 46–53.

[442] A. L. Biere, B. Ostaszewski, E. R. Stimson, B. T. Hyman, J. E. Maggio, D. J. Selkoe. Amyloid β-peptide is transported on lipoproteins and albumin in human plasma. *Journal of Biological Chemistry* **1996**, *271*, 32916–32922.

[443] Y. M. Kuo, M. R. Emmerling, C. L. Bisgaier, a. D. Essenburg, H. C. Lampert, D. Drumm, a. E. Roher. Elevated low-density lipoprotein in Alzheimer's disease correlates with brain Aβ 1-42 levels. *Biochemical and Biophysical Research Communications* **1998**, *252*, 711–715.

[444] G. Camejo, C. Halberg, A. Manschik-Lundin, E. Hurt-Camejo, B. Rosengren, H. Olsson, G. I. Hansson, G. B. Forsberg, B. Ylhen. Hemin binding and oxidation of lipoproteins in serum: mechanisms and effect on the interaction of LDL with human macrophages. *Journal of Lipid Research* **1998**, *39*, 755–766.

[445] P. Pattnaik. Surface Plasmon Resonance. *Applied Biochemistry and Biotechnology* **2005**, *126*, 79–92.

[446] R. Bakhtiar. Surface plasmon resonance spectroscopy: A versatile technique in a biochemist's toolbox. *Journal of Chemical Education* **2013**, *90*, 203–209.

[447] Y. Tang, X. Zeng, J. Liang. Surface plasmon resonance: An introduction to a surface spectroscopy technique. *Journal of Chemical Education* **2010**, *87*, 742–746.

[448] The UniProt Consortium. UniProt: The universal protein knowledgebase. *Nucleic Acids Research* **2017**, *45*, D158–D169.

[449] F. Sievers, A. Wilm, D. Dineen, T. J. Gibson, K. Karplus, W. Li, R. Lopez, H. McWilliam, M. Remmert, J. Söding, J. D. Thompson, D. G. Higgins. Fast, scalable generation of high-quality protein multiple sequence alignments using Clustal Omega. *Molecular Systems Biology* **2011**, *7*, 539.

[450] N. Goradia, A. Wißbrock, C. Wiedemann, R. Bordusa, Frank Ramachandran, D. Imhof, O. Ohlenschläger. (1)H, (13)C, and (15)N resonance assignments for the pro-inflammatory cytokine interleukin-36α. *Biomolecular NMR Assignments* **2016**, *10*, 329–333.

[451] Y. Chen, M. D. Barkley. Toward understanding tryptophan fluorescence in proteins. *Biochemistry* **1998**, *37*, 9976–9982.

[452] M. Möller, A. Denicola. Protein tryptophan accessibility studied by fluorescence quenching. *Biochemistry and Molecular Biology Education* **2002**, *30*, 175–178.

[453] S. M. Akbar, K. Sreeramulu, H. C. Sharma. Tryptophan fluorescence quenching as a binding assay to monitor protein conformation changes in the membrane of intact mitochondria. *Journal of Bioenergetics and Biomembranes* **2016**, *48*, 241–247.

[454] C. A. Royer. Probing protein folding and conformational transitions with fluorescence. *Chemical Reviews* **2006**, *106*, 1769–1784.

[455] D. Silva, C. M. Cortez, S. R. W. Louro. Chlorpromazine interactions to sera albumins: A study by the quenching of fluorescence. *Spectrochimica Acta Part A: Molecular and Biomolecular Spectroscopy* **2004**, *60*, 1215–1223.

[456] J. R. Lakowicz. Quenching of fluorescence. *in Principles of fluorescence spectroscopy* **2006**, 258–304.

[457] T. G. Spiro, J. M. Burke. Protein control of porphyrin conformation. Comparison of resonance raman spectra of heme proteins with mesoporphyrin IX analogs. *Journal of the American Chemical Society* **1976**, *98*, 5482–5489.

[458] T. Kitagawa, M. Abe, Y. Kyogoku, H. Ogoshi, E. Watanabe, Z. Yoshida. Resonance raman spectra of metallooctaethylporphyrins. Low frequency vibrations of porphyrin and iron-axial ligand stretching modes. *The Journal of Physical Chemistry* **1976**, *80*, 1181–1186.

[459] T. G. Spiro. Resonance Raman Spectroscopy as a Probe of Heme Protein Structure and Dynamics. *Advances in Protein Chemistry* **1985**, *37*, 111–159.

[460] J. A. Shelnutt, J. D. Satterlee, J. E. Erman. Raman difference spectroscopy of heme-linked ionizations in cytochrome c peroxidase. *Journal of Biological Chemistry* **1983**, *258*, 2168–2173.

[461] G. M. Giacometti, G. Giacometti. Spectroscopic techniques in biophysics. *IOS Press* **2001**.

[462] B. Krumm, Y. Xiang, J. Deng. Structural biology of the IL-1 superfamily: key cytokines in the regulation of immune and inflammatory responses. *Protein Science* **2014**, *23*, 526–538.

[463] D. Wang, S. Zhang, L. Li, X. Liu, K. Mei, X. Wang. Structural insights into the assembly and activation of IL-1β with its receptors. *Nature Immunology* **2010**, *11*, 905–911.

[464] O. Trott, A. J. Olson. AutoDock Vina: Improving the speed and accuracy of docking with a new scoring function, efficient optimization and multithreading. *Journal of Computational Chemistry* **2010**, *31*, 445–461.

[465] A. Derer, B. Groetsch, U. Harre, C. Böhm, J. E. Towne, G. Schett, S. Frey, H. A. J. Blockade of IL-36 receptor signaling does not prevent from TNF-induced arthritis. *PLoS One* **2014**, *9*, e101954.

[466] G. R. Nakayama, M. C. Caton, M. P. Nova, Z. Parandoosh, *Assessment of the Alamar Blue assay for cellular growth and viability in vitro*, **1997**.

[467] T. Zarubin, J. Han. Activation and signaling of the p38 MAP kinase pathway. *Cell Research* **2005**, *15*, 11–18.

Abbreviations

A	Absorbance
Aβ	Amyloid beta
Aa	Amino acid
AAA	Amino acid analysis
ABCB6	ATP-binding cassette subfamily B member 6
ABCB10	ATP-binding cassette subfamily B member 10
ABCG2	ATP-binding cassette super-family G member 2
ACD	Allergic contact dermatitis
AD	Alzheimer's disease
ALA	δ-Aminolevulinic acid
ALAS	δ-Aminolevulinic acid synthase
AP-1	Activated protein 1
APP	Amyloid precursor protein
APS	Ammonium persulfate
ASC	Apoptosis-associated speck-like protein containing CARD
ATP	Adenosine triphosphate
Bach1	Transcription regulator protein Bach1
Bmal1	Brain and muscle ARNT-like 1
BME	β-Mercaptoethanol
BOXes	Bilirubin oxidation products
BSA	Bovine serum albumin
BVR	Biliverdin reductase
C1q	Complement component 1q
C3	Complement component 3
CAA	Cerebral amyloid angiopathy
CBS	Cystathionine beta-synthase
CD	Circular dichroism
CD14	Cluster of differentiation receptor 14
CD91	Cluster of differentiation receptor 91
CD163	Cluster of differentiation receptor 163

CDK1	Cyclin-dependent kinase 1
CDK4	Cyclin-dependent kinase 4
CKIϵ	Casein kinase ϵ
ClpXP	ATP-dependent Clp protease ATP-binding subunit clpX-like, mitochondrial
Clock	Circadian locomotor output cycles protein kaput
CO	Carbon monoxide
CO_2	Carbon dioxide
CoA	Coenzyme A
COPD	Chronic obstructive pulmonary disease
COX	Cytochrome c oxidase
CPOX	Coproporphyrinogen oxidase
CRP	C-reactive protein
Cry	Cryptochrome
CSF	Cerebrospinal fluid (*Liquor cerebrospinalis*)
Cu	Copper
CYP_{450}	Cytochrome P_{450}
DAMP	Damage-associated molecular pattern
DCM	Dichloromethane
DGCR8	DiGeorgeCritical region 8
DIEA	*N,N*-Diisopropylethylamine
DITRA	Deficiency of interleukin thirty-six-receptor antagonist
DMEM	Dulbecco's modified Eagle's medium
DMF	*N,N*-Dimehtylformamide
DPP8	Dipeptiylpeptidase 8
DTT	Dithiothreitol
EDTA	Ethylenediaminetetraacetic acid
eIF2α	Eukaryotic initiation factor
ELISA	Enzyme-linked immunosorbent assay
EP	Erythrophagocytosis
ER	Endoplasmic reticulum
ERK1	Extracellular-signaling kinase 1
ERK2	Extracellular-signaling kinase 2
ESI	Electro spray ionization
FABP	Fatty acid binding protein
FECH	Ferrochelatase
Fl	Full-length
FLS	Fibroblast-like synoviocytes
FLVCR1a	Feline leukemia virus subgroup C receptor 1a

FLVCR1b	Feline leukemia virus subgroup C receptor 1b
FLVCR2	Feline leukemia virus subgroup C receptor 2
Fmoc	Fluorenylmethyloxycarbonyl (protecting group)
GAPDH	Glyceraldehyde-3-phosphate dehydrogenase
GATA-1	GATA-binding factor 1
GPCR	G protein-coupled receptor
GPP	General pustular psoriasis
GSH	Glutathione
H_2O	Water
H_2O_2	Hydrogene peroxide
H-bond	Hydrogen bond
HAP1	Heme activator protein 1
Hb	Hemoglobin
HBM	Heme-binding motif
HBP1	Heme-binding protein 1
HBP22	Heme-binding protein 22
HBP23	Heme-binding protein 23
HBTU	*O*-(Benzotriazol-1-yl)-*N,N,N',N'*-tetramethyluronium-hexafluorophosphate
HCl	Hydrochloric acid
HCP1	Heme carrier protein 1
HDL	High density lipoprotein
Hepes	4-(2-Hydroxyethyl)-1-piperazineethanesulfonic acid
HMB	Hydroxymethylbilane
HMGB1	High-mobility-group-protein B1
HRM	Heme-regulatory motif
HO-1	Heme oxygenase 1
HO-2	Heme oxygenase 2
HO-3	Heme oxygenase 3
HOBt	*N*-Hydroxybenzotriazole
HOIL1	Heme-oxidized IRP2 ubiquitin ligase 1
Hp	Haptoglobin
HPLC	High pressure liquid chromatography
HRG1	Heme-responsive gene 1 protein homolog
HRI	eIF2αkinase
HRP	Horseradish peroxidase
HSA	Human serum albumin
Hx	Hemopexin
IAA	Iodoacetamide

IκB	Inhibitory κB kinase
ICAM1	Intercellular adhesion molecule 1
ICH	Intracerebral hemorrhage
IFN	Interferon
IgG	Immunoglobulin G
IL	Interleukin
IL-1α	Interleukin-1α
IL-1β	Interleukin-1β
IL-1RII	Interleukin-1 receptor type II
IL-1RAcP	Interleukin-1 receptor accessory protein
IL-6	Interleukin-6
IL-8	Interleukin-8
IL-36	Interleukin-36
IL-36R	Interleukin-36 receptor
IL-36Ra	Interleukin-36 receptor antagonist
IMS	Intermembrane space
INFγ	Interferon-γ
IPTG	Isopropyl-β-D-1-thiogalactopyranoside
IRAK	Interleukin-1 receptor-associated kinase
IRE	Iron response element
IRP2	Iron regulatory protein 2
IRR	Iron responsive regulator
IUPAC	International Union of Pure and Applied Chemistry
JAK2	Janus kinase 2
JNK	c-Jun N-terminal kinase
KC	Keratinocyte-derived chemokine
K_D	Dissociation constant
$KMnO_4$	Potassium permanganate
LB	Lysogeny broth
LC	Liquid chromatography
LDL	Low density lipoprotein
LDL_{ox}	Oxidized LDL
LH	Labile heme
LPS	Lipopolysaccharid
LRP1	Low-density lipoprotein receptor-related protein 1 (CD91)
LTB_4	Leukotriene B_4
Maf	Musculoaponeurotic fibrosarcoma
MALDI	Matrix-assisted Laser Desorption/Ionization
MAMs	Mitochondria-associated membranes

MAPK	Mitogen-activated protein kinase
MARE	Maf recognition element
MD	Molecular dynamics
MD2	Myeloid differentiation factor 2
MDVs	Mitochondrial-derived vesicles
MEK1	Mitogen-activated protein kinase kinase 1
MEK2	Mitogen-activated protein kinase kinase 2
miRNA	MicroRNA
MKK	Mitogen-activated protein kinase
MPS	Mononuclear phagocytic system
MRP5	Multidrug resistance protein 5
mRNA	Messenger ribonucleic acid
MyD88	Myeloid differentiation primary response 88
NaCl	Sodium chloride
NAD(H)	Nicotinamide adenine dinucleotide
NADP(H)	Nicotinamide adenine dinucleotide phosphate
NaOH	Sodium hydroxide
NET	Neutrophil extracellular trap
Nf-κb	Nuclear factor kappa-light-chain-enhancer of activated B cells
NFTs	Neurofibrillary tau tangles
NH_4^+	Ammonium cation
NLRP3	Nucleotide-binding domain and leucine-rich repeat pyrin 3 (containing inflammasome)
NMM	N-methyl-morpholine
NMR	Nuclear magnetic resonance
NO	Nitric oxygen
NO_3^-	Nitrate
NOE	Nuclear Overhauser effect
NOESY	Nuclear Overhauser effect spectroscopy
NOS	NO-synthase
NPAS2	Neuronal PAS domain protein 2
O_2	Molecular oxygen
OD	Optical density
p38	P38 mitogen-activated protein kinases
p53	Tumor protein p53
PAGE	Polyacrylamide gel electrophoresis
PAMP	Pathogen-associated molecular pattern
PAS	Per-ARNT-Sim
PD	Parkinson's disease

PI_3K	Phosphoinositide 3-kinase
PKC	Protein kinase C
PBG	Porphobilinogen
PBGD	Porphobilinogen desaminase
PBGS	Porphobilinogen synthase
PCR	Polymerase chain reaction
PDPs	Propentdyopents
Per	Period
PPO	Porphyrinogen oxidase
PPIX	Protoporphyrin IX
PROS	Partially reduced oxygen species
PRR	Pattern recognition receptor
qRT-PCR	Quantitative real time PCR
RA	Rheumatoid arthritis
RAF	Rapidly accelerated fibrosarcoma
RBC	Red blood cell
RES	Reticuloendothelial system
RMSD	Root-mean-square deviation
RMSF	Root-mean-square fluctuation
Ro	Rodents
ROS	Reactive oxygen species
RPMI	Roswell Park Memorial Institute medium
*r*Raman	*Resonance* Raman spectroscopy
SAH	Subarachnoid hemorrhage
SASA	Solvent accessible surface area
SCD	Sickle cell disease
SDS	Sodium dodecyl sulfate
SEC	Size-exclusion chromatography
Slo1	Large-conductance calcium-dependent Slo1 BK channel
SPPS	Solid-phase peptide synthesis
SPR	Surface plasmon resonance
Src	Proto-oncogene tyrosine-protein kinase Src
TAB	TAK1-binding protein
TAK1	TGFβ1-activated kinase 1
TBST	Tris-buffered saline with Tween20
TEMED	Tetramethylethanediamine
TFA	Trifluoroacetic acid
ThT	Thioflavin T
TIR	Toll/interleukin-1 receptor

TLC	Thin-layer chromatography
TLR	Toll-like receptor
TLR4	Toll-like receptor 4
TMB	3,3',5,5'-Tetramethylbenzidine
TMB_{ox}	Oxidized 3,3',5,5'-Tetramethylbenzidine
TNF	Tumor necrosis factor
TOF	Time of flight
Tollip	Toll-interacting protein
Tr	Truncated
TRAF6	TNF receptor-associated factor 6
TRIF	TIR-domain-containing adapter-inducing interferon-β
Tris	Tris(hydroxymethyl)aminomethane
UROS	Uroporphyrinogen III synthase
UROD	Uroporphyrinogen III decarboxylase
VCAM1	Vascular cell adhesion molecule 1
vdW	Van der Waals
VLDL	Very-low-density lipoprotein
XLSA	X-linked sideroblastic anemia

List of Figures

List of Tables

Acknowledgments

During the past years I found myself taken on a roller coaster ride of tremendous ups and downs, delight and desperation, excitement and frustration, curiosity and anxiety as well as laughter and tears. Fortunately, I did not have to take this ride alone but had many people by my side.

First and foremost, I would like to express my deepest gratitude to my longtime supervisor and mentor Prof. Dr. Diana Imhof. I am very grateful for the chance to graduate in an empowering spirit and environment as the one that Prof. Dr. Imhof created. Apart from enabling me to perform my PhD thesis in her group, she also supported me in every way imaginable. I truly appreciated the opportunity to participate in several international conferences and even more to conduct a research stay in Washington D.C. that Prof. Dr. Imhof made possible. Due to the international climate sustained by her, I have crossed paths with many national and international graduate students, postdocs, and PIs who have influenced and enriched my personality and my research. Prof. Imhof's way of continuously being interested, encouraging, and enthusiastic has always been motivating and empowering. Many years of multifaceted conversations, scientific discussions, and abundant advice have not only had an enormous impact on my professional path but also on my personal development. Thank you!

I would like to thank Prof. Dr. Hofmann-Apitius (Bioinformatics, Fraunhofer Institute for Algorithms and Scientific Computing SCAI) for graciously contributing his time as a reader and second thesis supervisor. Together with Prof. Dr. med Oldenburg and Prof. Dr. Thiele I would like to thank all of the above-mentioned professors for forming the PhD committee.

Sincere thanks are given to Prof. Dr. Stefan Heinemann (Center for Molecular Biomedicine, Friedrich Schiller University) as the head of the DFG-founded research unit 'Heme and Heme Degradation Products - Alternative Functions and Signaling Mechanisms' (HHDP) for letting me participate in this marvelous research project, for

scientific advice, as well as many educational workshops and symposiums. Likewise, I would like to thank the Deutsche Forschungsgemeinschaft (DFG) for providing the financial footing of the present work within the HHDP.

Moreover, I would like to express my gratitude to the Deutsche Akademische Austauschdienst (DAAD), the Bonn Graduate Center (BGC), and the Bonn International Graduate School of Drug Sciences (BIGS DrugS) who financially enabled my participation at a Gordon Research Conference in Newport (Rhode Island, USA, 2018) and a research stay in College Park (Maryland, USA, 2017) in the lab of Prof. Dr. Iqbal Hamza by two scholarships. In addition, I would like to thank the managers of BIGS DrugS for organizing interesting and educational workshops and lectures.

At the turn of the year 2017/2018 I had the honor to join the lab of Prof. Dr. Iqbal Hamza (Department of Animal & Avian Sciences, University of Maryland) at the University of Maryland for a short-term research stay. The weeks I spent overseas have greatly enriched my perspective on science, culture, and people. I was welcomed with great hospitality and candor by Prof. Dr. Hamza himself and by his team members. Treating me like one of his students I was able to learn many lab-dependent and lab-independent matters. Therefore, I would like to express my sincere thanks for giving me this great opportunity!

Many projects of the present thesis have only been possible by the great support of several cooperation partners.

First of all, I am very grateful to Dr. Oliver Ohlenschläger, Dr. Nishit Goradia, and Amit Kumar (Leibniz Institute on Aging - Fritz-Lipmann-Institute, FLI, Jena) for recombinantly expressing the IL-36 cytokines, the NMR analysis, as well as the computational modeling of various peptides. I would also like to thank Dr. Oliver Ohlenschläger for being a member of my HHDP PhD board. Beyond that I want to thank them all for several short-term research stays at the FLI and many years of fruitful dialogues and discussions.

Prof. Dr. Ute Neugebauer, Prof. Dr. Jürgen Popp, Patrick Hoffmann, and Dr. Kerstin Galler (Leibniz-Institute of Photonic Technology, IPHT, Jena) enabled the resonance Raman spectroscopy measurements at the IPHT. Many thanks to Patrick who spend several long nights measuring samples and at the same time still provided fun and high spirits. Moreover, I would like to thank Prof. Dr. Ute Neugebauer for being the second member of my HHDP PhD board.

I am very grateful to Dr. Dr. Axel Hueber, Dr. Silke Frey, and Susanne Adams (Department of Medicine 3, Friedrich-Alexander University Hospital Erlangen) for testing the biological impact of heme on the IL-36 cytokines in *in vitro* cell assays.

The SPR analysis of heme binding to different proteins by Dr. Bastian Zimmermann and Dr. Kornelia Hampel from Biaffin GmbH & Co (Kassel) is also gratefully acknowledged.

CSF patient samples, kindly provided by Prof. Dr. Albert Becker (Department of Neuropathology, University of Bonn), are greatly appreciated.

I would also like to thank Ajay Abisheck Paul George (group of Prof. Dr. Imhof, Pharmaceutical Institute, University of Bonn) for the *in silico* analysis of heme binding to IL-36α and the IL-36α variants. Moreover, I gratefully appreciated the help of our technical assistant Sabrina Linden (group of Prof. Dr. Imhof, Pharmaceutical Institute, University of Bonn) who substantially supported the recombinant expression of the IL-36α cytokines. Furthermore, I would like to thank Marion Schneider (group of Prof. Dr. Müller, Pharmaceutical Institute, University of Bonn) who was always ready to help and support whenever needed for MS measurements. Moreover, I would like to thank Marie-Thérèse Hopp for reviewing parts of this thesis. I would also like to thank my dearest colleague Charlotte Bäuml for donating her time to read and correct the entire present thesis.

A very special thanks to the former and present group members of the AK Imhof for sharing dissertation woes, glimmers of hope, and many laughter as well as a chance to thrive! I deeply enjoyed being part of such a motivating, inspiring, and enriching environment. Your support and even more your distractions were greatly appreciated! Special thanks to Charlotte, Toni, Henning, Pascal, Ajay, and Marie!

Last but by no means least, I would like to thank my family and friends. I've been lucky to have their support, confidence, patience, pride, nurturing, and love over all these years!

Danke!

Publications

Manuscripts

Kühl, T., Wißbrock, A., Goradia, N., Sahoo, N., Galler, K., Neugebauer, U., Popp J., Heinemann, S. H., Ohlenschläger, O., Imhof, D. (2013) Analysis of Fe(III) heme binding to cysteine-containing heme-regulatory motifs in proteins, *ACS Chemical Biology*, 8, 1785-1793.

Goradia, N., Wißbrock, A., Wiedemann, C., Bordusa, F., Ramachandran, R., Imhof, D., Ohlenschläger, O. (2016) 1H, 13C, and 15N resonance assignments for the pro-inflammatory cytokine interleukin-36α, *Biomolecular NMR Assignments*, 10, 329-333.

Wißbrock, A.^{x}, Kühl, T.^{x}, Silbermann, K., Becker, A. J., Ohlenschläger, O., Imhof, D. (2017) Synthesis and evaluation of Aβ-derived and Aβ-independent enhancers of the peroxidase-like activity of heme, *Journal of Medicinal Chemistry*, 60, 373-385.

Wißbrock, A., Imhof D. (2017) A tough nut to crack: Intracellular detection and quantification of heme in malaria parasites by a genetically encoded protein sensor, *ChemBioChem*, 18, 1561-1564.

Kumar, A., Wißbrock, A., Goradia, N., Bellstedt, P., Ramachandran, R., Imhof, D., Ohlenschläger, O. (2018) Heme interaction of the intrinsically disordered N-terminal peptide segment of human cystathionine-β-synthase, *Scientifc Reports*, 8, 2474.

Peherstorfer, S., Brewitz, H. H., Paul George, A. A., Wißbrock, A., Adam, J. M., Schmitt, L., Imhof, D. (2018) Heme regulates activation of hemolysin A by binding to hemolysin-activating lysine acyltransferase HlyC from Escherichia coli, *Biochim Biophys Acta - General Subjects*, 1862, 1964-1972.

Wißbrock, A., Paul George, A. A., Brewitz, H. H., Kühl, T., Imhof, D., (2019) The Molecular Basis of Transient Heme-Protein Interactions: Analysis, Concept and Implementation, *Bioscience Reports*, 39, BSR20181940.

Kumar, A., Wißbrock, A., Bellstedt, P., Ramachandran, R., Imhof, D., Ohlenschläger, O. (2019) 1H, 13C, and 15N resonance assignments of the cytokine interleukin-36β, *Biomolecular NMR Assignments*, doi: 10.1007/s12104-018-09869-4.

Wißbrock, A.^{x}, Goradia, N. B.^{x}, Kumar, A., Paul George, A. A., Kühl, T., Bellstedt, P., Ramachandran, R., Hoffmann, P., Galler, K., Popp, J., Neugebauer, U., Hampel, K., Zimmermann, B., Adam, S., Wiendl, M., Krönke, G., Hamza, I., Heinemann, S. H., Frey, S., Hueber, A., Ohlenschläger, O., Imhof, D. (2019) Structural insights into heme binding to IL-36α proinflammatory cytokine, *Scientifc Reports*, 9(1), 16893.

Kumar, A., Bellstedt, P., Wiedemann, C., Wißbrock, A., Imhof, D., Ramachandran R., Ohlenschläger, O. (2019) NMR Experiments on the Transient Interaction of the Intrinsically Disordered N-terminal Peptide of cystathionine-β-synthase With Heme, *Journal of Magnetic Resonance*, 308,106561.

Goradia, N. B.[x], Wißbrock, A.[x], Kumar, A., Kühl, T., Brewitz, H. H., Sure, R., Koch, P., Groth, M., Wiedemann, C., Ramachandran, R., Grimme, S., Imhof, D., Ohlenschläger, O. (2019) NMR structural analysis and DFT calculations of CP-motifs reveal insight into the molecular architecture of heme-protein complexes, *In preparation.*
[x] *equal contribution*

Oral Presentations

Kühl, T., Wißbrock, A. (2012) A first glance at heme binding to CP-motifs, *Retreat FOR1738*, Siegmundsburg (Germany).

Wißbrock, A. (2015) Functional studies on Fe(III) heme interaction with the beta-amyloid peptide (short lecture), *12th German Peptide Symposium*, TU Darmstadt (Germany).

Wißbrock, A., Goradia, N. (2015) Impact of heme on peptides and proteins, *Retreat FOR1738*, Bad Blankenburg (Germany).

Wißbrock, A. (2017) Catalytically active peptide-heme complexes based on the Aβ-heme complex, *13th German Peptide Symposium*, University of Erlangen (Germany).

Wißbrock, A. (2017) Heme regulates the proinflammatory cytokine IL-36α, *Retreat FOR1738*, Bonn (Germany).

Wißbrock, A., Kühl, T., Brewitz, H. H., Imhof, I. (2018) Sequence Requirements for Transient Heme-Protein Interactions, *Heme Biosynthesis and the Porphyrias: Recent Advances*, Orlando (FL, United States of America).

Scientific Posters

Kühl, T., Wißbrock, A., Goradia, N., Sahoo, N., Galler, K., Neugebauer, U., Popp, J., Heinemann, S. H., Ohlenschläger, O., Imhof, D. (2013) Analysis of hemin binding to cysteine-containing heme-regulatory motifs in proteins, *11th German Peptide Symposium*, München (Germany).

Wißbrock, A., Kühl, T., Imhof, D. (2015) Functional studies on Fe(III) heme interaction with the beta-amyloid peptide, *12th German Peptide Symposium*, Darmstadt (Germany).

Brewitz, H. H., Schubert, E., Goradia, N., Galler, K., Kühl, T., Wißbrock, A., Popp, J., Neugebauer, U., Ohlenschläger, O., Hagelüken, G., Schiemann, O., Imhof, Spectroscopic Studies on Transient Heme-Binding to Peptides and Proteins, *SFB813: Graduate Talks on Chemistry@Spin Centers - Fall Retreat*, Trier (Germany).

Wißbrock, A., Kühl, T., Silbermann, K., Ohlenschläger, O., Imhof, D. (2016) Studies on the Aβ-Enhanced Peroxidase Activity of Heme: Implications for Sequence Deviations and LDL Resistance, *3rd HHDP Symposium*, Jena (Germany).

Wißbrock, A., Kühl, T., Silbermann, K., Ohlenschläger, O., Imhof, D. (2016) Peroxidase Activity of the Abeta-Heme Complex and Other Heme-Binding Peptides, *International Conference on Porphyrins and Phthalocyanines (ICPP)*, Nanjing (China).

Wißbrock, A., Kühl, T., Silbermann, K., Ohlenschläger, O., Imhof, D. (2016) Studies on heme-peptide complexes: Heme binding and catalytic activity in comparison to the heme-amyloid-β complex, Tetrapyrroles, *Chemistry and Biology of Gordon Research Conference*, Newport (RI, United States of America).

Wißbrock, A., Kühl, T., Silbermann, K., Ohlenschläger, O., Imhof, D. (2016) Catalytic Activity of Heme-Peptide Complexes: Amyloid-β Dependent and Independent Increase of the Peroxidase-like Activity, *34th European Peptide Symposium*, Leipzig (Germany).

Kumar, A., Wißbrock, A., Goradia, A., Ramachandran, R., Imhof, D., Ohlenschläger, O. (2017) Unraveling transient peptide/protein-heme interactions, *Advanced Isotopic Labelling Methods for Integrated Structural Biology*, Grenoble (France).

Imhof, D., Hopp, M.-T., Mai, S., Wißbrock, A., Hamedani, N. S., Pötzsch, B. (2017), Heme-regulated proteins within the blood coagulation cascade? Insights into the molecular basis of protein binding to free heme, *Congress of International Society on Thrombosis and Haemostasis (ISTH)*, Berlin (Germany).

Syllwasschy, B. F., Wißbrock, A., Brewitz, H. H., Schubert, E., Kühl, T., Ohlenschläger O., Schiemann, O., Hagelüken, G., Imhof, D. (2017) Investigation of heme-peptide complexes as models to explore heme-regulated proteins, *SFB 813 International Symposium 2017, Perspectives in Hypovalent Chemistry*, Bonn (Germany).

Wißbrock, A., Goradia, N. B., Kumar, A., Kühl, T., Hoffmann, P., Neugebauer, U., Frey, S., Hueber, A., Ohlenschläger, O., Imhof, D. (2018) Heme interacts with human interleukin-36 cytokines, *The Movement and Trafficking of Tetrapyrroles (Hemes, B12/Corrins, Bilins, and Chlorophyll) Gordon Research Conference*, Newport (RI, United States of America).

Syllwasschy, B. F., Hopp, M.-T., Paul George, A. A., Wißbrock, A., Imhof, D. (2018) Heme binding beyond Cys-Pro-motifs? – A systematic Analysis of His/Tyr-Based Motifs in Heme-Binding peptides and proteins, *35th European Peptide Symposium*, Dublin (Ireland).

Syllwasschy, B. F., Hopp, M.-T., Paul George, A. A., Wißbrock, A., Imhof, D. (2018) His/Tyr-based peptide motifs to study regulatory heme binding, *14th German Peptide Symposium*, Cologne (Germany).